AN INVESTIGATION INTO THE FEASIBILITY OF INCORPORATING KETOCONAZOLE INTO SOLID LIPID MICROPARTICLES

A Thesis Submitted to Rhodes University in
Fulfilment of the Requirements for the Degree of

MASTER OF SCIENCE (PHARMACY)

by

Henusha Devi Jhundoo

December 2014

Faculty of Pharmacy
Rhodes University
Grahamstown
South Africa

ABSTRACT

One of the major challenges of the oral administration of ketoconazole (KTZ), an inhibitor of sterol 14α-demethylase, used in the management of systemic and topical mycoses in immuno-compromised and paediatric patients is the lack of availability of liquid dosage forms. In order to overcome this challenge, extemporaneous preparations have been manufactured by care-givers and health care providers by crushing or breaking solid oral dosage forms of KTZ and mixing with a vehicle to produce a liquid dosage form that can be swallowed by patients. However, the use of extemporaneous preparations may lead to under or over-dosing if the care-givers are not guided accordingly. Furthermore, the dearth of information on the stability of these KTZ-containing extemporaneous preparations may lead to ineffective antifungal therapy and complicate the problems of resistance as it is difficult to estimate the shelf-lives of these extemporaneous products under varying storage conditions due to the susceptibility of KTZ to chemical degradation. Therefore, there is a need for formulation scientists to develop novel drug delivery systems that avoid the need for extemporaneous preparations, possess well-established limits of stability and minimize the risks of systemic adverse effects to facilitate KTZ therapy. The use of solid lipid microparticles (SLM) as potential carriers for the oral administration of KTZ was investigated since solid lipid carriers are known to exhibit the advantages of traditional colloidal carriers. The research undertaken in these studies aimed to investigate the feasibility of developing and manufacturing solid lipid microparticles (SLM), using a simple micro-emulsion technique, as a carrier for KTZ.

Prior to pre-formulation, formulation development and optimization studies of KTZ-loaded SLM, it was necessary to develop and validate an analytical method for the *in vitro* quantitation and characterization of KTZ in aqueous dispersions of SLM during development and assessment studies. An accurate, precise, specific and sensitive reversed-phase high performance liquid chromatographic (RP-HPLC) method coupled with UV detection at 206 nm was developed, optimized and validated for the analysis of KTZ in formulations.

Formulation development studies were preceded by solubility studies of KTZ in different lipids. Labrafil® M2130 CS was found to exhibit the best solubilising potential for KTZ. Pre-formulation studies were also designed to determine the polymorphic behavior and the crystallinity of KTZ and Labrafil® M2130 CS that was used for subsequent manufacture of the solid lipid carriers. DSC and FTIR studies revealed that there were no changes in the crystallinity of KTZ or

Labrafil® M2130 CS following exposure to a temperature of 60°C for 1 hour. In addition the potential for physicochemical interaction of KTZ with the lipid Labrafil® M2130 CS was investigated using DSC and FTIR and the results revealed that KTZ was molecularly dispersed in Labrafil® M2130 CS and that it is unlikely that KTZ would interact with the lipid. It was therefore established that KTZ and Labrafil® M2130 CS were thermo-stable at a temperature of 60°C and thus a micro-emulsion technique could be used to manufacture the KTZ-loaded SLM.

Drug-free and KTZ-loaded SLM were prepared using a modified micro-emulsion technique that required the use of an Ultra-Turrax® homogenizer set at 24 000 rpm for 5 minutes followed by the use of the Erweka GmbH homogenizer. SLM were characterized in terms of particle size (PS), zeta potential (ZP), shape and surface morphology using scanning electron microscopy (SEM) and transmission electron microscopy (TEM). In addition drug loading capacity (DLC) and encapsulation efficiency (EE) of SLM for KTZ were assessed using RP-HPLC. Formulation development and optimization studies of KTZ-loaded SLM were initially aimed at selecting an emulsifying system that was able to stabilize the SLM in an aqueous dispersion. Successful formulations were selected based on their ability to remain physically stable on the day of manufacture. Pluronic® F68 used in combination with Lutrol® E40, Soluphor® P, Soluplus® produced unstable dispersions on the day of manufacture and these combinations were not investigated further. However, the formulation of a stable KTZ-loaded SLM dispersion was accomplished by use of a combination of Pluronic® F68, Tween 80 and sodium cholate as the surfactant system. Increasing amounts of Labrafil® M2130 CS resulted in the production of particles with low DLC and EE, a large PS and a relatively unchanged ZP. An optimum concentration of 10% w/v Labrafil® M2130 CS was selected to manufacture the KTZ-loaded SLM. Studies to determine the influence of KTZ loading on the quality of SLM revealed that concentrations of KTZ > 5% w/v led to a reduction in DLC and EE and an increase in PS with minimal impact on the ZP. Stability studies conducted at 25°C/65% RH and 40°C/75% RH for up to 30 days following manufacture revealed that batch SLM 15 manufactured using 10% w/v Labrafil® M2130 CS, 5% w/v KTZ and a combination of 4% w/v Pluronic® F-68, 2% w/v Tween 80 and 1% w/v sodium cholate produced the most stable dosage form when stored at 25°C/65% RH for up to 30 days. However, storage at 40°C/75% RH resulted in instability of the formulation.

An aqueous dispersion of KTZ-loaded SLM has been developed and assessed and may offer an alternative to extemporaneous preparations used for KTZ therapy in paediatric and immuno-compromised patients.

ACKNOWLEDGEMENTS

I would like to express my sincere gratitude to the following people:

My supervisor, Professor Roderick B. Walker for giving me the opportunity to be part of his research group, for his patience, understanding and assistance throughout the course of my studies and during the preparation of this thesis and for the use of laboratory facilities. I would also like to thank him for granting me the opportunity to lecture an undergraduate course and co-ordinate undergraduate practicals which has immensely contributed to my personal growth and development.

Dr Sandile Khamanga, Dr Kasongo Wa Kasongo and Dr Adrienne Müller for being sources of inspiration, for their guidance, congenial company and support during my time as a post-graduate student. I would like to thank Dr Kasongo Wa Kasongo for his practical assistance and expertise throughout my studies and for being a role model in my academic career.

Professor Ros Dowse for her mentorship during the time that I lectured and coordinated practicals.

Members of the Faculty of Pharmacy at Rhodes University for their assistance during my time as a post-graduate student. The following members of the secretarial and technical staff are gratefully acknowledged for their invaluable assistance: Mr T. Samkange, Mr L. Purdon and Mr C. Nontyi, Ms L. Emslie, Ms T. Kent.

Members of the Faculty of Chemistry at Rhodes University for their assistance and technical expertise during the course of my DSC and FTIR studies.

Mrs S. Pinchuck and Mr M. Randall for their assistance, advice and patience during the course of my studies at the Electron Microscopy Unit.

Fellow post-graduate students, past and present in the Biopharmaceutics Research Group (BRG) for their help during my time as a post-graduate student.

Dr. Rosa Klein and Ms Candice Webber for their leadership, friendship and kindness during my time as a house warden in Drostdy Hall. The following members of Celeste House leadership committees are also gratefully acknowledged: Mr Zohaib Bholla, Ms Sarah D'Souza, Ms Spiwe Chidemo and Mr Sipho Khumalo.

Mrs Anthea Ribbink for her mentorship and guidance during my time as her sub-warden and a house warden and for her immense support and kindness during my time at Rhodes University.

My parents, my sister and my grandfather for their blessings, love, encouragement, motivation, understanding, financial assistance, advice and help throughout my life.

The Naran family: Mrs Sushilla Naran and late Mr Jayantylal Naran for their hospitality, kind-heartedness and for their support, understanding and encouragement during my time in Grahamstown. I would like to gratefully acknowledge their sons, Jitendra, Nitin and Anil and their families for their immense support, thoughtfulness and for taking care of me after the fire. I would also like to extend my gratitude to Mr and Mrs Tharkor Naran, Mrs Daksha Naran-Bills and family and Mrs Amalia Christelis for being family to me during my time in South Africa.

My cousin, Mr Thashveen Lutchmun for his hospitality after the fire incident, his support during my time at Rhodes University and his help during the submission of this thesis.

My friends, Ms Sonal Patel, Mrs Gurleen Manku and Mrs Bianca Mirino-Gutierrez who have been a source of support and encouragement and sometimes just laughter that kept me going throughout my life experiences. Special thanks to Ms Sonal Patel for her friendship, kindness, selflessness, help and hospitality during my time in Grahamstown.

Mr Andreas Gareis for his unwavering support, love, encouragement, patience and understanding especially in the last months leading up to the submission of this thesis and for kindly volunteering to proofread this manuscript.

Gattefossé SAS (Saint-Priest Cedex, France) for their donation of excipients.

The Andrew Mellon Foundation and the Joint Research Committee of Rhodes University for financial assistance during my studies.

Last but not least, I thank the Almighty God for his presence in my life and for providing me protection, strength and a life that I cherish. It is only through his grace and mercy that I was able to survive the fire incident on the 4th of June 2012 and that I was able to complete this work and see myself through to the end of this long journey and chapter of my life.

STUDY OBJECTIVES

Antifungal therapy is commonly required by immuno-compromised and paediatric patients in South Africa. The use of ketoconazole (KTZ) as an extemporaneous preparation is widespread for the treatment of systemic and topical fungal infections due to the lack of availability of antifungal medicines in child appropriate forms. Solid oral dosage forms of KTZ are usually broken or crushed and mixed with a vehicle to administer the molecule in a liquid dosage form that can be easily swallowed by the patients. The use of extemporaneous preparations of KTZ may lead to under or over-dosing by care-givers and the lack of stability data for these preparations makes it difficult to estimate the shelf-lives of these preparations under the variety of storage conditions to which they are exposed. Furthermore, prolonged KTZ therapy is associated with risks of hepatotoxicity. Novel drug delivery systems, that have well-defined stability limits, exhibit enhanced stability for KTZ and can minimize the risks of systemic adverse effects, are therefore required to facilitate the management of mycoses treated using KTZ. Therefore, the objectives of this study were:

1. To gather data relating to the physicochemical properties of KTZ that would assist in the development of novel drug delivery systems using empirical studies and literature sources.
2. To review current colloidal drug delivery systems and propose the need for oral lipid-based formulations such as solid lipid microparticles (SLM) formulations for KTZ.
3. To develop, optimize and validate a simple, selective, sensitive, precise and accurate reversed phase high performance liquid chromatographic method that was suitable for the quantitative analysis of KTZ in pharmaceutical formulations and the analysis of KTZ in aqueous dispersions of KTZ-loaded SLM.
4. To establish the thermal stability, polymorphic behaviour and crystallinity of KTZ and Labrafil® M2130 CS used for the manufacture of micro-particulate delivery systems.
5. To investigate the feasibility of incorporating KTZ into a SLM formulation.
6. To characterize the KTZ-loaded SLM formulations during formulation development and optimization studies.
7. To establish the stability of the KTZ-loaded SLM formulations developed in these studies.

TABLE OF CONTENTS

ABSTRACT ..... **I**
ACKNOWLEDGEMENTS ..... **III**
STUDY OBJECTIVES ..... **V**
TABLE OF CONTENTS ..... **VI**
LIST OF FIGURES ..... **XII**
LIST OF TABLES ..... **XIV**
LIST OF ACRONYMS ..... **XV**
CHAPTER ONE **1**
KETOCONAZOLE **1**
1.1. Introduction **1**
1.2. Physicochemical properties **2**
1.2.1. Description **2**
1.2.2. Solubility **2**
1.2.3. Dissociation constant **3**
1.2.4. Partition coefficient **3**
1.2.5. Ultraviolet Absorption Spectrum **3**
1.2.6. Infrared Spectrum **4**
1.2.7. Stereochemistry and structure activity relationship **5**
1.2.8. Specific rotation **6**
1.2.9. Melting characteristics **6**
1.3. Synthesis **7**
1.4. Stability **9**
1.4.1. Hydrolysis **9**
1.4.2. Oxidation **9**
1.4.3. Temperature **9**
1.4.4. Light **9**
1.5. Clinical Pharmacology **10**
1.5.1. Mechanism of action **10**
1.5.2. Spectrum of activity **11**
1.5.3. Clinical use and indications **11**
1.5.4. Resistance **11**
1.5.5. Dosage and administration **12**
1.5.6. Contraindications **13**

1.5.7. Drug interactions…….. 13

1.5.8. Adverse effects……14

1.5.9. High risk groups…….. 15
1.5.9.1. Pregnancy…….. 15
1.5.9.2. Lactation……. 16
1.5.9.3. Paediatric use……. 16
1.5.9.4. Geriatric use……. 16
1.5.9.5. Renal impairment……. 16

1.6. Pharmacokinetics…….. 17

1.6.1. Absorption……. 17

1.6.2. Distribution……. 18

1.6.3. Metabolism……. 19

1.6.4. Elimination……. 19

1.7. Conclusions…… 20

CHAPTER TWO 23

SOLID LIPID MICROPARTICLES AS A DRUG DELIVERY SYSTEM FOR KETOCONAZOLE 23

2.1. Introduction…….. 23

2.2. Description of colloidal drug delivery systems 24

2.3. Solid lipid microparticles…….. 26

2.3.1. Overview……. 26

2.3.2. Drug distribution in SLM matrices 28
2.3.2.1. Homogenous matrix model……. 29
2.3.2.2. Soft and hard drug-enriched shell models 29
2.3.2.3. Drug-enriched core…….. 30

2.4. Manufacture of solid lipid microparticles 30

2.5. Production of solid lipid microparticles (SLM) 31

2.5.1. Overview……. 31

2.5.2. High-pressure homogenization (HPH) 31
2.5.2.1. Hot high-pressure homogenization……. 34
2.5.2.2. Cold high-pressure homogenization 34

2.5.3. Micro-emulsion formation 35
2.5.3.1. Oil-in-water melt dispersion…….. 35
2.5.3.2. Water-in-oil melt dispersion…….. 36
2.5.3.3. Water-in-oil-in-water multiple emulsion 36

2.5.4. Solvent evaporation……. 36

2.5.5. Micro-channel emulsification 37

2.5.6. Cryogenic micronization 37

2.5.7. Spray congealing……. 37

2.5.8. Spray drying……. 38

2.6. Characterization of SLM…… 38

2.6.1. Overview……. 38

2.6.2. Image analysis……. 39
2.6.2.1. Overview…… 39
2.6.2.2. Scanning electron microscopy (SEM) 39
2.6.2.3. Transmission electron microscopy (TEM) 40
2.6.2.4. Atomic force microscopy……. 40

2.6.3. Particle size analysis…… 41

2.6.4. Zeta potential analysis……. 41

2.6.5. Crystallographic analysis 42
2.6.5.1. Differential scanning calorimetry……. 42
2.6.5.2. X-ray diffraction……. 43

2.6.6. Drug loading and encapsulation efficiency 43

2.7. Conclusions…… 44

CHAPTER THREE 47

DEVELOPMENT AND VALIDATION OF A HIGH PERFORMANCE LIQUID CHROMATOGRAPHIC METHOD FOR THE ANALYSIS OF KETOCONAZOLE 47

3.1. Introduction…….. 47

3.1.1. Overview……. 47

3.2. Principles of high performance liquid chromatography 48

3.3. HPLC method development 50

3.3.1. Overview……. 50

3.3.2. Experimental……. 52
3.3.2.1. Reagents……. 52
3.3.2.2. HPLC system……. 52
3.3.2.3. Selection of an analytical column ……..52
3.3.2.4. UV detection of KTZ……. 56
3.3.2.5. Choice of internal standard……. 58
3.3.2.6. Mobile phase selection ……59
3.3.2.7. Preparation of buffer……. 60
3.3.2.8. Preparation of mobile phase……. 61
3.3.2.9. Preparation of stock solutions and calibration standards 61

3.3.3. Optimization of the chromatographic conditions 62
3.3.3.1. Mobile phase selection…….. 62
3.3.3.1.1. Effect of concentration of organic modifier 62
3.3.3.1.2. Effect of flow rate……. 63
3.3.3.1.3. Effect of buffer pH…… 65
3.3.3.1.4. Effect of buffer molarity……. 66
3.3.3.1.5. Optimal mobile phase composition 66
3.3.3.2. Chromatographic conditions……. 67

3.4. Method validation……. 67

3.4.1. Overview……. 67

3.4.2. Linearity and range……. 68

3.4.3. Precision…… 69
3.4.3.1. Repeatability ……69
3.4.3.2. Intermediate precision…… 70
3.4.3.3. Reproducibility…….. 71

3.4.4. Accuracy…….. 71

3.4.5. Limits of quantitation (LOQ) and detection (LOD) 72

3.4.6. Specificity and selectivity 74
3.4.6.1. Analysis of KTZ in tablet dosage forms 74

3.4.7. Sample stability studies……. 76
3.4.7.1. Overview…… 76
3.4.7.2. Stability data analysis…….. 76
3.4.7.3. Stability of stock solutions…… 78

3.4.8. Method re-validation……. 79

3.4.8.1. Linearity and range……. 80

3.4.8.2. Precision…… 81
3.4.8.2.1. Repeatability…….. 81
3.4.8.2.2. Intermediate precision…….. 81

3.4.8.3. Accuracy……. 81

3.4.8.4. Specificity…….. 82

3.4.8.5. Limits of quantitation and detection. 84

3.4.9. Application of the HPLC method 84

3.5. Conclusions…….. 84

CHAPTER FOUR 87

EVALUATION OF POLYMORPHISM OF KETOCONAZOLE AND SELECTION AND CHARACTERIZATION OF SOLID LIPID FOR THE MANUFACTURE OF KETOCONAZOLE-LOADED SOLID LIPID MICROPARTICLES 87

4.1. Introduction…… 87

4.1.1. Differential scanning calorimetry 88

4.1.2. Fourier-transform infrared spectroscopy 91

4.2. Materials……. 93
4.2.1. Overview……. 93
4.2.2. Solid lipid excipients……. 93
4.2.2.1. Precirol® ATO5…….. 93
4.2.2.2. Compritol® 888……. 94
4.2.2.3. Labrafil® M2130 CS…….. 95
4.2.2.4. Gelucire® 44/14…….. 95
4.2.2.5. Gelucire® 50/13…… 96

4.2.3. Water…….. 97

4.3. Methods…….. 97

4.3.1. Characterization of KTZ 97
4.3.1.1. DSC characterization of KTZ……. 97
4.3.1.2. FTIR characterization of KTZ…….. 98

4.3.2. Selection of solid lipid excipient 98
4.3.2.1. Solubility studies…… 98
4.3.2.2. Polymorphism of bulk lipid…….. 99
4.3.2.2.1. DSC characterization of Labrafil® M2130 CS 99
4.3.2.2.2. FTIR characterization of Labrafil® M2130 CS 99
4.3.2.3. Interaction of bulk lipid with KTZ 99

4.4. Results and discussion…….. 100

4.4.1. Characterization of KTZ 100
4.4.1.1. DSC characterization of KTZ……. 100
4.4.1.2. FTIR characterization of KTZ……. 101

4.4.2. Selection of solid lipid excipient 103
4.4.2.1. Solubility studies…….. 103
4.4.2.2. Polymorphism of bulk lipid……. 104
4.4.2.2.1. DSC characterization of Labrafil® M2130 CS 104
4.4.2.2.2. FTIR characterization of Labrafil® M2130 CS 106
4.4.2.3. Interaction of bulk lipid with KTZ 109
4.4.2.3.1. DSC characterization of bulk lipid with KTZ 109
4.4.2.3.2. FTIR characterization of bulk lipid with KTZ 111

4.5. Conclusions…… 112

CHAPTER FIVE 114

FORMULATION AND CHARACTERIZATION OF AQUEOUS DISPERSIONS OF KTZ-LOADED SOLID LIPID MICROPARTICLES 114

5.1. Introduction……. 114

5.2. Materials……. 115

5.2.1. Solid lipid……. 115
5.2.1.1. Labrafil® M2130 CS……. 115

5.2.2. Emulsifying agents……. 115
5.2.2.1. Soluphor® P…… 115
5.2.2.2. Soluplus®……116
5.2.2.3. Lutrol® E400 ……..116
5.2.2.4. Pluronic® F68…….. 116
5.2.2.5. Sodium cholate……. 117
5.2.2.6. Tween 80…… 118

5.2.3. Water…….. 118

5.2.4. Formulation composition 119

5.3. Methods…….. 121

5.4. Characterization of KTZ-loaded SLM dispersions 122

5.4.1. SEM analysis……. 122

5.4.2. TEM analysis……. 122
5.4.3. Zeta potential analysis……..... 122
5.4.4. Drug loading capacity and encapsulation efficiency 123
5.4.5. Stability assessment of optimized formulations 123
5.5. Results and discussion……..... 124
5.5.1. Selection of surfactants…… 124
5.5.2. Selection of solid lipid concentration 131
5.5.3. Influence of drug-lipid ratio 134
5.5.4. Selection of production parameters 136
5.5.5. Stability assessment of optimized SLM formulations 139
5.5.5.1. Particle size analysis……..... 140
5.5.5.2. Zeta potential analysis ……...145
5.5.5.3. KTZ loading capacity and encapsulation efficiency 146
5.6. Conclusions……. 149
CHAPTER SIX..... 152
CONCLUSIONS..... 152
APPENDIX I..... 160
APPENDIX II 185
REFERENCES 193

LIST OF FIGURES

Figure 1.1 Ketoconazole 2
Figure 1.2 Ultraviolet spectrum of ketoconazole 4
Figure 1.3 Infra-red spectrum of ketoconazole 5
Figure 1.4 DSC curve for ketoconazole 7
Figure 1.5 Synthesis of cis-ketoconazole adapted from [39] 8
Figure 2.1 Proposed models of drug incorporation into SLN: (I) Homogenous matrix with molecular dispersion of the drug. (II) Lipid core surrounded by soft drug-enriched shell. (III) Drug-free lipid core surrounded by a hard shell consisting of lipid-drug mixture at eutectic concentrations. (IV) Lipid shell being drug-free or having low drug content surrounding the drug-enriched core [166, 173] 28
Figure 2.2 Schematic representation of hot and cold homogenization for the manufacture of SLN and SLM adapted from [102] 33
Figure 3.1 Typical chromatogram of a test mixture containing uracil (1), acetophenone (2), benzene (3), toluene (4) and naphthalene (5) after separation on a Beckman® Coulter ODS column 55
Figure 3.2 Effect of ACN composition on the retention times of KTZ and CLZ (n=6) 62
Figure 3.3 Effect of flow rate of the mobile phase on the retention times of KTZ and CLZ (n=6) 63
Figure 3.4 Typical chromatogram of a mixture of the internal standard, clotrimazole (CLZ, 80 µg/ml) and ketoconazole (KTZ, 120 µg/ml) using a mobile phase of 60% v/v ACN (60% v/v) and 50 mM phosphate buffer (pH 6.0) (40% v/v) at a flow rate of 1.0 ml/min 64
Figure 3.5 Effect of buffer pH used for the preparation of the mobile phase (comprising of 60% v/v ACN: phosphate buffer, 50 mM) on the retention times of KTZ and CLZ (n=6) 65
Figure 3.6 Effect of buffer molarity used for the preparation of the mobile phase (comprising of 60% v/v ACN: phosphate buffer, pH 6.0) on the retention times of KTZ and CLZ (n=6) 66
Figure 3.7 Typical calibration curve constructed for KTZ using peak height ratio of KTZ and CLZ versus concentration 69
Figure 3.8 Typical chromatogram obtained following analysis of Ketazol® 200 mg tablets using clotrimazole (CLZ) as internal standard. 75
Figure 3.9 Interpretation of stability data, as described by Timm et al. [340] 77
Figure 3.10 Interpretation of stability data for KTZ, as described by Timm et al. [340] 79
Figure 3.11 Calibration curve constructed for KTZ following least squares linear regression analysis of peak height ratio of KTZ and CLZ 80
Figure 3.12 Typical chromatogram obtained following analysis of Ketazol® cream (2% w/w) using clotrimazole (CLZ) as internal standard. 83
Figure 4.1 DSC profile of KTZ prior to and following exposure to 60°C for one (1) hour 100
Figure 4.2 Infra-red spectrum of KTZ following exposure to 60°C for one (1) hour 102
Figure 4.3 DSC profiles of Labrafil® M2130 CS generated prior to and following exposure of the lipid to heat at 60°C for one (1) hour 105
Figure 4.4 Infra-red spectrum of Labrafil® M2130 CS A) prior to exposure to 60°C for one (1) hour and B) following exposure to 60°C for one (1) hour 107
Figure 4.5 DSC profiles of a binary mixture of Labrafil® M2130 CS and KTZ generated prior to and following exposure of the lipid to heat at 60°C for one (1) hour 110
Figure 4.6 Infra-red spectrum of a binary mixture of Labrafil® M2130 CS and KTZ generated following exposure of the lipid to heat at 60°C for one (1) hour 111
Figure 5.1 Schematic representation of the modified micro-emulsion technique used to manufacture KTZ-loaded SLM 121
Figure 5.2 SEM micrographs of drug-free formulations, SLM 1 to SLM 9, manufactured using different surfactants or combinations of surfactants on the day of manufacture 126

Figure 5.3 TEM micrographs of drug-free formulations, SLM 1 to SLM 9, manufactured using different surfactants or combinations of surfactants on the day of manufacture 127
Figure 5.4 Mechanisms of instability in solid dispersions and emulsions adapted from [447] .. 130
Figure 5.5 SEM images of KTZ-loaded SLM manufactured using different concentrations of Labrafil® M2130 CS: 5% w/v (SLM 19), 10% w/v (SLM 15) and 15% w/v (SLM 20) on the day of manufacture 132
Figure 5.6 TEM images of KTZ-loaded SLM using different concentrations of Labrafil® M2130 CS: 5% w/v (SLM 19), 10% w/v (SLM 15) and 15% w/v (SLM 20) on the day of manufacture 132
Figure 5.7 ZP, PS, DLC, EE of KTZ-loaded SLM manufactured using different concentrations of Labrafil® M2130 CS: 5% w/v (SLM 19), 10% w/v (SLM 15) and 15% w/v (SLM 20) on the day of manufacture 133
Figure 5.8 SEM images of KTZ-loaded SLM manufactured using different concentrations of KTZ: 3.3% w/v (SLM 22), 5% w/v (SLM 15) and 10% w/v (SLM 21) on the day of manufacture 134
Figure 5.9 TEM images of KTZ-loaded SLM manufactured using different concentrations of KTZ: 3.3% w/v (SLM 22), 5% w/v (SLM 15) and 10% w/v (SLM 21) on the day of manufacture 134
Figure 5.10 PS, ZP, DLC and EE of KTZ-loaded SLM manufactured using different concentrations of KTZ: 3.3 % w/v (SLM 22), 5% w/v (SLM 15) and 10% w/v (SLM 21) on the day of manufacture 135
Figure 5.11 SEM images of KTZ-loaded SLM manufactured using 3 (A, SLM 23), 4 (B, SLM 24) and 5 (C, SLM 15) homogenization cycles on the day of manufacture 137
Figure 5.12 TEM images of KTZ-loaded SLM manufactured using 3 (A, SLM 23), 4 (B, SLM 24) and 5 (C, SLM 15) homogenization cycles on the day of manufacture 137
Figure 5.13 PS, ZP, DLC and EE of KTZ-loaded SLM manufactured using 3 (A, SLM 23), 4 (B, SLM 24) and 5 (C, SLM 15) homogenization cycles on the day of manufacture 138
Figure 5.14 SEM micrographs of SLM formulation 15 after storage at 25°C/60% RH on day 0 (A), 3 (B), 7 (C), 30 (D) after manufacture 141
Figure 5.15 SEM micrographs of SLM formulation 15 after storage at 40°C/75% RH on day 0 (A), 3 (B), 7 (C), 30 (D) after manufacture 142
Figure 5.16 TEM micrographs of SLM formulation 15 after storage at 25°C/60% RH (A) and 40°C/75% RH (B) on day 30 142
Figure 5.17 SEM micrographs of SLM formulation 16 after storage at 25°C/60% RH on day 0 (A), 3 (B), 7 (C), 30 (D) after manufacture 143
Figure 5.18 SEM micrographs of SLM formulation 16 after storage at 40°C/75% RH on day 0 (A), 3 (B), 7 (C), 30 (D) after manufacture 144
Figure 5.19 TEM micrographs of SLM formulation 16 after storage at 25°C/60°C RH (A) and 40°C/75°C RH (B) on day 30 144
Figure 5.20 Particle size (PS) of SLM formulations 15 and 16 after storage at 25°C/60% RH and 40°C/75% RH on day 0, 3, 7 and 30 after manufacture 145
Figure 5.21 Zeta potential (ZP) of SLM formulations 15 and 16 after storage at 25°C/60% RH and 40°C/75% RH on day 0, 3, 7 and 30 after manufacture 145
Figure 5.22 Drug loading capacity (DLC) and encapsulation efficiency (EE) of SLM 15 after storage at 25°C/60% RH and 40°C/75% RH on day 0, 3, 7 and 30 after manufacture 147
Figure 5.23 Drug loading capacity (DLC) and encapsulation efficiency (EE) of SLM 16 after storage at 25°C/60% RH and 40°C/75% RH on day 0, 3, 7 and 30 after manufacture 147

LIST OF TABLES

Table 1.1 Major infra-red band assignments for KTZ 5
Table 3.1 RP-HPLC methods used for the analysis of KTZ in dosage forms 51
Table 3.2 Retention times of KTZ and potential internal standards 59
Table 3.3 Optimized chromatographic conditions 67
Table 3.4 Intra-day precision data for HPLC analysis of KTZ 70
Table 3.5 Intermediate precision data for HPLC analysis of KTZ 71
Table 3.6 Accuracy data for HPLC analysis of KTZ (n = 3) 72
Table 3.7 LOQ data for HPLC analysis 74
Table 3.8 Intra-day precision data for HPLC analysis of KTZ during method revalidation 81
Table 3.9 Intermediate precision data for HPLC analysis of KTZ after method revalidation 81
Table 3.10 Accuracy data for HPLC analysis of KTZ (n = 3) after method revalidation 82
Table 3.11 LOQ data for HPLC analysis of KTZ 84
Table 4.1 DSC parameters for KTZ obtained prior to and after exposure to 60°C for one (1) hour 101
Table 4.2 Major infra-red band assignments for KTZ prior to and following exposure to 60°C for one (1) hour 102
Table 4.3 Solubility of KTZ in different solid lipid excipients 103
Table 4.4 DSC parameters for Labrafil® M2130 CS generated prior to and following exposure of the lipid to heat at 60°C for one (1) hour 105
Table 4.5 Major infra-red band assignments for Labrafil® M2130 CS prior to exposure to 60°C for one (1) hour 108
Table 4.6 Major infra-red band assignments for Labrafil® M2130 CS after exposure to 60°C for one (1) hour 108
Table 4.7 DSC parameters of a binary mixture of Labrafil® M2130 CS and KTZ obtained prior to and after exposure to heat at 60°C for one (1) hour 110
Table 4.8 Major infra-red band assignments for a binary mixture of Labrafil® M2130 CS and KTZ obtained following exposure to heat at 60°C for one (1) hour 111
Table 5.1 Formulation compositions of drug-free and KTZ-loaded SLM 120
Table 5.2 PS and ZP of drug-free batches, SLM 1 to SLM 9 and PS, ZP, DLC and EE of KTZ-loaded batches, SLM 10 to SLM 18 on the day of manufacture 127
Table 5.3 ZP, PS, DLC, EE of KTZ-loaded SLM manufactured using different concentrations of Labrafil® M2130 CS: 5% w/v (SLM 19), 10% w/v (SLM 15) and 15% w/v (SLM 20) on the day of manufacture 133
Table 5.4 PS, ZP, DLC and EE of KTZ-loaded SLM manufactured using different concentrations of KTZ: 3.3 % w/v (SLM 22), 5% w/v (SLM 15) and 10% w/v (SLM 21) on the day of manufacture 135
Table 5.5 PS, ZP, DLC and EE of KTZ-loaded SLM manufactured using 3 (A, SLM 23), 4 (B, SLM 24) and 5 (C, SLM 15) homogenization cycles on the day of manufacture 137
Table 5.6 PS, ZP, DLC and EE of KTZ-loaded SLM 15 manufactured using 10% w/v solid lipid, 5% w/v KTZ, 4% w/v Pluronic® F-68, 2% w/v Tween 80 and 1% w/v sodium cholate on days 0, 3, 7 and 30 after manufacture and after storage at 25°C/60% RH and 40°C/75% RH 140
Table 5.7 PS, ZP, DLC and EE of KTZ-loaded SLM 16 manufactured using 10% w/v solid lipid, 5% w/v KTZ, 5% w/v Pluronic® F-68, 1% w/v Tween 80 and 1% w/v sodium cholate on days 0, 3, 7 and 30 after manufacture and after storage at 25°C/60% RH and 40°C/75% RH 140

LIST OF ACRONYMS

ACN	Acetonitrile
ACTH	Adrenocorticotropic hormone
AFM	Atomic Force Microscopy
API	Active Pharmaceutical Ingredient
ATR	Attenuated Total Reflectance
BCS	Biopharmaceutics Classification System
BPC	Bonded-phase chromatography
CAPD	Continuing Ambulatory Peritoneal Dialysis
C.I.	Confidence Interval
CDDS	Colloidal drug delivery systems
CgERG11	ERG11 gene in *C. glabrata*
CLZ	Clotrimazole
CMC	Critical Micelle Concentration
CSF	Cerebrospinal Fluid
CYP P450	Cytochrome P450
DLC	Drug Loading Capacity
DLVO	Derjaguin and Landau, Verwey and Overbeek
DMA	Dimethylamine
DSC	Differential Scanning Calorimetry
ECZ	Econazole
EE	Encapsulation Efficiency
FDA	Food and Drug Administration
FTIR	Fourier-Transform Infra-Red
GIT	Gastrointestinal Tract
GRAS	Generally Regarded As Safe
HCl	Hydrochloric Acid
HLB	Hydrophilic-Lipophilic Balance
HPH	High-Pressure Homogenization
ICH	International Conference on Harmonization
IR	Infra-Red
IS	Internal Standard
IUPAC	International Union of Pure and Applied Chemistry
KBr	Potassium Bromide
KTZ	Ketoconazole
L.L.	Lower Limit
LD	Laser Diffraction
LDA	Laser Doppler Anemometry
LDL	Low Density Lipoprotein
LLOQ	Lower Limit of Quantitation
LOD	Limit of Detection
LOQ	Limit of Quantitation
MCZ	Miconazole
MeOH	Methanol
MW	Molecular Weight
NADPH	Nicotinamide Adenine Dinucleotide Phosphate
NaOH	Sodium hydroxide
NC	Nanocapsules
NE	Nanoemulsions
NMWL	Nominal Molecular Weight Limit

NS	Nanosuspensions
ODS	Octadecyl Silica
PCS	Photon Correlation Spectroscopy
PEG	Polyethylene Glycol
P-gp	P-glycoprotein
PN	Polymeric Nanoparticles
PS	Particle Size
RH	Relative Humidity
RP-HPLC	Reversed-phased High Performance Liquid Chromatography
RSD	Relative Standard Deviation
SAXD	Small Angle X-ray Diffraction
SDS	Sodium Dodecyl Sulphate
SEM	Scanning Electron Microscopy
SLM	Solid Lipid Microparticles
SLN	Solid Lipid Nanoparticles
$t_{1/2}$	Half-life
TEM	Transmission Electron Microscopy
U.L.	Upper Limit
USP	United States Pharmacopoeia
UV	Ultra-Violet
UV/Vis	Ultra-Violet/Visible
w/o/w	Water-in-oil-in-water
WAXD	Wide Angle X-ray Diffraction
WME	Width of melting event
ZnSe	Zinc selenide
ZP	Zeta Potential
2-BCM	2-body compartment

CHAPTER ONE

KETOCONAZOLE

1.1. Introduction

Ketoconazole (KTZ) is a synthetic imidazole antifungal molecule with a broad spectrum of antimicrobial activity. KTZ has been used for the management of a variety of systemic and topical fungal infections [1-7]. KTZ was the first azole antifungal agent of the dioxolane series to be introduced for clinical use, and was the first orally active azole type compound reported [1]. The development of KTZ stemmed from an attempt to vary the spectrum, specific level of antifungal activity, routes of administration and potential use of imidazole compounds [1, 8]. KTZ forms part of the *N*-substituted (mono) imidazole series in which substitutions are made at one of the two nitrogen atoms in the molecule whilst the imidazole ring is left intact [1, 8]. The incorporation of a dioxolane ring and a variety of side chains at the *N*-substituted imidazole of econazole and miconazole led to the discovery of KTZ in 1976 [9]. The dioxolane series of the azole compounds originated from substitutions made at the 1, 3-dioxolane configuration joined to the nitrogen atom [1].

Extensive studies were conducted on KTZ in the late 1970s following identification of its antifungal efficacy subsequent to oral administration [2, 3, 10-12]. It has been reported that KTZ is effective in the management of a range of fungal infections of the skin, fingernails, gastro-intestinal tract, respiratory tract and mucous membranes amongst others [5, 7, 11-17]. In 1981, Janssen Pharmaceutica introduced Nizoral® 200 mg tablets and received approval from the Food and Drug Administration (FDA) for the clinical use of KTZ as a prescription drug [18]. In recognition of his role in the discovery of KTZ in 1982, Jan Heeres was awarded the IUPAC-Richter Prize in 2008 for his work on azole chemistry, most specifically on KTZ [19]. KTZ is now widely used to treat fungal infections in adult and paediatric patients that do not respond to topical treatment and is occasionally used for the prophylaxis of fungal infections in immuno-compromised patients [7, 15]. Solid oral dosage forms of KTZ are usually crushed to produce extemporaneous preparations due to the dearth of antifungal medicine in liquid form. The lack of quality control in extemporaneous compounding makes it difficult to estimate the stability of such KTZ preparations. Therefore, the aim of this research was to investigate the feasibility of incorporating KTZ into a novel drug delivery system that possesses well-defined stability limits.

1.2. Physicochemical properties

1.2.1. Description

The chemical name of KTZ as defined by the IUPAC system is 1-Acetyl-4-[4[[(2*RS*, 4*SR*)-2-(2, 4-dichlorophenyl)-2-(1*H*-imidazol-1-ylmethyl)-1, 3-dioxolan-4-yl]methoxy]phenyl]piperazine [20]. KTZ is also known as (±)-*cis*-1-acetyl-4-{4-[2-(2, 4-dichlorophenyl)-2-(1*H*-imidazol-1-ylmethyl)-1, 3-dioxolan-4-yl-methoxy]phenyl}piperazine [15]. The structure of KTZ is depicted in Figure 1.1.

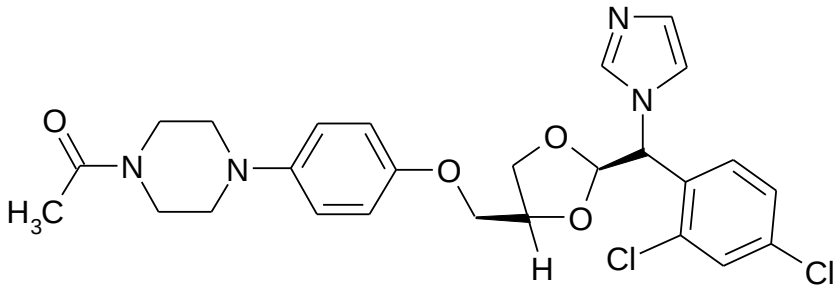

Figure 1.1 Ketoconazole

KTZ occurs as a white or almost white powder with a molecular formula and mass of $C_{26}H_{28}Cl_2N_4O_4$ and 531.4 g/mol respectively. One gram (1 g) of anhydrous KTZ contains not less than 99 % (0.99 g) and not more than 101.0% (1.01 g) ketoconazole.

1.2.2. Solubility

KTZ is practically insoluble in water, is sparingly soluble in ethanol, is soluble in toluene, ether and acetone and is freely soluble in methanol, chloroform and dichloromethane [15, 20, 21]. KTZ has been found to have an aqueous solubility of 0.017 mg/ml at 25°C [22]. KTZ is classified as a BCS Class II compound as it exhibits high permeability and low solubility in the gastrointestinal tract (GIT) [23]. The aqueous solubility of KTZ at pH 7.4 is 5.2 µM (0.0028 mg/ml) and 5.6 µM (0.0030 mg/ml) for the crystalline and amorphous forms, when measured using the shake flask method [24]. Amorphous KTZ, although known to be unstable, is more soluble than the crystalline form [25]. The dissolution of KTZ has been reported to be significantly reduced in solutions of pH > 5 [26].

1.2.3. Dissociation constant

The dissociation constant or pK_a, is a property of ionisable substances and expresses the ratio of ionized and unionized forms of a substance at equilibrium in water [27]. KTZ is a dibasic drug and therefore has two pK_a values *viz.*, 6.51 and 2.94 which are a consequence of the protonation of the imidazole and piperazine moieties respectively [28-30]. Ionisation of the piperazine group in the presence of gastric acid is vital for dissolution and subsequent absorption of KTZ [28-30].

1.2.4. Partition coefficient

The partition coefficient or log $P_{o/w}$ of a compound is a thermodynamic measure of the hydrophilic-lipophilic balance of the compound [31]. The log $P_{o/w}$ value of KTZ is 3.73 which is an indication that it is lipophilic and in part explains the poor water solubility of KTZ at neutral pH [29, 30]. Methods other than the traditional shake-flask method have been used to determine the partition coefficient of KTZ, including planar chromatography and the calculated log P value for KTZ is 4.45 [32]. Other reported values of log P for KTZ are 3.84 and 4.35 [33, 34].

1.2.5. Ultraviolet Absorption Spectrum

Ultraviolet/visible (UV/Vis) spectroscopy is widely used in qualitative and quantitative analysis, the determination of dissociation and equilibrium constants, trace analyses and photometric titration [35-37]. The range of wavelengths for UV/Vis spectroscopy is between 190 nm to 800 nm and although this range may seem limited, UV/Vis spectral studies can be of great value for the generation of information about molecules since most organic compounds and functional groups are transparent in this portion of the electromagnetic spectrum [35, 36].

UV studies were conducted to determine the λ_{max} of KTZ for high-performance liquid chromatographic analysis of KTZ coupled with UV detection. Since KTZ is insoluble in water and in the mobile phase constituents for analysis (§ 3.3.2.8), the UV absorption spectrum of KTZ in water or mobile phase was not assessed and the ultraviolet absorption spectrum of KTZ in a methanolic solution at a concentration of 10 µg/ml is depicted in Figure 1.2. The spectrum was generated using a double beam UV Vis spectrophotometer (GBC Scientific Equipment Pty Ltd, Melbourne, Victoria, Australia). The spectrum reveals a peak maximum at 205.9 nm and a minor peak at 247.8 nm. Shoulders at 217.4 nm and 221.5 nm were also noted in the spectrum.

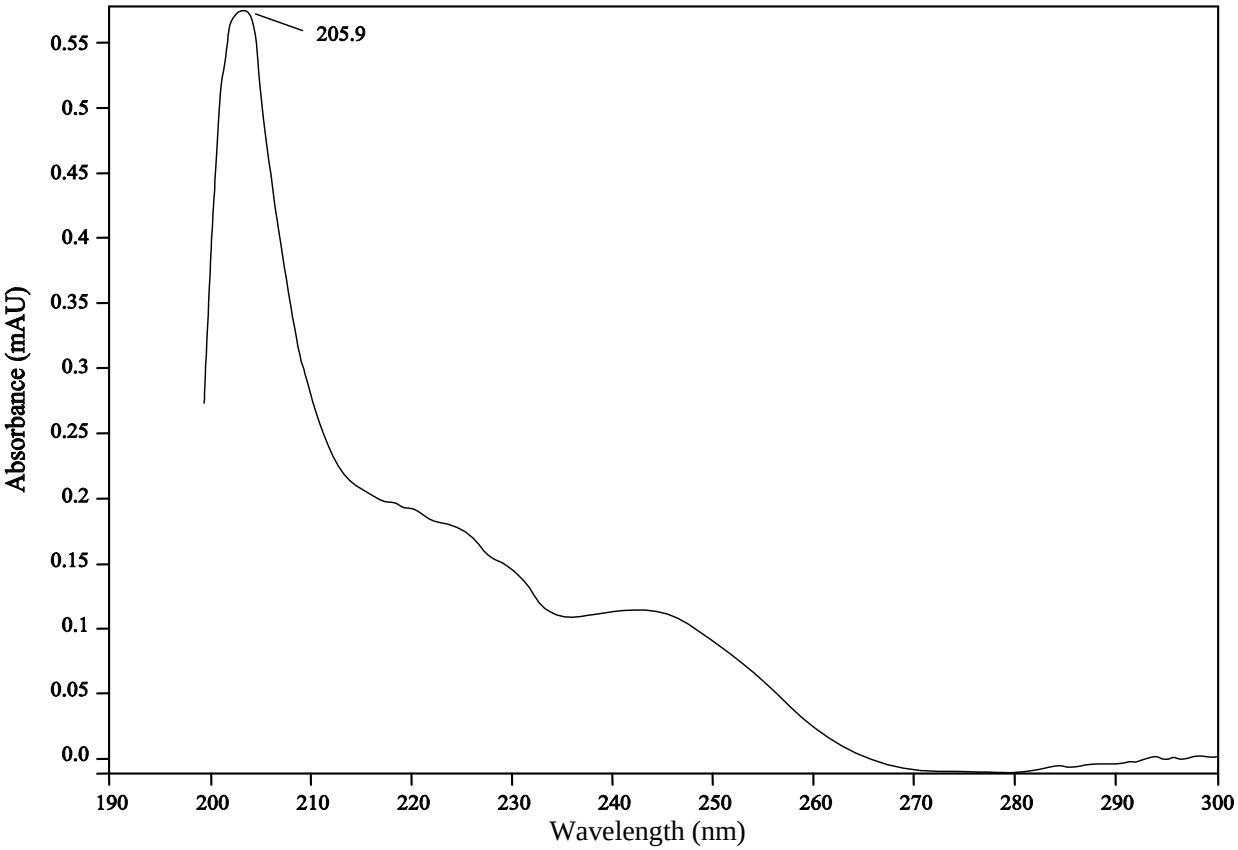

Figure 1.2 Ultraviolet spectrum of ketoconazole

1.2.6. Infrared Spectrum

Infrared (IR) spectroscopy is a useful and relatively easy technique that may be used to acquire structural information about a molecule and to identify unknown substances that may be present in a molecule [35, 36]. Molecules with covalent bonds that exhibit dipole moments absorb electromagnetic radiation in the infrared region of the electromagnetic spectrum and Consequently, display different natural vibration frequencies [35, 36]. Although different molecules might possess similar bonds, no two molecules will have the same infrared spectrum, as different molecules have different dipole moments [35, 36]. The IR spectrum of KTZ was generated using a Perkin-Elmer 100 FTIR spectrometer (Waltham, Massachusetts, USA) equipped with universal Attenuated Total Reflectance (ATR) technology in the range of 515-4000 cm^{-1}. The IR spectrum and relevant band assignments for KTZ are shown in Figure 1.3 and summarized in Table 1.1.

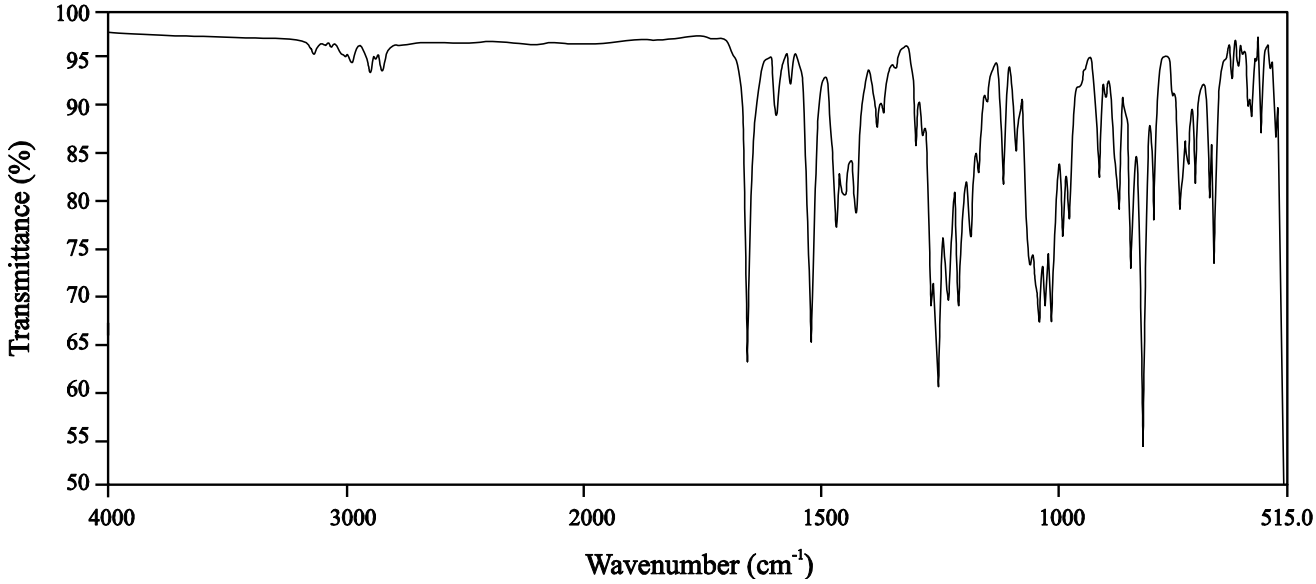

Figure 1.3 Infra-red spectrum of ketoconazole

Table 1.1 Major infra-red band assignments for KTZ

Band position (cm^{-1})	Assignment
3177	sp^2 C-H stretch
2976	sp^3 C-H stretch
1645	C=O stretching of the ketone (conjugation with imidazole ring)
1458	C-N stretching of the imidazole
1256	C-O stretching of the cyclic ether group
1240	C-C=O bend of the ketone | NR
1031	Ar-C-O stretching of the ether
737	C-Cl stretching of chlorine

The FTIR spectrum of KTZ reveals characteristic peaks showing the C=O stretching vibration of its carbonyl group, C-O stretching of its aliphatic ether group and C-O stretching of its cyclic ether at 1645 cm^{-1}, 1031 cm^{-1} and 1240 cm^{-1} respectively.

1.2.7. Stereochemistry and structure activity relationship

KTZ is the *cis* diastereomer of 1-acetyl-4-[4[[2-(2, 4-dichlorophenyl)-2-(1*H*-imidazole-1-ylmethyl)-1, 3-dioxolan-4-yl]methoxy]phenyl]piperazine, which has two centres of asymmetry and exists as two enantiomeric pairs of diastereomers [38]. KTZ is the most active antifungal agent of the diastereomers and is available commercially, as a racemic mixture with the R, S and S, R diastereomers in a 1:1 ratio [38]. The racemic mixture of KTZ is known to possess broad anti-infective properties and is effective against a large number of fungi, yeasts and

dermatophytes [38]. The racemic mixture of KTZ can be produced using the method described by Heeres et al. in in § 1.3 and individual diastereomers may be obtained following resolution with an optically active acid such as tartaric acid [38, 39]. The racemate of KTZ, albeit the most potent antifungal of the diastereomers, is associated with adverse effects such as hepatotoxicity of KTZ [40].

The development of KTZ commenced after an evaluation of miconazole revealed that it possessed certain key features responsible for antifungal activity [8]. Chemical modifications whilst maintaining the fundamental pharmacophore were introduced to generate azole compounds that were active against a wide range of mycoses [8]. The functional pharmacophore of KTZ is comprised of an imidazole ring joined to an asymmetric carbon atom to which a 2, 4-dihalogen-substituted benzene moiety is attached (Figure 1.1) [8]. During the early stages of azole drug development, chlorine atoms were attached to the benzene moiety whilst for the newer analogues, the chlorine atom has been substituted with fluorine atoms that result in increased potency [8].

The introduction of a dioxolane ring in KTZ improved the configuration of KTZ. Further substitutions of the dioxolane ring in addition to the introduction of a piperazine moiety, not only improved the antifungal efficacy of KTZ, but also enhanced oral activity [8]. The piperazine moiety is basic and is thought to be responsible for the water solubility and antimycotic activity of KTZ which is dependent on the extent of protonation of the piperazine group [41]. Increased protonation of the piperazine moiety leads to enhanced water solubility and antimycotic activity of KTZ and occurs when the pH of the medium is lower than the isoelectric point of the piperazine group substantiating the need for a low pH for adequate solubility and subsequent absorption of KTZ [41-43].

1.2.8. Specific rotation

The specific optical rotation of a 0.04 µg/ml KTZ solution in methanol at 20°C is between -1.0° and +1.0°.

1.2.9. Melting characteristics

The melting range of KTZ is 148°C and 152°C [20]. Changes in the melting behaviour of KTZ were investigated using Differential Scanning Calorimetry (DSC). The DSC thermogram of KTZ

was generated using a Perkin-Elmer DSC-7 Differential Scanning Calorimeter (Norwalk, Connecticut, USA) in a sealed aluminium pan, and is depicted in Figure 1.4. The DSC curve for KTZ reveals an endothermic peak of fusion at 149.27°C indicating that KTZ melts at this temperature. The melting range of KTZ was established as 146.42°C to 151.72°C.

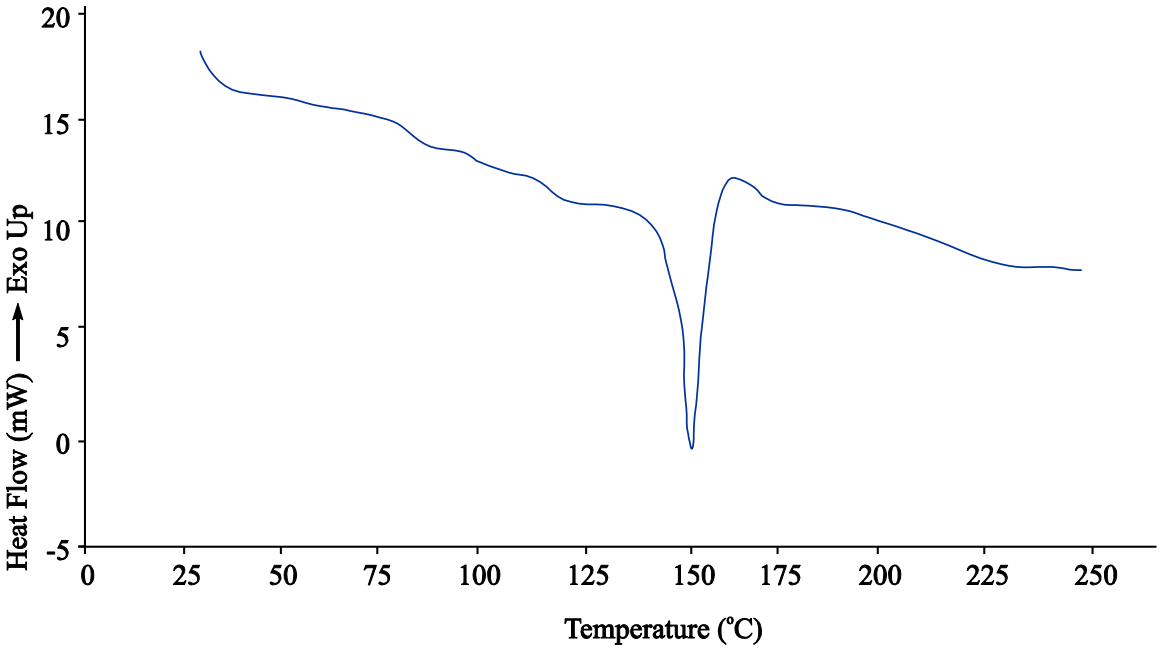

Figure 1.4 DSC curve for ketoconazole

1.3. Synthesis

The synthetic pathway for the manufacture of KTZ is illustrated in the reaction scheme depicted in Figure 1.5 [39]. The initial step in the synthesis of KTZ involves ketalisation of 2, 4-dichloroacetophenone (I) with glycerine in the presence of a benzene-1-butanol medium and *p*-toluenesulfonic acid. The ketal (II) is then brominated) at 30°C to form bromo ketal (III). Product III is then subjected to benzoylation in pyridine to form a cis/trans mixture, from which the cis form (IV) is isolated by recrystallization in ethanol. Coupling of product IV with imidazole in dry dimethylamine (DMA) produces an imidazole derivative and ester (V). Saponification of product V by refluxing in sodium hydroxide and dioxane-water leads to the formation of the alcohol (VI). Conversion of product VI to methylsulfonate (VII) followed by coupling with the sodium salt of VIII results in the production of ketoconazole (IX).

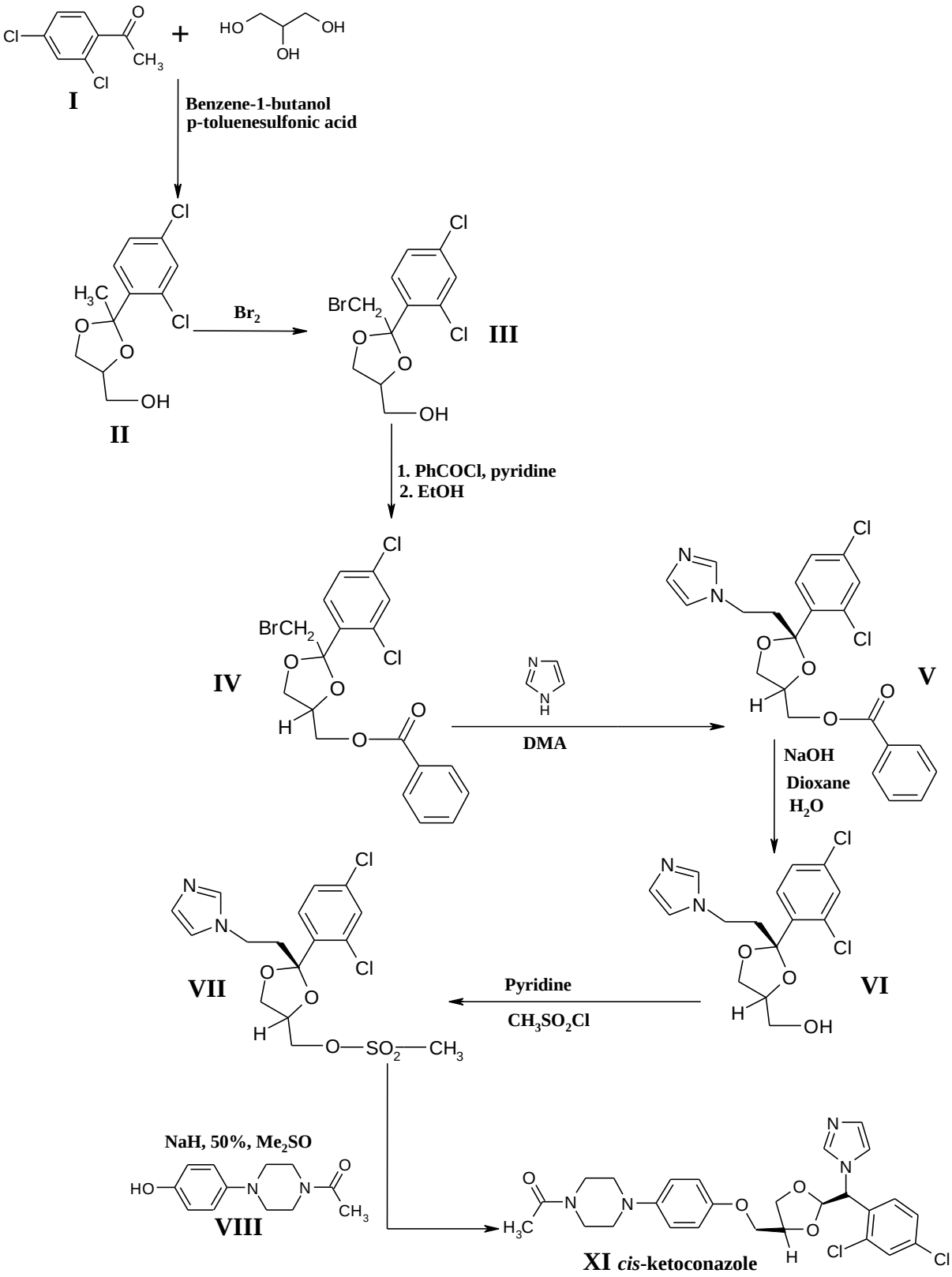

Figure 1.5 Synthesis of cis-ketoconazole adapted from [39]

1.4. Stability

1.4.1. Hydrolysis

KTZ undergoes hydrolysis at low pH [44]. Hydrolytic degradation is enhanced between pH 1-4 and the degradation rate has been found to be highest at pH 1 suggesting that KTZ is subject to specific acid catalysis in aqueous solution [44]. KTZ undergoes little hydrolysis at alkaline pH and optimum physical and chemical stability are observed at pH 7 [44]. It has been reported that KTZ may be subject to slow hydrolysis when heated under reflux conditions for 10 hours in a 10% v/v methanolic solution of sodium hydroxide [45].

1.4.2. Oxidation

KTZ is known to degrade through oxidation particularly in aqueous media [44]. It has been reported that the oxidation of KTZ is much higher at low pH [44]. In addition KTZ is subjected to chemically irreversible oxidation in solutions of pH 8-12 when it exists in the un-protonated form that exhibits an increased susceptibility of the imidazole and piperazine rings to oxidation [46-48]. KTZ has been found to undergo the least oxidation in the protonated form and is reported to be stable in a pH range of 4-7 [46-48].

1.4.3. Temperature

Accelerated stress studies conducted at 25°C and 50°C revealed that KTZ is relatively stable in aqueous media for approximately three months [44]. However, after three months pronounced degradation occurs at 50°C whereas only minimal degradation was noted at 25°C [44]. These results imply that KTZ is chemically stable in aqueous media at temperatures not exceeding 50°C for a maximum period of three months [44]. Moreover, it has been reported that there is no significant effect on the concentration of KTZ in ethanolic solution when stored at ambient temperature or under refrigerated conditions over a twenty-nine day period [49].

1.4.4. Light

Stability studies conducted in ethanolic solutions of two different concentrations of KTZ stored in clear and amber glass containers exposed to light over a period of twenty-nine days. The samples were analyzed on days 0, 1, 2, 3, 5, 8, 15, 22 and 29 using UV spectroscopy [49] and the results

revealed that exposure to light had no significant impact on the concentration of KTZ. No difference was observed between the UV spectrum of the test and reference samples revealing no sign of degradation [49].

1.5. Clinical Pharmacology

1.5.1. Mechanism of action

Azole compounds such as KTZ are known to exert their antifungal action by inhibiting sterol 14α-demethylase, a microsomal cytchrome P450-dependent enzyme system [4, 50-55]. This leads to the inhibition of ergosterol biosynthesis for the cytoplasmic membrane and results in the accumulation of lanosterol and other 14α-methylsterols [10, 50-52, 54]. The closely-packed arrangement of the acyl chains of the phospholipids is subsequently disturbed, thereby impairing the function of membrane-bound enzymes such as ATPase and the electron transport system [10, 50-52, 54]. The depletion of ergosterol therefore interferes with fungal cell growth and proliferation and inhibition of CYP P450 results in sensitization of fungal cells to oxidative metabolites produced by phagocytes [50].

KTZ also inhibits the biosynthesis of steroidal hormones in humans and specifically impacts the synthesis of testosterone and glucocorticoids [50]. The plasma levels of testosterone and androstenedione have been found to be lower in patients treated with KTZ [52, 56-59]. In addition an increase in 17α-hydroxyprogesterone levels implies that KTZ has an inhibitory effect on the enzyme C17, 20-lyase [56-58]. The reduction in androgen levels has been reported to be beneficial in the treatment of prostatic carcinoma and precocious puberty [57, 58]. KTZ has also proved useful in the treatment of Cushing's disease and adrenal adenoma due to its inhibition of adrenal 11β-hydroxylase and C17, 20-lyase leading to a reduction in the levels of cortisol and related corticosteroids produced by excessive adrenocorticotropic hormone (ACTH) secretion in these conditions [52, 56, 57]. KTZ has also been reported to inhibit cholesterol synthesis by blocking demethylation of lanosterol, leading to a marked decrease in low density lipoprotein (LDL) levels [60].

1.5.2. Spectrum of activity

KTZ exhibits a broad spectrum of activity against a variety of pathogenic fungi including the *Candida* species, *Cryptococcus neoformans*, *Coccidioides immitis*, *Histoplasma capsulatum*, *Blastomyces dermatitidis*, *Paracoccidioides brasiliensis* in addition to a wide range of dermatophytes or ringworm fungi [4, 11, 51, 61, 62]. The antibacterial and anti-parasitic activity of KTZ is restricted to protozoa of the *Leishmania major* species [4, 51].

1.5.3. Clinical use and indications

KTZ has been shown to be beneficial in the treatment of topical and oral pathogenic mycoses [2, 5, 7, 63]. The use of orally administered KTZ is required for the treatment of systemic mycoses such as paracoccidioidomycosis, blastomycosis, coccidiodomycosis, candidiasis and histoplasmosis [4, 7, 11, 14, 63-65]. KTZ may also be used to treat severe chronic muco-cutaneous candidiasis and disabling candidal chronic paronychia [5, 66]. KTZ is useful for the management of serious mycoses of the gastrointestinal tract (GIT), chronic vaginal candidiasis and dermatophyte infections which are not responsive to other therapies [5, 7, 66]. KTZ has also been used as prophylactic therapy in immuno-compromised patients with neoplastic and/or other malignant conditions [67].

High-dose KTZ has proved to be of therapeutic benefit in the treatment of metastatic prostate cancer since KTZ suppresses the biosynthesis of steroids and thus reduces androgen production. Topical KTZ is frequently used to treat ringworm, cutaneous candidiasis, pityriasis versicolor and seborrhoeic dermatitis and pityriasis capitis or dandruff caused by *Pityrosporum* spp.

1.5.4. Resistance

Over the years, resistant strains of *Candida* spp. to KTZ have emerged. The underlying mechanisms of resistance to azole antifungal agents involve gene overexpression and of efflux transport [50, 68-70]. Gene amplification or downregulation were found to be primary mechanisms of resistance in *C. albicans* [68]. Moreover, energy-requiring efflux pumps *viz.*, ATP-binding cassette multidrug transporters may account for resistance towards azole antifungals such as KTZ [50, 68]. Overexpression or downregulation of transporter genes such as CDR1 or BEN appear to mediate azole resistance in species such as *Saccharomyces cerevisiae* [68].

Modifications to the ERG11 gene, which encodes the azole target enzyme in *C. glabrata* (CgERG11) up-regulates the CgCDR1 and CgCDR2 genes which in turn encode efflux pumps and are primary causes of resistance to azole antifungal drugs [70]. A further mechanism of resistance is a reduction in ergosterol biosynthesis as observed in a number of post-treatment *C. albicans*, *C. neoformans* and *Histoplasma capsulatum* species [69]. Furthermore, mutations have been reported in the CYP51A1 genes of resistant *C. albicans* isolates and it appears that an overexpression of CYP51A1 in *C. albicans* and *C. glabrata* may also contribute to reduced susceptibility to azole antifungal agents [69].

1.5.5. Dosage and administration

KTZ is commercially available in South Africa as Nizoral® 200 mg tablets (Janssen-Cilag) and Ketazol® 200 mg tablets (Aspen Pharmacare) [61]. The adult dose for oral administration of KTZ for the management of chronic and recurrent vaginal candidiasis is 400 mg daily for five days [61]. Other indications usually require a dose of 200 mg KTZ daily which may be increased by 200 mg to 400 mg twice daily if an adequate response is not achieved [61]. It is imperative that KTZ therapy is continued for at least one week after the symptoms of the condition have disappeared [61]. Treatment with KTZ is usually 14 days in duration and may be longer if the initial clinical response is poor [66].

Topical preparations of KTZ include Nizcreme® cream (2%) (Janssen-Cilag) and Ketazol® cream (2%) (Aspen Pharmacare) [61]. In addition shampoo preparations of KTZ are also available for topical use and include Nizshampoo® (2%) (Janssen-Cilag), Adco-Dermed® shampoo (2%) (Adco Generics) and Kez® liquid (2%) (Pharma Dynamics) [61]. Topical administration of KTZ involves application of the product to the affected area(s) twice a day until a few days after the symptoms have disappeared [61].

There is a scarcity of appropriate paediatric formulations for KTZ in South Africa and extemporaneous preparations are generally manufactured and administered to paediatric patients in the public sector. These extemporaneous preparations of KTZ include suspensions that are manufactured by crushing KTZ tablets and mixing the resultant powder in a methylcellulose vehicle prior to administration. Limited data relating to the shelf-life and stability of these extemporaneous preparations is currently available and there is an increased potential for the stability of these extemporaneously prepared formulations to be adversely affected, thereby

possibly resulting in ineffective oral therapy with KTZ for the management of fungal infections in paediatric patients. Therefore, there is a need for the development of novel drug delivery systems for KTZ for paediatric use.

1.5.6. Contraindications

KTZ is contraindicated in patients with porphyria, pre-existing hepatic disease, hypersensitivity to imidazole drugs in pregnancy and nursing mothers [51, 61]. In mild liver disease it has been found that the pharmacokinetics of KTZ are not adversely affected, although the plasma levels of KTZ may be elevated due to impairment of metabolism [61, 71]. Hepatic damage is known to be a rare adverse effect of KTZ administration and may manifest itself with transient elevated levels of serum transaminase or fatal hepatitis [61, 71].

1.5.7. Drug interactions

Pharmacokinetic drug interaction studies revealed that KTZ may interact with a number of compounds as the molecule inhibits the cytochrome P450 isoenzyme 3A4 that is responsible for the hepatic metabolism of a large number of xenobiotics [53, 61, 72]. Animal studies have shown that KTZ inhibits N-demethylase and O-demethylase activity in hepatic microsomes as it binds to the CYP P450 component of the mono-oxygenase complex with little impact on NADPH-cytochrome *c* P450 reductase activity [53]. This effect on hepatic microsomes has been shown to persist at low concentrations and over a long period of time [53]. The mechanism of interaction involves the formation of a nitrogenous ligand to cytochrome P450 as a direct interaction exists between the azole-nitrogen and the haem functional group of the cytochrome P450 enzyme [53]. It has been intimated that different P450 isoenzymes may have different binding affinities for KTZ and therefore KTZ may be a mixed inhibitor of hepatic N-demethylation [53].

The consumption of alcohol while on KTZ therapy may lead to a disulfiram-like reaction characterized by nausea, vomiting and facial flushing that may result in the induction of hepato-toxicity [61, 73]. The anticoagulant effect of warfarin is known to be increased 3-fold with the concurrent administration of KTZ [61, 72]. The metabolism of compounds such as cyclosporine, tacrolimus and sirolimus are also known to be inhibited by KTZ resulting in elevated plasma concentrations of these compounds [61]. Raised levels of cyclosporine lead to nephrotoxicity and have been reported when cyclosporine and KTZ are co-administered. The mechanism of this

interaction is thought to be via inhibition of cyclosporine elimination by KTZ, increased absorption of cyclosporine or increased free cyclosporine caused by displacement from cell and protein binding by KTZ [72].

Drugs such as rifampicin, phenytoin, nevirapine and phenobarbitone are known to cause microsomal enzyme induction and have been reported to lower the plasma concentration of KTZ and therefore their concurrent use should be avoided [61, 72]. Conversely, the co-administration of protease inhibitors such as indinavir and ritonavir with KTZ may lead to increased levels of KTZ necessitating dose adjustment. The metabolism of corticosteroids is inhibited by KTZ and it is advised that the dose of corticosteroids such as methylprednisolone be halved when they are co-administered with KTZ [61, 72]. Other drugs for which a dose reduction may be necessary include calcium channel blockers such as dihydropyridines and verapamil that are metabolized by the CYP 3A4 system and the concomitant administration of KTZ with these compounds may lead to a marked antihypertensive effect in these patients [61].

Ebastine, mizolastine, pimozide, cisapride and quinidine are contraindicated when using KTZ as the metabolism of these drugs is inhibited and increased plasma concentrations may result in cardiotoxicity characterized by *torsade de pointes* [61]. An increased risk of rhabdomyolysis is possible due to increased plasma concentrations of HMG CoA reductase inhibitors on co-administration of KTZ and these drugs are therefore contraindicated when using KTZ [61]. A similar trend is observed with the concurrent administration of midazolam or triazolam which leads to a potentiation of the sedative effect of these compounds, therefore the oral use of these drugs is usually contraindicated and careful monitoring is necessary if used during KTZ therapy [61].

1.5.8. Adverse effects

The most common dose-dependent adverse effects of KTZ include nausea, dyspepsia, abdominal pain, diarrhoea, anorexia and vomiting [15, 51, 61]. The administration of KTZ with food or at bedtime or in divided doses may help to alleviate these effects [51]. Uncommon side effects such as headache, menstrual disruption, dizziness, photophobia, paraesthesia, hypersensitivity reactions, rash, pruritus, fever and chills may also be observed during KTZ therapy [61].

Since KTZ inhibits steroid biosynthesis in humans, endocrinologic anomalies such as gynaecomastia, erectile dysfunction, oligospermia and alopecia may be experienced during therapy [51, 61]. Hepatotoxicity whilst on KTZ therapy may be characterized by a mild and asymptomatic increase in serum aminoferase level which reverts to the normal range spontaneously or after a few days [51, 61, 74]. However, symptomatic KTZ-induced hepatitis may occur in rare cases and may be potentially fatal [15, 51, 61, 74]. It is advisable to perform liver function tests prior to and during long-term therapy with KTZ [15, 51, 61, 74]. The earliest symptoms of hepatitis include anorexia, malaise, nausea and vomiting with or without dull abdominal pain and liver function tests must be conducted and treatment with KTZ must be discontinued immediately [15, 51, 61, 74].

1.5.9. High risk groups

1.5.9.1. Pregnancy

KTZ has been found to be teratogenic, exhibits embryo-toxicity in animals and has been classified as a Category C compound [7, 61]. Although placental transfer is low a dose of 80 mg/kg/day of KTZ reduced the pregnancy rate in female Wistar rats and when administered on days 6 to 15 of gestation a decrease in body weight and consumption of food was also observed [7, 75]. Post-natal studies performed on the rats indicated that a dose of 40 mg/kg/day induced maternal toxicity and 50% of the litter were stillborn [7]. High doses of KTZ administered in food (160 mg/kg/day) produced small litter sizes with very few live births [7]. The newborn rats were small at birth showing signs of toxicity and were unable to gain weight which resulted in death a few days after birth [7]. In addition 60% of the pups had cleft palates, reduced ossification of skull bones and axial skeletal defects [75].

The effect of oral administration of KTZ on birth outcomes in human subjects has been investigated but failed to establish an increased risk for congenital malformation in infants that were born from mothers who received 200 mg oral KTZ once or twice daily during their second and third months of pregnancy [76]. Consequently, the *in utero* exposure of the human embryo to low doses of KTZ (<400 mg/day) during pregnancy is thought to be safe [75, 76].

1.5.9.2. Lactation

Breast-feeding is contraindicated in patients taking KTZ as the drug is excreted in breast milk and may cause kernicterus in the nursing infant [61]. It is advised that nursing mothers should express and discard the milk during and for 24 to 48 hours after treatment with KTZ [61]. Studies performed on dogs have reported that KTZ has been detected in the breast milk at a level that is 22% of the peak plasma concentration and KTZ use is therefore contraindicated during lactation [66].

1.5.9.3. Paediatric use

The safety of KTZ in children under two years of age has not yet been established. However, since the mid-1980s KTZ has been used to treat paediatric patients including infants [7, 61]. Extemporaneous suspensions are prepared by crushing KTZ tablets for administration to paediatric patients. A dose of between 3 mg/kg/day and 6.5 mg/kg/day has been administered orally for the management of fungal infections in paediatric patients [61, 66] and paediatric doses of KTZ are based on body weight. The recommended dosage regimen is 50 mg once daily for children weighing 20 kg or less, 100 mg once daily for children weighing between 20 kg and 40 kg and 200 mg once daily for children weighing more than 40 kg [7].

1.5.9.4. Geriatric use

It has been reported that normal doses of KTZ may be used in elderly patients [66]. Dosage adjustments of KTZ are therefore not required in the geriatric population unless underlying conditions necessitating such changes exist [66]. Caution should be exercised when treating the elderly, particularly if there is a history of hepatic disease or in case of poly-pharmacy, since elderly patients frequently have multiple chronic medical conditions for which they are prescribed medicines.

1.5.9.5. Renal impairment

The use of KTZ in patients with renal impairment is not contraindicated since KTZ is not eliminated via the kidneys [66]. Urinary excretion of unchanged KTZ was nominal in subjects with renal insufficiency compared to that observed in healthy subjects [7]. Renal elimination is not considered to be clinically relevant in patients with renal disease and in healthy subjects. In

patients with severe renal insufficiency the absorption of KTZ has been reported to be slower with peak plasma levels being lower than that observed in healthy subjects [7]. Nonetheless the extent of absorption did not differ between the two groups and the initial differences noted in absorption were not statistically significant [7]. It has been reported that renal failure does not affect the peak plasma concentrations or the elimination half-life of KTZ as the drug is extensively metabolized by the liver [77].

Consequently, dosage adjustments in patients with renal impairment are not required with KTZ [7, 66]. Studies performed in patients on continuing ambulatory peritoneal dialysis (CAPD) demonstrated minimal penetration into the CAPD fluid, thereby indicating that KTZ is unlikely to be effective in the treatment of fungal peritonitis [66].

1.6. Pharmacokinetics

Pharmacokinetic studies on KTZ suggest that KTZ exhibits linear kinetics over the dose range of 50 mg to 200 mg whilst higher doses of 400 mg to 600 mg exhibited non-linear kinetics [77]. The non-linear pattern noted in the kinetics of KTZ could be attributed to complete absorption, non-linear elimination, saturation of a first-pass effect or a reduction in the volume of distribution [77]. Single-dose administration of KTZ reveals no evidence of non-linear kinetics whereas multiple-dose administration of KTZ suggests some degree of non-linearity in the disposition of KTZ following oral administration [77]. Routine therapeutic drug monitoring of plasma or tissue concentrations achieved during treatment with KTZ may be unnecessary as there seems to be no correlation between peak plasma levels of KTZ and the clinical response in patients with superficial or deep mycoses [7, 72].

1.6.1. Absorption

KTZ, unlike miconazole and econazole, is known to be well absorbed following oral administration. The absorption of KTZ is usually complete within two to four hours after ingestion. Peak plasma concentrations after administration of 200 mg and 400 mg doses have been found to be 3 to 4.5 µg/ml [7] and 5 to 7µg/ml respectively [78]. It is worth noting that higher and more consistent plasma concentrations are observed when KTZ is administered with a meal which may be due to the highly lipophilic character of the molecule (log $P_{o/w}$ = 3.73) [7, 77, 79]. The acidic environment of the stomach plays an important role in facilitating the dissolution

and subsequent absorption of KTZ [42, 44, 78]. Concomitant therapy with drugs that interfere with gastric pH or acid production in the stomach, including antacids such as sodium bicarbonate, aluminium oxide and H_2-receptor antagonists such as cimetidine can therefore markedly reduce the absorption of KTZ following oral delivery [7, 28, 80].

Other drugs that reduce gastric acidity include sucralfate, ranitidine, anticholinergic drugs and proton-pump inhibitors such as omeprazole [7, 51, 81]. Didanosine formulations in which antacids or buffers have been incorporated to prevent acid degradation of didanosine have also been shown to exert a similar effect on gastric pH [61]. Moreover, the concurrent administration of KTZ with Maalox®, an antacid preparation containing magnesium and aluminium hydroxide resulted in variable effects on plasma levels of KTZ [77]. It has been suggested that drugs or formulations that may impair the absorption of KTZ should be taken at least two hours before or after KTZ administration to ensure that an optimal therapeutic effect can be achieved [61, 66].

It has been postulated that the absorption of KTZ may be impaired as a result of a reduction in gastric acid secretion caused by gastrointestinal tract abnormalities in patients infected with HIV [82]. It has been suggested that the co-administration of KTZ with 200 ml of 0.1 M hydrochloric acid (HCl) can improve the absorption of KTZ although the administration of HCl can be problematic due to its effect on dental enamel and potential irritation of the oesophagus [83]. In addition the preparation and administration of HCl may not always be convenient and therefore alternatives to HCl, *viz.*, glutamic acid have been used in conjunction with KTZ administration [83]. Glutamic acid is available as glutamic acid hydrochloride which reacts with the aqueous contents of the stomach to release HCl following oral administration and it has been reported that glutamic acid hydrochloride exhibits fewer adverse effects than HCl [84]. The bioavailability of KTZ after oral administration of a 200 mg single-dose tablet was found to be approximately 75%, which may suggest that KTZ undergoes first-pass metabolism or significant pre-systemic metabolism during the absorption phase [7, 66].

1.6.2. Distribution

The distribution of KTZ is wide (99%) as KTZ is extensively bound to plasma proteins (84%) and erythrocytes (15%), although the volume of distribution is only 0.361 Lkg^{-1} for persons weighing 70 kg [61, 66]. Obesity does not have a significant impact on the distribution pattern of KTZ [66]. The distribution of KTZ, albeit extensive in the body, appears to be poor in respect of

the cerebrospinal fluid (CSF) and detectable levels of KTZ have been observed in the CSF of patients with inflammation of the meninges [5, 61, 66, 85]. Therefore, the concentrations of KTZ that are likely to be achieved in the CSF are insufficient for the effective treatment of fungal meningitis [66, 72, 85]. However, the penetration of KTZ into saliva, urine, sebum and the cerumen has been found to be high and the drug can therefore be used to treat fungal conditions associated with these secretions [77].

1.6.3. Metabolism

KTZ undergoes extensive hepatic metabolism and major metabolites are excreted in the bile [7, 77]. Various metabolic pathways have been identified for the metabolism of KTZ in humans. The main metabolic reaction includes oxidation of the imidazole ring followed by degradation of the oxidized imidazole [66]. Other pathways for the metabolism of KTZ include oxidative *O*-dealkylation, oxidative degradation of the piperazine ring and aromatic hydroxylation. The metabolites of KTZ are not pharmacologically active [7, 66]. KTZ inhibits the metabolism of substrates of P450-dependent oxidation, *viz.*, the P450 III A isoenzyme which appears to be responsible for the oxidation of KTZ [66]. Therefore, compounds that are inducers of P450 IIIA are capable of causing a reduction of plasma concentrations of KTZ and conversely, concomitant administration of KTZ with drugs metabolized by P450 III A may lead to increased levels of these molecules with the consequence of adverse drug reactions [51, 61, 66].

1.6.4. Elimination

The elimination half-life ($t_{1/2}$) of KTZ has been reported to be between six and ten hours [66]. It has been suggested that the $t_{1/2}$ of KTZ increases with dose and that after repeated dosing it may take between eight and ten hours for elimination to occur [51, 72, 79, 86-88]. In patients with neoplastic disease a mean $t_{1/2}$ of 3.7 hours has been reported [67], contrary to a $t_{1/2}$ of 55 minutes observed in severely immuno-compromised patients administered 400 mg KTZ on a daily basis [89]. KTZ has been shown to exhibit slow and dose-dependent elimination at concentrations of less than 0.1 mg/ml. The elimination half-life ($t_{1/2\beta}$) of KTZ following administration of single oral doses of 100 mg, 200 mg and 400 mg was found to be 6.5, 8.1 and 9.6 hours respectively implying that the pharmacokinetics of KTZ may be best fitted to a 2 body-compartment (2-BCM) model [7, 79].

The excretion of KTZ in man occurs mostly in the faeces (57%) and in the urine (13%) [7]. Unchanged KTZ accounts for 20% to 65% of the drug recovered in the faeces and for approximately 2% to 4% of that in the urine [7]. The metabolites of KTZ in the urine include basic, polar acidic and conjugates of polar acidic compounds [7]. In cancer patients it was reported that less than 1% of the KTZ administered could be recovered in the urine six hours post administration [67]. The urinary excretion of KTZ is therefore minor and this is considered to be an insignificant route of elimination of the drug.

1.7. Conclusions

A review of the literature on ketoconazole including the description, physicochemical properties, stereochemistry and structure-activity-relationships, clinical pharmacology and clinical pharmacokinetics has been presented. The chemical name of KTZ is 1-Acetyl-4-[4[[(2*RS*, 4*SR*)-2-(2, 4-dichlorophenyl)-2-(1*H*-imidazol-1-ylmethyl) 1, 3-dioxolan-4-yl]methoxy] phenyl]piperazine. The molecular formula of KTZ is $C_{26}H_{28}Cl_2N_4O_4$ and its molecular weight is 531.4. KTZ is a synthetic imidazole antifungal agent of the dioxolane series and occurs as a white or almost white powder.

KTZ exhibits poor water solubility and is a dibasic compound with two pK_a values of 6.51 and 2.94 that are due to the ionisable imidazole and piperazine groups respectively. The piperazine moiety is ionized at low pH and thus the solubility of KTZ in an acidic environment is enhanced, which is essential for the absorption of the drug. The lipophilic nature of KTZ can be explained by the relatively high octanol/water partition coefficient or log P of 3.73 and the even higher calculated log P values. KTZ is soluble in organic solvents such as ethanol, toluene, ether, acetone, methanol, chloroform and dichloromethane.

The ultraviolet (UV) absorption spectrum of KTZ reveals that KTZ has a wavelength of maximum absorption (λ_{max}) of 205.6 nm. Infrared spectral studies reveal characteristic bond stretching in KTZ specifically for the C=O, C-Cl, C-O, C-C and C-N bonds. The stereochemistry of KTZ is particularly important for optimal antifungal activity and the *cis*-ketoconazole is thought to be the most potent antifungal of the four possible diastereomers of KTZ. It has been found that the pharmacophore of KTZ responsible for antifungal action consists of an imidazole ring joined to an asymmetric carbon atom to which a 2, 4-dichlorobenzene moiety is attached.

Introduction of a dioxolane ring and piperazine moiety in the KTZ structure are thought to improve the oral and antimycotic activity of the drug.

A Differential Scanning Calorimetry (DSC) thermogram for KTZ reveals that the melting range is 146.42°C to 151.72°C and that the melting point of KTZ was found to be 149.27°C. An understanding of the DSC thermogram for KTZ is essential to elucidate the melting behaviour of KTZ prior to and after exposure to heat during formulation and manufacturing to identify if any polymorphic forms of KTZ may arise as a result of these processes. KTZ has been found to undergo increased hydrolysis at low pH and irreversible oxidation in aqueous media when it is in the un-protonated form in solution of pH between 8 and 12, whereas at temperatures < 50 °C there does not appear to be an impact on KTZ stability in solution. The mechanism of action of KTZ involves inhibition of sterol 14α-demethylase, a microsomal cytchrome P450-dependent enzyme system that leads to depletion of ergosterol in fungal cells, thereby affecting cell growth and proliferation. KTZ has also been found to inhibit the biosynthesis of steroids in humans that in turn impacts on the synthesis of testosterone and glucocorticoids.

The broad spectrum of activity of KTZ makes it suitable for the treatment of a variety of fungal conditions including oral and topical infections. Systemic mycoses requiring oral KTZ therapy include paracoccidioidomycosis, blastomycosis, coccidiodomycosis, candidiasis, histoplasmosis, chronic mucocutaneous candidiasis, candidal paronychia, mycoses of the GIT, vaginal candidiasis and dermatophyte infections. KTZ is also useful for prophylaxis when treating immuno-compromised patients suffering from neoplastic disease or malignant cancer. High-dose KTZ may also be used for the treatment of metastatic prostate cancer. KTZ is also used for topical application for the treatment of ringworm, cutaneous candidiasis, pityriasis versicolor and seborrhoeic dermatitis and pityriasis capitis. Resistance to azole antifungals over the years has been found to be the consequence of overexpression of genes and efflux pump activity.

KTZ is contraindicated in hepatic disease, porphyria, pregnancy and nursing mothers. Drug interactions have been noted with the concomitant use of compounds such as cyclosporine, tacrolimus, sirolimus, rifampicin, phenytoin, nevirapine, phenobarbitone, indinavir, ritonavir, corticosteroids such as methylprednisolone, calcium channel blockers, verapamil, ebastine, mizolastine, pimozide, cisapride, quinidine, HMG CoA reductase inhibitors, midazolam and triazolam with KTZ. Therefore, dosage adjustments and careful monitoring are often required during concurrent therapy.

Pharmacokinetic studies of KTZ reveal that it exhibits linear kinetics at doses of between 50 mg and 200 mg, whereas non-linear patterns have been observed at higher doses. The absorption of KTZ has been reported to be impaired by drugs such as antacids, H_2-receptor antagonists, proton pump inhibitors and sucralfate which reduce gastric acidity, thereby indicating that a low pH is essential for the absorption of KTZ. This may be explained by the protonation of the piperazine group of KTZ at pH < 3, which increases the solubility and subsequent absorption of KTZ. It has been found that KTZ is extensively distributed in the body and it binds to plasma proteins and red blood cells. KTZ is metabolized in the liver and a number of different metabolic pathways for KTZ exist. Renal excretion is not a major elimination route of KTZ as it is mostly excreted in the faeces as unchanged drug.

KTZ has physicochemical and pharmacological properties such as a high lipophilicity and oral antifungal activity, making it a suitable candidate for inclusion in an oral lipid formulation. Since there is a dearth of appropriate paediatric formulations, in particular for KTZ, it was deemed important to develop oral paediatric formulations of KTZ to optimize antifungal drug therapy in such patients. A liquid dosage form of KTZ with well-defined stability limits would be an advantage in antifungal therapy as it would circumvent the need for extemporaneous compounding by care-givers thus minimizing the risks associated with the lack of quality control of such preparations. Solid lipid microparticles (SLM) are novel solid lipid carriers that have been found to possess advantages over traditional colloidal carriers and therefore, it may be considered appropriate to develop SLM carriers for the delivery of KTZ to paediatric patients.

CHAPTER TWO

SOLID LIPID MICROPARTICLES AS A DRUG DELIVERY SYSTEM FOR KETOCONAZOLE

2.1. Introduction

The development of advanced drug delivery systems is a challenging interdisciplinary field integrating areas of research such as pharmaceutics, biochemistry and physical chemistry, amongst others [90, 91]. Colloidal drug delivery systems (CDDS) have been investigated intensively over the past thirty years and delivery technologies *viz.*, liposomes, polymeric nanoparticles and solid lipid nanoparticles have since been commercialized for therapeutic use [90-102]. With increasing numbers of lipophilic compounds emerging through drug discovery studies, it has become crucial that pharmaceutical scientists develop novel drug delivery systems that improve the aqueous solubility, increase dissolution rates and subsequently enhance oral bioavailability of hydrophobic drugs [103-105]. Furthermore, during the development of novel drug delivery systems important delivery considerations such as the toxicity of the system and protection of the active pharmaceutical ingredient (API) against chemical degradation must not be overlooked [93, 101, 106-108]. In addition an essential requirement of modern drug therapy is that controlled delivery of an API to the site of action in therapeutic concentrations is desired [109-112].

A number of CDDS have been reported over the years and include liposomes [92-94, 113-120], nanoemulsions (NE) [121, 122], nanosuspensions (NS) [123-125], nanocapsules (NC) [126-131], polymeric particles [98, 111-113, 124, 128-130, 132-143] and solid lipid particles for which the dimensions are in the micrometeter and nanometer ranges [100-102, 106, 110, 144-157]. Although liposomes, NS and NE technologies have been successfully introduced commercially, there are major obstacles associated with the use of such CDDS that include costly excipients and equipment. In addition sustained drug release from formulations is not always possible through the use of CDDS [90, 94, 158]. The use of polymeric nano- and microparticles has been associated with numerous challenges including the lack of large scale production methods that yield products of appropriate quality and that are acceptable to regulatory authorities [159-162]. In contrast, the use of CDDS consisting of lipids that are physiologically well tolerated and have a Generally Regarded as Safe (GRAS) status, have been deemed advantageous and lipid

formulations appear to be an attractive delivery system since they have the potential to modify drug release profiles and prolong drug release due to slower degradation of the lipid and protection of API from chemical degradation [101, 102, 163-166]. In addition lipid formulations have been used as an approach to solubilize hydrophobic drug candidates with the aim of enhancing oral bioavailability of poorly soluble compounds [103, 104, 123, 125]. The incorporation of a model lipophilic drug such as KTZ into a CDDS that possesses the ability to control the release of the API may not only assist in reducing the incidence of systemic adverse effects associated with long-term antifungal therapy but may also lower the frequency of dosing which would be beneficial in the treatment of immunocompromised and paediatric patients who are often unable to swallow large solid dosage forms and require intravenous therapy or extemporaneous preparations made by care-givers. Solid lipid particles in the nanometer or micrometer range have been shown to possess advantages of other CDDS in addition to being physiologically compatible, sustaining drug release and having the ability to be manufactured using large-scale production methods [99, 101, 102, 106, 163, 164, 166]. KTZ is known to be highly lipophilic and thus may be a good candidate for inclusion into a solid lipid carrier. Furthermore, the encapsulation of KTZ into a solid lipid carrier prior to incorporation into a liquid dosage form intended for paediatric use may offer a promising alternative drug delivery system for this population as KTZ is susceptible to chemical degradation.

2.2. Description of colloidal drug delivery systems

Liposomes have been extensively studied during the development of CDDS as the formulations are known to achieve a high drug loading, have low inherent toxicity and immunogenicity and are biodegradable [90, 93, 116, 118, 167]. However, liposomes tend to exhibit limited physicochemical stability on storage and undergo degradation in the gastrointestinal tract (GIT) following oral administration [94, 102, 162, 168]. Liposomal formulations have therefore not been considered promising systems for oral drug delivery and have rather been used for cosmetic applications [90, 125]. Cosmetic liposomal formulations have been successfully introduced into the clinical and pharmaceutical markets, despite limited data and information relating to these systems being available [90]. Furthermore, the excipients used in the manufacture of liposomes tend to be expensive and the possibilities for large-scale production of liposomal formulations are often limited [90, 125, 167, 169, 170].

Nanoemulsions (NE) were initially used as CDDS for the purposes of parenteral nutrition and were later applied to the intravenous administration of hydrophobic molecules [101, 122, 157, 171-173]. As the extent of haemolysis and pain experienced at the site of injection are reduced with NE formulations such preparations have proved to be beneficial when administered intravenously [173]. One of the challenges of using NE as CDDS is the possibility of partitioning an API from the dispersed oil droplets into the continuous aqueous phase, which may impact on the stability of the API if it is susceptible to degradation in an aqueous environment [173, 174]. In addition the potential for controlled drug delivery is restricted in NE formulations as the API may easily diffuse from dispersed oil droplets [121, 175, 176].

Another CDDS used for the formulation of poorly soluble drugs are nanosuspensions (NS), which were developed to enhance the oral bioavailability of hydrophobic compounds. The formulation of NS does not require the use of a matrix material and no excipients besides a vehicle comprised of oils or liquid polymers are required. Consequently, NS are relatively simple systems that can be produced on a large-scale using high pressure homogenization [123, 125]. A major disadvantage of liposomes, NE and NS is their inability to protect an API against chemical degradation due to the absence of a matrix material to encapsulate the API [125, 127, 140, 177].

Nanocapsules (NC) and polymeric nanoparticles (PN) were developed in an attempt to incorporate an API into a matrix in order to prevent the compound from being exposed to a hostile environment that may precipitate hydrolytic or light-induced degradation [127, 140, 177]. The presence of a polymeric membrane in NC and PN not only physically impedes the movement of an API within the matrix but also offers possibilities of retarding or modifying drug release from the matrix system [127, 140, 141, 177]. Although the polymeric membrane offers the advantage of a solid matrix and allows flexibility in the control of drug release and protection of the API against chemical degradation, PN have not been extensively commercialized due to the challenges associated with polymer chemistry, toxicity and the lack of possibilities of industrial scale production of PN [132, 178-180]. In addition the production of PN tends to be covered by broad patents which do not guarantee exclusivity and it may not always be profitable for research groups working in collaboration with pharmaceutical industries to develop PN products [90].

Müller and his research group developed solid lipid nanoparticles (SLN™) [164] that were designed to avoid the shortcomings of existing technologies [164, 173, 181-187]. SLN are promising particulate carrier systems that are biodegradable, physico-chemically stable, have low

toxicity and can be manufactured on a large scale using high pressure homogenization [101, 108, 110, 173, 182]. SLN are manufactured using biocompatible lipids which may be used to incorporate lipophilic, hydrophilic and poorly water-soluble drugs [101, 102, 108, 110, 173, 182]. Another advantage of SLN is that they exist in the solid state and therefore, can protect an incorporated API against chemical degradation and further offer possibilities of modifying drug release profiles [101, 108, 110, 165, 173, 182]. In addition the degradation velocity of SLN *in vivo* is slower than that observed for traditional colloidal systems [166]. SLN are known to be in the sub-micron size range of between 50 and 1000 nm, whilst solid lipid microparticles (SLM) range in size between 10 and 1000 μm [91, 99]. The qualitative composition of SLM is known to be equivalent to that of SLN and therefore, SLM may also be considered physiologically compatible, biodegradable, non-toxic and may be produced on a large scale [99, 188]. The respective size ranges of SLN and SLM essentially account for the differences in the applications and routes of administration applicable for both types of delivery system [99, 188]. The use of SLM in drug delivery has not been comprehensively explored, although SLM may have some applications for the *in vivo* targeting and selective administration of some therapeutic compounds [91, 99]. A broad list of drugs, miscellaneous and macrocyclic entities that have already been incorporated into SLM by various research groups, has recently been published [102, 139, 143, 189-204]. However, no attempts have been made to incorporate ketoconazole (KTZ) into SLM for the purposes of oral drug delivery. Therefore, this project involved an investigation into the feasibility of incorporating KTZ into solid lipid microparticles (SLM) in an attempt to improve oral drug delivery of the compound for paediatric patients. Consequently, aqueous dispersions of KTZ-loaded SLM were developed, optimized and characterized during these studies.

2.3. Solid lipid microparticles

2.3.1. Overview

Innovative solid lipid carriers have a wide range of applications including topical [205, 206], intravenous [207, 208] and solid lipid formulations for parenteral [207, 208], oral [209, 210], dermal [206], ocular [211, 212], pulmonary [163, 204, 213, 214] and rectal [215] routes of delivery. One of the major advantages of SLM over polymeric nanoparticles and o/w fat emulsions is the high degree of tolerability and the good oral bioavailability associated with these drug delivery systems when compared to polyester PN [101, 209]. Cosmetic and pharmaceutical

agents may be formulated into SLM in order to protect these compounds from the surrounding and potentially hostile environment [173, 174, 212, 216].

In essence, SLM consist of an oil-in-water emulsion, similar to the emulsions used for parenteral nutrition except for the substitution of a liquid lipid or oil with a lipid that is solid at both room and body temperatures and that forms solid lipid microparticles [166]. Solid lipid carriers such as SLN and SLM consist of a lipid matrix manufactured by using physiologically well-tolerated lipids or a mixture of lipids *viz.,* fatty acid esters of glycerol and polyglycerol, fatty acids, fatty alcohols, hydrogenated fatty acid esters and polar wax, amongst others [143, 189-204, 217]. The use of solid lipids or solid lipid mixtures with relatively different molecular structures has been reported to increase the drug loading capacity (DLC) and encapsulation efficiency (EE) of these technologies [108, 173]. SLM may be manufactured using a variety of manufacturing techniques as described in § 2.4, *vide infra*. However, small particles made from glycerides with short-chain fatty acids may not easily be produced as these often do not recrystallize during the manufacturing process [100, 218].

Various liquid media such as highly ethylcellulose solutions and non-aqueous or aqueous media of PEG-600 have been used as the outer or dispersed phase for SLM dispersions [166, 219]. Aqueous dispersions of SLM may be stabilized using a single or combination of surfactants by means of electrostatic interaction using ionic surfactants such as sodium dodecyl sulphate (SDS) or by steric hindrance using non-ionic surfactants such as Tween 80 and/or Poloxamer 188 (Pluronic® F68) [220, 221]. The aqueous drug-loaded SLM dispersions may be used as a granulating fluid and incorporated in the manufacture of traditional dosage forms such as tablets or pellets that are designed to release SLM in a completely non-aggregated form following disintegration [166]. In addition SLM can be dried by spray-drying or lyophilization to enhance their long-term stability. The dry powder may be reconstituted with water to produce a suspension that would be useful as a paediatric dosage form [102, 166, 173].

The use of SLM has been associated with shortcomings such as particle growth particularly on ageing and storage, unpredictable tendencies to gel, cream or coalescence. Furthermore, limited DLC and drug expulsion may occur on prolonged storage and can be attributed to dynamic changes within the lipid structure during polymorphic transitions following production [102, 151, 222]. The burst release associated with SLM has also been reported as a result of phase separation during cooling in production of SLM with drug-enriched shells (Figure 2.1. III) [102, 108].

Consequently, there is an urgent need for research to be undertaken to develop SLM carriers that circumvent these challenges and enhance the potential for oral drug delivery using such carriers.

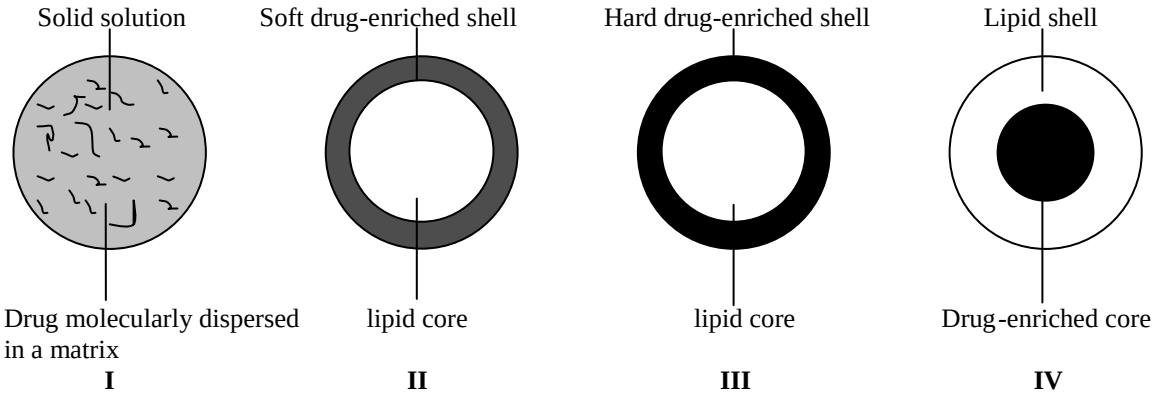

Figure 2.1 Proposed models of drug incorporation into SLN: (I) Homogenous matrix with molecular dispersion of the drug. (II) Lipid core surrounded by soft drug-enriched shell. (III) Drug-free lipid core surrounded by a hard shell consisting of lipid-drug mixture at eutectic concentrations. (IV) Lipid shell being drug-free or having low drug content surrounding the drug-enriched core [166, 173]

2.3.2. Drug distribution in SLM matrices

Drug distribution within SLM matrices may influence drug release performance of the SLM formulation [188]. Incorporation of a drug into the SLM matrix may be complex and can be affected by several factors, including the solubility of the drug in the lipid and the physicochemical characteristics of the drug or the lipid carrier and stabilizer used in the production of the SLM. Furthermore, the techniques used to manufacture the SLM may impact on the model of drug incorporation into the SLM and production parameters may need to be altered to achieve appropriate loading for the desired model [166, 223]. A diagrammatic representation of four different models of drug incorporation into SLM postulated by Müller *et al.,* is depicted in Figure 2.1 [166, 173, 188].

These models include a homogenous matrix model, the soft and hard drug-enriched shell models and the drug-enriched core model. The proposed models of drug incorporation are applicable to ideal situations and in practice may occur concurrently [188]. The structure of the SLM matrix is chiefly influenced by the chemical nature of an API, the excipients used and associated interactions also depend on production process parameters [166, 173, 188]. However, it may not be feasible to observe the physical distribution of a drug in an SLM matrix since lipid excipients

are soft and have a low melting point [188]. Therefore, other means of visualization using computer simulation may have to be used to explore the microstructure of SLM systems [188].

2.3.2.1. Homogenous matrix model

The homogenous matrix model (Figure 2.1 I) refers to a situation in which the drug is molecularly distributed or forms amorphous clusters within a solid lipid matrix [101, 166]. This model may be produced when highly lipophilic drugs are incorporated into a solid lipid matrix using hot high-pressure homogenization (HPH) or when cold HPH is used to produce drug-loaded SLM [101]. No phase separation of the lipid and the API occurs during the production process and the homogenous matrix is formed following cooling and recrystallization of the oil droplets obtained from the homogenization of the drug-loaded micro-emulsion using HPH [101]. Drug release from these systems is determined by the rate of diffusion of the drug within the solid lipid matrix and this model has been reported to be ideal for sustaining and controlling drug release [166].

2.3.2.2. Soft and hard drug-enriched shell models

In contrast, drug-enriched shell models (Figure 2.1 II and III, respectively) are produced when phase separation occurs during the production process and may be described as a solid lipid core surrounded by an outer shell enriched with drug [101, 166]. Models II and III are also produced using hot HPH and re-partitioning occurs during the cooling process [101]. However, the soft shell model (Figure 2.1 II) consists of a drug-enriched outer shell due to lipid precipitating initially, thereby forming a drug-free lipid core during cooling of the crude drug-containing micro-emulsion [166]. The rest of the drug-lipid mixture is continuously enriched with drug content until eutectic concentrations are reached and simultaneous crystallization of the lipid and the drug occurs leading to the formation of a soft shell surrounding the lipid core [166]. Conversely, the hard drug-enriched shell model (Figure 2.1 III) may be obtained when the API and the lipid have structural characteristics enabling them to fit together to form a layered solid brick-like structure [166]. The API fits into the imperfections of the lipid lattice thus forming a hard outer shell [166]. Burst release is observed from soft and hard drug-enriched shell models as the drug has a relatively short diffusion distance for release [166].

2.3.2.3. Drug-enriched core

The drug-enriched core model (Figure 2.1 IV) is formed when a drug precipitates as it reaches its saturation solubility and a drug-enriched core and a poorly enriched shell is formed on cooling [166]. The liquid mixture is enriched within the lipid until eutectic concentrations are reached and on further cooling a mixture of drug and lipid precipitate simultaneously [166]. This model describes a situation in which the drug precipitates prior to crystallization of the lipid and oil droplets surrounding the drug-enriched core subsequently recrystallize to form a solid lipid shell that serves as a membrane through which the drug must diffuse, from the inner core [166]. The drug-enriched core model has been used to describe the incorporation of an API into SLM which demonstrates an initial burst release followed by controlled release of the API from the SLM [166]. This model therefore describes a situation where membrane-controlled release occurs in accordance with Fick's first law of diffusion [166, 188].

2.4. Manufacture of solid lipid microparticles

Solid lipid carriers such as SLM consist of a lipid matrix manufactured using physiologically well-tolerated lipids such as mono-, di- and/or triglycerides composed of fatty acid esters, fatty alcohols or fatty acids, waxes, cholesterol and phospholipids, amongst others [102, 139, 143, 189-204]. The SLM matrices are produced and stabilized using surfactants such as poloxamers, polysorbates, lecithin amongst others and water which comprises the aqueous vehicle of the dispersion [102, 139, 190, 192, 199-201, 204]. Perusal of the literature reveals extensive lists of lipids and emulsifiers that may be used for the manufacture of SLM [102, 139, 143, 189-204]. The typical excipients used for the manufacture of SLM usually have a GRAS status and suggesting that SLM formulations are of suitable quality, are acceptable to international regulatory authorities and do not show signs of acute and/or chronic toxicity during *in vivo* use that have been observed when polymeric particles, particularly those made of polyester derivatives, are used [102, 164].

SLM may be manufactured from solid lipids or a mixture of solid lipids using different manufacturing techniques (§ 2.5 *vide infra*). Solid lipids or solid lipid mixtures with different molecular structures may be used to increase the drug loading capacity and encapsulation efficiency of SLM [108, 173]. One of the crucial steps in the manufacturing process of SLM includes the dissolution or dispersion of a drug into a lipid to achieve controlled release profiles

for the SLM formulations [102, 207, 224]. Therefore, physical mixing of a drug and a lipid phase is not sufficient if drug release is to be prolonged and the melting of the lipid to incorporate the API is an essential requirement for the successful manufacture of sustained released SLM [102, 207, 224]. Another important step in the manufacture of SLM is the dispersion of a molten lipid phase into an aqueous medium which may be undertaken using either mechanical or thermodynamic methods to promote the formation of SLM [102, 207, 224]. The emulsifying agent or stabilizer may be added either to the lipid or aqueous phase to produce a thermodynamically stable system depending on the predominant properties of the surfactant used and include hydrophilicity or lipophilicity, which may be deduced from its hydrophilic lipophilic balance (HLB) value of the compound [166].

2.5. Production of solid lipid microparticles (SLM)

2.5.1. Overview

A number of methods have been used for the production of SLM *viz.*, high pressure homogenization [164, 225], micro-emulsion formation [183, 225, 226], solvent evaporation [151, 160, 193, 225, 227, 228], micro-channel emulsification [229, 230], cryogenic micronization [196], spray congealing [139, 143, 195, 198, 199, 203, 217, 231] and spray drying [203, 231]. High pressure homogenization (HPH) is preferred as it is efficient, reliable and does not involve the use of toxic organic solvents. In addition HPH does not require the use of large volumes of water for dilution of micro-emulsions compared to the other methods of production of SLM [102]. Nevertheless, HPH requires the use of costly equipment often not routinely available in small-scale laboratories [102]. An alternative method of production of SLM that does not require complex equipment and toxic organic solvents was therefore selected for the laboratory-scale production of SLM. A micro-emulsion technique was selected for use due to its simplicity and involves the use of high shear devices such as an Ultra Turrax® homogenizer that is routinely available in research laboratories.

2.5.2. High-pressure homogenization (HPH)

High-pressure homogenization (HPH) has been used for a number of applications for many years for the production of emulsions and suspensions [102, 125]. HPH has also been used in the food industry for the homogenization of food products such as milk and in the pharmaceutical industry to produce parenteral emulsions [125]. The major advantage associated with the use of HPH is

the ease of scale-up of batch sizes, which makes it valuable in the large-scale production of solid lipid nano- or microparticles depending on the formulation composition and process parameters required [125]. The method of producing SLM by HPH is similar to that used for the production of parenteral oil-in-water (o/w) emulsions [101, 125]. The underlying principle of HPH is based on the fact that the pre- or crude micro-emulsion is passed through a small gap, the piston-gap, which is approximately 10 µm, at a high velocity and pressure. Particle size is reduced due to shear force, cavitation and impaction [125]. Instead of using a piston-gap homogenizer, a jet-stream homogenizer may also be used for particle size reduction. In such homogenizers the impact of two colliding high-velocity streams of the micro-emulsion results in particle diminution [125]. The jet stream homogenizer is preferred for the production of nano-crystals [125]. HPH can be conducted at high temperatures *viz.*, hot HPH or at lower temperatures *viz.*, cold HPH [101, 125]. In both cases an API is dissolved or solubilized in a lipid at a temperature approximately 5-10°C above its melting point [101]. A schematic representation of the manufacture of SLN or SLM using cold and hot HPH is shown in Figure 2.2.

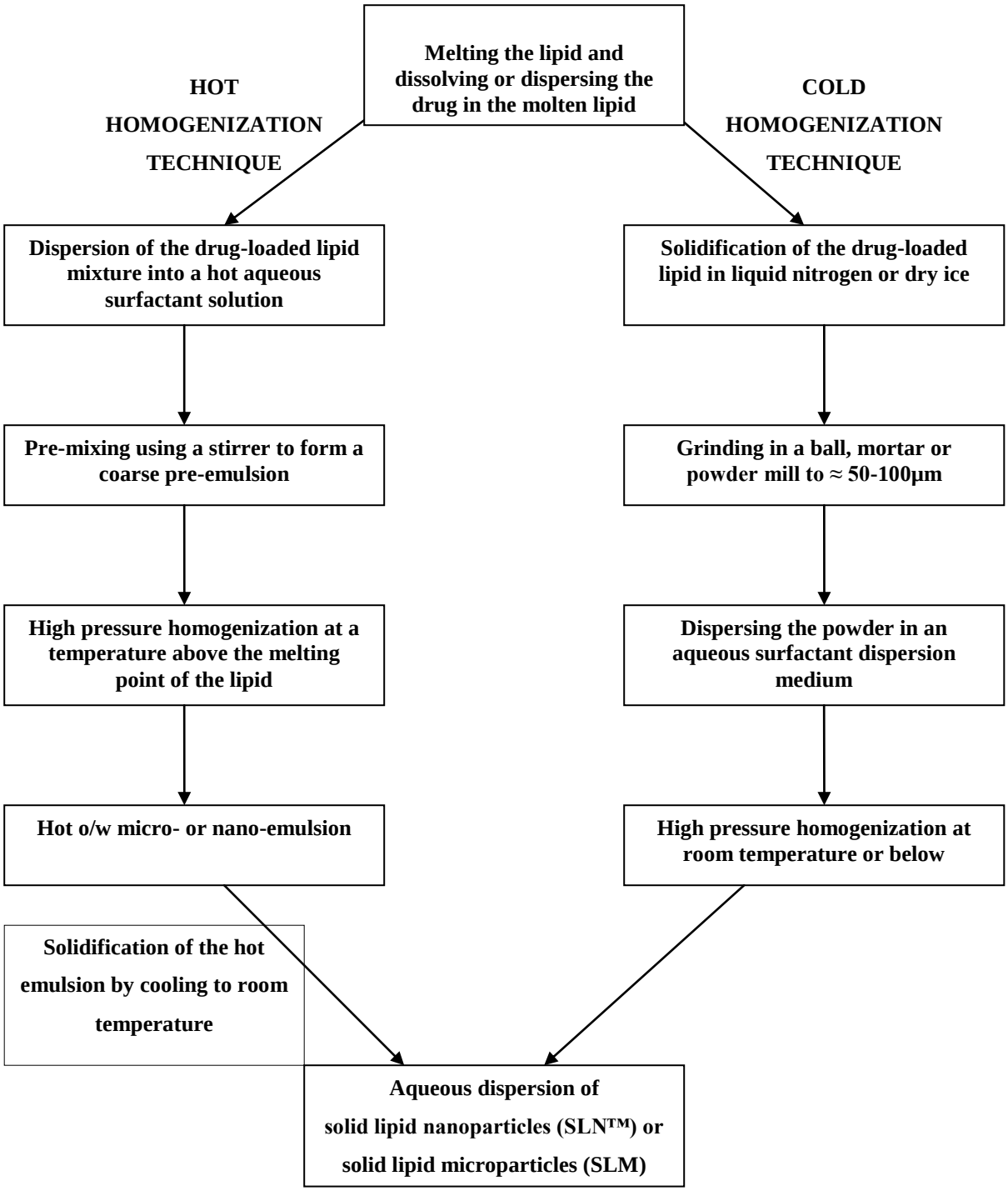

Figure 2.2 Schematic representation of hot and cold homogenization for the manufacture of SLN and SLM adapted from [102]

2.5.2.1. Hot high-pressure homogenization

In the hot HPH technique, a drug-lipid molten phase is dispersed in a hot aqueous surfactant solution heated to the same temperature as the lipid phase whilst stirring to form a micro- or pre-emulsion [102]. The pre-emulsion is homogenized using a high-pressure homogenizer such as a piston-gap homogenizer or a jet stream homogenizer to produce a nano- or micro-emulsion [101, 102, 125]. The emulsion is subsequently cooled to room temperature (25ºC) to allow crystallization of the dispersed lipid droplets in the nano- or micro-emulsion to form nano- or microparticles, respectively [101, 102].

Hot HPH is associated with major shortcomings such as temperature-induced degradation of API, partitioning of drug into the aqueous phase during homogenization and the complexity of the crystallization process of the micro-emulsion, which may result in lipid modification and/or the formation of super-cooled melts [102]. Therefore, hot HPH is ideal for the production of SLM containing lipophilic and thermostable drugs. In addition coalescence of particles may occur during homogenization due to the high kinetic energy of the particles if the homogenization pressure is too high or the number of homogenization cycles is excessive [125, 187]. It has been reported that the use of 3-5 homogenization cycles at a homogenization pressure between 500-1500 bar tends to produce SLN or SLM products of high quality [100, 225].

2.5.2.2. Cold high-pressure homogenization

Cold HPH involves rapid cooling of a drug-lipid molten phase with dry ice or liquid nitrogen in order to increase the brittleness of the lipid to permit uniform distribution of the API throughout the lipid. The drug-containing solid lipid is then ground to form lipid particles of sizes ranging between 50 and 100 µm [102]. The lipid particles are dispersed in a cold surfactant solution using a high speed stirrer to form a pre-suspension which may then be homogenized at or below room temperature [102]. The cold HPH technique is preferred for thermolabile drugs as the exposure to high temperature during the dispersion of the drug in the lipid is relatively short [102]. Furthermore, cold HPH may be used for hydrophilic drugs since this technique minimizes the partitioning of hydrophilic molecules from the lipid phase into the aqueous phase of the dispersion, during the high pressure homogenization process [102, 232]. However, a major drawback of cold HPH is that the method increases the fragility of the lipid at low temperatures

that may lead to particle aggregation and result in the formation of relatively large particles with a wide particle size distribution [101].

2.5.3. Micro-emulsion formation

The micro-emulsion technique, developed and patented by Gasco [183, 184], involves the formation of a micro-emulsion at a temperature above the melting point of the lipid used. The micro-emulsion may be produced by heating a mixture of water, surfactant and co-surfactant to the same temperature as the molten lipid phase [102]. The lipid phase containing the drug is then mixed under mild stirring conditions with the aqueous surfactant solution [102]. The micro-emulsion formed is then dispersed in a cold (2-3°C) aqueous medium under mild mechanical stirring to promote precipitation of nano- or microparticles [102]. The volume ratio of hot micro-emulsion to cold water is usually in the range of 1:25 to 1:50 [102]. Micro-emulsions already contain droplets of submicron size which are formed spontaneously without application of energy [102, 183] and it has been reported that the particle size is influenced by the velocity of the distribution processes [233]. The process of producing the micro-emulsion may be modified to produce different products variants, including oil-in-water and water-in-oil melt dispersions and water-in-oil-in-water multiple emulsions [200, 201].

2.5.3.1. Oil-in-water melt dispersion

An oil-in-water (o/w) melt dispersion technique, also known as hot melt microencapsulation is generally used when lipophilic drugs are to be included in the product and it is similar to the micro-emulsion technique [160, 190, 191, 193, 194, 200, 204, 228]. The drug to be included is dissolved in molten lipid at a temperature of 5-10 ºC above the melting point of the lipid and the drug-lipid mixture is subjected to emulsification in an aqueous surfactant solution at the same temperature using a high-shear device such as an Ultra-Turrax® or Silverson® mixer [160, 191, 193, 200, 204, 228]. The o/w emulsion, that is produced, may then be dispersed into a large volume of an ice-cooled aqueous phase to produce SLM in an aqueous dispersion [160, 191, 193, 200, 204, 228]. The hardened microparticles are harvested following filtration, rinsing with water and drying using a vacuum desiccator [200].

2.5.3.2. Water-in-oil melt dispersion

The water-in-oil (w/o) melt dispersion technique is a variation of the o/w melt dispersion approach and is used for the incorporation of hydrophilic API into SLM [199]. The w/o dispersion method avoids the use of water to prevent the drug from partitioning into the external aqueous phase that results in low drug loading in the microparticles [199]. The API and the surfactant are dispersed into the molten lipid, followed by addition of a hot non-aqueous continuous phase such as silicone oil to produce a w/o dispersion [199]. The w/o dispersion is subsequently subjected to rapid cooling by immersion in an ice bath and cold oil is incorporated into the mixture as it cools, to form solid lipid microparticles [199]. Centrifugation may be used to separate the microparticles from the oil followed by washing and drying to obtain the SLM [199].

2.5.3.3. Water-in-oil-in-water multiple emulsion

The water-in-oil-in-water (w/o/w) multiple emulsion technique is preferred for water-soluble drugs [201]. The lipid is melted and the API is dissolved in an aqueous surfactant solution which is heated to the same temperature as the lipid phase [201]. The aqueous solution is then emulsified with the molten lipid to produce a primary w/o emulsion which is then mixed in an external aqueous phase to generate the w/o/w emulsion [201]. The dispersion obtained is cooled in an ice bath [201] or at room temperature [228] prior to filtering, rinsing and drying the particles that are produced in a vacuum desiccator.

2.5.4. Solvent evaporation

The solvent evaporation technique, also known as solvent emulsification, was developed by Sjöström and Bergenståhl and involves the formation of solid lipid nano- or microparticles by precipitation from o/w emulsions [227]. A water-immiscible organic liquid such as chloroform is used to dissolve the lipid and the drug is incorporated as a solid which has been finely ground using liquid nitrogen or as an aqueous solution [160, 193]. The drug-containing organic phase is then subjected to emulsification with an aqueous phase containing an emulsifying agent [102]. The solvent is subsequently evaporated and the emulsion produced is transferred into an ice-cooled aqueous phase and stirred to induce precipitation of lipid microparticles from the aqueous phase [102]. Evaporation can be performed under low pressure, for example between 4-6 kPa [234]. The major advantage of this technique is that it precludes the drug and the lipid carrier

from being exposed to high temperatures as experienced in high-pressure homogenization and melt dispersion approaches to manufacture. However, the use of organic solvents limits the use of the method particularly in development of parenteral and paediatric formulations and it was therefore not selected for the manufacture of SLM in these studies.

2.5.5. Micro-channel emulsification

Micro-channel emulsification is a novel technique used to manufacture mono-disperse o/w and w/o emulsions without the need for high mechanical shear and requires lower energy inputs compared to traditional emulsification processes [229, 230]. This is achieved by use of a silicon micro-channel plate through which the dispersed and continuous phases are forced to generate mono-disperse emulsion droplets [229, 230]. The sizes of these droplets are controlled by the structure of the micro-channel plate and the SLM aqueous dispersion is obtained on cooling the emulsion to room temperature [229, 230].

2.5.6. Cryogenic micronization

The cryogenic micronization technique requires the use of drug-containing lipid matrices formed by melt dispersion or solvent stripping for the production of SLM. The drug may be dispersed into the molten lipid using a magnetic stirrer or the drug and the lipid may be dispersed into an organic solvent mixture to produce the lipid matrices. These lipid matrices are stored at temperatures as low as -80ºC and are micronized in an apparatus through which liquid nitrogen is purged to produce finely divided powders. These may be sieved using an automatic sieving apparatus [196]. The SLM particles obtained may vary from 5-5000 µm in diameter, depending on the sieve selected to segregate the powders [196].

2.5.7. Spray congealing

The spray congealing method of producing SLM is often referred to as spray chilling. The API is initially dissolved in a lipid carrier that has previously been heated to a temperature above its melting point and the drug-lipid melt is subsequently atomized, with a pneumatic nozzle, into a vessel that is placed into a dry ice bath, prior to drying using vacuum at room temperature for several hours [139, 143, 198, 199, 203, 217, 231]. The drug-lipid mixture may also be atomized by use of ultrasound to generate small droplets that fall freely and solidify upon cooling at room temperature [195, 198, 199]. An alternative means of producing the SLM particles may involve

the use of a high-speed rotating disc onto which the drug-lipid melt is poured [143]. The rotation of the disc in a cooling chamber causes the drug-lipid mixture to spread evenly and spray from the peripheral edges of the disc onto a chiller, which forms a surface from which the microparticles may be collected [143].

2.5.8. Spray drying

This technique is often used for the production of SLM containing lipophilic drugs as it is a relatively simple process [203, 231]. The lipid and hydrophobic API are dispersed concurrently into an organic solvent to form a drug-containing lipid mixture [203, 231]. The mixture produced is then spray-dried, resulting in the formation of microparticles [203, 231]. The major drawback of this technique is the use of organic solvents which is not desirable in the formulation of SLM intended for oral drug delivery, particularly for paediatric patients.

2.6. Characterization of SLM

2.6.1. Overview

The characterization of aqueous dispersions of SLM is an important step in the formulation development and assessment process as it gives the formulation scientist an opportunity to make predictions regarding the physical stability, release kinetics and quality of the resultant product [101, 102]. Nonetheless, it is worth noting that owing to the small colloidal particle size range of SLM systems and the multiple dynamic phenomena involved with the use of lipids *viz.*, the kinetics in hysteresis and the super cooling phenomena, characterization of SLM dispersions can be complicated [102]. Sample preparation may for instance, result in changes in the physical properties of SLM such as the kinetics, crystallization patterns or lipid modification of the particles which in turn, may produce erroneous results [102]. Subsequently, such physical changes may lead to spontaneous gelation or other macroscopically visible changes in the SLM formulation [102]. It is therefore imperative that samples be handled with care, particularly during sample preparation during analysis of SLM formulations. Acquaintance with techniques used in sample manipulation is essential for optimal results to be derived from characterization studies. Typical performance characteristics of SLM systems that must be evaluated include particle size and zeta potential. However, it should be borne in mind that other parameters such as the degree of crystallinity and lipid modification, in addition to the possibility of coexistence of multiple colloidal systems, must also be assessed.

2.6.2. Image analysis

2.6.2.1. Overview

Image analysis provides direct information about the size, shape and surface morphology of SLM, which may not be accessible when techniques that measure the particle diameter such as for example laser diffraction (LD) and/or photon correlation spectroscopy (PCS) that rely on light scattering effects are used [102]. In addition, image analysis allows the type of particle surface to be evaluated from direct observation with microscopic methods. Image analysis may be performed using light and electron microscopy. Light microscopy permits the visualization of particles with sizes in the micrometer range and high-resolution microscopy such as electron microscopy using a scanning electron microscope (SEM) and/or a transmission electron microscope (TEM), are required to view particles in the micrometer or nanometer range [102].

The main disadvantage of image analysis is the need for pre-treatment of samples prior to visualization. This may result in particle aggregation or solvent removal and thus may adversely affect the size and/or shape of the SLM [102, 235]. Image analysis methods are complementary, and each approach has advantages and disadvantages [102]. Different information may therefore be extracted from each of the methods and different characteristics of the microparticles may subsequently be elucidated [102].

2.6.2.2. Scanning electron microscopy (SEM)

Scanning electron microscopy (SEM) allows for visualization of microparticles under dehydrated conditions since the preparation of samples prior to analysis involves drying using either an oven or a vacuum pump. Imaging is performed at high voltages under high vacuum [235]. The sample is deposited on a graphite strip and allowed to air- or oven-dry for a few minutes, after which it is metalized with gold and viewed under an accelerating voltage of approximately 10-20 kV [235]. SEM produces three-dimensional images of microparticles which facilitates the viewing of surface morphology. However, shrinking of the microparticles may occur as a result of drying of the sample under high vacuum or removal of the solvent which may change the molecular structure of the microparticles [235].

2.6.2.3. Transmission electron microscopy (TEM)

Transmission electron microscopy (TEM) can be used to investigate the size, shape and surface morphology of a variety of colloidal particles [236]. TEM generally has a higher resolution than SEM and provides a better indication of the particle size distribution of colloidal dispersions. Samples may be prepared prior to TEM analysis using techniques such as staining, freeze-fracturing or cryo-electron microscopy. Staining is generally sufficient to obtain accurate information relating to particle size, shape and surface morphology of aqueous SLM dispersions. The sample is usually plated on a copper grid coated with a carbon film and is left to dry for 30 seconds prior to staining with a dye such as phosphotungstic acid or uranyl acetate. The stained sample is dried at room temperature for approximately 30 seconds prior to visualization using TEM [236].

2.6.2.4. Atomic force microscopy

Atomic force microscopy (AFM) is another imaging technique used to visualize the shape and surface morphology of colloidal particles. AFM monitors the force acting between a surface and a probe tip to obtain spatial resolution of 0.01 nm, which is then used for imaging [102]. AFM is an imaging technique that does not require sample pre-treatment and the need for sample conductivity [102, 235]. The hydrated sample is usually plated onto a microscope slide or a mica plate and since this approach permits rapid visualization of SLM, *in situ* changes which occur at the interface of the particles may also be observed [102]. A fine AFM probe is used to assess the outer layer of the particle. The hardness of the particle surface can be determined by contact AFM by comparing it to that for a standard silicon surface [166, 221]. Therefore, the model of drug incorporation into the SLM matrices may be predicted using AFM analysis [102]. Immobilization of particles by contact AFM can be easily accomplished for particles in the micrometer range due to their higher rate of sedimentation [101]. However, smaller particles that are inherently in constant and rapid motion may not be accurately viewed using contact AFM without removal of the solvent in which they are dispersed. In addition it has been established that solvent removal may distort the shape of SLM as well as their molecular structures [102, 235]. AFM was not used in these studies.

2.6.3. Particle size analysis

Photon correlation spectroscopy (PCS) and laser diffraction (LD) are routine approaches for the assessment of particle size in colloidal dispersions. PCS may also be used in conjunction with LD to determine the polydispersity indices of colloidal dispersions [102]. Both LD and PCS do not directly measure particle size but measure the light scattering effects of colloidal dispersions, which may then be used to calculate particle size [102]. Inaccurate data may be obtained in cases where non-spherical or platelet-like particles are present in a colloidal dispersion [237]. The use of LD and PCS may not provide an exact representation of the size of SLM for samples with large particle size distribution (PSD) or polydispersity indices (PI) and in such cases, the use of electron microscopy may be more appropriate. PCS, also known as dynamic light scattering, measures the intensity fluctuations of scattered light upon particle movement and allows the measurement of particles in the size range of a few nanometers to approximately 3 µm. PCS is more likely to detect nanoparticles than microparticles. LD is generally used to characterize particles in the micrometer range and covers a broad range from nanometer to the lower millimeter size range [102]. Since LD technology was not available in our laboratory, particle size analysis was performed using imaging analysis coupled with Soft Scanning Imaging Software (SSIS) as PCS was deemed inappropriate for measuring SLM particles, which were larger than 3 µm in diameter.

2.6.4. Zeta potential analysis

The zeta potential (ZP) of a colloidal dispersion represents the electric potential at the hydrodynamic plane of shear and is a key property of a dispersion that is used to predict the physical stability of dispersions, particularly during and following storage for extended periods of time [102, 148, 238, 239]. The ZP of SLM depends not only on particle charge but also on the dispersant used [235, 238]. It has been established that small changes in pH or ionic strength of a medium may have an impact on the ZP of SLM and may result in the interaction of particles according to their zeta potential and not according to their surface charge [235, 238]. A large negative or positive zeta potential results in mutual repulsion of particles, thereby enhancing the physical stability of a colloidal dispersion by preventing aggregation of the particles [238]. The ZP of SLM dispersions may be determined using Laser Doppler Anemometry (LDA) coupled with a zetasizer and subsequently applying the Helmholtz-Smoluchowsky equation (Equation 2.1) to the resultant data [235, 239].

$$\upsilon = \frac{\varepsilon \xi}{\eta}$$

Equation 2.1

where,

υ = electrophoretic mobility
ε = dielectric constant
ξ = zeta potential
η = viscosity of the dispersion medium

The measurement of the ZP of particles in distilled water or water with low conductivity provides a comprehensive assessment of the dispersion or aggregation behaviour of colloidal particles. The ZP of a colloidal dispersion, stabilized by electrostatic stabilizers alone, indicates stability of the dispersion if the ZP is ≤ -30 mV or ≥ +30 mV [238]. A zeta potential of magnitude < -30 mV or < +30 mV is indicative of a stable colloidal dispersion when steric stabilizers are used in combination with electrostatic stabilizers, since steric stabilizers decrease the ZP due to a shift in the shear plane of a particle [235, 238]. The measurement of ZP was therefore used to predict the stability of the SLM dispersions throughout the formulation development process and following storage of the dispersions.

2.6.5. Crystallographic analysis

2.6.5.1. Differential scanning calorimetry

Differential scanning calorimetry (DSC) is used to establish the melting point(s) and melting enthalpies of different modifications of solids including lipids and may therefore be used to predict the stability associated with different modifications of a lipid [102, 148, 240, 241]. The principles of DSC are described in detail in Chapter 4, § 4.1.1, *vide infra*. DSC was used in preformulation studies to assess the polymorphism of KTZ and solid lipids prior to the production of KTZ-loaded SLM. The melting enthalpies observed following DSC analyses of aqueous SLM dispersions may be used to calculate the recrystallization index (RI) of SLM formulations. The RI value may be used as a measure of the percentage lipid that has recrystallized during storage of aqueous SLM dispersions and may be calculated using Equation 2.2 [240].

$$\text{RI (\%)} = \frac{\Delta H_{\text{aqueous SLM}}}{\Delta H_{\text{bulk lipid}} \times \text{Lipid concentration}} \times 100$$

Equation 2.2

where RI = recrystallization index

ΔH = molar melting enthalpy

2.6.5.2. X-ray diffraction

X-ray diffraction (XRD) assesses the dimensions and length of the long and short spacing within a lipid lattice [102]. Synchrotron radiation can be used to avoid the long measurement times and associated sensitivity issues of conventional X-ray determinations. Wide-angle X-ray diffraction (WAXD) may be used to establish the lamellar arrangement of lipid molecules, elucidate the polymorphic behaviour and degree of crystallinity of fatty acid chains in triacylglyceride compounds [241, 242]. WAXD measures the length of long and short spacings between alkyl side chains in a triglyceride lipid layer such that discrimination between crystalline and amorphous substances may be made based on the number of reflection bands in the WAXD spectrum [243]. WAXD may be used to fully elucidate the polymorphism and crystallinity of lipids, SLM or an API in a SLM dispersion. It is a powerful tool when used in conjunction with DSC for the characterization of SLM [244, 245]. Accessibility of WAXD equipment remains a challenge for the routine characterization of lipids [102] and the method was therefore not used in the analysis of SLM dispersions. Crystallographic analyses were performed during preformulation studies using DSC only.

2.6.6. Drug loading and encapsulation efficiency

The drug loading capacity of a carrier system for a specific API determines the suitability of the carrier system. It is a crucial parameter that needs to be evaluated during formulation development and optimization studies [101, 207, 246]. CDDS such as SLM are expected to protect an API from chemical and light-induced degradation and therefore, the API should remain encapsulated within the lipid matrix [207]. Furthermore, it is desirable that such delivery systems have a high encapsulation efficiency (EE) and long-term retention of the entrapped drug [207]. Consequently, DLC and EE are essential characteristics of SLM which need to be assessed during formulation development as these may impact on the drug release characteristics of SLM formulations. Drug loading capacity (DLC) is generally expressed as the amount of drug added to

a colloidal dispersion relative to the total amount of lipid phase used [101, 247] and includes the lipid and API. DLC is calculated using Equation 2.3.

$$\text{DLC}\ (\%) = \left(\frac{\text{Amount of drug entrapped}}{\text{Total amount of lipidic phase}}\right) \times 100 \qquad \textit{Equation 2.3}$$

Several factors affect the drug loading capacity of SLM including the solubility of the API in the molten lipid, miscibility of the drug melt and molten lipid, the chemical and physical structure of the solid lipid matrix and the polymorphic state of the lipid material (s) [101]. In order to achieve a high drug loading capacity, a drug needs to be sufficiently soluble in the lipid melt and demonstrate a higher solubility than required in the melt as solubility decreases on cooling and may therefore be lower in the solid lipid form [101]. Solubilizers may be used to increase the solubility of a drug in the lipid phase. The use of lipids with a mixture of mono-, di- and triglycerides increases the solubilization of a drug [101]. In addition the use of lipid mixtures may promote the formation of imperfections in a crystal lattice, thereby creating more space to accommodate the drug within the lipid matrix [101]. The polymorphic form of a lipid may also dictate whether drug will be retained in the lipid matrix or expelled following crystallization and during storage [101].

The encapsulation efficiency of a drug depends on the total amount of drug added to the lipid. The higher the drug content, the higher the theoretical EE [248]. EE is usually expressed as the amount of drug entrapped in the particles relative to the total amount of drug added and can be calculated using Equation 2.4 [246, 247]. The extent of drug incorporation into the SLM may be quantified using analytical techniques such as UV spectrophotometry or high performance liquid chromatography (HPLC). The DLC and EE of KTZ-loaded SLM were investigated using a RP-HPLC method that was developed, optimized and validated as described in Chapter 3, *vide infra*.

$$\text{EE}(\%) = \left(\frac{\text{Amount of drug entrapped}}{\text{Total amount of drug}}\right) \times 100 \qquad \textit{Equation 2.4}$$

2.7. Conclusions

The development of advanced colloidal drug delivery systems (CDDS) stemmed from attempts to address challenges in drug delivery such as enhancing the bioavailability of hydrophobic drugs, protecting API from chemical degradation and achieving controlled drug delivery to the site of

action. Colloidal systems such as liposomes, nano-emulsions, nanosuspensions, nano-capsules, polymeric particles and solid lipid carriers have been developed and these CDDS demonstrate advantages and limitations which restrict their application in human and veterinary drug delivery. In an attempt to minimize the shortcomings of the existing systems, novel drug delivery systems such as solid lipid nano- (SLN) and microparticles (SLM) have been developed using physiologically compatible lipids such as glycerides of fatty acids. The major difference between SLN and SLM is directly related to their respective size ranges. SLN are known to range between 50 and 1000 µm in size whereas SLM range between 10 and 1000 µm in diameter. SLN or SLM dispersions are suspended in an aqueous medium and are formulated using lipid(s) that are solid at room temperature and a surfactant or combination of surfactants to stabilize the resultant particles.

The use of solid lipid carriers has numerous advantages over other CDDS technologies such as polymeric nanoparticles and liposomes, including their biocompatibility, good oral bioavailability, possibility of drug targeting to various parts of the body and large-scale production. In addition it is possible to control or modify drug release profiles as the degradation velocity of solid lipid carriers *in vivo* is slower than that of other colloidal systems. Furthermore, the solid lipid matrix provides excellent protection against chemical or light-induced degradation and SLN and SLM carriers have been shown to exhibit the potential for drug delivery via the oral, topical, parenteral, dermal, ocular, pulmonary and rectal routes of administration. Drug incorporation into SLM matrices depends on a number of factors including solubility of the drug in the lipid melt, physicochemical properties of the drug, lipids and surface active agents in addition to production parameters used in the manufacture of SLM formulations. Three models of API incorporation have been proposed for SLM matrices although in practice, these may occur simultaneously. The models of drug incorporation include a homogenous matrix, soft and hard drug-enriched and the drug-enriched core models.

The production of SLM may be achieved using different approaches including high pressure homogenization, micro-emulsion techniques, solvent evaporation, micro-channel emulsification, cryogenic micronization, spray congealing and spray drying. The quality of SLM formulations must be evaluated during formulation development and optimization and parameters such as particle size (PS), shape, surface morphology, zeta potential (ZP) and lipid polymorphism must be determined. SLM formulations may be characterized using photon correlation spectroscopy (PCS) which can be used in conjunction with laser diffraction (LD) to measure the particle size of

SLM. The physical stability of an aqueous SLM dispersion may be assessed using Laser Doppler Anemometry (LDA) to determine the zeta potential of the SLM which enables predictions to be made regarding the long-term stability of the SLM dispersion. It is important to note that PCS and LD provide information only on the particle size of the SLM which is indirectly measured from light scattering effects. Information relating to shape and surface morphology are not obtained from PCS and LD analysis. Imaging analysis is required to elucidate the shape and surface morphology of SLM and is usually achieved using high-resolution microscopy such as SEM and TEM.

Crystallographic analysis of SLM dispersions may be performed using complementary techniques such as differential scanning calorimetry (DSC) and wide-angle X-ray diffraction (WAXD) which reveal polymorphic modifications and the presence of crystalline structures. The stability associated with lipid modifications may be deduced from DSC analyses which may therefore be used to predict the behaviour of a lipid after being exposed to heat and the extent of recrystallization during storage.

It is essential that the loading capacity of the SLM carriers be assessed to determine the suitability and usefulness of a specific drug carrier system. Analytical techniques such as UV spectrophotometry and high performance liquid chromatography (HPLC) may be used to determine the drug loading capacity (DLC) and the encapsulation efficiency (EE) of SLM for an API.

The feasibility of incorporating the hydrophobic drug, KTZ into SLM as potential drug carriers was investigated and is reported in Chapter 5, *vide infra*, where aqueous dispersions of KTZ-loaded SLM were developed using a micro-emulsion technique. The KTZ-loaded SLM formulations were characterized in terms of PS, particle shape and morphology and ZP using some of the techniques reviewed in this chapter. In addition the DLC and EE of the SLM preparations were established using RP-HPLC during formulation development and stability studies.

CHAPTER THREE

DEVELOPMENT AND VALIDATION OF A HIGH PERFORMANCE LIQUID CHROMATOGRAPHIC METHOD FOR THE ANALYSIS OF KETOCONAZOLE

3.1. Introduction

3.1.1. Overview

The quantitative analysis of ketoconazole (KTZ) in biological fluids [249-259] and pharmaceutical dosage forms has been accomplished using a variety of analytical techniques [260-269]. Analytical approaches such as microbiological assay [259, 269], capillary zone electrophoresis [270, 271], spectrophotometry [256, 263, 264, 267], TLC-densitometry [262] and high-performance liquid chromatography (HPLC) [249-258, 260-266, 268, 271] have been used for the quantitation of KTZ in a variety of matrices. Perusal of the literature reveals the inherent complexity of most of these methods and the high cost associated with the equipment required and that is often not available in many laboratories [262, 270, 271]. Techniques such as microbiological assay are neither adequately sensitive nor selective for the routine analysis of KTZ in biological fluids or pharmaceutical dosage forms [259, 269]. Previously reported HPLC methods demonstrated higher sensitivity and selectivity than microbiological assays for the analysis of KTZ but tend to involve complicated extraction procedures or require mobile phase compositions that are tedious to prepare due to the inclusion of hydrophobic ion-pair reagents or amine-containing mobile phase modifiers [253, 254, 260, 272, 273].

The objective of this study was to develop a rapid, cost-effective, simple, sensitive, selective, precise and accurate analytical method that could be used for the quantitation of KTZ for the routine *in vitro* analysis of KTZ containing pharmaceutical dosage forms. Reversed-phase high-performance liquid chromatography (RP-HPLC) coupled with UV detection was selected as the preferred method of analysis for KTZ, based on the frequency of use reported in the literature, simplicity relative to other analytical techniques and the availability of equipment in our laboratory.

3.2. Principles of high performance liquid chromatography

High performance liquid chromatography (HPLC) is an analytical technique used to separate and isolate compounds based on their physico-chemical properties. It is suitable for the analysis of macromolecular and/or thermolabile analytes that may not be readily analysed using gas chromatography (GC) [274-281]. HPLC analysis of low molecular weight compounds can be achieved using various approaches such as normal-phase or adsorption, ion-exchange and bonded-phase chromatography all of which require the compound of interest to have specific properties *viz.*, polarity, electric charge amongst others [282-285].

Adsorption chromatography is also known as liquid-solid or normal-phase chromatography and was the most widely used chromatographic technique until the development of derivatized silica for use as a stationary phase was initiated [286]. Normal-phase chromatography requires the use of polar stationary and non-polar mobile phases and is suitable for the chromatographic separation of polar compounds [281, 282, 286]. In contrast, ion-exchange chromatography involves the reversible exchange of ions between the mobile and stationary phases. Ion-exchange separations are based on the different strengths of solute-ion or resin-ion pair interactions. The solute-ion competes with the mobile phase ion for ionic sites in the ion exchange backbone [282, 284, 286]. Bonded-phase chromatography was developed in the late 1960s to improve the efficiency and reproducibility of performance of stationary phases used in liquid chromatography. Functional groups are chemically bonded onto spherical silica particles through carefully monitored reaction conditions to produce highly efficient and reproducible stationary phases. The level of cross-linking and the amount of silane bonded to the surface are determined by the reaction conditions used to produce the column. The degree of silanization determines the surface chemistry of the stationary phase and therefore, the performance of separations on that stationary phase [286].

Bonded-phase chromatography (BPC) can be of two types, *viz.*, normal- and reversed-phase chromatography. In normal-phase chromatography the stationary phase is generally more polar than the mobile phase and the retention of solutes decreases with increasing solvent polarity [282-284, 286]. In reversed-phase chromatography the stationary phase is non-polar whilst the eluent or mobile phase is polar and the strength of the mobile phase may be adjusted by the addition of polar organic solvents [286-288]. The mobile phases used in reversed-phase HPLC are optically transparent, are compatible with electrochemical detectors and biological samples and have weak

interactions with the stationary phase, thereby enhancing mass transfer during a separation and reducing equilibration times when solvent changes are made [283, 286, 287].

Reversed-phase HPLC was selected for the analysis of KTZ as it has a number of advantages with respect to versatility, convenience and reproducibility of the analytical technique [275]. The use of hydrocarbon bonded phases such as octyl or octadecyl silica as the stationary phase in RP-HPLC enhances the stability and lifetime of columns when compared to micro-particulate bonded phases as hydrocarbon phases are usually stable in aqueous solutions of pH < 8 [275]. RP-HPLC may be used for the chromatographic separation of a variety of compounds possessing different chemical properties using a broad range of solvents of varying strength that may be used in combination with complexation in the mobile phase [275]. The convenience associated with using RP-HPLC stems from the extended operational life of columns leading to the use of a single column for the analysis of a compound of interest over an extended period of time [275].

Many theories to explain retention mechanisms of a solute in RP-HPLC have been postulated. The hydrophobic and/or solvophobic theory refers to the partitioning of a solute from a hydrophilic mobile phase onto a hydrophobic stationary phase which is not expected to retain the solute by ionic attraction, hydrogen bonding, formation of charge transfer complexes or any strong non-covalent interactions due to the non-polar nature of this phase [275, 289-291]. Another theory that explains the retention of large non-polar moieties in RP-HPLC may be attributed to silanophilic interactions with surface silanols [275, 289]. Interactions between the solute and residual silanol groups on the surface of a stationary phase involve hydrogen bonding and/or ionic interactions [275, 289-291].

RP-HPLC has been widely used in pharmaceutical and drug analysis where the separation of compounds of interest or constituents from biological fluids, fatty acids, hydrocarbons with varying degrees of isotopic substitution and naturally occurring samples are performed routinely [283, 292-294]. BPC has been used for high precision analysis and trace analyses in environmental sample studies [283, 294]. In addition BPC has been widely used for the separation of excipients in pharmaceutical formulations, measurement of cations and anions after the formation of derivatives with appropriate reagents and characterization of some oligomeric mixtures [283, 292].

3.3. HPLC method development

3.3.1. Overview

It is worth noting that many considerations drive the development of an analytical method *viz*., the physical and chemical nature of an analyte of interest, knowledge of the type of matrix from which the analyte is to be separated and the structure, stability and reactivity of the analyte [287, 295-297]. The solubility and sensitivity of the analyte of interest to changes in pH, temperature, dissolved oxygen and light must be considered in addition to functional parameters such the accuracy and precision of the method, the complexity and time required for sample preparation, manipulation and analysis [287, 295]. Furthermore, the concentration range of the analyte and its chemical properties may influence detection and are important parameters that need to be established prior to commencing analytical method development [287, 295].

Several HPLC methods have been reported for the analysis of KTZ [249-258, 260-266, 268, 271]. A summary of the methods published for the analysis of KTZ is listed in Table 3.1. Most of the methods involve the use of RP-HPLC coupled with UV detection for the analysis of KTZ in biological matrices [249, 253, 254, 272, 273, 298-300] or pharmaceutical dosage forms [260, 262, 265, 268].

Table 3.1 RP-HPLC methods used for the analysis of KTZ in dosage forms

Column	Mobile phase composition	Sample matrix	Flow rate (ml/min)	Detection wavelength	Retention time	Internal standard	Ref.
Bakerbond® C_{18} (5µm, 4.6 × 250 mm I.D.)	Diisopropylamine in MeOH (1:500) and ammonium acetate solution (1:200), 70:30	Oral liquid mixture	3.0	225 nm	3.1	-	[265]
Interchrom Nucleosil® C_8 (5µm, 4.6 × 250 mm I.D.)	ACN and 0.025 M phosphate buffer, 45:55, pH 4.	Shampoo	1.0	250 nm	-	Formaldehyde	[268]
RP-Hypersil® BDS-C_{18} (5µm, 4.6 × 150 mm I.D.)	MeOH-water-diethylamine, 74:26:1	Canine plasma	1.0	240 nm	8.0	9-acetyl anthracene	[253]
RP-µ-Bondapak™ C_{18} cartridge column (10µm, 4.6 × 250 mm I.D.)	ACN and 0.025 M trishydroxymethyl aminomethane in phosphate buffer, 55:45, pH 7	Formulations: Nizoral™ cream and tablets	2.0	260 nm	5.7	Clotrimazole	[262]
Inertsil® ODS-80A (5µm, 4.6 × 150 mm I.D.)	ACN-water-tetrahydrofuran-ammonium hydroxide-triethylamine, 50.2:45:2.5:0.1:0.1, pH 6.0	Human plasma	1.0	206 nm	5.9	Clotrimazole	[254]
Hypersil® ODS RP-column (5µm, 4.6 × 150 mm I.D.)	ACN-0.1 Sorensen buffer, 60:40, pH 6.6	Human plasma	-	206 nm	5.75	-	[298]
Beckman® C_{18} (5µm, 4.6 × 250 mm I.D.)	ACN:50 mM phosphoric acid, 60:40, pH 2.2	Blood	2	207 nm	-	-	[300]
RP-µ-Bondapak™ C_{18} (5µm, 4.5 × 300 mm I.D.)	MeOH:25 mM KH_2PO_4 and 4 mM heptanesulfonic acid buffer, 60:40, pH 8.0	Blood	1.8	226 nm	-	Terconazole	[273]
Nova-Pak® C_{18} (5µm, 3.9 × 150 mm I.D.)	MeOH:ACN:20 mM KH_2PO_4, 30:30:35, pH 6.8	Blood	2	254 nm	4.3	Clotrimazole	[249]
Hypersil® ODS C_{18} (5µm, 3 × 100 mm I.D.)	ACN:water, 45:55, with 500 µL/L diethylamine, pH 8.0	Blood	0.6	254 nm	5.0	Terconazole	[272]
Spherisorb® CN (5µm, 4.6 × 250 mm I.D.)	THF: phosphoric acid, 50 mM triethylamine, 30:70, pH 3.0)	Formulations: tablets and cream	1	230 nm	7	Clotrimazole	[260]
Whatman® RP-C18 (5µm, 4.5 × 125 mm I.D.)	ACN:10 mM KH_2PO_4, 65:35, pH 6.0	Human stratum corneum	0.7	254 nm	8.6	-	[299]

3.3.2. Experimental

3.3.2.1. Reagents

All chemicals were at least of analytical reagent grade. HPLC-grade acetonitrile (UV cutoff at 200 nm) was purchased from Romil-SpS® Ltd. (Waterbeach, Cambridge, UK). Potassium dihydrogen phosphate and sodium hydroxide pellets were purchased from Associated Chemical Enterprises (Southdale, Gauteng, RSA). HPLC-grade water was prepared by reverse osmosis using a Milli-RO® 15 water purification system (Millipore Co., Bedford, MA, USA) consisting of a Super-C® carbon cartridge, two Ion-X® ion-exchange cartridges and an Organex-Q® cartridge and the resistivity of the water was maintained at 18 MΩcm. The water was filtered through a 0.22 μm Millipak® 40 stack filter (Millipore Co., Bedford, MA, USA) prior to use. Ketoconazole (KTZ) and clotrimazole (CLZ) were purchased from Sigma-Aldrich (Johannesburg, Gauteng, RSA). Ketazol® tablets (Aspen Pharmacare, Port Elizabeth, Eastern Cape, RSA) were purchased from Wallaces Pharmacy (Grahamstown, Eastern Cape, RSA).

3.3.2.2. HPLC system

The modular HPLC system consisted of an Isochrom LC dual piston solvent delivery module (Spectra-Physics, San Jose, CA, USA), a WISP™ Model 712 Autosampler (Millipore® Waters Associates, Milford, MA, USA) and a linear UV-100 detector (Spectrachrom, NV, USA) set at a λ = 206 nm. Data acquisition was performed using an SP-4600 Integrator (Spectra-Physics, San Jose, CA, USA).

3.3.2.3. Selection of an analytical column

The analytical column is a significant component of any HPLC system [275, 282-284]. In RP-HPLC the column packing is usually comprised of spherical or irregularly shaped silica particles which form the surface of the support to which organic ligands containing functional groups *viz.*, *n*-octadecyl or *n*-octyl are covalently bonded [275, 282-284]. The column surfaces are known to possess favourable kinetic properties for mobile phase equilibration and eluent adsorption and exhibit relatively good stability in respect of hydrolytic decomposition. The particle shape, size and pore size distribution, nature of ligands, morphology of the bonded surface layer and the magnitude of surface coverage are responsible for the differences in retention behaviour exhibited by different commercial columns [275]. Most columns used in HPLC are generally 150 mm in

length, with an inner diameter of approximately 4-5 mm and a narrow particle size distribution with a mean diameter of < 10 µm [275, 282, 283]. Analytical columns are expected to display lasting efficiency, stability, rapid responses to changing conditions, reproducibility, reliability and durability during analysis [275].

Ketoconazole is a dibasic imidazole compound with two pK_a values of 2.91 and 6.54, respectively [29, 30, 301]. The lipophilic characteristics of the molecule are due to the presence of a benzene ring and hydrophobic alkyl chains, whilst the presence of nitrogen atoms in the piperazine and imidazole moieties account for a small degree of polarity of the molecule. These properties make KTZ a suitable candidate for separation using a reversed-phase packing material, as KTZ is expected to be retained on a hydrophobic stationary phase. A search of available literature revealed that liquid chromatographic studies of KTZ have been undertaken using a C_{18} packed column for *in vitro* and *in vivo* analyses. A Beckman® Coulter ODS 5µm, 150 × 4.6 mm i.d. column was selected for these studies following efficiency testing to evaluate its performance.

The most common measure of efficiency of a chromatographic system is the theoretical plate number, *N*, that is also known as the number of theoretical plates contained in a chromatographic column [284], a definition that has now become universally accepted. The plate number, *N* for a test substance under specified favourable conditions can be quantitatively expressed using Equation 3.1 [284].

$$N = 5.54\left(\frac{t_R}{W_{1/2}}\right)^2 \qquad \textbf{\textit{Equation 3. 1}}$$

where,

t_R = the retention time of a test peak

$W_{1/2}$ = the peak width at half peak height

The assumption for the measurement of peak width in Equation 3.1 is that the peak is Gaussian in nature. This assumption is not often observed in practice, in particular for basic compounds which tend to show evidence of tailing as a consequence of the interaction with acidic silanol groups of the stationary phase [284, 289]. Nevertheless, the calculation of the theoretical plate number permits an analyst to select an appropriate analytical column based on the efficiency and

performance of that stationary phase. For the purposes of these studies only columns displaying plate counts of > 5000 were considered acceptable for use.

In general, the smaller the diameter of particles of the support material or the adsorbent, the greater the separation efficiency and the higher the value for *N* is expected due to an increase in the associated surface area of the stationary phase, which in turn enhances the potential for interaction between the eluent and the compound(s) of interest [276, 279]. The smaller the particle diameter of a packing material the higher the inlet pressure and subsequently, high pressures and flow rates used for a separation may result in removal of the stationary phase from the support. Chemically bonded stationary phases have been developed to avoid the stripping of the stationary phase from the column, particularly when highly polar solvents are used to elute strongly retained sample components [276].

Column packing and preparation is a critical step for the optimization and efficiency of a separation and for prolonging the column life during use. When packing the stationary phase it is vital that the support is packed optimally with solid adsorbents to avoid the development of stagnant pools and to allow the pores of the support to be completely filled with the stationary phase [276, 302]. Equilibration of a column with mobile phase at a flow rate of 1 ml/min for approximately one hour is also important to allow the adsorbent material to equilibrate to the mobile phase and to remove entrapped air from the packing material. It has been reported that a properly packed HPLC column should provide an efficiency of at least 6000 theoretical plates with 5-10 μm particles [276]. Packing materials of 5 μm diameter have been reported to double column efficiency when compared to 10 μm packing materials although system back pressures at higher flow rates are significantly greater for these systems [279].

The efficiency of a chromatographic column is best evaluated using an ideal test system under specified conditions, rather than using the analyte of interest for which the method is to be developed using the conditions for HPLC method development. The use of small, neutral test compounds such as toluene or naphthalene, a flow rate of 1 ml/min and a mobile phase with a viscosity (η) of less than 1 cP, with a composition of 0 to 100% acetonitrile-water mixtures kept at temperatures < 20˚C are ideal test conditions [284].

The efficiency of the 5μm, 150 × 4.6 mm i.d. Beckman® Coulter ODS column was assessed by performing replicate injections (n=6) of a test mixture containing uracil, acetophenone, benzene,

toluene and naphthalene at room temperature (22˚C). A wavelength of 254 nm and a mobile phase composition of acetonitrile-water (70:30) at a flow rate of 1 ml/min were used for the separation. A typical chromatogram of the separation of the test mixture using these conditions is depicted in Figure 3.1.

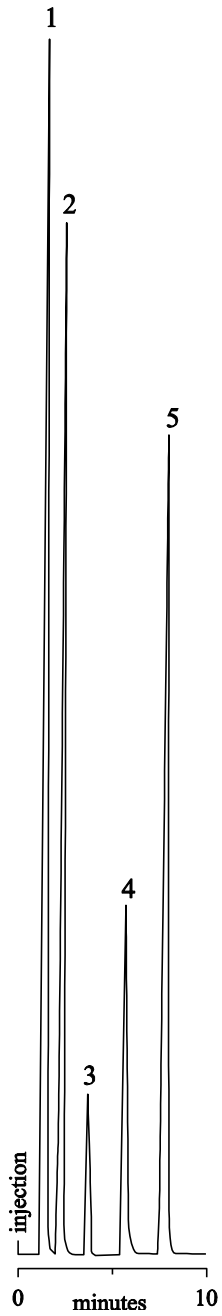

Figure 3.1 Typical chromatogram of a test mixture containing uracil (1), acetophenone (2), benzene (3), toluene (4) and naphthalene (5) after separation on a Beckman® Coulter ODS column

The theoretical plate number for the Beckman® column was found to be 7544 ± 532 (n=6). Such a column with a particle size diameter of 4 µm and a length of 150 mm is expected to give a theoretical plate number of more than 10 000. However, since the column had been used, it was regarded as suitable for use in development and validation of a method for the analysis of KTZ using low flow rates.

3.3.2.4. UV detection of KTZ

The selection of a detector is an important consideration for quantitative analysis by HPLC, as the detector is used to monitor the concentration of a solute in a mobile phase when it leaves the stationary phase and column [303]. It is desirable that detectors used in liquid chromatography show a response that increases linearly with solute concentration and displays a broad range of linearity with high sensitivity and predictable specificity [303, 304]. Ideal HPLC detectors should be able to respond to all solutes universally without contributing to extra-column band broadening, be non-destructive of the solute molecules, have a reasonably fast response independent of the mobile phase and be unaffected by changes in temperature and mobile-phase flow rates [303-306]. The HPLC detector should be able to operate under moderate pressures, be versatile, reliable, convenient to use and easy to maintain. In practice, no currently available detector possesses all these characteristics and the selection of an HPLC detector is based on the characteristics of the solute, sensitivity and specificity required in addition to the convenience and versatility necessary to facilitate analysis [304, 306].

Since the late 1960s, UV detection has been the most commonly used method of detection in HPLC analysis [304, 307]. The measurement of the ultraviolet (UV) absorbance of a solute in the mobile phase is achieved using either a variable-wavelength spectrophotometric or diode-array detector [304]. UV detectors offer a number of advantages over other detection systems as they are simple to use, relatively cheap to purchase, trouble-free to operate, easy to maintain, are sensitive and non-destructive to solute molecules [308, 309]. UV detection is generally selected as the detection method of choice, particularly if samples to be analyzed absorb light in the UV or visible region of the electromagnetic spectrum between 190-600 nm unless analyte concentrations are too low for detection, sample interference is significant or qualitative structural information for the analyte is needed [304]. KTZ is an imidazole antifungal compound whose chemical structure consists of light-absorbing chromophores including an aromatic ring, an imidazole and a

piperazine moiety, double bonds (π electrons) including C=O, thereby making it a suitable candidate for UV detection following separation using HPLC.

The principle of UV detection is based on the Beer-Lambert law which states that the analyte concentration, *C,* is proportional to the fraction of light transmitted through the detector flow cell, $\left(\frac{I_0}{I}\right)$ and is related to absorbance, *A*, molar absorptivity or molar extinction coefficient of the analyte, ε and the path length, *L*, of the flow cell as shown in Equation 3.2 [304, 307, 310].

$$A = \log\left(\frac{I_0}{I}\right) = \varepsilon CL \qquad \textbf{\textit{Equation 3.2}}$$

where,

A = absorbance

I_0 = intensity of the incident light

I = intensity of the transmitted light

ε = molar absorptivity or molar extinction coefficient of absorbing species

C = analyte concentration

L = path length of flow cell

Successful chromatographic monitoring using UV detection can only be achieved if the wavelength of detection is carefully selected since it can potentially impact the sensitivity, selectivity and baseline noise of a detector [310]. A good understanding of the UV spectrum of the sample to be analyzed is therefore required prior to selecting a wavelength of detection for use during method development studies.

A review of the literature indicated that different wavelengths have been used for RP-HPLC analysis of KTZ and include 206 nm [254, 298], 207 nm [300], 225 nm [265], 226 nm [273], 230 nm [260], 240 nm [253], 250 nm [268], 254 nm [249, 272, 299] and 260 nm [262]. The differences in the wavelengths used for HPLC analysis may be due to the fact that the λ_{max} is also in part a function of the solvent which is used to dissolve KTZ. The wavelength of maximum absorption (λ_{max}) was found to be 206 nm following assessment of the UV absorption spectrum of KTZ in methanol (§ 1.2.5) and was therefore selected as the wavelength of choice for maximal sensitivity during the analysis of KTZ. The use of higher wavelengths has been previously

reported for the analysis of KTZ and this choice may have been based on the need to exclude the likelihood of interference from other compounds at wavelengths close to 200 nm. In these studies, high selectivity for KTZ was obtained at 206 nm without any significant interference from the solvent or excipients observed. Although the RP-HPLC method involved the use of the internal standard, clotrimazole, the eluent was monitored at 206 nm and not at the λ_{max} of clotrimazole as it is possible to include adequate amounts of the internal standard during analysis with appropriate attenuation to ensure that a satisfactory response from the analyte(s) of interest is generated.

3.3.2.5. Choice of internal standard

The use of an internal standard (IS) improves the accuracy of an analytical method and minimizes system and procedural deviations that may result in variations in precision as a function of sample size or instrumental response [278, 311]. An internal standard is usually structurally similar to the analyte of interest and is added to a sample mixture during the preparation of standards and solutions of unknown concentration [282, 284, 311]. The unknown concentration of a compound of interest is calculated following the measurement of the peak area or peak height ratio of the analyte and IS [280]. In these studies, peak height ratio was chosen over peak area as the measurement criteria since the amount of tailing observed during the analysis of KTZ was not considered substantial. The internal standard method compensates for sample volume changes and day-to-day changes in chromatographic conditions, which may affect the IS and the sample of interest uniformly [280, 312]. The choice of an internal standard is therefore crucial to facilitate the optimization of the analytical method.

An internal standard should be well resolved from the API and should as far as possible be commercially available [278, 282, 284]. In addition the IS must not be a potential impurity or degradation product of the analyte of interest. The most important consideration while selecting an IS is to ensure that it has similar physicochemical characteristics and chromatographic behaviour to the analyte of interest, although it might not be structurally related to the compound of interest [284]. Therefore, the method developed for the compound of interest must be suitable and applicable for the quantitation of both the compound of interest and the IS.

Perusal of the literature revealed that imidazole antifungals agents are often used as IS for the HPLC analysis of KTZ. Potential internal standards investigated included clotrimazole (CLZ),

econazole (ECZ) and miconazole (MCZ). Separation was achieved using a mobile phase composition of acetonitrile and 50 mM phosphate buffer (pH 6) in a ratio of 65:35 at a flow rate of 1 ml/min and detected at 206 nm. The retention times of the potential IS are listed in Table 3.2.

Table 3.2 Retention times of KTZ and potential internal standards

Compound	Retention time of KTZ (min)	Retention time of IS (min)
Clotrimazole	3.8	6.7
Econazole	3.9	8.7
Miconazole	3.8	14.1

MCZ eluted at a retention time of 14.1 min which was considered too long for routine analysis of KTZ and was therefore not considered further as an IS. The retention times of CLZ and ECZ suggest that these compounds may be appropriate for use as IS for the analysis of KTZ. The peak for ECZ however exhibited considerable tailing and as ECZ eluted at 8.7 min, the run time may be prolonged, which was again considered undesirable. Conversely, the peak for CLZ was sharp, with good baseline resolution and a retention time of 6.7 min, therefore CLZ was selected as the IS for this analysis.

3.3.2.6. Mobile phase selection

Mobile phases used in HPLC analyses offer a series of challenges and often differ in respect of their spectral, chemical and chromatographic separation performance. Based on the retention characteristics of the analyte of interest when a particular solvent mixture, organic solvent concentration or choice of organic solvent is made further adjustment to modify retention times may be necessary [283].

It is desirable that the solvents used in liquid chromatography are miscible with all components of the mobile phase. In addition they should be of appropriate purity and stability, have acceptable toxicity, possess low viscosities to reduce pressure drops and have high diffusivities to produce sharper peaks. Solvents used in HPLC with UV detection must be UV transparent and solvents transparent below 220 nm are preferred. It is particularly important to avoid contamination of solvents as impurities are known to make the solvent opaque, or shift the UV cut off to higher wavelengths. It is preferred that solvents used in HPLC have boiling points below 100°C to ensure high sample recovery and if mass spectrometry detectors are to be used, low molecular weight solvents are preferred [281].

The most commonly used solvent mixtures for RP-HPLC include water-methanol (MeOH) or water-acetonitrile (ACN). The optimum mobile phase composition is often found by trial and error and a convenient approach for method development is to start with 1:1 water-MeOH or water-ACN mixtures [283, 296]. Methanol is widely used for reversed-phase separations as it has a hydroxyl functional group which can act as a hydrogen bond donor and/or acceptor. Furthermore, MeOH is readily available as a high-purity liquid, is chemically stable, possesses minimal health and safety hazards when handled carefully, is usually miscible with a wide range of solvents and is relatively inexpensive [287]. MeOH is more polar than other solvents due to its hydrogen-bonding properties and its ability to form hydrogen bonds with a stationary phase may influence adsorption of the solvent and partitioning of the solute with a resultant impact on the chromatographic separation [313].

In contrast, acetonitrile is a moderately polar and weak hydrogen bond acceptor as it is an aprotic compound. ACN offers a unique combination of properties that distinguish it from other HPLC solvents. ACN is known to be a solubilizing solvent that typically produces sharp well-defined peaks and is miscible with a wide range of organic solvents. Moreover, ACN-water mixtures have a low viscosity in comparison to analogous hydro-alcoholic solutions such as water-MeOH mixtures. ACN also has a midrange solvent strength and has a very low UV cutoff, making it suitable for use in systems in which low wavelength UV detection is essential [287].

KTZ is a lipophilic compound that is practically insoluble in aqueous solution, whilst it is freely soluble in methanol and solvents such as chloroform and dichloromethane (§1.2.2). HPLC methods for the analysis of KTZ have been developed using bonded phase columns (C_{18}) and mobile phases consisting of ACN and sometimes MeOH as the organic modifier (Table 3.1). A mixture of water and MeOH was used as the mobile phase for the analysis of KTZ and produced broad, asymmetric peaks with tailing and poor baseline resolution. Conversely, binary mixtures of ACN and water produced well-defined sharp peaks with good baseline resolution and reduced tailing. Therefore, ACN was selected as the organic solvent of choice for further method development studies for the analysis of KTZ.

3.3.2.7. Preparation of buffer

Buffer solutions of 20, 30, 40, 50, 60 and 70 mM were prepared by accurately weighing appropriate amounts of potassium dihydrogen phosphate into a 1 litre A-grade volumetric flask

and making up to volume with HPLC grade water. The resulting solution was then adjusted to the desired pH using a 1.0 M NaOH solution that had been prepared by accurately weighing 4.0 g of sodium hydroxide pellets into a 100 ml A-grade volumetric flask and making the solution up to volume with HPLC grade water.

3.3.2.8. Preparation of mobile phase

Solutions of mobile phase were prepared by adding the desired volume of HPLC-grade acetonitrile and buffer to a glass Duran® Schott solvent mixing bottle (Schott Duran GmbH, Mainz, Germany). The mixture was allowed to equilibrate to room temperature and the mobile phase was then filtered through a 0.45 µm Millipore® HVLP filter (Millipore, Bedford, MA, USA) and degassed under vacuum using a Model A-2S Eyela Aspirator (Rikakikai Co., Ltd, Tokyo, Japan) prior to use. Freshly prepared mobile phase was used daily and mobile phase was not recycled during use. It is necessary to degas the mobile phase as dissolved gases may lead to the formation of small air bubbles in the flow cell of a detector or in the connecting tubing at high inlet pressures subsequently causing chromatographic interference. The more polar the mobile phase, the more likely it is to dissolve air and degassing aids in the removal of oxygen which may react with the stationary phase. Air bubbles disrupt detectors, particularly those used to monitor eluent by detection of optical properties of solutes. The presence of dissolved gasses may result in baseline drift and random noise which in turn could affect the sensitivity and reproducibility of a system [282].

3.3.2.9. Preparation of stock solutions and calibration standards

Standard stock solutions of KTZ (250 µg/ml) and CLZ (200 µg/ml) were prepared by accurately weighing approximately 25 mg of KTZ and 20 mg of CLZ using a Model AG-135 Mettler Toledo top-loading analytical balance (Mettler Instruments, Zurich, Switzerland) directly into 100 ml A-grade volumetric flasks and dissolving in 20 ml of MeOH. The stock solutions were placed in a Model 8845-30 ultrasonic bath (Cole-Parmer Instrument Comp. Chicago, IL, USA) for 2 min in order to ensure complete dissolution of the analytes after which samples were made up to volume with MeOH. Stock solutions were stored in a refrigerator (4˚C). Stock solutions were used within a maximum period of one (1) week, based on stability study data generated as described in § 3.4.7.2 *vide infra*. Calibration standards of KTZ were prepared by serial dilution of the stock standard solution on a daily basis to produce solutions of 2, 10, 20, 40, 60, 80, 100 and 120 µg/ml concentration and were made up to volume using MeOH.

3.3.3. Optimization of the chromatographic conditions

3.3.3.1. Mobile phase selection

The mobile phase in RP-HPLC has a significant influence on sample retention and separation characteristics. Separation selectivity in RP-HPLC can be altered by changing the concentration of the organic modifier or altering the pH of the mobile phase if the sample components are acidic or basic in nature. The use of buffers or pH adjustment can lead to ion suppression and hence reduce peak tailing if the analyte is in the non-ionised form. For strongly basic analytes, basic modifiers *viz.*, tertiary amines such as triethylamine may be added to the mobile phase to eliminate peak tailing. Furthermore, the addition of salts or ion-pair reagents may affect the solubility of the analyte and hence influence retention and selectivity characteristics of that compound.

3.3.3.1.1. Effect of concentration of organic modifier

The influence of the concentration of ACN on the retention times of KTZ and CLZ was assessed using binary mixtures of ACN and 50 mM phosphate buffer in different proportions at pH 6.0. The mixtures ranged between 55 and 75% ACN and the results are depicted in Figure 3.2.

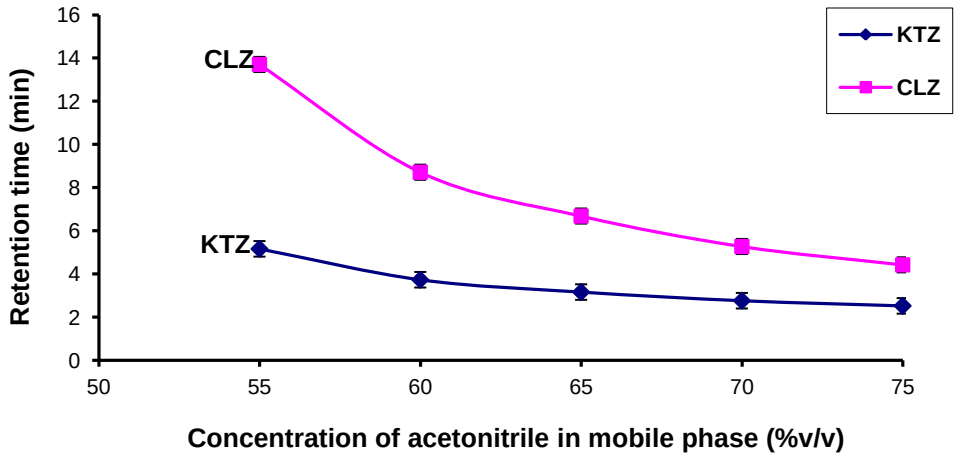

Figure 3.2 Effect of ACN composition on the retention times of KTZ and CLZ (n=6)

It was observed that the retention time (R_t) of KTZ was shorter than that for CLZ with any of the ACN/water binary mixture used. This can be explained in part by the lipophilic characteristics of CLZ enhancing the hydrophobic interactions between CLZ and the stationary phase used. It was also observed that the retention times of both KTZ and CLZ were inversely proportional to the

ACN concentration in the mobile phase, implying that an increase in ACN concentration in the mobile phase would lead to a shorter retention time for KTZ and CLZ. This reduction in retention time may be due to an increase in the extent of interactions between the solute and the solvent and a decrease in the extent of interaction between the solute and the stationary phase.

These studies were conducted to determine an optimal concentration of ACN for use in the mobile phase such that reasonable retention times for both KTZ and CLZ were possible. Retention times considered acceptable were approximately 4 min for the first peak of interest and an approximate difference of 2-6 min between the elution of the first peak and second peaks, giving rise to a run time of approximately 10-12 min. A binary mixture consisting of ACN and 50 mM phosphate buffer (pH 6.0) in a ratio of 60:40 was selected as the mobile phase of choice for the separation of KTZ and CLZ based on criteria set in our laboratory. The retention times for KTZ and CLZ using this particular mobile phase were 3.7 and 8.7 min, respectively.

3.3.3.1.2. Effect of flow rate

One of the aims of these studies was to develop an HPLC method with a run time of approximately 10-12 min for the analysis of KTZ in pharmaceutical dosage forms. Therefore, the influence of flow rate on the retention times of KTZ and CLZ was also evaluated. The effect of changing flow rate is depicted in Figure 3.3. These studies indicate that the retention times of KTZ and CLZ decrease as the flow rate of the mobile phase increases. A flow rate of < 1.0 ml/min resulted in a retention time of > 10 min for CLZ, which was considered undesirable since the method would be time-consuming.

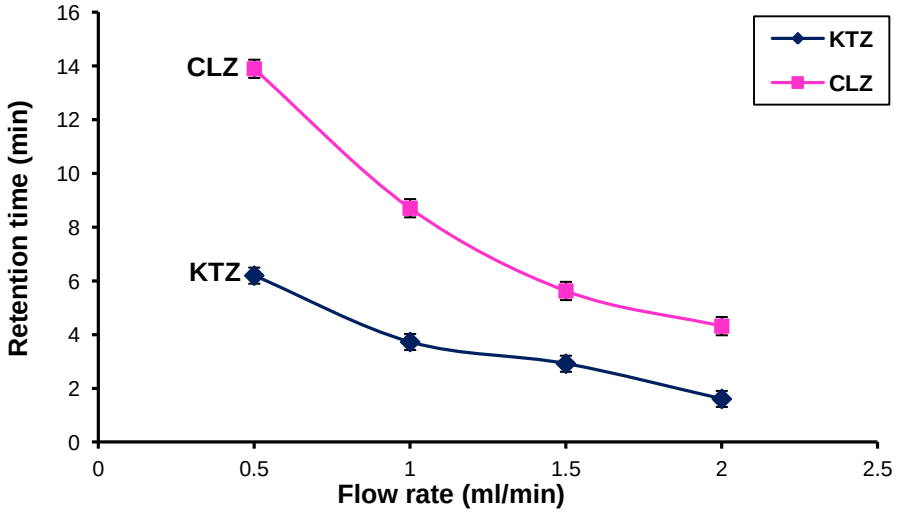

Figure 3.3 Effect of flow rate of the mobile phase on the retention times of KTZ and CLZ (n=6)

The use of high flow rates such as 1.5 ml/min and 2 ml/min resulted in short retention times for KTZ and CLZ which were considered too close to the solvent front for quantitation in addition to back pressures exceeding 2000 psi (13.8 MPa). Moreover, the resolution of the peaks was not adequate at high flow rates. A flow rate of 1.0 ml/min produced sharp, well-resolved peaks with acceptable retention times for KTZ and CLZ (Figure 3.4). The mobile phase flow rate selected for further use was 1.0 ml/min.

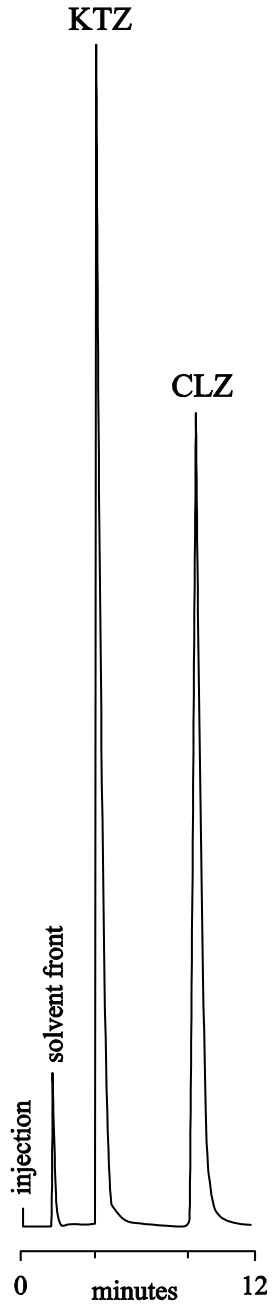

Figure 3.4 Typical chromatogram of a mixture of the internal standard, clotrimazole (CLZ, 80 µg/ml) and ketoconazole (KTZ, 120 µg/ml) using a mobile phase of 60% v/v ACN (60% v/v) and 50 mM phosphate buffer (pH 6.0) (40% v/v) at a flow rate of 1.0 ml/min

3.3.3.1.3. Effect of buffer pH

The effect of the pH of the buffer, used to prepare the mobile phase, on the retention times of KTZ and CLZ is depicted in Figure 3.5. These studies were conducted using a mixture of ACN (60% v/v) and 50 mM phosphate buffer ranging from pH 4.0 to 7.0. No difference was noted in the retention times of KTZ and CLZ as the pH of the buffer was increased. However, poor resolution was noted at pH < 5.

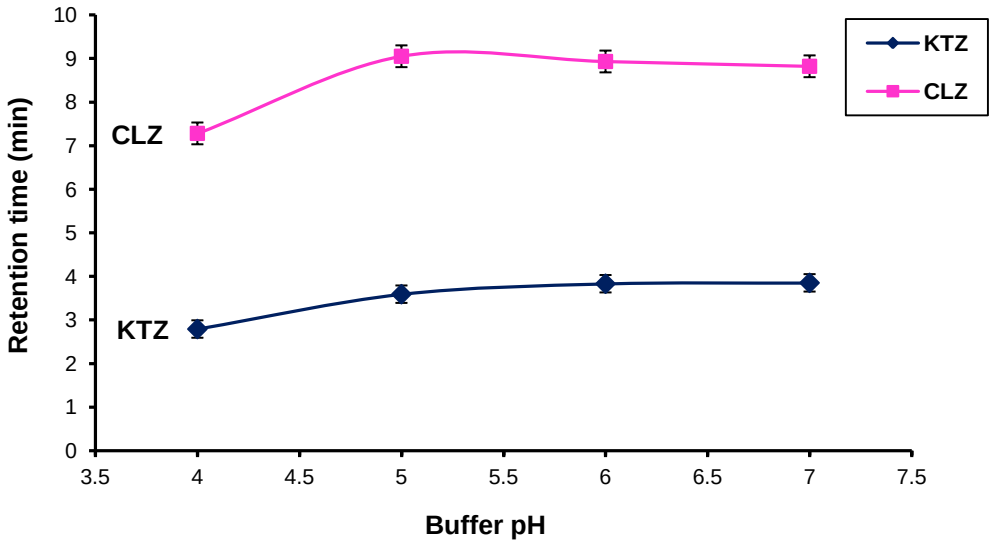

Figure 3.5 Effect of buffer pH used for the preparation of the mobile phase (comprising of 60% v/v ACN: phosphate buffer, 50 mM) on the retention times of KTZ and CLZ (n=6)

Close inspection of the chromatograms revealed slight shouldering and an increase in tailing of the peaks at higher pH, e.g. pH 7.0. Buffers of pH > 7.0 were not used as silica-based columns such as the Beckman® ODS column may undergo hydrolysis at pH ≥ 8. The increased shouldering and tailing observed at high pH was attributed to the poor performance of the column and a pH of 6.0 resulted in sharp and well-resolved peaks.

3.3.3.1.4. Effect of buffer molarity

The effect of buffer molarity on the chromatographic separation of KTZ and CLZ was also investigated and studies were conducted over the range of 20 to 100 mM using potassium dihydrogen phosphate buffer (pH 6.0). The influence of buffer molarity on the retention times of both KTZ and CLZ is shown in Figure 3.6.

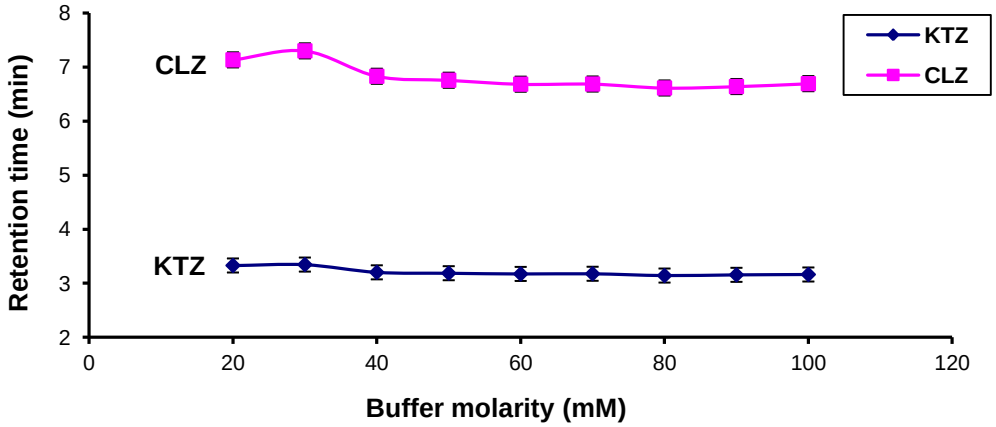

Figure 3.6 Effect of buffer molarity used for the preparation of the mobile phase (comprising of 60% v/v ACN: phosphate buffer, pH 6.0) on the retention times of KTZ and CLZ (n=6)

No significant differences were observed in the retention times of KTZ and CLZ as the buffer molarity was increased from 20 to 100 mM. However, poorly resolved asymmetric peaks were observed when buffers of low and high molarity were used. A buffer of intermediate molarity of 50 mM was therefore selected for further optimization studies.

3.3.3.1.5. Optimal mobile phase composition

The mobile phase selected for further investigation for the analysis of KTZ using CLZ as an IS was comprised of a binary mixture of ACN and 50 mM phosphate buffer (pH 6.0) in a ratio of 60:40. The KTZ peak was well resolved from the CLZ peak when the optimal mobile phase was used and sharp well-defined peaks were observed. A typical chromatogram generated using these separation conditions and a flow rate of 1.0 ml/min is depicted in Figure 3.4. The peaks for KTZ and CLZ eluted at 3.7 min and 8.7 min, respectively. A total run time of 12 min was selected for the analysis, which resulted in a relatively low volume of mobile phase and solvent use for the analysis of KTZ in test samples.

3.3.3.2. Chromatographic conditions

The final chromatographic conditions selected for validation of the HPLC analysis of KTZ are summarized in Table 3.3.

Table 3.3 Optimized chromatographic conditions

Column	Beckman® Coulter ODS column (5µm, 150 × 4.6 mm I.D.) ®
Flow rate	1.0 ml/min
Detection wavelength	206 nm
Injection volume	10 µL
Temperature	Ambient
Mobile phase composition	ACN:50 mM phosphate buffer, pH 6.0 (60:40)
Sensitivity	2.0 AUFS
Recorder	SP-4600 Integrator (Spectra-Physics, San Jose, CA, USA)
Integrator speed	0.25 mm/min

3.4. Method validation

3.4.1. Overview

The validation of an analytical method is a critical process that is used to establish the performance characteristics of a method and to establish whether the method meets the requirements for its intended purpose [314-319]. The validation process provides significant data with respect to the reliability, accuracy and precision of an analytical method and enables the analyst to identify or foresee potential problems [320, 321]. Nevertheless, it may not be possible to identify all potential problems of a particular analytical method during the validation process and only common problems such as column degeneration, changes in column behaviour and co-elution of impurities may be identified [318, 322]. Method validation is therefore a distinct process that is used to certify that the analytical method performs in a specific manner for the purpose for which it was developed [315, 318, 319].

Guidelines outlining the validation of analytical methods used for the routine analysis of pharmaceutical dosage forms have been published in the United States Pharmacopoeia (USP), by FDA, regulatory authorities in Europe and the International Conference on Harmonization (ICH) [314, 315, 323-325]. All provide useful information on the type of studies to be conducted and define key validation parameters to be investigated [314, 315, 323-325]. However, these guidelines fail to provide information with respect to how the validation studies must be conducted, and therefore, perusal of the literature for published approaches to analytical method validation is essential.

It is imperative that the objective of the intended method is established before proceeding with a particular validation protocol even if validation procedures for HPLC methods essentially include similar parameters [321, 322]. A Level I or quantitative assay method is usually applied to the determination of potency, evaluation of drug release, monitoring of drug levels in blood or assessment of impurities or contaminants in human drug products [321]. On the other hand, a Level II or qualitative assay method is intended for qualitative analyses for the purposes of identification. The FDA for instance recommends that an analytical method developed for a pharmaceutical product be validated with regard to accuracy, precision, sensitivity, specificity and reproducibility [320]. The USP and ICH guidelines include validation parameters such as accuracy, precision, specificity, limits of detection (LOD) and of quantitation (LOQ), linearity, range and sample stability [314, 315, 323-325]. In addition the ICH guidelines also include an evaluation of robustness and system suitability [323, 324]. The validation of a RP-HPLC method for the analysis and quantification of KTZ from pharmaceutical dosage forms during formulation development and assessment was therefore performed as detailed in the FDA [316, 325] and USP [314] guidelines with reference to the ICH recommendations [323, 324].

3.4.2. Linearity and range

The evaluation of linearity is vital to demonstrate whether proportionality exists between a quantitative response and the concentration of the analyte within the range of analysis [314, 317, 326]. The range of analysis refers to the inclusive interval between the upper and lower levels of analyte concentration that have been quantitated with the necessary accuracy, precision and linearity [282, 283, 295, 323, 324]. The linearity of the analytical method was assessed within the range of concentrations expected, using a standard calibration curve which was evaluated by calculation of a least squares linear regression curve [327]. Linearity must be established when using UV spectrophotometry as it is fundamental that the absorptive response follows the Beer-Lambert law over the range of concentrations analyzed [274, 283, 284].

A minimum of five concentrations spanning the concentration range to be analyzed must be used for the assessment of linearity. Linearity studies were therefore conducted by performing replicate measurements (n=6) at eight concentration levels covering the concentration range of 2-120 µg/ml for KTZ. The mean peak height ratio of KTZ and internal standard was plotted against concentration to produce the calibration curve. The acceptability of the linearity data was judged from an examination of the correlation coefficient (R^2) for the regression line of the standard

calibration curve. An R^2 value of between 0.999 and 1 was considered to be adequate to demonstrate the linearity of the method and to show the presence of a direct response-concentration relationship [317, 323, 324]. A typical calibration curve for the analysis of KTZ is depicted in Figure 3.7.

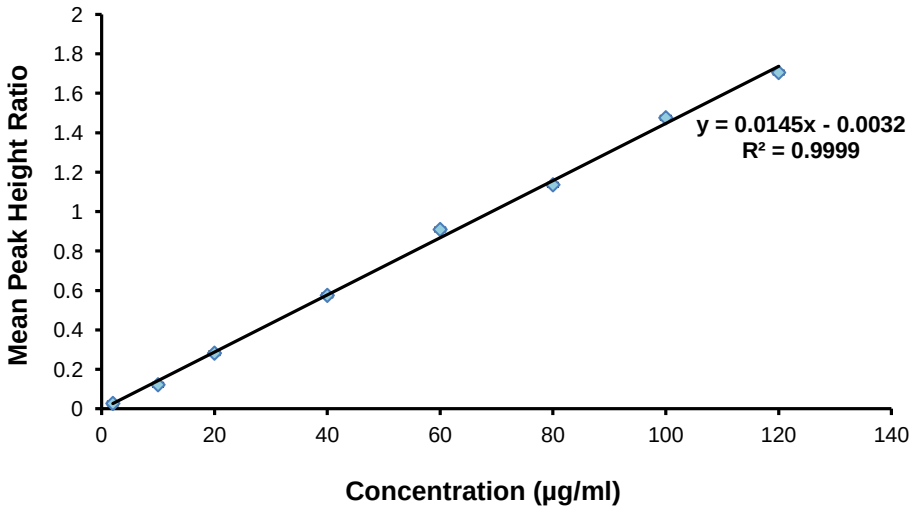

Figure 3.7 Typical calibration curve constructed for KTZ using peak height ratio of KTZ and CLZ versus concentration

3.4.3. Precision

Precision is a measure of the extent of closeness of data from repeated analysis of an homogenous sample [326, 328]. Precision quantifies the variability of an analytical method on account of the performance of the analyst, manipulations made in performing the analysis and day-to-day environmental changes [315, 328]. All official or approved analytical methods are required to include an assessment and quantification of precision, which indicates the repeatability and reproducibility of a method. The ICH guidelines recommend that precision be assessed at three levels *viz.*, repeatability, intermediate precision and reproducibility [315, 323, 324]. Precision is usually expressed as the percent relative standard deviation (% RSD) and a percent RSD of ± 5% was set as the acceptable tolerance for precision studies in our laboratory.

3.4.3.1. Repeatability

The repeatability of a method of analysis is a measure of the intra-day variation and expresses the ability of the method to withstand small experimental variations over a short time interval under the same operating conditions [323, 324]. Repeatability studies therefore need to be conducted by

the same analyst, in the same laboratory using the same equipment on the same day [323, 324, 328]. A minimum of nine determinations spanning the range of analysis or a minimum of six determinations at 100 % of the expected test concentration are suggested in the ICH guidelines as adequate for repeatability evaluation. The % RSD for an assay method must be ≤ 2 % [320], whereas the % RSD for the determination of impurities at trace levels must be ≤ 10 % [329].

The repeatability of the analytical method was assessed through replicate analysis (n=6) of samples at low, medium and high concentrations interpolated from the calibration curve and which were within the range of concentrations analyzed. Analyses were performed at concentrations of 5, 45 and 115 µg/ml. The % RSD values obtained for the intra-day precision were ≤ 2% indicating that the analytical method was repeatable. The results from repeatability studies (n = 6) are summarized in Table 3.4.

Table 3.4 Intra-day precision data for HPLC analysis of KTZ

Concentration (µg/ml)	Mean Peak Height Ratio	Standard Deviation (SD)	% RSD
5.00	0.058	0.0006	0.960
45.0	0.572	0.0049	0.853
115	1.454	0.0061	0.417

3.4.3.2. Intermediate precision

Intermediate precision is also expressed as the ruggedness of an assay and refers to the ability of an analytical method to withstand variations within a laboratory and therefore, assesses the reliability of the procedure when conducted on different days using different analysts and/or instruments [314, 320, 323, 330]. The assessment of inter-day precision is important to establish the long-term variability of an analytical method within the same environment and to ensure the validity of the method once method development has been completed [320, 328]. The intermediate precision of this method was determined by performing replicate analyses (n=6) of samples of concentration 5, 45 and 115 µg/ml on three consecutive days. The intra-day precision data, expressed as the coefficient of variation or % RSD of the mean peak height ratio of KTZ to internal standard are summarized in Table 3.5. The criterion for acceptable intermediate precision was set at ≤ 2% for each concentration level. The data reveal that the % RSD values were < 2%, thereby indicating that the day-to-day precision of the analytical method was acceptable.

Table 3.5 Intermediate precision data for HPLC analysis of KTZ

Day	Concentration (µg/ml)	Mean Peak Height Ratio	Standard Deviation (SD)	% RSD
1	5.00	0.059	0.0011	1.931
	45.00	0.584	0.0111	1.792
	115.00	1.460	0.0098	0.670
2	5.00	0.059	0.0001	0.297
	45.00	0.591	0.0068	1.159
	115.00	1.461	0.0122	0.833
3	5.00	0.061	0.0001	0.149
	45.00	0.595	0.0012	0.197
	115.00	1.461	0.0063	0.435

3.4.3.3. Reproducibility

The reproducibility of an analytical method refers to the ability of the method to maintain precision when used in different laboratories. Reproducibility tests should be performed using homogenous samples by different analysts in different laboratories to establish whether the method can be transferred from one laboratory to another [328]. It is not usually expected to perform reproducibility tests if intermediate precision has been established unless the analytical method is intended for a standardized procedure which is to be published in an official compendium [324]. Tests for reproducibility were therefore not conducted in these studies as all analyses were performed by the same analyst in the same laboratory.

3.4.4. Accuracy

The accuracy of an analytical method refers to the closeness of results of an analysis to a known standard or reference value within the established range of analysis [314, 317, 326]. Accuracy and precision are two most important validation tests, as they are used to determine the error of an analytical procedure [317, 331, 332]. As recommended by the ICH, accuracy may be established by performing replicate analysis of samples containing known amounts of the analyte of interest and comparing the experimentally determined values to the nominal theoretical values. Another approach that can be used to investigate the accuracy of an analytical method involves comparing analytical results from a new method to the results from an existing or well-established procedure, or by spiking known amounts of the API of interest into blank matrices and establishing and evaluating the percent recovery from that matrix [320]. Statistical analysis of the data generated may also be used to demonstrate accuracy [315]. A two-sided t-test may be performed to determine whether significant differences exist between the mean data generated by a test method and a nominal value with a 95% level of confidence [317, 320]. FDA requires that

recovery values > 90% be demonstrated for biological samples if the analytical method is to be approved and recommends that accuracy be investigated at 80%, 100% and 120% of label claim for analytical methods used for analysis of drug substances or products [321, 332].

The accuracy of the HPLC method was determined by performing triplicate analyses (n=3) of samples containing known amounts of KTZ *viz.*, 5, 45 and 115 µg/ml analyzed in replicates of six. The accuracy of the analytical method was represented as the percent recovery, % RSD and % bias. Bias reflects the influence of an analyst on the performance of the method and hence the accuracy of sample preparation prior to analysis [326]. By definition, bias refers to the deviation from the mean value determined for the API of interest [326]. FDA recommends that the acceptance criteria for recovery and % RSD be 100 ± 2% and ≤ 2% respectively at each concentration level studied over the range 80-120% of the target concentration. The tolerance limit for percent bias was set to 5% in our laboratory.

The data generated during accuracy studies are summarized in Table 3.6. The percent bias was < 5% for all samples tested. Based on the acceptable test criteria for our laboratory, the analytical method was considered accurate.

Table 3.6 Accuracy data for HPLC analysis of KTZ (n = 3)

Theoretical concentration (µg/ml)	Actual concentration (µg/ml)	SD	% RSD	% Bias	% Recovery
5.00	4.96	0.0907	1.829	-0.867	99.28
45.00	45.30	0.5240	1.164	+0.674	100.67
115.00	115.51	1.1410	0.986	+0.443	100.44

3.4.5. Limits of quantitation (LOQ) and detection (LOD)

The LOQ, sometimes termed the lower limit of quantitation or LLOQ, refers to the lowest concentration of an analyte that can be accurately and precisely quantitated under the stated operational conditions of an analytical method. The LOD refers to the lowest concentration that will yield an identifiable or detectable peak that might not necessarily be quantifiable under the stated operational conditions of the analytical method [295]. UV detectors may not have the highest precision at low analyte concentrations as a result of a loss of sensitivity of the detector lamp on ageing or due to variations in the noise levels of the detector, particularly if it has been acquired from a different manufacturer or has a different model number [321]. The LOQ is generally taken to be the lowest concentration level of the calibration curve, whereas the LOD is

a limit test that enables the analyst to determine whether the concentration of an analyte is above or below a specific level or amount [314, 333].

The ICH outlines different approaches that can be used to establish the LOQ and LOD of an analytical method. The different approaches yield similar results and none have similar identifiable trends that are a specific characteristic of the method. The LOQ and LOD can be determined by visual evaluation of the data. Another commonly used approach used in the determination of LOQ and LOD is the signal-to-noise ratio approach that may However, only be used in analytical methods that display significant baseline noise. The LOQ is said to have a signal to noise ratio of 10:1, whereas the LOD is established at a signal to noise ratio of 3:1 when measured signals from samples with known low analyte concentrations are compared [324]. This approach, albeit recommended by the USP, is not very practical as noise levels vary from detector to detector. Another technique used for the assessment of LOQ and LOD involves the calculation of the standard deviation of the response and slope of the line using Equations 3.3 and 3.4 to determine the value for these limits [286].

$$LOQ = \frac{10\sigma}{S} \qquad \textbf{\textit{Equation 3.3}}$$

$$LOD = \frac{3.3\,\sigma}{S} \qquad \textbf{\textit{Equation 3.4}}$$

where,

σ = standard deviation of the response

S = slope of the calibration curve

A fourth approach, where a plot of standard deviation versus concentration is constructed and the equation of the line determined, may be used. The LOQ and LOD are then calculated by multiplying the y-intercept by 10 and 3 respectively. The LOQ can also be taken as the lowest concentration with a % RSD of < 5% following multiple injection. The LOD can subsequently be taken as 30% of the LOQ [333]. The % RSD approach was used in these studies for the determination of LOQ and LOD. Six concentrations of KTZ were selected as potential LOQ values and analyzed in replicates of six. The results generated for this approach are listed in Table 3.7. Using this technique, the LOQ was found to be 2.5 µg/ml with a % RSD of 2.13%. By convention, the LOD was calculated to be 0.75 µg/ml.

Table 3.7 LOQ data for HPLC analysis

Concentration (µg/ml)	Mean Peak Height Ratio (n = 6)	SD	% RSD
2.50	0.0375	0.0008	2.13
2.00	0.0292	0.0015	5.24
1.50	0.0289	0.0025	8.57
1.00	0.0184	0.0014	7.44
0.75	0.0099	0.0006	6.32
0.50	0.0068	0.0006	8.92
0.25	0.0029	0.0005	18.82

3.4.6. Specificity and selectivity

The specificity or selectivity of an analytical method is defined as the ability of an analytical method to accurately and specifically determine the concentration of the analyte of interest in the presence of other components of a mixture or a sample matrix [318, 321, 334-336]. For the analytical method to be considered specific and selective, the analyte of interest must be well resolved from extraneous components of that mixture or matrix [284, 314, 321, 324]. For the chromatographic analysis of pharmaceutical dosage forms, it is important that the analytical procedure exhibits good resolution of the peak of interest from possible excipients or contaminants that might be present in dosage forms.

3.4.6.1. Analysis of KTZ in tablet dosage forms

The specificity and selectivity of the RP-HPLC method developed for the analysis of KTZ can be demonstrated from the chromatogram depicted in Figure 3.8, which was generated following the analysis of Ketazol® 200 mg tablets. A composite of 20 tablets was prepared by grinding the tablets into a fine powder and accurately weighing aliquots of the powder (n = 3), each of which was equivalent to the average weight of a single tablet. The powders were transferred into three respective volumetric flasks containing the IS and made up to volume using methanol. The solution was filtered through a 0.22 µm Millipore® membrane filter and appropriate aliquots were analyzed using the validated HPLC method. No interference from tablet excipients or contaminants was observed. The drug of interest, i.e. KTZ, eluted at 3.7 min and was well resolved from the internal standard, CLZ, which in turn eluted at 9.0 min.

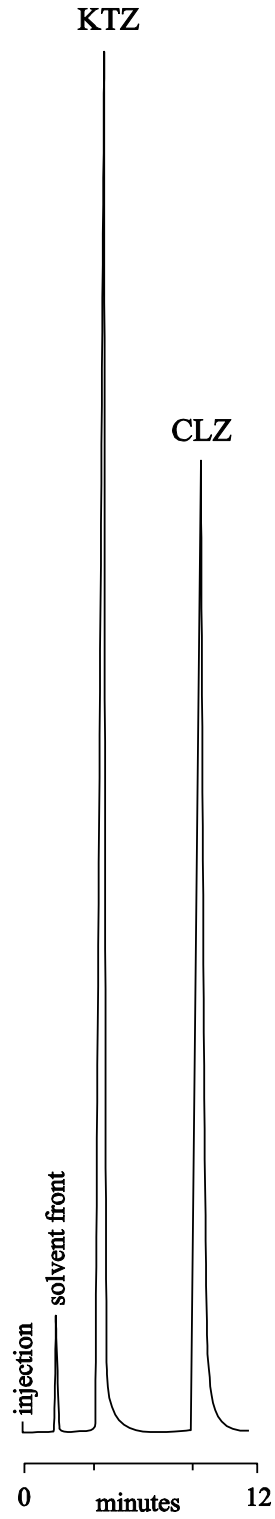

Figure 3.8 Typical chromatogram obtained following analysis of Ketazol® 200 mg tablets using clotrimazole (CLZ) as internal standard.

3.4.7. Sample stability studies

3.4.7.1. Overview

Part of a validation process necessitates an evaluation of the stability of analytes in the sample matrix and solvents used under the conditions to which the analytical samples will be subjected during analysis [321]. A compound may be considered stable under certain conditions for a specified period of time when there is no significant difference between the detector response for the API of interest following analysis of stored samples, compared to the response produced from freshly prepared solutions of that drug in a similar matrix or solvent [317]. Drugs that undergo hydrolysis, photolysis or that are sequestered onto glassware may need to be investigated for stability under normal laboratory operating conditions or following storage. It has been suggested that the stability of standard stock solutions used for the preparation of calibration curve standards should be assessed over the duration for which these solutions will be stored, under the same conditions of light or dark, at the same temperature(s) and in the same solvent(s) and container(s) that will be used prior to and during analysis [317, 337, 338].

The stability of KTZ in the standard stock solution used to prepare the calibration standards (§ 3.3.2.9) was assessed over a one week period as this was the maximum period over which the sample was likely to be stored. The aim of these stability studies was to establish whether KTZ degrades during this time i.e. from sample preparation through storage and to ensure that the integrity of the samples is maintained until analysis is performed [337-339]. In cases where data on stability are not available, it is recommended that standard stock solutions be prepared on a daily basis during sample analysis. Failure to prepare fresh solutions may result in the construction of a calibration curve from standards that do not reflect the true concentration of drug and therefore, leads to an inaccurate estimation of the drug concentration in unknown samples [338].

3.4.7.2. Stability data analysis

A systematic statistical procedure was used for the analysis of data generated during stability studies. This statistical approach is particularly useful since it accounts for the influence of the analytical method. In addition any error that may be associated with the procedure has been reported. The method, initially developed for the determination of stability of drugs in biological fluids, is based on the calculation of a 90 % confidence interval (C.I.) for the difference in

concentration or detector response (D) generated from replicate analysis of stored and freshly prepared samples. The true percentage change in response between stored and freshly prepared samples lies within a limit defined by the lower limit (L.L.) and the upper limit (U.L.) with 90% certainty [340].

According to this approach, a change may be statistically significant albeit not pharmacokinetically relevant i.e. a change may be regarded as significant if the C.I. does not include zero and relevant if the U.L. and L.L. of the C.I. are > 10% or < 10% respectively. This concept is illustrated in Figure 3.9, which displays the possible results that could be obtained from the analysis of stored samples using the approach described by Timm *et al.*, for stability data assessment [340].

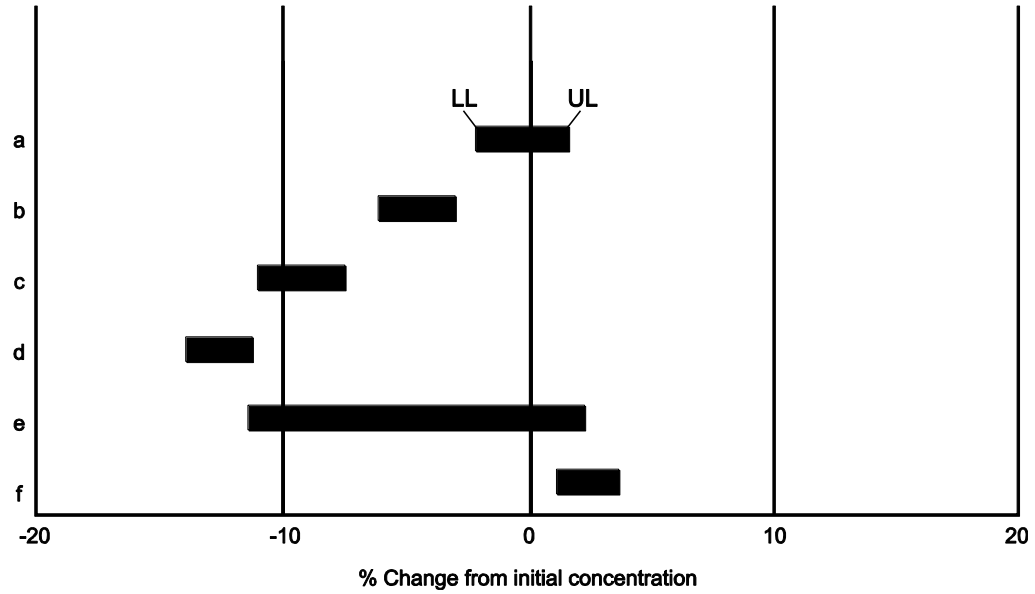

The bars represent the C.I. for the possible scenarios:

a) change of response, not significant and not relevant
b) decrease of response, significant but not relevant
c) decrease of response, significant and possibly relevant
d) decrease of response, significant and relevant
e) decrease of response, not significant but possibly relevant
f) increase of response, significant

Figure 3.9 Interpretation of stability data, as described by Timm et al. [340]

3.4.7.3. Stability of stock solutions

The stability of KTZ stock solutions prepared, as previously described in § 3.3.2.9, was assessed during storage for one week at 4°C. Aliquots of 400 and 4800 µl of KTZ stock solutions were measured using single-channel model electronic pipettes (Hamilton Soft Touch ™, Nevada, US) covering the volume range of 50-1200 and 500-5000 µl respectively and these were transferred into 10 ml A-grade volumetric flasks and made up to volume with ACN to yield solutions of 10 µg/ml and 120 µg/ml representing low and high concentrations respectively. Five replicate samples at each concentration were prepared for analysis on days 0, 1, 2, 3 and 7 following storage at 4°C. Consequently, a total of twenty-five separate samples were analyzed. Fresh samples of KTZ at each concentration studied were also prepared from a freshly prepared KTZ stock solution (§ 3.3.2.9) and analyzed on the same day as the stored samples on each day of analysis. A 40 µl aliquot of the internal standard (CLZ) stock solution measured using an electronic pipette (Hamilton Soft Touch™, 1-100 µl, Nevada, US) was added to the solutions prior to analysis and the peak height ratio of KTZ to internal standard was measured.

The results obtained from stability studies of KTZ stock solutions at both the lower and upper concentrations stored at 4˚C for 1, 2, 3, 7 days are depicted in Figure 3.10. The data generated reveal that the change of response for KTZ was neither significant nor relevant at the lower (10 µg/ml) and upper (120 µg/ml) concentration levels when stored at 4˚C for 7 days as the U.L. and L.L. of the C.I. were found to be within 5%. The wider C.I. calculated for both concentrations on day 3 could possibly be attributed to poor precision during sample preparation. However, the stability studies indicate that KTZ is stable in methanolic solution at 4°C following storage for one week. Therefore, it was acceptable to prepare stock solutions of KTZ in methanol and use them within one week prior to storage at 4°C.

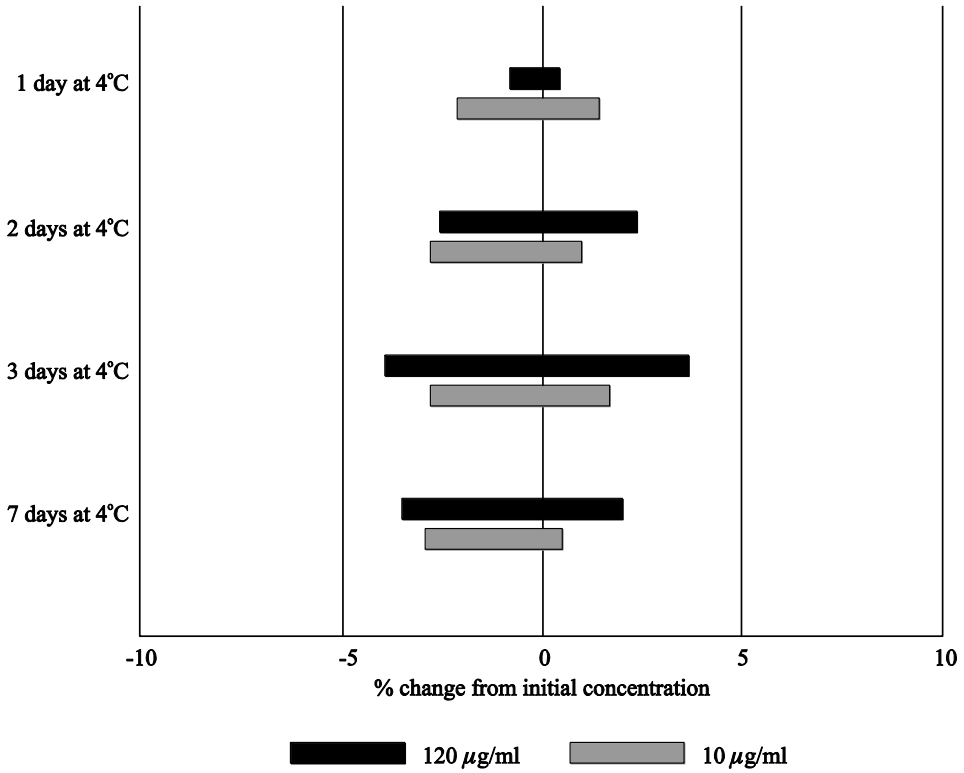

Figure 3.10 Interpretation of stability data for KTZ, as described by Timm et al. [340]

3.4.8. Method re-validation

Re-validation studies might have to be performed to ensure the validity of an analytical method when an original procedure has been changed or its validated operating conditions have been altered according to FDA guidelines. The extent of re-validation depends on the nature of the change to that analytical method and it might not be obligatory to re-validate the method completely if it has previously been validated according to the specifications of an international protocol [321]. Changes in the raw material or drug substance, changes in the manufacturing process of the raw material or in the composition of the product may require re-validation of the analytical method to ensure that the method continues to resolve the right strength, quality, purity and potency of the drug of interest and/or drug product. The re-validation process may only require an evaluation of performance characteristics likely to be affected by the change in the analytical method [315]. Nonetheless, it is advisable to conduct an evaluation of linearity, accuracy and precision of a method as an absolute minimum requirement should there be any change to the analytical method [315].

The RP-HPLC method developed for KTZ was revalidated since the column used initially in validation studies was replaced with a new column. Replacing a chromatographic column may lead to changes in specificity and resolution and quantitative aspects of the HPLC method [315]. Therefore, all method validation parameters were reassessed when the new column was installed for use. The definitions and accepted validation parameters of the performance characteristics discussed below have been described in § 3.4. In addition the column efficiency for the new column was evaluated using an ideal test system as described in § 3.3.2.3. The theoretical plate number for the new column was 13495 ± 742 (n=6).

3.4.8.1. Linearity and range

The linearity of the method was evaluated within the concentration range expected from the *in vitro* analysis of KTZ from lyophilized KTZ-loaded solid lipid microparticles that were to be developed. Calibration standards were prepared as previously described in § 3.3.2.9, and linearity was assessed as described in § 3.4.2. The calibration curve shown in Figure 3.11 was generated after replicate analysis (n=6) of samples in the range 2-120 µg/ml. The calibration curve represented by the equation $y = 0.0124x + 0.0004$, with a linear regression coefficient of 0.9998 obtained after revalidation, indicates that the HPLC method is linear.

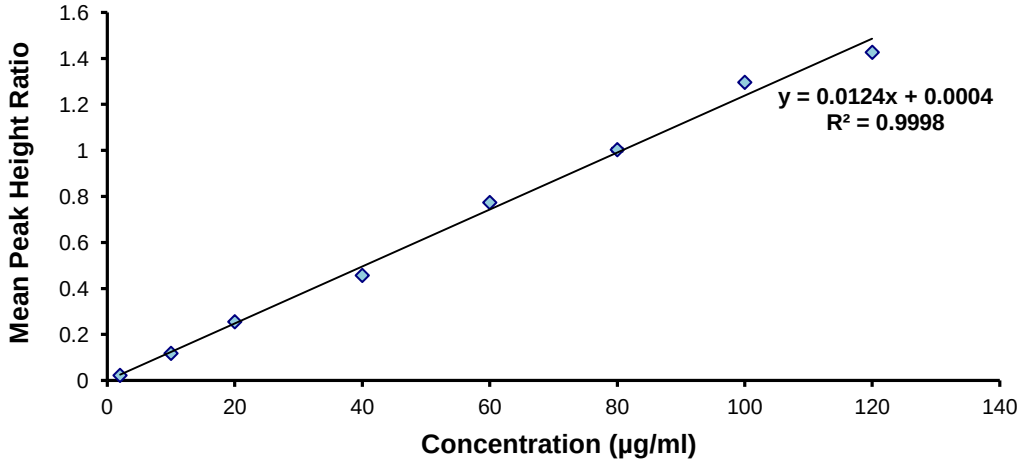

Figure 3.11 Calibration curve constructed for KTZ following least squares linear regression analysis of peak height ratio of KTZ and CLZ

3.4.8.2. Precision

The repeatability and inter-day precision of the analytical method were evaluated during the revalidation process as described in § 3.4.3.

3.4.8.2.1. Repeatability

The repeatability of the HPLC method was determined as described in § 3.4.3.1 at three concentration levels *viz.*, 5, 45 and 115 µg/ml in triplicate. The results generated in this study reveal that the HPLC method is repeatable and are summarized in Table 3.8.

Table 3.8 Intra-day precision data for HPLC analysis of KTZ during method revalidation

Concentration (µg/ml)	Mean Peak Height Ratio	Standard Deviation (SD)	% RSD
5.00	0.059	0.0005	0.786
45.00	0.601	0.0050	0.835
115.00	1.461	0.0070	0.480

3.4.8.2.2. Intermediate precision

The inter-day precision was of the method was assessed as described in § 3.4.3.2, and was determined at three concentration levels *viz.*, 5, 45 and 115 µg/ml in triplicate (n=3) for three consecutive days. The results of the intermediate precision studies are depicted in Table 3.9. The HPLC method was found to be precise over several days as the % RSD values observed were < 5%.

Table 3.9 Intermediate precision data for HPLC analysis of KTZ after method revalidation

Day	Concentration (µg/ml)	Mean Peak Height Ratio	Standard Deviation (SD)	% RSD
1	5.00	0.058	0.0011	1.879
	45.00	0.593	0.0095	1.600
	115.00	1.514	0.0089	0.590
2	5.00	0.058	0.0001	0.117
	45.00	0.587	0.0086	1.460
	115.00	1.493	0.0097	0.653
3	5.00	0.061	0.0001	0.176
	45.00	0.565	0.0007	0.124
	115.00	1.482	0.0064	0.423

3.4.8.3. Accuracy

The accuracy of the HPLC method was evaluated as described in § 3.4.4, and was determined at three different levels *viz.*, 5, 45 and 115 µg/ml in triplicate (n=3). The results of these studies are summarized in Table 3.10 and reveal that the percent bias was < 5% at the concentration levels studied, thus the HPLC method can be said to be accurate.

Table 3.10 Accuracy data for HPLC analysis of KTZ (n = 3) after method revalidation

Theoretical concentration (µg/ml)	Actual concentration (µg/ml)	SD	% RSD	% Bias	% Recovery
5.00	4.86	0.125	2.572	-0.028	97.20
45.00	44.80	0.264	0.589	-0.005	99.60
115.00	116.01	0.273	0.235	+0.008	100.88

3.4.8.4. Specificity

The specificity of the HPLC method developed for the analysis of KTZ was assessed using analysis of Ketazol® 200 mg tablets as described in § 3.4.6.1. The specificity of the analytical method for KTZ was also evaluated using Ketazol® 20mg/g cream. A typical chromatogram obtained from these studies is depicted in Figure 3.12, and reveals that there was no interference from the formulation excipients. KTZ eluted at 3.6 min and was well resolved from the internal standard, CLZ, which in turn eluted at 8.8 min.

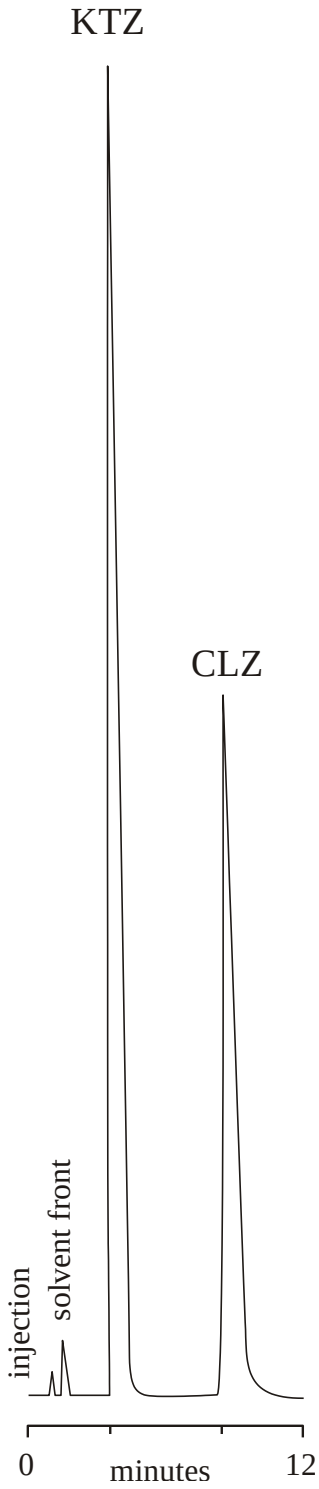

Figure 3.12 Typical chromatogram obtained following analysis of Ketazol® cream (2% w/w) using clotrimazole (CLZ) as internal standard.

3.4.8.5. Limits of quantitation and detection

The LOQ was established using the % RSD method as described in § 3.4.5, and was found to be 2 µg/ml with a % RSD of 3.38% after replicate analyses (n=6) of samples at that concentration. The LOD was therefore taken to be 30% of the LOQ by convention and was calculated to be 0.6 µg/ml. The results obtained for LOQ determination are listed in Table 3.11.

Table 3.11 LOQ data for HPLC analysis of KTZ

Concentration (µg/ml)	Mean Peak Height Ratio (n = 6)	SD	% RSD
2.50	0.0361	0.0002	0.526
2.00	0.0287	0.0010	3.380
1.50	0.0211	0.0013	5.972
1.00	0.0163	0.0010	6.319
0.50	0.0061	0.0005	7.541
0.25	0.0023	0.0004	17.826

3.4.9. Application of the HPLC method

Following development and validation studies, the RP-HPLC analytical method for KTZ was applied to the quantitative determination of KTZ in aqueous dispersions of solid lipid microparticles during drug loading capacity (DLC) and encapsulation efficiency (EE) studies.

3.5. Conclusions

A reversed-phase HPLC method has been developed for the analysis of KTZ and has been optimized and validated for use in the *in vitro* analysis of KTZ in solid lipid microparticles formulations. Method development studies reveal that the RP-HPLC method developed was relatively simple and convenient to use in comparison with those previously reported which are generally complicated and require mobile phase compositions that include the use of hydrophobic ion pair reagents or amine modifiers.

UV detection was selected due to its versatility and simplicity. The choice of wavelength of analysis must take into account the need for maximum sensitivity and selectivity for the drug of interest. The ultraviolet absorption spectrum of KTZ revealed that the wavelength of maximum absorption of KTZ was 206 nm. The analytical column was selected based on the physicochemical characteristics of KTZ, the column length and the type and size of packing material. The efficiency of the column was evaluated using an ideal test system prior to selection of a particular column for analysis of KTZ. A 5µm, 150 × 4.6 mm I.D Beckman® ODS column

was selected for use, based on these criteria before commencing method development studies for the analysis of KTZ.

An internal standard (IS) was used during analysis of KTZ. A few azole antifungal agents were screened as potential IS prior to the selection of CLZ as the IS of choice. Optimization of a high-performance chromatographic method was achieved by alteration of the pH and molarity of the buffer, and concentration of the organic modifier used in the mobile phase. The separation of KTZ was eventually achieved using reversed-phase HPLC on a non-polar *n*-octadecylsilane (C_{18} or ODS) stationary phase, whilst the polarity of the mobile phase was adjusted using a mixture of acetonitrile (ACN) and phosphate buffer. ACN was preferred to methanol as the organic modifier since ACN possesses moderate polarity and produced sharp and well resolved peaks.

During the analysis of basic compounds, such as KTZ, it is important to maintain the pH < 8 and conduct the analysis at an intermediate pH to avoid hydrolysis of silica-based columns [275, 284, 289]. Since increased tailing was observed at pH values > 6.0 due to interactions of the basic KTZ and the acidic silanol groups, it was necessary to alter the pH of the buffer accordingly. The influence of parameters such as the mobile phase flow rate and the mobile phase composition on the retention times of KTZ and CLZ were also investigated. A binary mixture of ACN-50 mM phosphate buffer, pH 6.0 (60:40) was considered the most appropriate mobile phase composition for the separation of KTZ and CLZ when used at a flow rate of 1 ml/min. KTZ and CLZ eluted at 3.7 and 8.7 min respectively and the total run time for the analytical procedure was approximately 12 min.

The HPLC method developed for the analysis of KTZ was validated in accordance with the recommendations specified in the United States Pharmacopeia (USP) and by the International Conference on Harmonization (ICH) [314, 323, 324]. Based on the criteria defined in these international protocols, the RP-HPLC method was found to be linear, precise, accurate, specific and sensitive. Stability studies indicated that KTZ is stable in methanol following storage at 4°C for at least 7 days. Since the analytical column was replaced by a new one, re-validation of the method of analysis was essential to ensure validity of the method and to evaluate the performance characteristics of the method with the new column [315]. The data generated during re-validation studies indicated that the HPLC method was linear, precise, accurate, specific and sensitive for

the analysis of KTZ from pharmaceutical formulations. A RP-HPLC method that is simple, rapid, linear, accurate, precise, sensitive and selective and has application for the *in vitro* analysis of KTZ-containing dosage forms has therefore been developed and validated.

CHAPTER FOUR

EVALUATION OF POLYMORPHISM OF KETOCONAZOLE AND SELECTION AND CHARACTERIZATION OF SOLID LIPID FOR THE MANUFACTURE OF KETOCONAZOLE-LOADED SOLID LIPID MICROPARTICLES

4.1. Introduction

The manufacture of solid lipid microparticles (SLM) using hot high pressure homogenization and micro-emulsion techniques require the active pharmaceutical ingredient (API) to be subjected to high temperatures [341]. The hot high pressure homogenization (HPH) technique is associated with the formation of a pre-emulsion prior to homogenization using a piston gap homogenizer [99, 341]. Similarly, the micro-emulsion technique involves the formation of a micro-emulsion at temperatures above the melting point of the lipid [183]. The drug-lipid molten phase is formed following heating of the lipid to a temperature that is 5-10°C above its melting point and incorporating the API into the molten lipid [99, 341]. The melting process in these production techniques, albeit essential for the incorporation of the API into the bulk lipid, may precipitate temperature-induced degradation of the API or lipid carrier and may lead to changes in their physicochemical properties [183, 245, 342, 343].

Perusal of the literature reveals that KTZ melts at 146°C with no mass-dependent decomposition occurring in the range of 25-200°C supporting the fact that KTZ is likely to be chemically stable under the production conditions used during the manufacture of KTZ-loaded SLM using hot HPH and micro-emulsion techniques [343]. The chemical degradation of KTZ leads to a change in colour from white to purple that is visible to the naked eye [343]. Therefore, for the purposes of this research visual assessment of the KTZ-loaded SLM formulations was deemed sufficient to detect signs of chemical instability and no colour changes were observed in any event.

Investigating the solubility of KTZ in lipids prior to formulation of KTZ-loaded SLM is essential as the solubility of the API in lipids is likely to dictate the drug loading capacity (DLC) and encapsulation efficiency (EE) [99, 182, 341]. One of the phases of these studies therefore included an assessment of the solubility of KTZ in several lipids to determine the lipid excipient that should be used during formulation development and optimization studies. Preliminary

solubility studies were performed to select a solid lipid with the highest solubilizing potential for KTZ.

It has been intimated that the methods used in the formulation of SLM may lead to changes in the polymorphic and crystalline states of the SLM in relation to those of the bulk lipid from which the microparticles were manufactured [241, 344]. The objectives of these studies were to establish the thermal stability, polymorphic behaviour and crystallinity of KTZ and Labrafil® M2130 CS used for the manufacture of micro-particulate delivery systems. These studies therefore included an investigation of the polymorphic and crystalline behaviour of the lipid carrier, Labrafil® M2130 CS and KTZ and a 1:1 combination of Labrafil® M2130 CS and KTZ prior to and after exposure to a temperature of 60°C for 1 hour using differential scanning calorimetry (DSC) in conjunction with Fourier-transform infra-red (FTIR) spectroscopy. The thermal and spectroscopic analyses of a mixture of KTZ and Labrafil® M2130 CS were performed to establish whether Labrafil® M2130 CS interacted with KTZ in any manner.

4.1.1. Differential scanning calorimetry

DSC is a simple thermo-analytical technique that is commonly used to assess the purity, thermal kinetic constants, phase equilibria and transitions of substances [345-349]. In addition DSC is used in the characterization of drugs and excipients during preformulation studies where it is applied to elucidate potential structural changes caused by solid-state interactions and polymorph formation [349-352]. Interactions such as drug-excipient incompatibility are easily detected using DSC which makes it a valuable tool during product development [351, 353-355]. Furthermore, due to its convenience and relative speed, DSC has been reported to have a wide scope of practical applications *viz.*, the evaluation of thermal stability, chemical reactivity, decomposition behaviour and the qualitative and quantitative analysis of drugs and drug mixtures [351, 355-358]. One of the main advantages of DSC is that small samples of between 2 and 5 mg are required for analysis [359]. A common application of DSC in the food and pharmaceutical industry includes the characterization and determination of the phase behaviour of lipids and starches such as in the discrimination of olive oil categories, determination of oil quality and stability with regards to lipid oxidation in vegetable oils, thermal analysis of starches and in the screening of lipid excipients which are of potential use in drug delivery [360-366].

The principle of DSC is based on the manipulation of temperature to obtain an indirect measurement of differential power during thermal events such as melting, dehydration, crystallization or glass transition phenomena [359]. DSC is a thermal analytical method in which two samples, the reference or control sample and the substance of interest are heated at a constant rate using a controlled temperature-heating programme in identical sample holders or cells [346-348, 359]. In heat flux DSC the temperature of the reference sample and the substance of interest usually increase at the same rate during the controlled heating programme and under ideal conditions there are no differences between the temperatures of the two cells, provided no cooperative structural changes occur in the sample of interest [345, 346, 348]. Melting and crystallization are accompanied by the uptake and emission of heat respectively whilst polymorphic transitions may absorb or release heat into a system [345, 348, 359]. During such transitions the energy input into the system is used for the transition resulting in the sample temperature remaining constant [345, 348]. A temperature difference therefore exists between the reference and the sample cells and this temperature difference is measured using a thermal electric device for which the voltage is proportional to this temperature difference [348]. The voltage is subsequently converted to a differential heat flow signal through a calibration procedure and the signal obtained is plotted as a thermogram [348]. In power compensation DSC the two cells are heated by separate energy sources in a heat sink and the samples are maintained at a constant temperature by an automatic adjustment of the heating power in case of temperature differences [347, 348, 367]. The amount of energy or heat required to attain the desired sample temperature is measured in both cells and is directly correlated to the heat flow into or out of the samples [347]. The heating power or energy input is lower in the reference sample compared to the material of interest and this differential heat flow may be plotted on a thermogram as a function of temperature or time [347]. The DSC curve may be used to retrieve the transition temperature and precisely calculate the standard enthalpy and entropy changes of the thermal event [348, 359, 367]. The standard enthalpy change may be determined from the integral of the signal obtained during a particular transition [348, 367].

Peak-shaped signals are generally obtained during first-order transitions such as melting, crystallization and polymorphic transitions [348, 367]. The shape of the DSC curve may also provide useful information about the presence of polymorphs and the character of the transition itself and indicate the presence of impurities which lead to broadening of the curve and in which case peak asymmetry may be indicative of the type of interaction of the impurity with the material of interest [348, 367]. Glass transitions tend to have a characteristic step-like deviation

from the baseline position [348]. Any large shift in melting point may be indicative of a strong solid-solid interaction although it may not necessarily indicate an incompatibility. Smaller peaks, extra-thermal effects or peaks which have completely disappeared may also indicate incompatibilities [347, 348]. In addition DSC may be used for the identification of solvates that are known to modify pharmaceutical properties such as solubility, dissolution rate, bioavailability and chemical stability and preformulation studies may have to include thermal characterization of the solvent of crystallization to determine the enthalpy of desolvation [346, 368, 369].

DSC is a powerful screening tool in preformulation studies as it is possible to derive information relating to potential physical or chemical incompatibilities between an API and potential excipients, thereby facilitating the rational selection of materials for use in dosage form design and development [370]. However, it is worth noting that DSC alone may not be adequate in establishing solid-solid interactions arising from formulation processes which may only be conclusively identified using other supportive analytical techniques and long-term stability studies [367, 370]. Although it may be possible to monitor and quantify minute thermal events in a sample and the temperatures at which these occur, DSC may not definitely determine the cause of a thermal event and it may not be possible to clearly differentiate between certain thermal events. For instance, a shift in a melting endotherm may be due to degradation, polymorphism, presence of solvates, transformation or changes in the crystalline structure of the compound of interest which may be need to be substantiated using complementary methods such as thermogravimetric analysis, spectroscopic approaches and/or X-ray diffraction [348, 367, 370, 371]. During thermal analysis of lipids, DSC may be used to predict the polymorphic behavior of lipids although X-ray diffraction techniques such as wide angle X-ray diffraction (WAXD) and small angle X-ray diffraction (SAXD) may be required to confirm the polymorphic states and the crystalline behaviour of the bulk lipid [363, 372, 373]. It was therefore deemed necessary to use a spectroscopic technique to rule out possibilities of degradation, transformation and presence of solvates in preformulation studies when the API and the lipid excipients are subjected to elevated production temperatures. Fourier-transform infra-red (FTIR) spectroscopy was considered an appropriate complementary technique for these preformulation studies and was used in conjunction with DSC to elucidate the thermal behavior of KTZ and lipid excipients. DSC provides thermodynamic data on the phase behaviour of lipids whilst FTIR spectroscopy provides molecular level details relating to interactions and changes occurring in lipids prior to and following exposure to heat [363, 374].

4.1.2. Fourier-transform infrared spectroscopy

Fourier transform infra-red spectroscopy (FTIR) is commonly used in the characterization of the solid-state properties of solid dispersion co-precipitates in routine pharmaceutical analysis [369, 375, 376]. FTIR analysis may be useful in identifying potential interactions between an API and a carrier from an assessment of the chemical bond shifts in the infra-red (IR) spectrum [355, 377, 378]. In addition FTIR spectroscopy may be used to derive important structural information on chain conformation and packing arrangements in molecules such as lipids, polypeptides and polymers since IR absorption patterns are known to be different for all molecules even when similar frequencies of vibration are present [363, 379-382]. The use of FTIR in the study of fats, oils and solid lipids is common and invaluable for the determination and verification of organic structures as these molecules absorb electromagnetic radiation in the infra-red region (4000 and 700 cm^{-1}) resulting in differences in intensities and frequencies of absorption by different types of bonds [363, 380, 383-386].

FTIR has been widely used in the characterization of pharmaceutical systems, particularly in raw material identification and qualification, solid-state characterization of drugs and physiochemical characterization of lipids and excipients for the identification of polymorphic and crystal forms [376, 380-383, 387-393]. FTIR spectrometers are usually preferred for IR analysis as they acquire data in a few minutes using only a few milligrams of sample and are accurate even in the presence of trace amounts of impurities which may also be identified [387, 394, 395]. Furthermore, FTIR spectrometers, particularly those equipped with attenuated total reflectance (ATR) technology are convenient, rapid and easy-to-use for routine fingerprinting of molecules [374, 379].

The IR absorption process is based on the excitation of molecules to a higher energy state when they absorb IR radiation which is a quantized process leading to the stretching and bending of bonds in covalent molecules [367, 375, 394, 396, 397]. It is important to note that only bonds with a dipole moment are capable of absorbing IR radiation and therefore symmetrical bonds such as those of alkenes and alkynes do not absorb IR radiation [396, 397]. Analysis of solids using FTIR may be performed using different methods of sample preparation including the potassium bromide (KBr) pellet method and the Nujol mull method [367, 374, 375]. The KBr pellet approach involves finely grinding the solid substance with powdered KBr and pressing the mixture under high pressure which melts the KBr and incorporates the sample into a matrix

forming a KBr pellet [374, 396, 397]. The solid sample may also be ground with the mineral oil known as Nujol to form a suspension with the finely ground solid dispersed in the oil or dissolved in an organic solvent such as carbon tetrachloride prior to analysis [396-398]. These methods of sample preparation have limitations: for instance, KBr tends to be hygroscopic which may interfere with the spectrum and the use of Nujol oil or carbon tetrachloride during sample preparation may produce obscure spectra [374, 398]. An alternative to these techniques for IR analysis includes the use of attenuated total reflectance (ATR) technology which addresses the main challenges of IR analysis namely sample preparation and spectral reproducibility [374, 379, 399]. FTIR coupled with ATR technology offers practical advantages over other spectroscopic methods as no sample preparation is required prior to analysis. In traditional FTIR spectroscopy sample preparation may induce solid-state transformations and introduce interferences as a result of environmental humidity [374, 379, 399]. Spectral bands obtained during FTIR analysis may be assigned to specific features of the molecule under investigation and the presence of polymorphic forms may be identified due to the appearance of unique bands or peak shifting in the IR spectrum [367]. Furthermore, the co-existence of amorphous states of the drug may be detected from broadening of the peaks in the IR spectrum [367, 396].

The principle of ATR FTIR is based on the measurement of the changes that are produced when an IR beam is subjected to total internal reflection when it comes into contact with a sample placed on an optically dense crystal surface [399]. The quantum mechanical properties of light leads to an extension of the electromagnetic field beyond the crystal surface such that an evanescent wave, produced for approximately 0.5 to 5 µm above the surface, senses the IR-absorbing sample [399]. The evanescent wave or field is subsequently attenuated or altered before returning to the IR beam producing the IR spectrum [399]. When using ATR technology it is imperative that the sample must be in direct contact with the crystal surface as the evanescent wave only protrudes above the crystal surface for a few microns [399]. In addition the refractive index of the crystal must be higher than that of the sample for total internal reflection to be produced and ATR crystals typically have refractive indices between 2.38 and 4.01 at 2000 cm^{-1} as solids and liquids tend to have lower refractive indices [399]. Crystal materials commonly used for ATR analysis include zinc selenide (ZnSe), germanium and diamond of which diamond has been reported to exhibit greater robustness and durability and exhibits minimal lifetime replacement costs [399]. However, ZnSe and germanium are often selected as crystal materials of choice for routine ATR sampling due to the high original purchase costs associated with diamond [399]. FTIR coupled with ATR technology was used in these studies to identify potential

molecular changes that may occur in KTZ and the lipid after exposure to high temperatures used during production of SLM.

4.2. Materials

4.2.1. Overview

The materials that were used in solubility studies and thermal analyses are known to have GRAS status and are approved for oral and/or IV use in humans by one or more international regulatory authority [400-402]. The physicochemical parameters of KTZ have been previously summarized in Chapter 1, § 1.2 *vide infra*. KTZ used during these studies was purchased from Oman Chemicals and Pharmaceuticals, Al Buraimi, Sultanate of Oman. The materials used in these studies were at least of analytical reagent grade and were used as received from the suppliers without further testing.

4.2.2. Solid lipid excipients

4.2.2.1. Precirol® ATO5

Precirol® ATO 5 (Gattefossé SAS, Saint-Priest Cedex, France) is the proprietary name for glyceryl palmitostearate, which consists of a mixture of relatively short chain length acylglycerols of distearate, tripalmitin and tristearin [403, 404]. Precirol® ATO 5 occurs as a fine white or almost white powder of well-controlled particle-size distribution with an indicative particle size of 50 µm and has a faint odour [403, 405, 406]. The melting point of Precirol® ATO 5 lies between 52 and 55°C [403]. It has been reported that Precirol® ATO 5 is freely soluble in chloroform and dichloromethane and practically insoluble in ethanol, mineral oil and water [403]. Precirol® ATO 5 is classified as a non-ionic agent with a low HLB value of 2.0 [403-405]. It is advisable not to store Precirol® ATO 5 at temperatures exceeding 35°C and Precirol® ATO 5 must be stored at a temperature of between 5 and 15°C in an airtight container protected from light and moisture [403]. Precirol® ATO 5 has a hydroxyl value of 90-110, an acid number of < 6, an iodine number < 3 and a saponification number ranging from 175 to 195 [404]. The manufacture of Precirol® ATO 5 involves direct esterification of palmitic and stearic acids with glycerol without a catalyst and Precirol® ATO 5 is regarded as an essentially non-toxic and non-irritant material, with a GRAS status [403]. The uses of Precirol® ATO 5 are diverse, ranging from being used as a lipophilic agent, excipient, tableting binder to a lubricant for solid and

semisolid sustained release formulations [404, 406]. It has been reported that Precirol® ATO 5 protects drugs and improves the stability of dosage forms [404].

4.2.2.2. Compritol® 888

Compritol® 888 (Gattefossé SAS, Saint-Priest Cedex, France) is the proprietary name for glyceryl behenate [407]. Glyceryl behenate is described as a mixture of glycerides of fatty acids, mainly behenic acid with a content of 1-monoglycerides between 12.0 and 18.0% [407]. The non-proprietary name for Compritol® 888 is glyceryl dibehenate and Compritol® 888 occurs as a mixture of diacylglycerols, mainly dibehenylglycerol, with varying amounts of mono- and triacylglycerols [408]. Compritol® 888 occurs as fine white or almost white to yellow powder or hard waxy mass or unctuous flakes with a faint odour and a low HLB value of 2.0 [404, 405, 407, 408]. The melting point of Compritol® 888 falls between 65 and 77°C [407, 408]. Compritol® 888 is practically insoluble in hexane, mineral oil and water and is soluble, on heating, in chloroform, dichloromethane and ethanol (96%) [404, 407, 408]. Compritol® 888 decomposes on heating to produce acrid smoke and irritating fumes [407]. It has been reported that Compritol® 888 has an acid number < 4, an iodine number < 3 and a saponification number between 145 and 165 [404].

The production of Compritol® 888 occurs via esterification of glycerin by behenic acid (C_{22} fatty acid) without the addition of catalysts [407]. Raw materials of vegetable origin are used for the preparation of Compritol® 888 and the resulting esterified material is atomized by spray-cooling [407]. Compritol® 888 has a GRAS status and is generally regarded as a relatively non-irritant and non-toxic material [407]. Compritol® 888 should be stored in its original airtight container at a temperature < 35°C and it is recommended to prevent the exposure of Compritol® 888 to air, light, heat and moisture [404, 407]. Compritol® 888 has a hydroxyl value of 80-105 [238]. The fatty acid fractions of glycerol dibehenate, as determined by gas chromatography consist of palmitic, stearic, arachidic, erucic and lignoceric acids [408]. Compritol® 888 has been used in the formulation of modified release tablets, as a lubricant for tablets produced by direct compression and as a lipid excipient in melt processing techniques such as spray cooling and hot melt extrusion [409].

4.2.2.3. Labrafil® M2130 CS

Labrafil® M2130 CS (Gattefossé SAS, Saint-Priest Cedex, France) is the proprietary name for lauroyl macrogol-6-glycerides EP or lauroyl polyoxyl-6 glycerides NF [410]. Labrafil® M2130 CS occurs as a pale yellow waxy semisolid with a relatively low HLB value of 4 [410]. The manufacture of Labrafil® M2130 CS occurs via a trans-esterification procedure involving a C_{12-18} glyceride and polyethylene glycol [411]. Labrafil® M2130 CS has a melting range of 38 to 40°C [404, 410, 411]. Labrafil® M2130 CS has a hydroxyl value of 90-110, an acid value < 2, a saponification value between 185 and 200 and an iodine value < 3 [411]. Labrafil® M2130 CS is freely soluble in chloroform and dichloromethane, partly soluble in ethanol and practically insoluble in mineral oils and water [404]. Labrafil® M2130 CS must be stored at a temperature of 5-15°C in an airtight container protected from light and moisture and should not be stored at temperatures exceeding 35°C [410]. Labrafil® M2130 CS is composed of well-characterized PEG-esters and a glyceride fraction and is regarded as an essentially non-toxic and non-irritant material with GRAS status [410]. The safety of use of Labrafil® M2130 CS has been established by substantial toxicological data and its precedence of use in approved pharmaceutical formulations [410]. Labrafil® M2130 CS may be used in oral and topical formulations as a solubilizer and is known to act as a bioavailability enhancer for oral formulations [410]. Furthermore, Labrafil® M2130 CS is able to self-emulsify when in contact with aqueous media resulting in a coarse dispersion or a fine micro-emulsion and its surface-active properties improve the solubility of poorly soluble API *in vitro* and *in vivo* making it valuable in the formulation of self-emulsifying lipid formulations [410]. In topical ointments, microemulsions and emulsions, Labrafil® M2130 CS is able to act as a water-in-oil surfactant which enhances drug penetration [410]. In addition Labrafil® M2130 CS is also used in the formulation of tablets and hard and soft gelatin capsules [410].

4.2.2.4. Gelucire® 44/14

Gelucire® 44/14 (Gattefossé SAS, Saint-Priest Cedex, France) is the proprietary name for lauroyl macrogolglycerides or polyoxyglycerides [412]. Gelucire® 44/14 is produced from hydrogenated palm kernel oil and polyethylene glycol and is comprised of a mixture of polyethylene glycol 33 (PEG 33, MW 1500), glycerides, glycerol and PEG mono- and diesters of fatty acids, with the most common fatty acid chain in the mixture being lauric acid in a proportion of 40-50% w/w, of which more than 80% are saturated [412, 413]. The final composition of Gelucire® 44/14 is

approximately 72% w/w PEG esters, 20% w/w glycerides, 8% w/w pure PEG and 2% w/w glycerol [412, 413]. Gelucire® 44/14 occurs as a waxy solid with a faint odour and melts at 44ºC, with its drop point ranging between 42.5 and 47.5°C [404]. It has been reported that Gelucire® 44/14 dissolves in chloroform, dichloromethane and ethanol but is insoluble in mineral oils [404]. The properties of Gelucire® 44/14 such as its high HLB value of 14 make it a good additive as a bioavailability enhancer and solubilizer for inclusion in the formulation of poorly soluble drugs [404, 412, 413]. The safety of Gelucire® 44/14 is substantiated by in-depth toxicological evaluations and precedence of use in approved pharmaceutical products [412]. Gelucire® 44/14 is often used to improve the release of poorly soluble API in a number of oral delivery systems such as granules, tablets, hard gelatin capsules, and self-emulsifying lipid formulations [404, 412, 413]. Gelucire® 44/14 has an acid number < 2, an iodine number < 2, a saponification number between 79 and 93 and a hydration number between 36 and 56 [404]. Studies have shown that Gelucire® 44/14 is susceptible to hydration in the presence of at least 5% w/w water content at high humidity levels such as 75% RH [414]. It is therefore advisable to store Gelucire® 44/14 in its original airtight container away from air, light, heat and moisture [404, 412, 414].

4.2.2.5. Gelucire® 50/13

Gelucire® 50/13 is the proprietary name for stearoyl macrogolglycerides or polyoxyglycerides [415]. Gelucire® 50/13 occurs as white waxy solid pellets with an HLB value of 13 [415]. Gelucire® 50/13 melts at 50ºC with a drop point ranging between 46 and 51°C [404]. Gelucire® 50/13 is used in the formulation of a number of delivery systems such as capsules, granules, tablets and self-emulsifying lipid formulations as it forms a fine dispersion or micro-emulsion by self-emulsification when in contact with aqueous media [415]. Gelucire® 50/13 possesses surface-active characteristics that enhance *in vivo* drug solubilization thus improving the bioavailability of poorly soluble drugs and facilitating their absorption [413, 415]. The use of Gelucire® 50/13 tends to result in immediate release preparations due to its high HLB value particularly when used in melt granulations [415]. However, Gelucire® 50/13 may also be used as an excipient in hard gelatin capsules as a controlled-release agent and to protect API [413, 415]. In addition Gelucire® 50/13 exhibits good thermo-plasticity for use as a binder in melt processes and is a good excipient for use in melt processing approaches for capsule filling [415]. Gelucire® 50/13 has an acid number < 2, an iodine number < 2 and a saponification number between 65 and 80 [404]. Gelucire® 50/13 has GRAS status supported by toxicological data and precedence of use in approved products [404, 415].

4.2.3. Water

Water used in these studies was of HPLC ultra pure grade and was prepared using a Milli-RO® 15 water purification system (Millipore Co., Bedford, MA, USA) that consisted of a Super-C® carbon cartridge, two Ion-X® ion-exchange cartridges and an Organex-Q® cartridge. The water was filtered through a 0.22 μm Millipak® 40 stack filter (Millipore Co., Bedford, MA, USA) prior to use.

4.3. Methods

4.3.1. Characterization of KTZ

4.3.1.1. DSC characterization of KTZ

The melting range and changes in the melting behaviour of KTZ were determined using a Perkin-Elmer DSC-7 Differential Scanning Calorimeter (Perkin-Elmer, Norwalk, Connecticut, USA). A 2.6402 mg sample of KTZ was weighed using a Mettler Toledo top-loading analytical balance (Mettler Instruments, Zurich, Greifensee, Switzerland) and was hermetically sealed into a standard 40 μl aluminium pan. The instrument was calibrated for temperature using 5.0 mg high purity indium and DSC curves for KTZ samples were generated by heating the sample from 25ºC to 250ºC and subsequently cooling to 25ºC at heating and cooling rates of 10ºC/min. The reference standard used was an empty pin-holed aluminium pan sealed in a similar manner to the pan containing the sample. The DSC profile for KTZ was generated prior to and following exposure of the API to a temperature of 60ºC for 1 hour in order to determine the influence of heat on the physicochemical properties of KTZ. Parameters such as temperature onset, maximum peak and enthalpy were established using Pyris™ Thermal Analysis Manager software (Perkin-Elmer, Shelton, Connecticut, USA) coupled to the Perkin-Elmer DSC-7 Differential Scanning Calorimeter.

4.3.1.2. FTIR characterization of KTZ

The FTIR spectra of KTZ prior to exposure to heat was generated as described in § 1.2.6 using a sample of KTZ weighing approximately 2 mg. FTIR analysis was also performed on a sample of KTZ following exposure to heat to identify any changes in chemical bond shifts, broadening of peaks or the presence of unique bands in the IR spectrum which might be indicative of polymorphic modifications that may have occurred following heating. A 10 mg sample of KTZ was weighed using a Mettler Toledo top-loading analytical balance (Mettler Instruments, Greifensee, Zurich, Switzerland) and transferred to a screw-capped test tube that was heated at 60ºC for one hour and cooled to cooling 25ºC. Spectral data were collected over the IR spectrum in the region of 515-4000 cm^{-1} using samples weighing approximately 5 mg. The resultant chemical bond shifts were used to analyze the spectra for possible interactions and polymorphic changes in the IR spectrum of KTZ.

4.3.2. Selection of solid lipid excipient

4.3.2.1. Solubility studies

As there are no standard methods to determine the solubility of a drug in a solid lipid, the solubility of KTZ was investigated by dissolving increasing amounts of KTZ in the different lipids in the molten state and visually assessing the drug-lipid melt to establish whether drug crystals had dissolved in the molten lipid dispersion. The solubility of KTZ in solid lipids was determined using a shaking water bath (Laboratory Thermal Equipment, Greenfield, Oldham, United Kingdom) set to 50 rpm and with the temperature set to 60°C. Briefly 1.0 g of solid lipid and 0.05 g of KTZ were accurately weighed using a top-loading analytical balance (Mettler Instruments, Greifensee, Zurich, Switzerland) and transferred to a screw-capped test-tube. The solid lipid-KTZ mixture was melted in the water bath at 60°C and then mixed using a vortex mixer to facilitate the dissolution of the KTZ in the molten lipid. The drug-lipid mixture was allowed to shake and the solubility of KTZ in the molten lipid was assessed visually by observing the clarity of the molten lipid after the addition of KTZ. Following dissolution of KTZ the initial concentration of 5% w/w was increased to 10% w/w, 15% w/w, 20% w/w and higher until saturation solubility of KTZ in the solid lipid was reached. The point at which the saturation solubility was reached occurred when KTZ crystals failed to dissolve in the molten lipid after allowing the mixture to shake for 12 hours at 60ºC. The solid lipid that was found to exhibit the best solubilising potential for KTZ was selected for further thermal and spectroscopic analyses.

4.3.2.2. Polymorphism of bulk lipid

Polymorphic modifications that might occur when bulk lipid material is subjected to temperatures used in the production of SLM were established by assessing the crystallinity of the solid lipids prior to and following heating using DSC. The first step in the production of SLM involves heating the bulk lipid prior to dispersing the molten lipid in a hot aqueous surfactant solution. The initial melting of the lipid materials before homogenization may result in changes in the polymorphic form of the lipid, which may in turn affect the crystallinity of the lipid in the SLM, thereby impacting on the stability of the SLM.

4.3.2.2.1. DSC characterization of Labrafil® M2130 CS

The DSC system used in these studies has been described in § 4.3.1.1. The DSC thermograms for the bulk solid lipid excipient were generated from a scan of a sample of the solid lipid prior to exposure to heat and scanning the solid lipid that had been heated from 25ºC to 60ºC for one (1) hour and left to cool to 25ºC. The weight of the samples analyzed was between 2 to 5 mg and the reference used was an empty pin-holed 40 µl aluminium pan.

4.3.2.2.2. FTIR characterization of Labrafil® M2130 CS

The FTIR spectrum of the solid lipid was generated as described in § 1.2.6 for a sample weighing approximately 2 mg at room temperature, prior to exposure to heat. Thereafter, analysis of a sample of the solid lipid following heating to 60ºC for one (1) hour and then cooled to 25ºC was conducted. Spectral data were collected over the IR spectrum in the region of 515-4000 cm^{-1} and resultant chemical bond shifts were used to analyze the spectra for possible polymorphic modifications of KTZ.

4.3.2.3. Interaction of bulk lipid with KTZ

DSC and FTIR analyses were also used to investigate for potential interactions between Labrafil® M2130 CS and KTZ using methods similar to those described in § 4.3.1.1 and 4.3.1.2, respectively. The concentration of KTZ in the solid lipid-drug mixture was 50% w/w to ensure saturation solubility had been reached. DSC and FTIR scans were performed on an unheated sample of KTZ and the lipid and a homogenous sample of the drug-lipid mixture that had been exposed to heat. The unheated binary mixture of KTZ and solid lipid was prepared by crushing

the lipid with KTZ in a 1:1 ratio using a mortar and pestle. The binary mixture that was exposed to heat was prepared by heating KTZ and the solid lipid (1:1) to 60ºC for one (1) hour and allowing the mixture to stand at room temperature (25ºC) for 24 hours. The weights of the samples used for the DSC analysis were between 2 and 5 mg.

4.4. Results and discussion

4.4.1. Characterization of KTZ

4.4.1.1. DSC characterization of KTZ

DSC was used to elucidate the melting, crystalline and polymorphic nature of KTZ prior to and following exposure to a temperature of 60ºC for one (1) hour. The DSC profile of KTZ generated before and after exposure to heat is depicted in Figure 4.1. The melting events are summarised in Table 4.1 including the width of the melting events (WME) which is calculated as the difference between melting and onset temperatures. The magnitude of the WME may be used as a measure of lattice defects within the crystal structure [241].

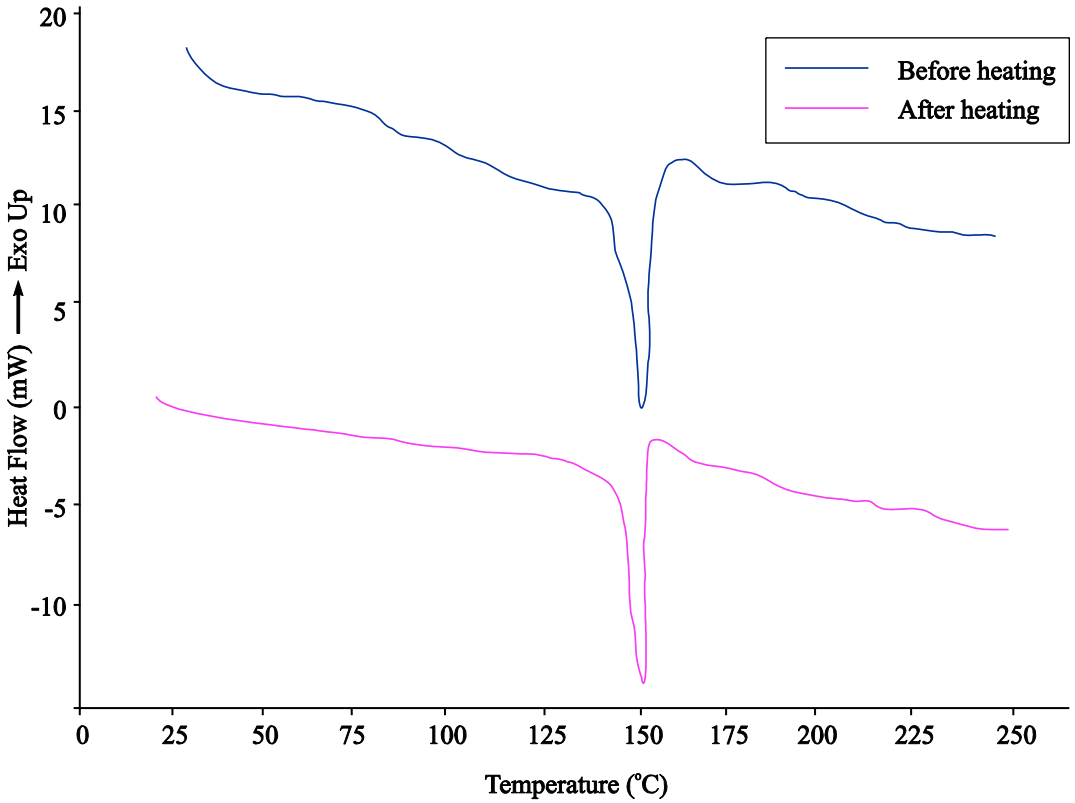

Figure 4.1 DSC profile of KTZ prior to and following exposure to 60°C for one (1) hour

Table 4.1 DSC parameters for KTZ obtained prior to and after exposure to 60°C for one (1) hour

KTZ	Thermal event	Onset (°C)	MP (°C)	Enthalpy (J/g)	WME (°C)
Prior to heating	Endothermic	146.42	149.27	156.84	2.85
After heating	Endothermic	145.85	149.13	138.37	3.28

The DSC curve for KTZ prior to exposure to heat shows the presence of an endothermic thermal event with an extrapolated onset temperature and peak maximum occurring at 146.42°C and 149.27°C, respectively with a corresponding enthalpy of 156.84 J/g. This event is indicative of the melting of a stable polymorphic modification of KTZ and the relatively narrow width of the melting event of 2.85°C and sharp and distinct endothermic peak reveal the highly crystalline structure of KTZ. No major changes were observed in the melting behaviour of KTZ after exposure to 60ºC for one (1) hour although a slight decrease from 149.27°C to 149.13 °C was noted in the peak maximum. This decrease in peak temperature was considered insignificant and could not be associated with the presence of new polymorphic modifications as only changes of more than two degrees in the peak maximum are known to be related to the formation of new crystalline forms [416, 417].

In addition a reduction in enthalpy and extrapolated onset temperature from 156.84 J/g and 146.42°C to 138.73 J/g and 145.85°C were noted, coupled with a broader WME of 3.28°C following exposure to heat. The broadening of the WME accompanied by a decrease in enthalpy, onset temperature and intensity of the endotherm obtained for KTZ scanned after exposure to heat may possibly be attributed to a slight reduction in the degree of crystallinity of KTZ.

4.4.1.2. FTIR characterization of KTZ

FTIR was used to determine if any molecular changes occurred in KTZ following exposure to heat and differences in peak temperatures observed in DSC may imply the occurrence of chemical changes in the structure of KTZ or the presence of polymorphic modifications which may result in a change in crystalline forms after exposure to heat. The IR spectrum of KTZ exposed to a temperature of 60ºC for one (1) hour was compared to the spectrum obtained for KTZ prior to heating (Chapter 1, Figure 1.2 *vide infra*) to identify any changes in the characterisitic band assignments. The relevant band assignments are depicted in Figure 4.2 and summarized in Table 4.2.

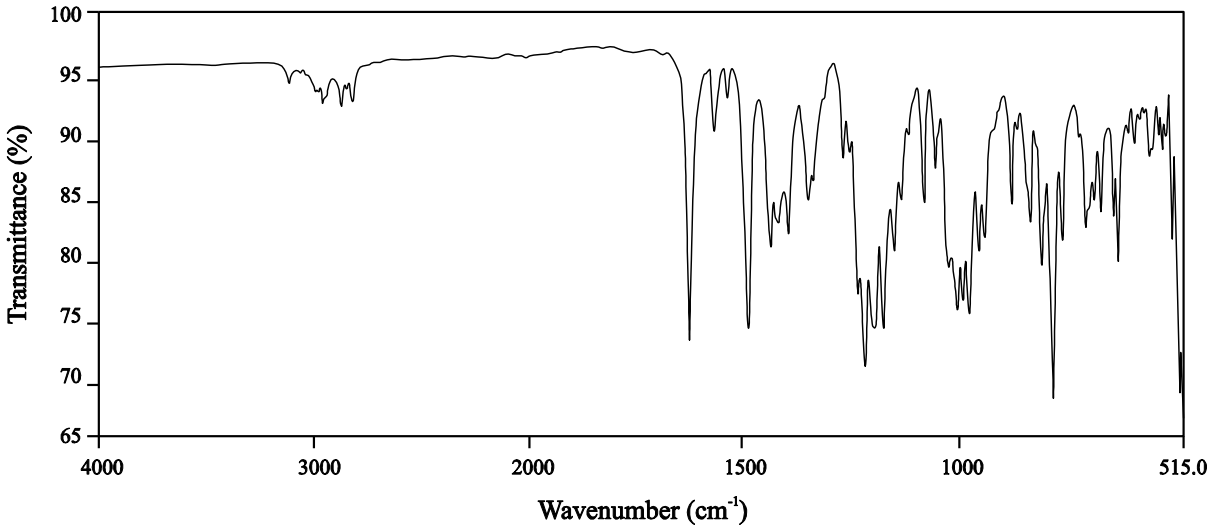

Figure 4.2 Infra-red spectrum of KTZ following exposure to 60°C for one (1) hour

Table 4.2 Major infra-red band assignments for KTZ prior to and following exposure to 60°C for one (1) hour

Band position (cm^{-1})		**Assignment**
Prior to exposure to 60°C for 1 hour	**After exposure to 60°C for 1 hour**	
3177	3179	sp^2 C-H stretch
2976	2976	sp^3 C-H stretch
1645	1643	C=O stretching of the ketone (conjugation with imidazole ring)
1458	1457	C-N stretching of the imidazole
1256	1255	C-O stretching of the cyclic ether group
1240	1241	C-C=O bend of the ketone NR
1031	1030	Ar-C-O stretching of the ether
737	740	C-Cl stretching of chlorine

The wavelengths characteristic of KTZ, 1643, 1457, 1255, 1241, 1030, 740 cm^{-1} remained unchanged indicating the absence of new crystal forms. The baseline height was also almost constant prior to and following exposure of KTZ to heat. Therefore, major differences in the degree of crystallinity of KTZ are unlikely. A decrease in the intensity of some peaks was recorded after exposure of the KTZ sample to heat and this may be attributed to changes in the crystal habits during crystal growth resulting in changes in the physicochemical properties of KTZ as observed from the differences in peak maxima during DSC studies [416]. Conversely, it is evident from FTIR studies conducted on KTZ prior to and following exposure to heat that KTZ consists of the same polymorphic modification and that new polymorphic forms of KTZ are not produced when heated to a temperature of 60°C. Nevertheless, it is worth noting that further studies using complementary tools such as X-ray diffraction may be required to expound the significance of the possible changes in crystallinity and crystal habit of KTZ observed during

DSC and FTIR analysis. The main objective of these studies were to elucidate if polymorphic modifications had occurred following exposure of KTZ to a temperature of 60ºC for one (1) hour from changes in chemical bond shifts, broadening of peaks or occurrence of unique bands in the IR spectrum and FTIR was therefore deemed sufficient when used with DSC for this purpose.

4.4.2. Selection of solid lipid excipient

4.4.2.1. Solubility studies

Investigating the solubility of KTZ in lipids prior to formulation development and optimization studies is essential as the solubility of the API in lipids will impact on the DLC and EE of particles [99, 182, 341]. Preliminary solubility studies were performed to select a solid lipid with the highest solubilizing potential for KTZ and further analyses using DSC and FTIR were subsequently performed on the solid lipid selected. A summary of the solubility data obtained for KTZ in different solid lipids is listed in Table 4.3.

Table 4.3 Solubility of KTZ in different solid lipid excipients

No.	Solid lipid	MP (°C)	5% w/w KTZ	10% w/w KTZ	15% w/w KTZ	20% w/w KTZ
1	Precirol® ATO5	52-55	Soluble	Partially soluble	Insoluble	N/A
2	Compritol® 888	65-77	Soluble	Partially soluble	Insoluble	N/A
3	Labrafil® M2130 CS	38-40	Soluble	Soluble	Soluble	Insoluble
4	Gelucire® 44/14	42.5-47.5	Soluble	Soluble	Insoluble	N/A
5	Gelucire® 50/13	46-51	Soluble	Partially soluble	Insoluble	N/A

The data generated from the solubility studies reveal that KTZ is not very soluble in the solid lipids tested at concentrations exceeding 5% w/w. It appears that Labrafil® M2130 CS has the best solubilising potential for KTZ. The higher solubility of KTZ in Labrafil® M2130 CS compared to the other solid lipid excipients tested could be attributed to the composition of Labrafil® M2130 CS. Solid lipids which consist of mixtures of short-chain length acylglycerols and PEG-esters *viz.*, Labrafil® M2130 CS and Gelucire® 50/13 seem to exhibit a higher solubilising potential for KTZ due to their average lipophilicity and good self-emulsifying properties. Labrafil® M2130 CS consists of PEG-esters and a C_{12} glyceride fraction that is partly unsaturated thus improving the potential for hydrogen bond formation between the API and solid lipid since Labrafil® M2130 CS has a hydroxyl value of 90-110 [410, 411]. Esterification of the PEG components may also lead to an increased potential for formation of hydrogen bonds between the ester components and the KTZ molecule facilitating the dissolution of KTZ. Furthermore, the PEG moiety in Labrafil® M2130 CS imparts self-emulsifying characteristics to the solid lipid which improve its surface-active properties thus enhancing the solubility of poorly

soluble compounds such as KTZ. Labrafil® M2130 CS also has an HLB value of 4 which suggests that it is a good water-in-oil surfactant and wetting agent that reduces the interfacial tension between KTZ and lipid molecules and promotes dissolution of KTZ [410].

Gelucire® 44/14 showed good solubilising potential for KTZ at concentrations of 5-10% w/w. This could be attributed to the PEG-33 moiety in Gelucire® 44/14 that improves its surface active properties and its relatively short chain acylglycerol consisting of a lauric acid (C_{12}) backbone that imparts an average lipophilic character to the lipid [412]. In addition Gelucire® 44/14 has a high HLB value of 14 that contributes to its self-emulsifying characteristics and promotes dissolution of KTZ. Conversely, it appears that Gelucire® 50/13 exhibits a poor solubilising potential for KTZ which may be explained by its longer steroyl backbone (C_{18}), resulting in lipophilicity outweighing self-emulsifying properties [415]. KTZ exhibits poor solubility in solid lipids such as Precirol® ATO5 and Compritol® 888 as these consist of long chain acylglycerols such as stearic (C_{18}) and behenic acids (C_{22}) that tend to increase the lipophilicity of these materials [405]. Furthermore, these lipids have low HLB values of 2.0 which do not seem to promote good wetting of the lipid and KTZ. Consequently, Labrafil® M2130 CS was selected as the solid lipid of choice for use in the development of KTZ-loaded SLM and was subsequently used for thermal and spectroscopic analyses in preformulation studies using DSC and FTIR.

4.4.2.2. Polymorphism of bulk lipid

4.4.2.2.1. DSC characterization of Labrafil® M2130 CS

The DSC profile of Labrafil® M2130 CS generated prior to and following exposure to 60°C for one (1) hour is depicted in Figure 4.3 and the relevant DSC data generated in these studies is listed in Table 4.4.

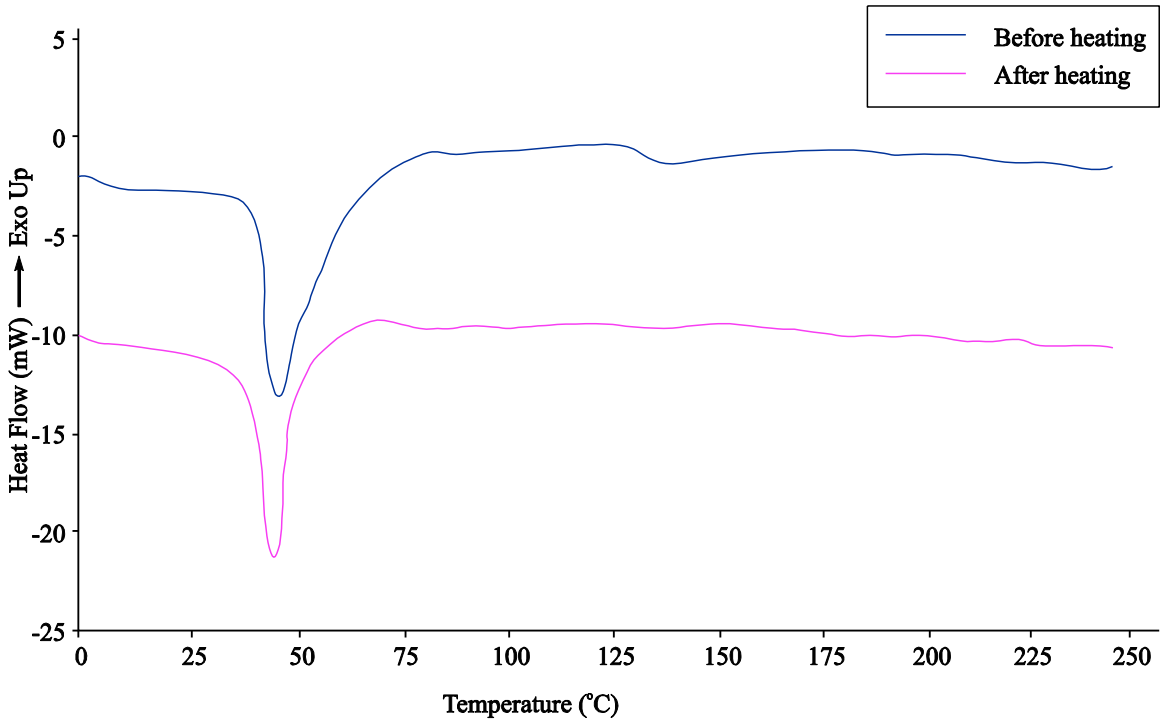

Figure 4.3 DSC profiles of Labrafil® M2130 CS generated prior to and following exposure of the lipid to heat at 60°C for one (1) hour

Table 4.4 DSC parameters for Labrafil® M2130 CS generated prior to and following exposure of the lipid to heat at 60°C for one (1) hour

Labrafil® M2130 CS	Thermal event	Onset (°C)	MP (°C)	Enthalpy (J/g)	WME (°C)
Prior to heating	Endothermic	37.52	39.81	32.41	2.29
After heating	Endothermic	36.40	40.02	35.89	3.62

The DSC scan of Labrafil® M2130 CS generated prior to exposure of the lipid to heat reveals the presence of a single peak with an onset and peak maximum at 37.5°C and 39.8°C thus confirming the presence of a single polymorphic form. The WME of the thermogram is relatively narrow with a value of 2.3°C which may be explained by the slightly amorphous and disordered crystalline structure of the lipid prior to heating. The DSC thermogram of the sample that was exposed to 60°C for one (1) hour before scanning reveals a single melting event at 40.0°C with an onset temperature at 36.4°C. The WME of the DSC curve of Labrafil® M2130 CS after exposure to heat is wider compared to that observed for the unheated lipid. A WME value of 3.6°C could be explained by the presence of defects within the lipid structure, thereby impacting the crystalline structure of Labrafil® M2130 CS. DSC alone cannot be used to confirm the presence of different polymorphic forms of Labrafil® M2130 CS following exposure of the lipid to heat

and it was necessary to use FTIR to confirm if changes in the crystallinity within the lipid structure had occurred.

4.4.2.2.2. FTIR characterization of Labrafil® M2130 CS

The IR spectra of Labrafil® M2130 CS are depicted in Figure 4.4 and the band assignments are summarized in Tables 4.5 and 4.6 for samples investigated prior to and following exposure to heat. The IR spectrum of Labrafil® M2130 CS exposed to a temperature of 60ºC for one (1) hour (Figure 4.4. B) was compared to the spectrum obtained for Labrafil® M2130 CS prior to heating (Figure 4.4. A) to identify if any changes in the characterisitic band assignments for the compound had occurred.

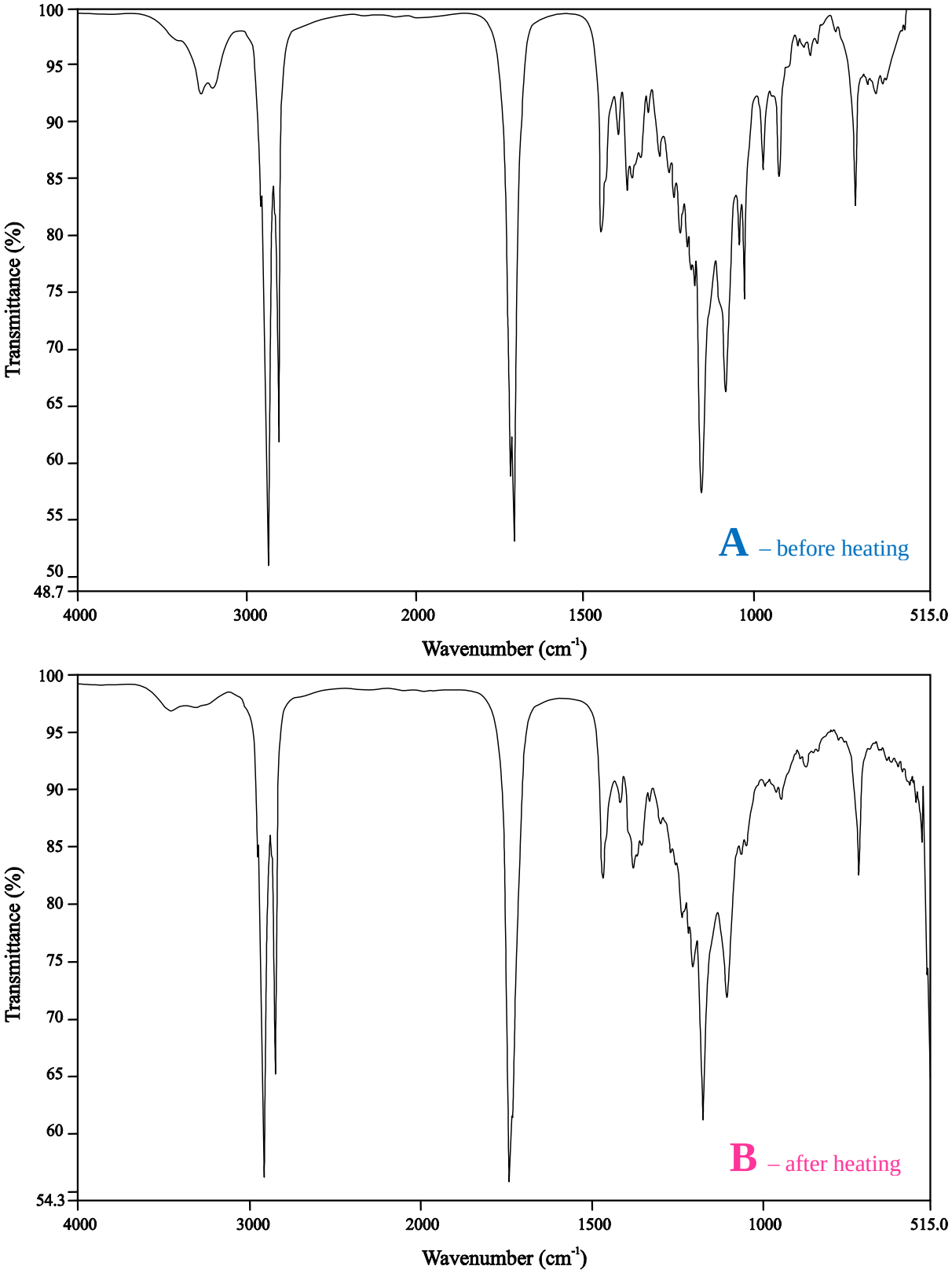

Figure 4.4 Infra-red spectrum of Labrafil® M2130 CS A) prior to exposure to 60°C for one (1) hour and B) following exposure to 60°C for one (1) hour

Table 4.5 Major infra-red band assignments for Labrafil® M2130 CS prior to exposure to 60°C for one (1) hour

Band position (cm^{-1})	Assignment
3405	O-H stretching (water band)
2923	Symmetric stretching of CH_2 *(cis* double bond stretching)
2850	Asymmetric stretching of CH_2
1720	C=O stretching of the ester carbonyl group
1466	Bending vibrations of CH_2 and CH_3 aliphatic groups
1105	Stretching vibration of the C-O ester group
1030	C-O stretching
720	$=CH_2$ wagging

Table 4.6 Major infra-red band assignments for Labrafil® M2130 CS after exposure to 60°C for one (1) hour

Band position (cm^{-1})	Assignment
3380	O-H stretching (water band)
2924	Symmetric stretching of CH_2 *(cis* double bond stretching)
2860	Asymmetric stretching of CH_2
1725	C=O stretching of the ester carbonyl group
1465	Bending vibrations of CH_2 and CH_3 aliphatic groups
1127	Stretching vibration of the C-O ester group
1032	C-O stretching
721	$=CH_2$ wagging

The FTIR spectra of Labrafil® M2130 CS depicted in Figure 4.4 A and B revealed that there is no significant difference in the spectrum of the solid lipid prior to and following exposure to a temperature of 60°C for one (1) hour indicating that the chemical structure of Labrafil® M2130 CS does not change after heating. In addition FTIR analysis of Labrafil® M2130 CS revealed a lack of significant change in broadening of peaks or occurrence of unique bands in the IR spectrum, thereby supporting the data observed in DSC studies suggesting that exposure of the lipid to relatively high temperatures does not change the polymorphic form. The minor differences observed between the two spectra from the band assignments for Labrafil® M2130 CS before and after exposure to 60°C for one (1) hour and summarized in Tables 4.5 and 4.6. The FTIR spectra of Labrafil® M2130 CS showed typical characteristic absorption bands for common triglycerides which may be attributed to the specific functional groups of the principal components of the solid lipid [380, 386, 418, 419]. The differences observed between the two spectra occur due to the stretching, wagging, bending, scissoring vibrations of the CH_2 groups of the acyl chains, a phenomenon known to occur during IR analysis of lipid structures [381]. The band assignments observed for Labrafil® M2130 CS prior to exposure to heat at 2923, 2850, 1466 and 720 cm^{-1} can be explained by the different vibrations of the CH_2 and CH_3 groups and it can be noted that these absorption bands were not significantly different following exposure of the solid lipid to heat on comparison of the two spectra as the corresponding band assignments were noted at 2924, 2860, 1465 and 721 cm^{-1} after exposure to 60°C for one (1) hour. In addition the

presence of water in Labrafil® M2130 CS was detected prior to and after heating of the lipid from the broad bands observed at 3405 and 3380 cm^{-1} respectively in the IR spectra enhancing the possibility of hydrogen bonding occurring within the lipid structure [379]. Furthermore, the interfacial region of the lipid causes strong absorption bands from the ester C=O groups in the triglyceride esters which may be seen in the 1720 to 1750 cm^{-1} region of the IR spectra [379, 381]. In IR analysis of Labrafil® M2130 CS, the carbonyl group stretching prior to and after exposure to heat was observed at 1720 and 1725 cm^{-1}. The lower peak frequency observed for the ester group prior to heating of Labrafil® M2130 CS may be due to the formation of hydrogen bonds between the carbonyl functional group and water [379].

4.4.2.3. Interaction of bulk lipid with KTZ

DSC and FTIR were also used to determine if any interaction occurred between KTZ and Labrafil® M2130. A binary mixture of KTZ and Labrafil® M2130 CS (1:1) was used for thermal and spectroscopic analyses.

4.4.2.3.1. DSC characterization of bulk lipid with KTZ

The DSC profiles generated following analysis of a mixture of KTZ and Labrafil® M2130 CS following heating to 60°C for one (1) hour is depicted in Figure 4.5 and the DSC parameters are summarized in Table 4.7.

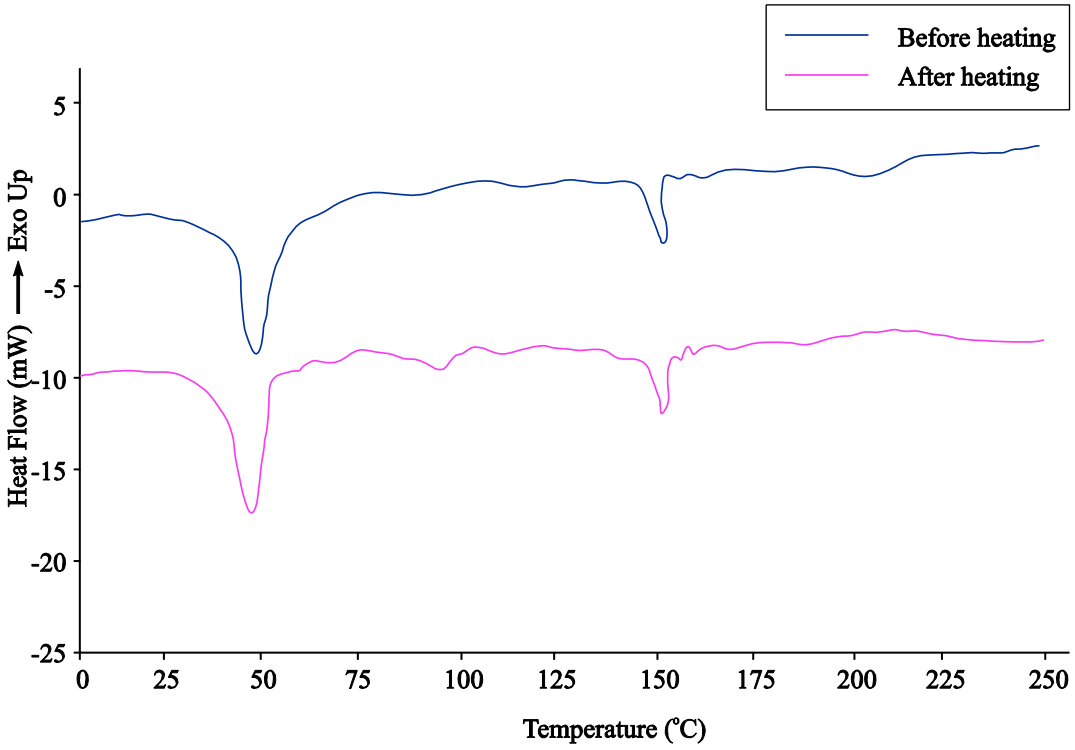

Figure 4.5 DSC profiles of a binary mixture of Labrafil® M2130 CS and KTZ generated prior to and following exposure of the lipid to heat at 60°C for one (1) hour

Table 4.7 DSC parameters of a binary mixture of Labrafil® M2130 CS and KTZ obtained prior to and after exposure to heat at 60°C for one (1) hour

Labrafil® M2130 CS and KTZ	Thermal event	Onset (°C)	MP (°C)	Enthalpy (J/g)
Prior to heating	Endothermic	37.52	40.10	119.45
	Endothermic	146.49	151.31	2.63
After heating	Endothermic	37.12	39.91	128.76
	Endothermic	145.32	150.86	7.38

The DSC profiles of the binary mixture of KTZ and Labrafil® M2130 CS prior to and following heating to 60°C for one (1) hour reveals the presence of peaks that are due to both KTZ and Labrafil® M2130 CS which are present at their typical melting points as reported in § 4.4.1.1 and 4.4.2.2.1 indicating that there is no obvious interaction between KTZ and the solid lipid. The presence of a separate peak for KTZ both prior to and after exposure to heating of the binary mixture suggests that KTZ was not soluble in Labrafil® M2130 CS at a concentration of 50% w/w as indicated by the solubility studies. KTZ is therefore molecularly dispersed in Labrafil® M2130 CS.

4.4.2.3.2. FTIR characterization of bulk lipid with KTZ

The IR absorption bands of a 1:1 mixture of Labrafil® M2130 CS and KTZ after exposure to 60ºC for one (1) hour are shown in Figure 4.6 and summarized in Table 4.8. The IR spectra of the binary mixture can be compared to the individual spectrum and relevant band assignments of Labrafil® M2130 CS (Figure 4.4 A, Table 4.5) and KTZ (Chapter 1, Figure 1.3, Table 1.1 *vide infra*) prior to heating to identify if any significant changes in the characterisitic absorption bands had occurred.

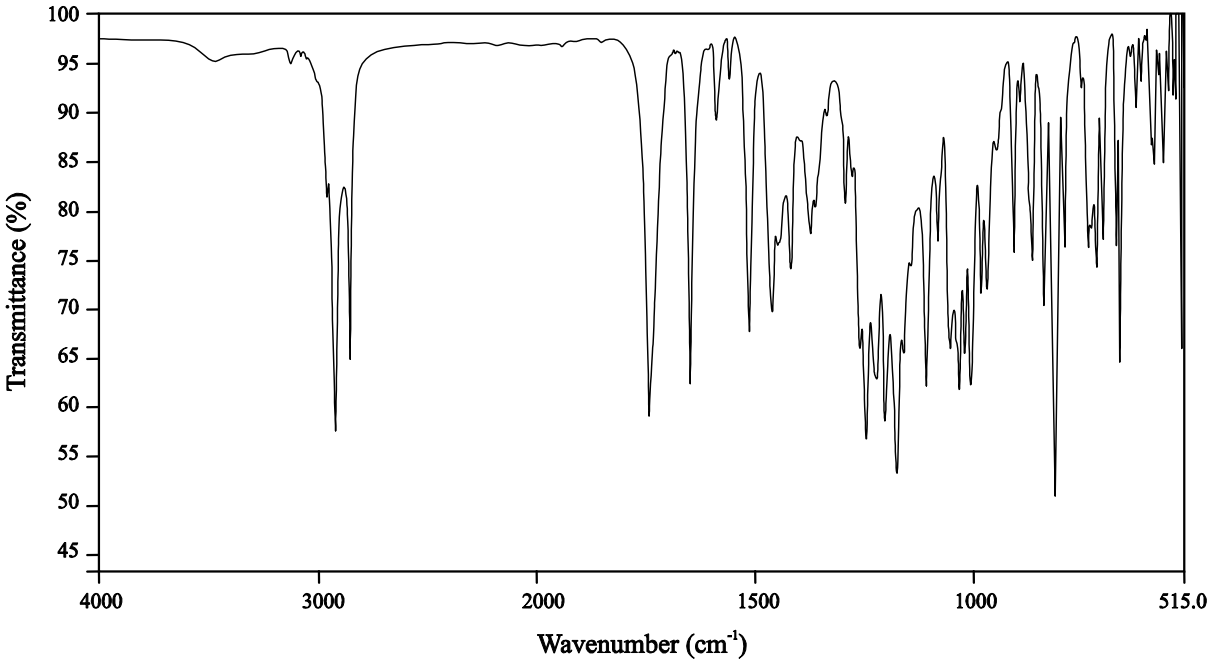

Figure 4.6 Infra-red spectrum of a binary mixture of Labrafil® M2130 CS and KTZ generated following exposure of the lipid to heat at 60°C for one (1) hour

Table 4.8 Major infra-red band assignments for a binary mixture of Labrafil® M2130 CS and KTZ obtained following exposure to heat at 60°C for one (1) hour

Band position (cm^{-1})	**Assignment**
3406	O-H stretching (water band)
3175	Symmetric stretching of CH_2 *(cis* double bond stretching)
2920	Symmetric stretching of CH_2 *(cis* double bond stretching)
2853	Asymmetric stretching of CH_2
1745	C=O stretching of the ester carbonyl group
1642	C=O stretching of the ketone (conjugation with imidazole ring in KTZ)
1496	Bending vibrations of CH_2 and CH_3aliphatic groups
1422	C-N stretching of the imidazole in KTZ
1260	C-O stretching of the cyclic ether group in KTZ
1245	C-C=O bend of the ketone in KTZ | NR
1185	Stretching vibration of the C-O ester group
1027	Ar-C-O stretching of the ether in KTZ
1020	C-O stretching
797	$=CH_2$ wagging

The FTIR spectrum of the binary mixture of Labrafil® M2130 CS and KTZ depicted in Figure 4.6 revealed that it was similar to the individual spectra of Labrafil® M2130 CS and KTZ. The absence of broadened peaks or additional absorption bands suggests that there is no interaction between the solid lipid Labrafil® M2130 CS and KTZ in the solid state. The typical characteristic absorption bands for Labrafil® M2130 CS and KTZ can be observed in Figure 4.6 and no new absorption band was detected indicating that no physicochemical interaction resulting in the formation of new chemical bonds had occurred in a mixture of the solid lipid and KTZ. The slight differences in the intensity and frequency of the peaks may be attributed to the formation of hydrogen bonds between Labrafil® M2130 CS and KTZ as KTZ is comprised of polar head groups that may give rise to dipole-dipole electrostatic interactions that produce different absorption bands. In addition these studies also confirm that the KTZ is molecularly dispersed in the lipid Labrafil® M2130 CS which demonstrates the fairly good affinity of KTZ for the lipid.

4.5. Conclusions

These studies have revealed that KTZ is stable to heat and therefore, a micro-emulsion approach may be used for the production of KTZ-loaded SLM. The lipid screening studies performed to establish lipids with the best solubilising potential for KTZ revealed that KTZ is moderately soluble in several lipids and that Labrafil® 2130M CS was found to exhibit the best solubilising potential for KTZ. Thermal analysis used in conjunction with FTIR proved useful in analyzing the polymorphic behaviour of KTZ and Labrafil® M2130 CS. No significant change in crystallinity was observed after heating KTZ to 60ºC for one (1) hour from DSC studies and similar results were observed using FTIR analysis. In addition no polymorphic change was noted in the lipid structure of Labrafil® M2130 CS when it is heated to 60ºC for one (1) hour as there was only a slight shift in the melting endotherm from 39.8ºC to 40.0ºC observed from DSC studies. FTIR analysis of Labrafil® M2130 CS prior to and after heating to 60ºC for one (1) hour also revealed no significant change in chemical bond shift, broadening of peaks or occurrence of unique bands in the IR spectrum, thereby supporting the information obtained from DSC studies and suggesting that exposure of the lipid to relatively high temperatures does not result in a change in polymorphic form. No interaction was detected between KTZ and the bulk solid lipid Labrafil® M2130 CS from DSC and FTIR studies after analysis of the 1:1 drug-lipid mixture heated at 60ºC for one hour. This lack of interaction could be detected from the typical peaks obtained for both Labrafil® M2130 CS and KTZ in the DSC thermogram after heating hence indicating that KTZ exists in its molecular form in the lipid. The relatively high solubility of KTZ

in Labrafil® M2130 CS compared to Precirol® ATO5, Compritol® 888, Gelucire® 44/14 and Gelucire® 50/13 suggests that a solid lipid matrix prepared from Labrafil® M2130 CS is likely to have a higher DLC and EE for KTZ than a matrix consisting of any other lipids tested. Consequently, an investigation into the feasibility of incorporating KTZ into SLM using this lipid was undertaken.

CHAPTER FIVE

FORMULATION AND CHARACTERIZATION OF AQUEOUS DISPERSIONS OF KTZ-LOADED SOLID LIPID MICROPARTICLES

5.1. Introduction

Formulation studies entailed an investigation into the feasibility of incorporating KTZ into SLM to improve delivery for paediatric and other patients. In many cases it is difficult to administer tablets or solid oral dosage forms to paediatric patients due to their inability to swallow [420, 421]. Therefore, liquid formulations are preferred for paediatric drug delivery for convenience and ease of administration [420, 421]. As it is common practice in South Africa to administer KTZ to paediatric patients in the form of extemporaneous preparations made by crushing tablets and mixing the resultant powder with a suspension vehicle it was thought that KTZ would be a good candidate for inclusion in aqueous dispersions of SLM as it is a highly lipophilic molecule. This novel strategy was also aimed at minimizing the risks of adverse effects associated with the lack of stability data available for extemporaneous preparations. Consequently, aqueous dispersions of KTZ-loaded SLM were developed, optimized and characterized during these studies.

The KTZ-loaded SLM consisted of the lipid Labrafil® M2130 CS. An alternative method of production of SLM which does not require the use of complex equipment and toxic organic solvents was developed for the laboratory-scale production of KTZ containing SLM. A micro-emulsion technique was selected due to its simplicity and involves the use of high shear devices such as the Ultra Turrax® homogenizer that tends to be routinely available in laboratories when compared to high-pressure homogenizers. Formulation development studies were initially conducted to identify an appropriate surfactant or combination of surfactants for the incorporation of KTZ in SLM. Following selection of the surfactant or surfactant mixture further studies were performed to investigate the influence of other formulation parameters such as the concentration of the solid lipid, the KTZ:solid lipid ratio and the number of homogenization cycles on the quality of the SLM produced. In addition these studies entailed an investigation into the quality of the aqueous SLM dispersions throughout formulation development and optimization in terms of particle size (PS), particle shape and morphology, zeta potential (ZP), drug loading capacity (DLC) and encapsulation efficiency (EE). Furthermore, the stability of the optimized SLM

formulations was assessed on days 0, 3, 7 and 30 following manufacture to establish the quality and stability of aqueous dispersions after storage at 25°C/65% RH and 40°C/75% RH. The objectives of these studies were therefore to investigate the feasibility of incorporating KTZ into solid lipid microparticles.

5.2. Materials

5.2.1. Solid lipid

5.2.1.1. Labrafil® M2130 CS

The physicochemical parameters of the solid lipid Labrafil® M2130 CS have been summarized in Chapter 4, § 4.2.2.3 *vide infra*. Labrafil® M2130 CS used in these studies was purchased from Gattefossé SAS, Saint-Priest Cedex, France and was used as received from the suppliers without further testing. Labrafil® M2130 CS has GRAS status and is physiologically compatible and biodegradable.

5.2.2. Emulsifying agents

5.2.2.1. Soluphor® P

Soluphor® P (BASF Corporation, Florham Park, NJ, USA) is the proprietary name for 2-pyrrolidone which is used as a solvent with water in combination with low molecular polyvinylpyrrolidone in injectable preparations [404, 422, 423]. Soluphor® P occurs as a colourless or slightly coloured liquid which has a faint characteristic odour and tends to solidify at room temperature as its melting range is 25-26ºC [423]. Soluphor® P is miscible with water and an aqueous solution of 100 g/L of Soluphor® P at 20ºC has a pH of between 8.2 and 10.8 and solutions up to 50% v/v tend to have a viscosity of about 4 mPa s [423]. Soluphor® P must be stored in airtight containers and storage below 25ºC is recommended to avoid discolouration. When stored in unopened original containers at room temperature (20-25ºC), Soluphor® P is stable for at least 12 months [422, 423]. Soluphor® P is soluble in water and a variety of organic solvents including ethanol, isopropyl alcohol and aromatic hydrocarbons [424]. Soluphor® P has a bulk density of 1.103 g/cm^3 and a partition coefficient (log $P_{o/w}$) of 0.71 at 25ºC and a dynamic viscosity of 10.2 mPas at 30 ºC [422]. Soluphor® P is also used in veterinary injectable products

as a solvent with water and has been reported to be of use in solutions for oral delivery of poorly soluble API [422, 423].

5.2.2.2. Soluplus®

Soluplus® (BASF Corporation, Florham Park, NJ, USA) is the proprietary name for polyvinyl caprolactam-polyvinyl acetate-polyethylene glycol graft copolymer [425]. It occurs as a free flowing white to slightly yellowish granule that has practically no taste [425]. Soluplus® is a novel polymer that has been designed for solid solutions in an attempt to improve the solubility and bioavailability of poorly soluble drugs as it has a unique structure that enables ideal interactions with API through hydrogen bonding, thereby positively impacting the stability and solubility of drugs [425-427]. Soluplus® is a polymeric solubilizer that can be used to prepare solid dispersions by spray drying, melt granulation and co-precipitation [427]. Soluplus® is known to be ideal for use in manufacturing approaches such as hot melt extrusion as it possess exceptional extrudability and may be easily processed [426]. Toxicological studies performed with Soluplus® reveal that its safety has been documented in comprehensive toxicological studies [426]. Soluplus® may be used at a broader pH range, since it is non-ionic, without compromising its solubilization capacity. Soluplus® is known to improve the solubility of KTZ [426].

5.2.2.3. Lutrol® E400

Lutrol® E400 (BASF Corporation, Florham Park, NJ, USA) is the proprietary name for polyethylene glycol (PEG-8) and is used as solvent for oral, topical and parenteral formulations [428-431]. Lutrol® E400 occurs as a colourless, almost odourless and tasteless liquid at room temperature with a density of 1.13 g/cm^3 and a molecular weight of 380 to 420 [429]. Lutrol® E400 is miscible with water and a 5% v/v aqueous solution has a pH of between 4.5 and 7.5 [430]. The viscosity of Lutrol® E400 at 20ºC is 6.8 to 8.0 mPas and it has a hydroxyl value of 267 to 295 [429, 430].

5.2.2.4. Pluronic® F68

Pluronic® F-68 (BASF Corporation, Florham Park, NJ, USA) is the proprietary name for a polyoxypropylene-polyoxyethylene block copolymer [432]. Pluronic® F-68 is a non-ionic surfactant that is a difunctional block copolymer of ethylene oxide and propylene oxide that terminates in primary hydroxyl groups [432]. The polyoxyethylene portion of the Poloxamer 188

molecule is hydrophilic whilst the polyoxypropylene portion is hydrophobic [432]. Pluronic® F-68 occurs as white, waxy, free-flowing prilled granules or cast solids or as white or almost white, waxy powders, micro-beads or flakes [432]. Pluronic® F-68 has a melting point range of between 52 and 57°C and is generally odourless and tasteless [432]. The HLB value of Pluronic® F-68 is 29 [404, 432, 433]. The aqueous solubility of Pluronic® F-68 at 25°C is > 100 mg/ml and Pluronic® F-68 is freely soluble in water at temperatures < 10°C and produces a clear solution of pH 5.0 to 7.5 [404, 432]. Pluronic® F-68 is also soluble in alcohol and practically insoluble in light petrolatum [404, 432]. Pluronic® F-68 has been reported to be hygroscopic only at relative humidities > 80% [432]. Pluronic® F-68 is used as an emulsifying agent or solubilising agent and may also be used as an excipient in inhalation, ophthalmic, oral, topical products and IV injections [404, 432].

The first digit in the name Pluronic® F-68 arbitrarily represents the molecular weight of the polyoxypropylene and the second digit represents the weight percent of the oxyethylene portion [432]. The letter 'L', 'P' and 'F' represent the physical properties of the poloxamer, such as liquid, paste or flakes [432]. Poloxamer 188 is the non-proprietary name of Pluronic® F-68 and contains the number 188, the first two digits when multiplied by 100, correspond to the average molecular weight of the polyoxypropylene segment of the copolymer molecule and the third digit, when multiplied by 10, corresponds to the percentage by weight of the polyoxyethylene segment of the molecule [432]. Poloxamer 188 has 75-85 ethylene oxide units, 2-30 propylene oxide units with a content of oxyethylene of between 79.9-83.7% and an average molecular weight of between 7680-9510 [404, 432]. Poloxamers are regarded as non-toxic and non-irritant materials and are not metabolised *in vivo* [404, 432].

5.2.2.5. Sodium cholate

Sodium cholate (Sigma-Aldrich, Saint Louis, MO, USA) is the monosodium salt of 3, 7, 12 - trihydroxy-5β-cholan-24-oic acid and is a hydrophilic anionic surfactant that occurs in bile salts [434, 435]. Sodium cholate is obtained in the form of a dark yellowish or sometimes white to off-white powder and has a critical micelle concentration (CMC) of 6.028% w/v or 9-15 mM at 20-25ºC above which sodium cholate forms micelles with a MW of approximately 900-1300 [434-436]. Sodium cholate has an HLB value of 18 and is manufactured by high temperature alkaline hydrolysis of bovine, ox or sheep bile as a by-product of the meat processing industry [434-437].

5.2.2.6. Tween 80

Tween 80 (Sharon Bolel Chemical Marketing, Houghton, Gauteng, South Africa) is also known as polyoxyethylene 20 sorbitan monooleate, polysorbate 80, PEG (80) sorbitan monoleate and is a yellow oily liquid with a characteristic odour [438]. Tween 80 is miscible in water (0.1 ml/ml) and yields a clear to slightly hazy faint yellow solution when dispersed. A 1% v/v solution has a pH ranging between 5.5 to 7.2 [438]. Tween 80 is miscible with alcohol, cottonseed oil, corn oil, ethylacetate, methanol and toluene and is immiscible with mineral and vegetable oils. Tween 80 has a GRAS status and is a non-toxic non-irritant material that may be used as a non-ionic emulsifying agent, a wetting agent, solubilizing agent in parenteral, food, oral, topical and cosmetic products [438]. Furthermore, Tween 80 improves the solubility of KTZ [439].

Tween 80 has a molecular weight of 1310 Da assuming that it has twenty ethylene oxide units, one sorbitol and one unit of oleic acid as the primary fatty acid [438]. The typical fatty acid constitution of Tween 80 determined by trans-esterification to yield fatty acid methyl esters, is approximately 70% oleic acid and other fatty acids that have been indicated include palmitic acid [438]. The HLB value and hydroxyl value of Tween 80 have been established as 15 and 65-60 mg KOH/g respectively [438]. Tween 80 has a specific gravity of 1.07 and a dynamic viscosity of 400 to 620 cP at 25°C [438, 440]. Tween 80 has a saponification value ranging between 45 and 55 mg KOH/g, an acid value of 2.0% and a surface tension of 42.5 mN/m at 20°C [438]. Tween 80 auto-oxidizes and is hygroscopic and should therefore be stored in a well-sealed container away from light in a cool and dry environment [438] and prolonged storage of Tween 80 may result in the formation of peroxides [438]. Tween 80 has been reported to be incompatible with alkalis, heavy metal salts, phenols and tannic acid [438, 440].

5.2.3. Water

Water used in these studies was purified water of HPLC grade and was prepared using the purification system described in § 3.3.2.1.

5.2.4. Formulation composition

Aqueous dispersions of SLM were prepared using a micro-emulsion approach adapted and modified from that described in § 2.5.3.1. A summary of the SLM preparations investigated in these studies is listed in Table 5.1 which shows the composition of all the formulations used for these studies. To ensure the selection of optimised formulations in terms of particle size, drug loading capacity and encapsulation efficiency of the SLM for further studies, a number of formulation parameters were investigated during the initial stages of formulation development and included the use of different surfactant(s), solid lipid concentration, drug-lipid ratio and number of homogenization cycles.

Table 5.1 Formulation compositions of drug-free and KTZ-loaded SLM

	Drug-free SLM									KTZ-loaded SLM												
SLM no.	**1**	**2**	**3**	**4**	**5**	**6**	**7**	**8**	**9**	**10**	**11**	**12**	**13**	**14**	**15**	**16**	**17**	**18**	**19**	**20**	**21**	**22**
Excipients																						
KTZ	-	-	-	-	-	-	-	-	-	5	5	5	5	5	5	5	5	5	5	5	10	3.3
Labrafil M2130 CS	10	10	10	10	10	10	10	10	10	10	10	10	10	10	10	10	10	10	5	15	10	10
Pluronic® F68	4	4	4	4	4	4	5	6	7	4	4	4	4	4	4	5	6	7	4	4	4	4
Sodium cholate	-	-	-	-	2	1	1	1	-	-	-	-	-	2	1	1	1	-	1	1	1	1
Tween 80	-	-	-	3	1	2	1	-	-	-	-	-	3	1	2	1	-	-	2	2	2	2
Lutrol® E400	3	-	-	-	-	-	-	-	-	3	-	-	-	-	-	-	-	-	-	-	-	-
Soluphor ® P	-	3	-	-	-	-	-	-	-	-	3	-	-	-	-	-	-	-	-	-	-	-
Soluplus ®	-	-	3	-	-	-	-	-	-	-	-	3	-	-	-	-	-	-	-	-	-	-
Purified water ad	100	100	100	100	100	100	100	100	100	100	100	100	100	100	100	100	100	100	100	100	100	100

5.3. Methods

A modified micro-emulsion approach (Chapter 2, § 2.5.3 *vide infra*) was used to manufacture the KTZ-loaded SLM dispersions and a summary is illustrated schematically in Figure 5.1. An aqueous mixture of surfactant and co-surfactant was prepared by dispersing the surfactant in water at 4°C followed by the addition of the co-surfactant. The micro-emulsion was formed by addition of an aqueous surfactant mixture heated to 60°C to the molten lipid phase containing KTZ that had been maintained at the same temperature. Following mixing with a vortex mixer the hot micro-emulsion was dispersed in cold water maintained at 2-3°C. The micro-emulsion dispersion was then homogenized using an Ultra-Turrax® homogenizer (Janke & Kunkel KG, Ika Werk, Staufen I. Breisgau, Germany) at 24 000 rpm for 5 minutes prior to homogenization with an Erweka GmbH homogenizer (Erweka AR400, Heusenstamm, Offenbach, Germany) for five (5) cycles. The aqueous dispersions were stored at room temperature prior to imaging analysis, ZP, DLC and EE assessment that were conducted on the day of manufacture.

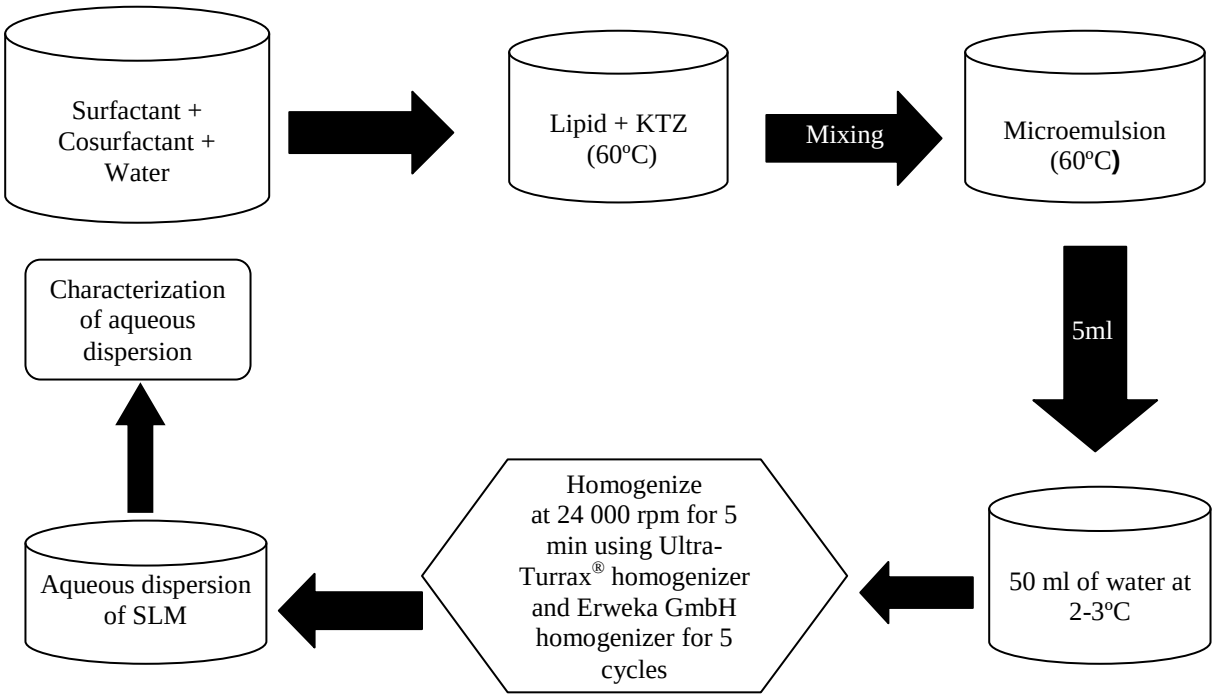

Figure 5.1 Schematic representation of the modified micro-emulsion technique used to manufacture KTZ-loaded SLM

5.4. Characterization of KTZ-loaded SLM dispersions

5.4.1. SEM analysis

The shape and surface morphology of SLM from aqueous dispersion samples obtained in these studies were investigated using a Model TS 5136LM Vega Tescan SEM (Tescan USA, Cranberry Twp, PA, USA). A sample was deposited on a graphite plate and air-dried for one (1) minute after which the sample was metallized with gold under vacuum. Samples were visualized under an accelerated voltage of 20 kV.

5.4.2. TEM analysis

The particle size of SLM was determined using Scandium Soft Imaging software (SSIS) (Olympus Soft Imaging Solutions, Center Valley, Philadelphia, USA) coupled to TEM. The aqueous dispersions of SLM were plated on a copper grid with a carbon film and allowed to dry for thirty (30) seconds after which it was stained with uranyl acetate (1% w/v) and allowed to dry at ambient temperature (25ºC) for thirty (30) seconds prior to examination using a Model JEOL-1210 transmission electron microscope (JEOL 1210, JEOL Inc., Boston, Massachusetts, USA) to obtain two-dimensional (2-D) images of the microspheres and to determine the particle size and particle size distribution of the product.

5.4.3. Zeta potential analysis

The ZP of the microparticles was assessed using a Nano-ZS Zetasizer (Malvern Instruments Ltd, Worcestershire, United Kingdom) in the Laser Doppler Anemometry (LDA) mode. Measurements were performed after dilution of each sample in distilled HPLC grade water prepared as detailed in § 3.3.2.1. A 20 µL aliquot of each sample was diluted with 10 ml of deionized HPLC grade water maintained at a resistivity of 18 MΩcm and the resulting dispersion was placed into a cell designed for ZP measurements. LDA measurements were performed in triplicates on each sample at an applied field of 20 V/cm and the Helmholtz-Smoluchowsky equation (Equation 2.1, § 2.6.4, *vide infra*) was used *in situ* to calculate the ZP value automatically.

5.4.4. Drug loading capacity and encapsulation efficiency

The DLC and EE of KTZ-loaded SLM from aqueous dispersions were determined in triplicate by accurately pipetting 0.5 ml of homogenous aqueous SLM dispersion using a micropipette (Hamilton Soft Touch™ 100-1200 µL). The mixture was placed in the sample reservoir of a Microcon® centrifugal filter device (Merck Millipore, Massachusetts, USA) equipped with an Ultracel YM filter membrane with a nominal molecular weight limit (NMWL) 100 000 Da (Merck Millipore, Massachusetts, USA). The sample was centrifuged at 10 000 rpm for 20 min using a Model 1EC HN-SII Damon centrifuge (International Equipment Company, Needham Heights, Massachusetts, USA). After centrifugation the filtrate was collected from the sample reservoir and transferred into a vial or recovery chamber which contained the aqueous phase that had been filtered through the membrane. The amount of KTZ in the aqueous phase was quantitated using the RP-HPLC method that was developed and validated as described in Chapter 3. The DLC and EE of the SLM were calculated using Equations 2.3 and 2.4 respectively (Chapter 2, § 2.6.6, *vide infra*).

5.4.5. Stability assessment of optimized formulations

An evaluation of the stability of two (2) optimized formulations selected from the formulation development process was conducted by determining the PS, ZP, DLC and EE on days 0, 3, 7 and 30 following manufacture. Approximately 8 ml of each SLM dispersion were pippetted (Hamilton Soft Touch™ 500-5000 µL) (n=3) into three (3) separate 10 ml glass vials. The vials were closed with airtight closures, covered using aluminum foil and placed in stability chambers maintained at 25°C±1/60% RH and 40°C±1/75% RH (Binder GmbH, KBF 240, E5.2, Tuttlingen, Germany). The stability chambers used in these studies were appropriate for stability tests conducted according to the ICH guideline Q1A as they were able to operate under extreme climate and site conditions and maintain homogenous climate conditions within the interior of the chamber thus ensuring the reproducibility of results. The system consisted of an APT.line™ preheating chamber and cooling system that were equipped with a controlled humidification and dehumidification system which were connected to a water supply. Samples were withdrawn for analysis when required and immediately placed back into the chambers. The PS, ZP, DLC and EE were assessed on days 0, 3, 7 and 30 after manufacture as detailed in § 5.4.1, 5.4.2, 5.4.3 and 5.4.4, respectively.

5.5. Results and discussion

5.5.1. Selection of surfactants

Solid lipid carriers may be produced using ionic, non-ionic or a combination of surfactants. The choice of an emulsifying system and the concentration of the emulsifiers has a direct influence on the resultant quality of the SLM formulations produced [182]. The choice of the surfactant is known to influence the surface morphology of the particles and the use of surfactant mixtures has been reported to lower the particle size and improve the stability of solid lipid carriers on storage [187, 441-443]. Five surfactants, *viz.*, Soluphor® P, Soluplus®, Lutrol® E400, Pluronic® F-68, sodium cholate and Tween 80 were investigated to determine their potential to stabilize SLM formulations. The choice of a suitable emulsifying system for use in the preparation of aqueous drug-free and KTZ-loaded SLM formulations was based on the ability to produce formulations with stable, spherical and smooth particles on the day of manufacture when stored at 22°C. Non-ionic surfactants can be used at concentrations between 2 and 10% w/w to produce solid lipid carriers. The use of high concentrations of surfactants is known to produce particles of smaller size and surface tension thus preventing particle aggregation [102, 187]. Pluronic® F68 is of use in the formulation of solid lipid carriers intended for oral administration due to the ability of the block copolymer to prevent enzymatic degradation of the lipids in the presence of lipase. Furthermore, Pluronic® F68 is known to exhibit surface-like steric effects when used in combination with ionic surfactants [442]. Therefore, Pluronic® F68 was used in combination with other surfactants up to a concentration of 7% w/v during these studies to determine the most appropriate emulsifying system for the production of KTZ-loaded SLM.

Drug-free (SLM 1-9, Table 5.1) and KTZ-loaded SLM (SLM 10-18, Table 5.1) were manufactured using different surfactants, combinations of surfactants and concentrations of surfactants. A lipid concentration of 10% w/v was used to manufacture these formulations and the physical stability of the SLM formulations was evaluated by determining the particle size (PS), shape and surface morphology and zeta potential (ZP). Formulations were considered stable only if the particles were discreet, spherical and showed no signs of aggregation on the day of manufacture (day 0). The quality of the SLM formulations in terms of particle size, shape and surface morphology were assessed using SEM and TEM.

The ZP is a good indicator of instability and ZP values of ± 30 mV are generally considered the limit of stable and unstable dispersions. However, optimal electrostatic repulsion only occurs at > ± 60 mV [238]. A large positive or negative ZP value is indicative of greater stability as the particles have a higher charge and repulsive potential, thereby avoiding aggregation [444]. Limited flocculation occurs in systems that exhibit ZP values of 5-15 mV and rapid flocculation occurs below 5 mV [237]. In a formulation containing a combination of surfactants both the electrostatic effect and the steric stabilization effect are cumulative and provide additional stability at ZP values lower than ± 30 mV [238]. A ZP of -20 to -11 mV corresponds to the threshold of agglomeration in dispersions [445]. The tendency of the particles to agglomerate may be attributed to an inadequate electrostatic repulsion potential energy that is necessary for a good quality of the interface between the particles as postulated by the DLVO theory [446]. The DLVO theory may be used to explain the interaction forces over large distances in colloidal systems although it cannot be used explain interactive forces between particles that are very close to each other such as particles that are separated by distances in the nanometer size range. At small separation distances the particle size, shape and chemistry affect the interactions between the particles and forces such as solvation, hydration, hydrophobic forces and steric interactions may predominate over the attractive and repulsive potentials suggested by the DLVO theory [446, 447]. However, the DLVO theory gives a good indication of the macroscopic stability of the system as the formation of agglomerates within a dispersion reveals that the particles are able to overcome the energy barrier of electrostatic repulsion and therefore implying dominating attractive Van der Waals forces are present [448].

The SEM and TEM micrographs of SLM formulation are depicted in Figures 5.2 and 5.3 and reveal potential differences in the quality of the particles produced using different surfactants. The mean PS was established using TEM and the ZP of the particles were measured on the day of manufacture for all formulations. The DLC and EE of the drug-loaded SLM formulations 10-18 were also evaluated and the data generated in these studies is summarized in Table 5.2.

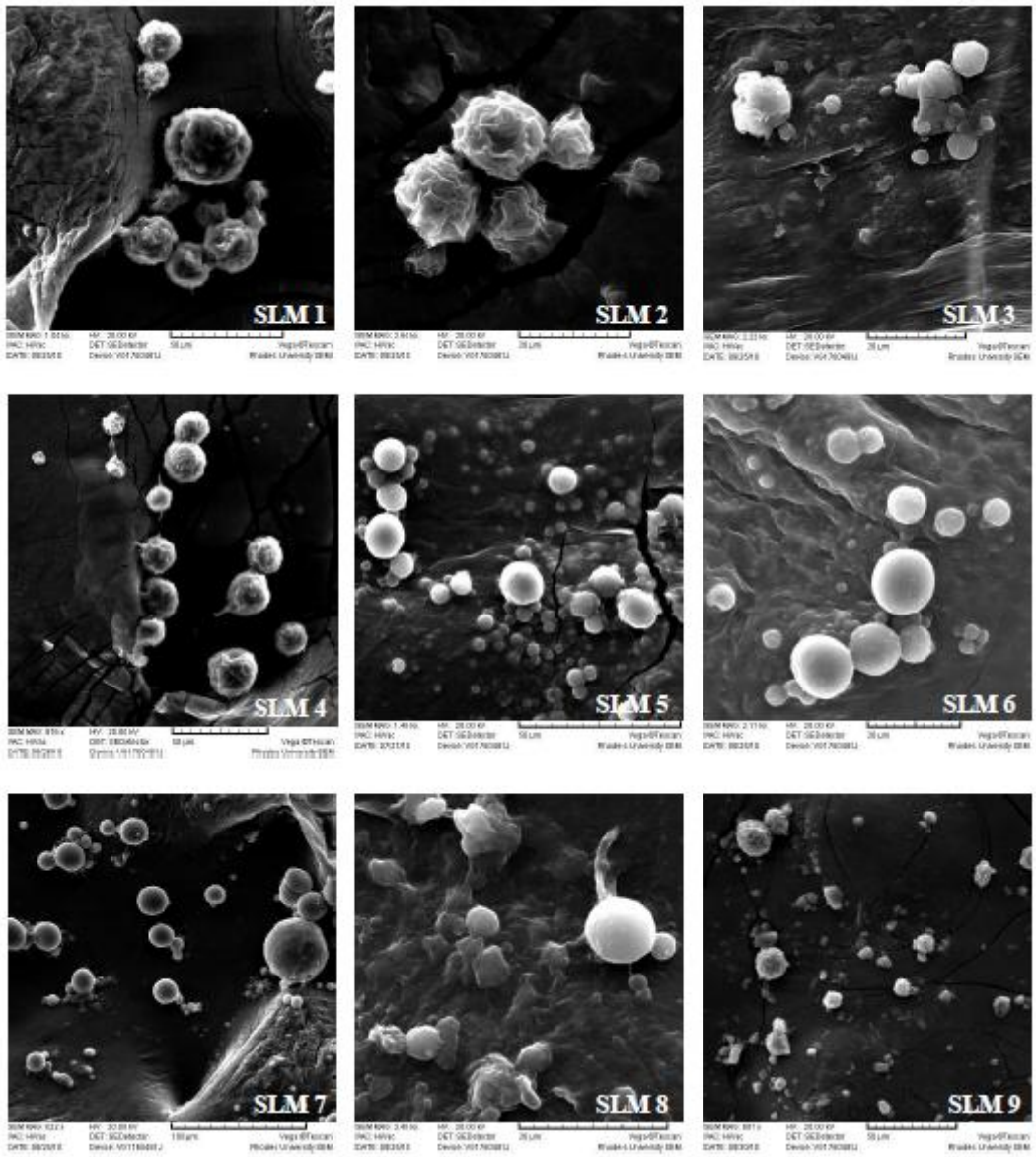

Figure 5.2 SEM micrographs of drug-free formulations, SLM 1 to SLM 9, manufactured using different surfactants or combinations of surfactants on the day of manufacture

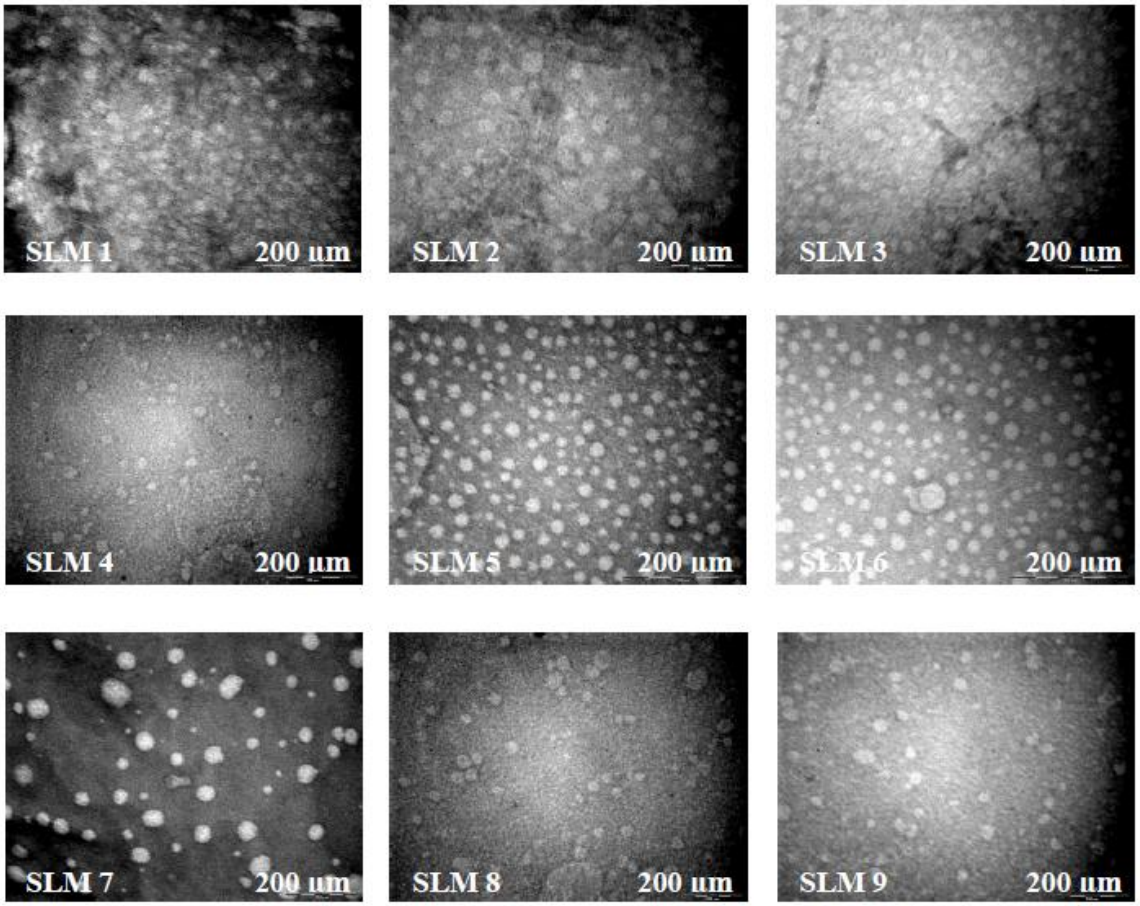

Figure 5.3 TEM micrographs of drug-free formulations, SLM 1 to SLM 9, manufactured using different surfactants or combinations of surfactants on the day of manufacture

Table 5.2 PS and ZP of drug-free batches, SLM 1 to SLM 9 and PS, ZP, DLC and EE of KTZ-loaded batches, SLM 10 to SLM 18 on the day of manufacture

BATCH	**SLM 1**	**SLM 2**	**SLM 3**	**SLM 4**	**SLM 5**
Parameter	**Day 0**	**Day 0**	**Day 0**	**Day 0**	**Day 0**
PS (µm)	43.7 ± 3.1	17.3 ± 4.4	21.7 ± 8.6	37.4 ± 6.5	40.6 ± 9.2
ZP (mV)	-18.3 ± 0.5	-13.9 ± 0.2	-14.8 ± 0.6	-18.7 ± 0.9	-11.6 ± 0.7
BATCH	**SLM 6**	**SLM 7**	**SLM 8**	**SLM 9**	
Parameter	**Day 0**	**Day 0**	**Day 0**	**Day 0**	
PS (µm)	25.5 ± 2.6	22.6 ± 4.1	22.2 ± 7.9	33.4 ± 5.8	
ZP (mV)	-31.1 ± 0.2	-32.7 ± 0.1	-19.3 ± 0.3	-15.5 ± 0.3	
BATCH	**SLM 10**	**SLM 11**	**SLM 12**	**SLM 13**	**SLM 14**
Parameter	**Day 0**	**Day 0**	**Day 0**	**Day 0**	**Day 0**
PS (µm)	39.2 ± 8.1	33.6 ± 4.4	15.7 ± 8.6	24.4 ± 5.2	23.6 ± 7.7
ZP (mV)	-18.3 ± 0.5	-13.9 ± 0.2	-14.8 ± 0.6	-18.3 ± 0.4	-30.9 ± 0.8
DLC (%)	0.04 ± 0.007	0.89 ± 0.02	0.97 ± 0.07	6.9 ± 1.2	7.3 ± 0.18
EE (%)	0.09 ± 0.006	1.85 ± 0.09	1.93 ± 0.18	11.5 ± 1.8	13.3 ± 0.74
BATCH	**SLM 15**	**SLM 16**	**SLM 17**	**SLM 18**	
Parameter	**Day 0**	**Day 0**	**Day 0**	**Day 0**	
PS (µm)	18.6 ± 3.6	15.6 ± 2.1	24.2 ± 6.5	28.4 ± 8.8	
ZP (mV)	-30.1 ± 0.2	-31.6 ± 0.1	-20.7 ± 0.3	-15.6 ± 0.2	
DLC (%)	23.6 ± 1.8	18.6 ± 0.3	17.4 ± 0.1	10.1 ± 0.2	
EE (%)	58.2 ± 2.3	43.2 ± 1.4	29.7 ± 0.9	17.9 ± 0.4	

The SLM products that were produced were all aqueous dispersions with an off-white appearance on the day of manufacture. The mean PS data measured from the TEM micrographs demonstrate that the particle size for all batches was < 50 µm although the PS was relatively high for batches 1 and 10 that were manufactured using a combination of Pluronic® F68 and Lutrol® E400. In addition the SEM micrographs depicted in Figure 5.2 reveal that the particles for SLM 1, SLM 2 and SLM 3 possessed non-spherical shapes and had an irregular surface morphology. The particles were not discrete and seemed to exhibit signs of aggregation from the day of manufacture. A similar pattern was observed for the KTZ-loaded batch SLM 10, 11 and 12 that also contained Lutrol® E400, Soluphor® P and Soluplus® respectively (Table 5.1). It can be noted that SLM 1, SLM 2 and SLM 3 produced a semi-solid-like dispersion within a few hours of storage at room temperature with the effect being more pronounced for SLM formulations 1 and 3. The change of state of the SLM formulation was used as a direct indication of the physical instability of the dispersion. Therefore, formulations SLM 1, SLM 2 and SLM 3 were not considered stable and appropriate for future formulation development studies. The concentration of 3% w/v Lutrol® E400, Soluphor ® P, Soluplus ® were not optimum for adequate reduction of surface tension and formation of a protective surfactant layer around the lipid particle. Particle partition may therefore have been hindered leading to the agglomeration of uncovered lipid surfaces. The surfactants Lutrol® E400, Soluphor® P, Soluplus® were not used in further optimization studies for the manufacture of KTZ-loaded SLM as the use of Pluronic® F68, Tween 80 and sodium cholate produced particles of better quality in these preliminary studies. Furthermore, DLC and EE of KTZ-loaded formulations, SLM 10, SLM 11 and SLM 12 that were produced using Lutrol® E400, Soluphor ® P, Soluplus® (Table 5.1) were very low which revealed poor encapsulation of KTZ due to a lack of stabilization of the particles by the emulsifying system used and is evident from the data summarized in Table 5.2.

Drug-free batches, SLM 4 to SLM 9 were manufactured using Pluronic® F68 in combination with the ionic surfactant, sodium cholate and the non-ionic surfactant, Tween 80 (Table 5.1). SLM formulations 4 to 9 were made up of relatively spherical particles irrespective of the surfactant used (Figure 5.1). Batch SLM 9 manufactured using Pluronic® F-68 alone contained discrete but rough surfaced particles compared to SLM 5, 6 and 7 that contained sodium cholate and Tween 80 in combination with Pluronic® F-68 (Figure 5.2). Pluronic® F-68 and Tween 80 enhance the stability of SLM by steric stabilization whereas sodium cholate increases the electrostatic repulsive potential energy of the particles and can circumvent flocculation within an aqueous dispersion [185]. The use of Pluronic® F-68 in combination with Tween 80 has been found to

reduce the PS of solid lipid carriers and improve the oral absorption of poorly soluble drugs. The surfactants Pluronic® F-68 and Tween 80 may also increase the permeability of the intestinal membrane and promote the interaction between the intestinal membrane and lipid particles. Furthermore, Pluronic® F-68 and Tween 80 possess moderate inhibiting effects on the P-glycoprotein (P-gp) efflux system increasing the oral absorption of poorly soluble drugs [449, 450]. It appears that Pluronic® F-68 alone did not produce adequate stabilization through steric effects and the use of Pluronic® F-68 without other surfactants was deemed insufficient for stabilization of SLM dispersions. Similarly, the use of Tween 80 in combination with Pluronic® F-68 in SLM 4 produced rough particles which tend to coalesce via the formation of bridges possibly due to inadequate steric hindrance (Figure 5.2). Block copolymers such as Pluronic® F-68 may act as a plasticizer and gelling agent possibly via the presence of bridging effects that result in the incorporation of water within the intralamellar areas of SLM causing the hardening of the gel with time [448]. The SLM aqueous dispersions were found to exhibit a slight gelation tendency particularly on storage.

The ZP measured for SLM 4 was -18.7 ± 0.9 mV (Table 5.2) which appears insufficient to hinder coalescence via steric effects as a ZP range of -20 mV to -11 mV is known to correspond to the threshold of agglomeration in dispersions [448]. The SEM micrographs of SLM 8 manufactured using a combination of Pluronic® F-68 and sodium cholate revealed spherical and smooth particles (Figure 5.2) but the particles seemed to agglomerate. The ZP measured for SLM 8 was -19.3 ± 0.3 mV (Table 5.2) which also appears insufficient for cumulative electrostatic and steric stabilization from a combination of 6% w/w Pluronic® F-68 and 1% w/w sodium cholate. The particles of batch SLM 8 appear to be in a state of limited flocculation which could trigger subsequent mechanisms of instability such as sedimentation, aggregation and caking (Figure 5.4). It was reported that dispersions may undergo solidification once the ZP values fall within the threshold of agglomeration of -20 mV to -11 mV [448].

TEM micrographs of batches SLM 4, 8 and 9 reveal the presence of a wide particle size distribution (Figure 5.3 and Table 5.2). The KTZ-loaded SLM formulations 13, 17 and 18 were also stabilized using Pluronic® F-68 and Tween 80, Pluronic® F-68 and sodium cholate and yielded similar results (Table 5.2). The wide particle size distribution in SLM formulations 4, 8, 9, 13, 17, 18 could contribute to the aggregation tendency due to Ostwald ripening (Figure 5.4). The large differences in particle sizes leads to small particles preferentially dissolving in the outermost layer of larger particles to form a supersaturated solution resulting in crystal growth

and an increase in particle size [238, 447]. The DLC and EE of SLM 13, 17 and 18 were relatively low and SLM 17 manufactured using a combination of Pluronic® F-68 and sodium cholate, exhibited the highest EE (Table 5.2). Therefore, a combination of surfactants was considered necessary to ensure a high entrapment efficiency for KTZ and further investigations were undertaken using a combination of Pluronic® F-68, Tween 80 and sodium cholate to stabilize the SLM dispersions.

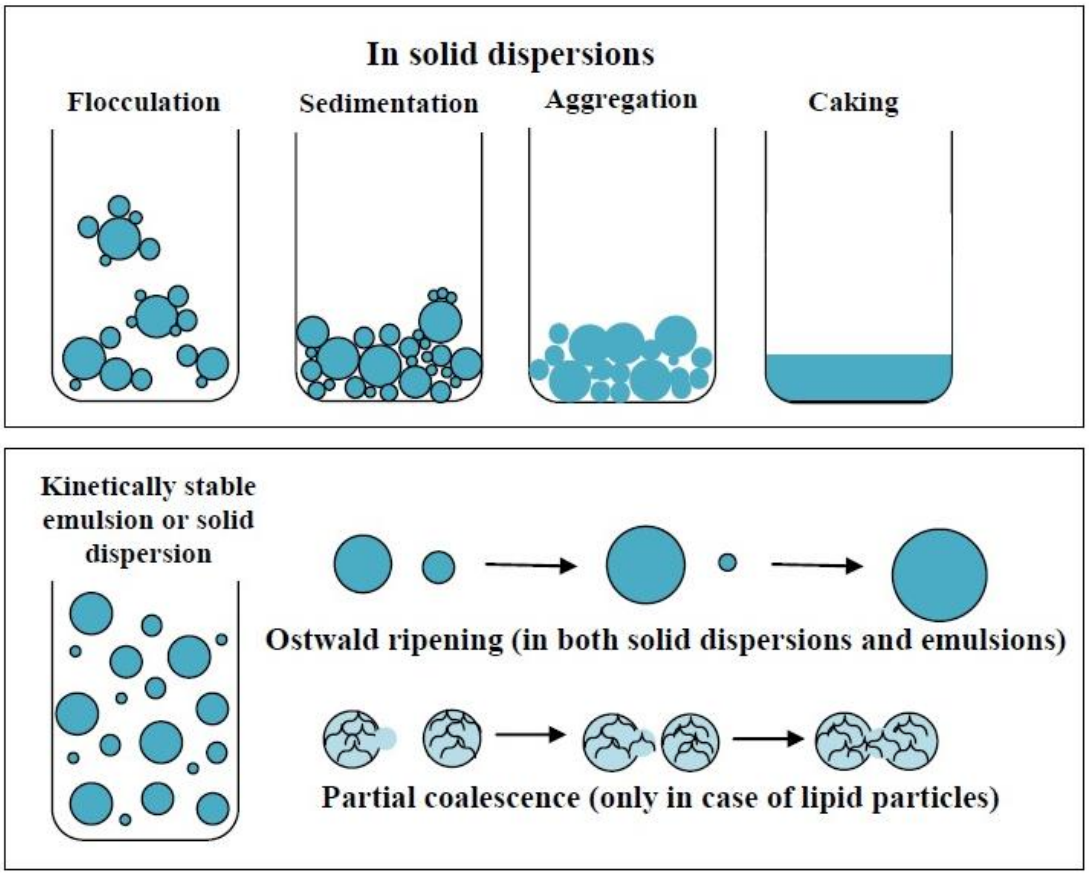

Figure 5.4 Mechanisms of instability in solid dispersions and emulsions adapted from [447]

It has been suggested that increasing the concentration of surfactants in a formulation leads to a reduction in particle size up to a point [451]. Drug-free batches SLM 5, 6 and 7 and KTZ-loaded SLM 14, 15 and 16 were manufactured using a combination of Pluronic® F-68, Tween 80 and sodium cholate in different concentrations (Table 5.1). The SEM micrographs of drug-free SLM 5, 6 and 7 depicts spherical and smooth particles on day 0 (Figure 5.2) with particle sizes < 50 µm and a wide particle size distribution was observed for SLM 5 (Table 5.2). However, the KTZ-loaded SLM manufactured with a similar formulation composition (SLM 14) has smaller particles of 23.6 ± 7.7 µm in diameter and a ZP of -30.9 ± 0.8 mV with DLC and EE values of 7.3 ± 0.18% and 13.3 ± 0.74% respectively (Table 5.2). Conversely, particles from batches SLM 16

and SLM 17 demonstrated higher DLC and EE values than those of batch SLM 14 inferring that the stability of the emulsifying system also resulted in a higher retention capability for KTZ. The particles observed in the SEM micrograph of particles from batch SLM 14 (Figure 5.2) revealed signs of agglomeration and a wide particle size distribution which is likely to promote instability of the dispersion due to Ostwald ripening. Batches SLM 15 and 16 produced discrete particles with a small particle size and high ZP values of -30.1 ± 0.2 mV and -31.6 ± 0.1 mV respectively. The large negative ZP value could be attributed to the presence of the anionic sodium cholate and additional steric stabilization due to the presence of Tween 80 that exerts a cumulative effect on the stability of the colloidal dispersion. The combination of steric and electrostatic surfactants has a synergistic effect leading to a decrease in particle size and improved stability. Therefore, particles from batches SLM 15 and 16 manufactured using a combination of three surfactants *viz.*, Pluronic® F-68 (4-5% w/v), sodium cholate (1% w/v) and Tween 80 (1-2% w/v) were considered to be promising colloidal dispersions and further studies were performed to assess their stability and are detailed in § 5.4.5, *vide infra*.

5.5.2. Selection of solid lipid concentration

The influence of solid lipid concentration on the quality of KTZ-loaded SLM was investigated using three different levels *viz.*, 5% w/v, 10% w/v and 15% w/v Labrafil® M2130 CS (SLM 15, 19 and 20, Table 5.1). The potential differences in terms of size, shape and surface morphology of KTZ-loaded SLM obtained in these studies were assessed using TEM and SEM (Figures 5.5 and 5.6). Furthermore, the influence of solid lipid concentration on ZP, DLC and EE of KTZ-loaded SLM were evaluated in these studies the results of which are summarized in Table 5.3 and Figure 5.7 which depict the effect(s) of Labrafil® M2130 CS concentration on PS, ZP, DLC and EE of KTZ-loaded SLM batches 15, 19 and 20.

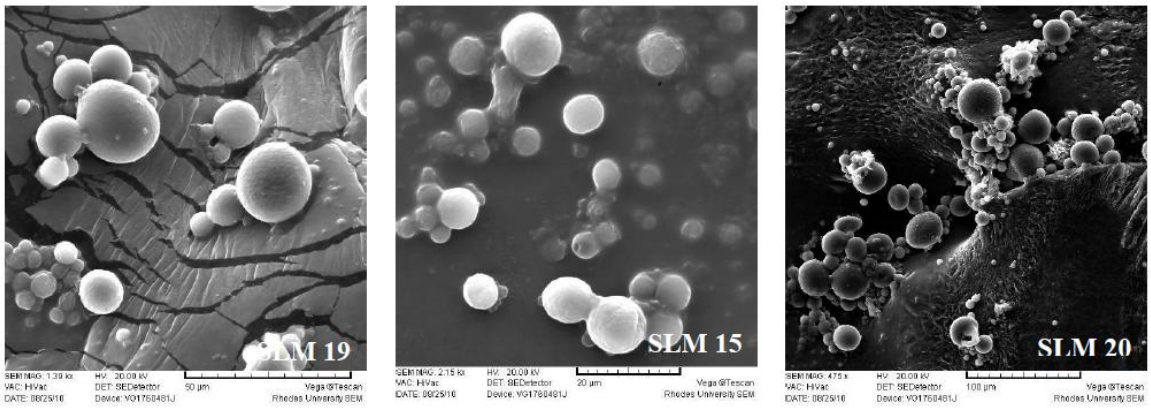

Figure 5.5 SEM images of KTZ-loaded SLM manufactured using different concentrations of Labrafil® M2130 CS: 5% w/v (SLM 19), 10% w/v (SLM 15) and 15% w/v (SLM 20) on the day of manufacture

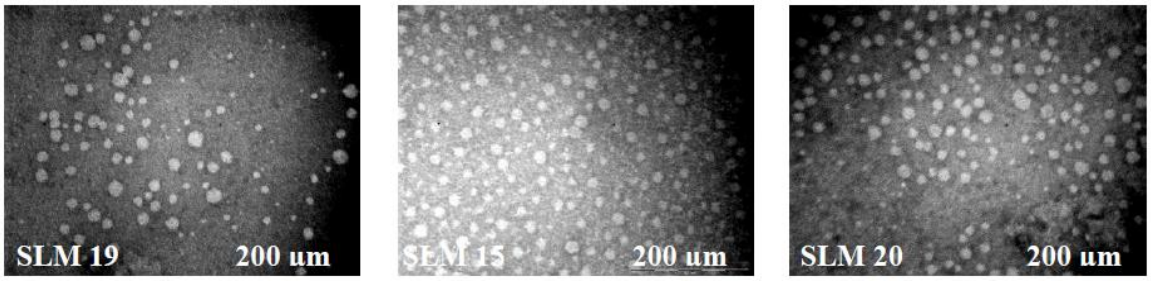

Figure 5.6 TEM images of KTZ-loaded SLM using different concentrations of Labrafil® M2130 CS: 5% w/v (SLM 19), 10% w/v (SLM 15) and 15% w/v (SLM 20) on the day of manufacture

The SEM micrographs depicted in Figure 5.5 (SLM 19, SLM 15 and SLM 20) reveal that the particles were mostly spherical and had a regular and smooth surface. However, TEM images (Figure 5.6) reveal that the particles of SLM 19 were relatively large with a mean PS of 40.2 ± 3.5 µm. In addition signs of agglomeration were observed on the day of manufacture for batches SLM 19 and 20 (Figure 5.5) and this could lead to increased instability due to coalescence on storage. Particles prepared using high lipid concentrations require modification of certain process parameters such as stabilizer concentration(s) and/or temperature and the formation of lipid formulations depends on the concentration of lipid used as lipid aggregates generated during diffusion tend to coalesce at high lipid concentrations [451]. The difference in density between the lipid and aqueous phases may also lead to an increase in the formation of lipid aggregates at high lipid concentrations [452]. The increase in PS may also be attributed to an increase in the viscosity of the continuous phase which results in a lower diffusion rate of suspended particles and subsequently leads to an increase in aggregation [453]. Although the mean PS on the day of manufacture did not increase with increasing concentration of Labrafil® M2130 CS a larger number of lipid aggregates was noted for batch SLM 20 (Figures 5.5 and 5.6).

Table 5.3 ZP, PS, DLC, EE of KTZ-loaded SLM manufactured using different concentrations of Labrafil® M2130 CS: 5% w/v (SLM 19), 10% w/v (SLM 15) and 15% w/v (SLM 20) on the day of manufacture

Concentration of Labrafil® M2130 CS (% w/v)	**5**	**10**	**15**
Parameter on day 0	**SLM 19**	**SLM 15**	**SLM 20**
PS (µm)	40.2 ± 3.5	18.6 ± 3.6	32.2 ± 4.2
ZP (mV)	-30.2 ± 0.3	-30.1 ± 0.2	-29.5 ± 0.1
DLC (%)	24.5 ± 2.1	23.6 ± 1.8	15.1 ± 0.23
EE (%)	59.3 ± 3.5	58.2 ± 2.3	32.9 ± 0.34

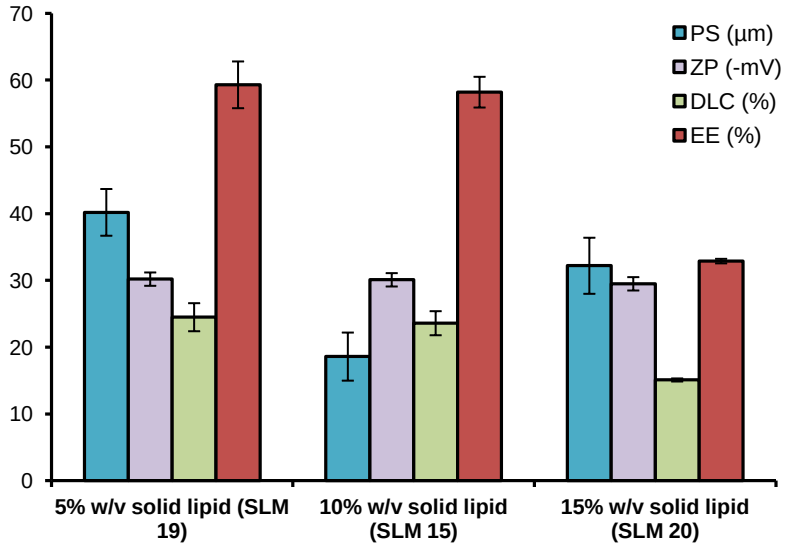

Figure 5.7 ZP, PS, DLC, EE of KTZ-loaded SLM manufactured using different concentrations of Labrafil® M2130 CS: 5% w/v (SLM 19), 10% w/v (SLM 15) and 15% w/v (SLM 20) on the day of manufacture

The ZP of SLM 19, SLM 15 and SLM 20 were not significantly different which indicates that the use of different lipid concentrations did not affect the electrostatic stability of the KTZ-loaded SLM formulations ($p > 0.05$, Table 5.3 and Figure 5.7). In addition DLC and EE studies revealed that poor encapsulation of KTZ occurred with a lipid concentration of 15% w/v. A decrease in lipid concentration yielded particles with a higher DLC and EE and stability (Table 5.3). However, the optimum lipid concentration was considered to be 10% w/v Labrafil® M2130 CS as the particles produced with 10% w/v solid lipid (SLM 15) were discrete and relatively small with a mean PS of 18.6 ± 3.6 µm and these exhibited fewer signs of aggregation on the day of manufacture (Figure 5.5). As the concentration of lipid was increased and the concentration of stabilizer was kept constant, flocculation occurred resulting in the formation of larger aggregate structures [237]. Increasing the concentration of Labrafil® M2130 CS (Figure 5.7) from 10% w/v to 15% w/v led to a decrease in DLC and EE. The decrease in KTZ entrapment could be attributed to an increase in drug expulsion due to the occurrence of physical instability within the dispersion and possible reduction in the crystallinity of KTZ. Therefore, a concentration of 10% w/v Labrafil® M2130 CS was used during further formulation development studies to investigate

the influence of KTZ loading on the quality of SLM formulations and these studies are detailed in § 5.5.3.

5.5.3. Influence of drug-lipid ratio

Aqueous SLM dispersions containing different amounts of KTZ (Table 5.1) were manufactured in order to investigate the influence of KTZ loading on the quality of the SLM that were produced. The PS, ZP, EE for KTZ-loaded SLM formulations were measured on the day of manufacture and the data generated from these studies are summarized in Table 5.4. The influence of drug:solid lipid concentration on the quality of KTZ-loaded SLM was investigated using three different concentrations *viz.,* 3.3% w/v, 5% w/v and 10% w/v of KTZ (SLM 22, 15 and 21, Table 5.1). SEM and TEM images (Figures 5.8 and 5.9) depict images of SLM prepared using three different concentrations of KTZ. In addition the influence of KTZ loading on ZP, DLC and EE of KTZ-loaded SLM were also evaluated. The effect of Labrafil® M2130 CS concentration on PS, ZP, DLC and EE of KTZ-loaded SLM batches 22, 15 and 21 are summarized in Table 5.4 and depicted in Figure 5.10.

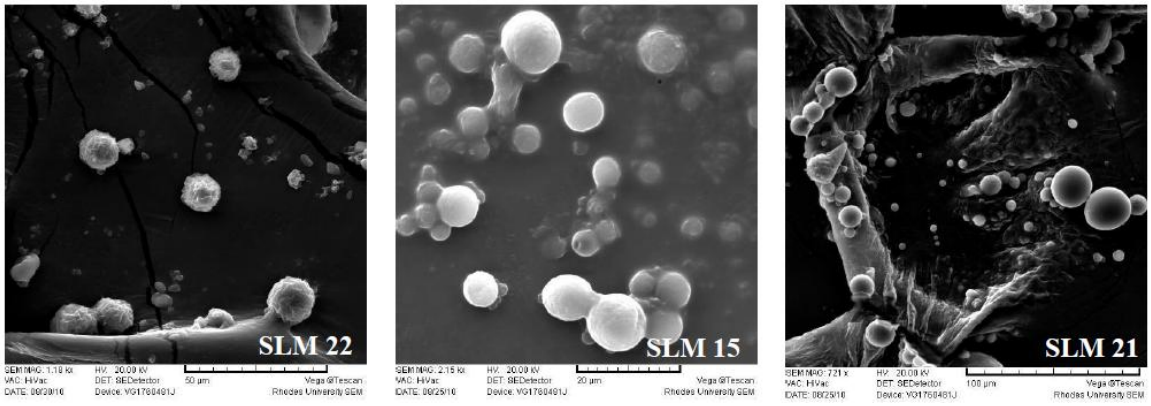

Figure 5.8 SEM images of KTZ-loaded SLM manufactured using different concentrations of KTZ: 3.3% w/v (SLM 22), 5% w/v (SLM 15) and 10% w/v (SLM 21) on the day of manufacture

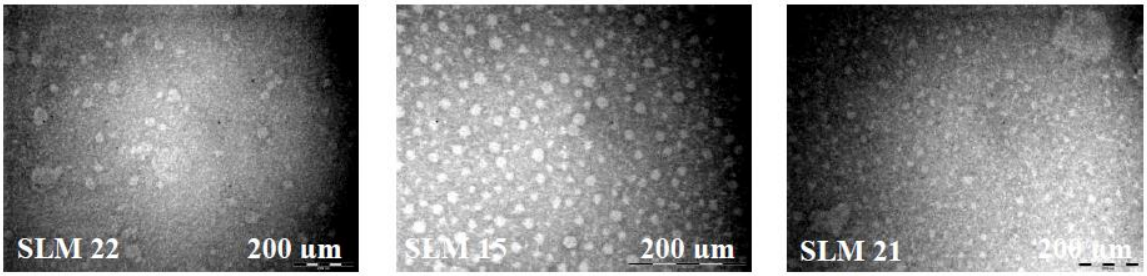

Figure 5.9 TEM images of KTZ-loaded SLM manufactured using different concentrations of KTZ: 3.3% w/v (SLM 22), 5% w/v (SLM 15) and 10% w/v (SLM 21) on the day of manufacture

Table 5.4 PS, ZP, DLC and EE of KTZ-loaded SLM manufactured using different concentrations of KTZ: 3.3 % w/v (SLM 22), 5% w/v (SLM 15) and 10% w/v (SLM 21) on the day of manufacture

Concentration of KTZ (% w/w)	**3.3**	**5**	**10**
Drug:lipid ratio	**1:3**	**1:2**	**1:1**
Parameter on day 0	**SLM 22**	**SLM 15**	**SLM 21**
PS (µm)	27.5 ± 4.9	18.6 ± 3.6	28.3 ± 3.8
ZP (mV)	-30.8 ± 0.6	-30.1 ± 0.2	-28.1 ± 0.1
DLC (%)	22.5 ± 1.2	23.6 ± 1.8	19.4 ± 0.37
EE (%)	48.5 ± 2.9	58.2 ± 2.3	49.5 ± 0.79

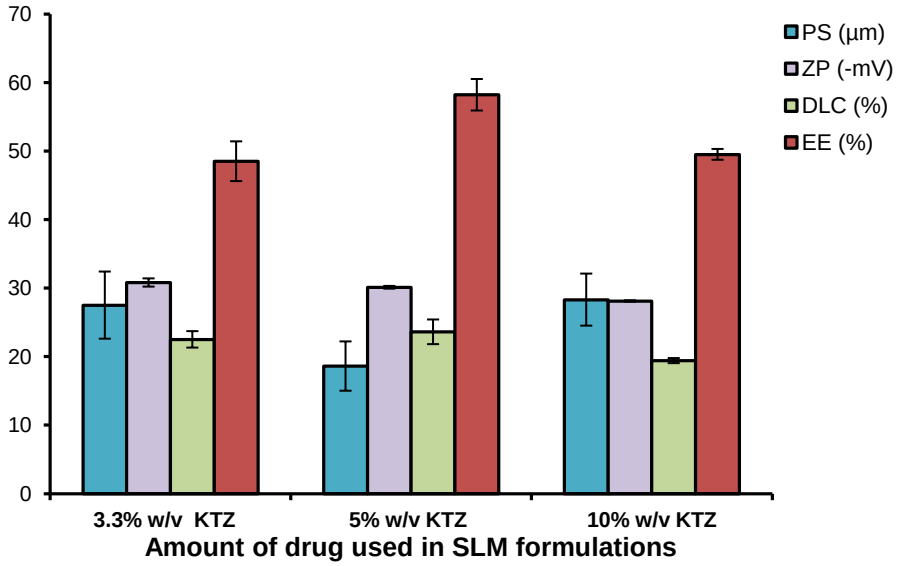

Figure 5.10 PS, ZP, DLC and EE of KTZ-loaded SLM manufactured using different concentrations of KTZ: 3.3 % w/v (SLM 22), 5% w/v (SLM 15) and 10% w/v (SLM 21) on the day of manufacture

On the day of manufacture the KTZ-loaded SLM formulations appeared to be more spherical and smooth as the concentration of KTZ was increased although differences in shape and surface morphology of KTZ-loaded particles were not significant at concentrations of 5% w/v and 10% w/v KTZ (Figure 5.8). The measurement of PS revealed that the mean PS of KTZ-loaded SLM was between 18.6 and 28.3 µm with a relatively narrow particle size distribution. Loading concentrations have been reported to exert no influence on the PS of solid lipid nanoparticle formulations of trans retinoic acid [454]. The findings observed in these studies reveal that the PS was not significantly altered when increasing loading concentrations of KTZ as the mean PS measured for the drug-free SLM formulation manufactured using the same combination of surfactants and lipid concentration ($p > 0.05$, SLM 6, Table 5.1) depicted a similar PS range. The use of techniques that measure the particle diameter through light scattering effects may be required to further investigate the effects of KTZ loading on the PS of SLM formulations.

Similarly, the ZP of KTZ-loaded SLM were not significantly different when increasing KTZ concentrations were used to manufacture the formulations ($p > 0.05$, Figure 5.10). The KTZ-free

SLM formulation prepared using the same formulation composition as SLM 15 was found to exhibit a similar ZP on the day of manufacture (SLM 6, Table 5.2). The ZP values were negative due to the presence of sodium cholate and were close to -30 mV which defines the limit for stability of colloidal dispersions stabilized by electrostatic interactions alone. The stability of the SLM formulations was further improved by the addition of steric surfactants such as Pluronic® F-68 and Tween 80.

DLC and EE are important properties that can influence drug release characteristics and formed an integral part of these formulation development studies. KTZ is known to be a lipophilic API and is therefore a good candidate for inclusion in SLM formulations. However, KTZ did not exhibit an extremely high solubility in the lipids used during lipid screening studies and due to the average solubility of KTZ in Labrafil® M2130 CS only small amounts of KTZ were used to investigate the feasibility of SLM to encapsulate KTZ. Concentrations of 3.3% w/v, 5% w/v and 10% w/v were deemed sufficient for the intended purpose of these studies. The data summarized in Table 5.4 and depicted in Figure 5.10 demonstrate that a concentration of 5% w/v KTZ yielded maximum entrapment of KTZ with DLC and EE values of 23.6 ± 1.8% and 58.2 ± 2.3%, respectively. The data also reveal that the amount of KTZ entrapped in the microparticles for each formulation investigated did not vary significantly and seemed to decrease as the concentration of KTZ was increased to levels > 5% w/v ($p > 0.05$). The use of 10% w/v KTZ led to a reduction in DLC and EE and an increase in PS (Table 5.4 and Figure 5.10). Therefore, a concentration of 5% w/v KTZ, 10% w/v Labrafil® M2130 CS and a combination of three surfactants, Pluronic® F-68 (4% w/v), sodium cholate (1% w/v) and Tween 80 (2% w/v) were used during further formulation development studies to establish the effect of process parameters such as the number of homogenization cycles on the quality of SLM formulations manufactured and these studies are described in § 5.5.4.

5.5.4. Selection of production parameters

The method used to manufacture SLM formulations using an Ultra-Turrax® homogenizer at 24000 rpm for 5 minutes prior to homogenization with an Erweka GmbH homogenizer (Erweka AR400, Heusenstamm, Offenbach, Germany) required that an appropriate number of homogenization cycles be used to produce particles in an acceptable micrometer PS range and that exhibited sufficient entrapment of KTZ. The number of homogenization cycles was changed between 3 and 5 and the quality of the SLM dispersion was characterized in terms of particle

shape and surface morphology, PS, ZP, DLC and EE. The SEM and TEM micrographs (Figures 5.11 and 5.12) depict the SLM formulations manufactured using 5% w/v KTZ, 10% w/v Labrafil® M2130 CS and a combination of 4% w/v Pluronic® F-68, 1% w/v sodium cholate and 2% w/v Tween 80 using different numbers of homogenization cycles. The effect of the number of homogenization cycles on PS, ZP, DLC and EE of KTZ-loaded SLM batches manufactured using 3 (SLM 23), 4 (SLM 24) and 5 (SLM 15) homogenization cycles are summarized in Tables 5.5 and depicted in Figure 5.13.

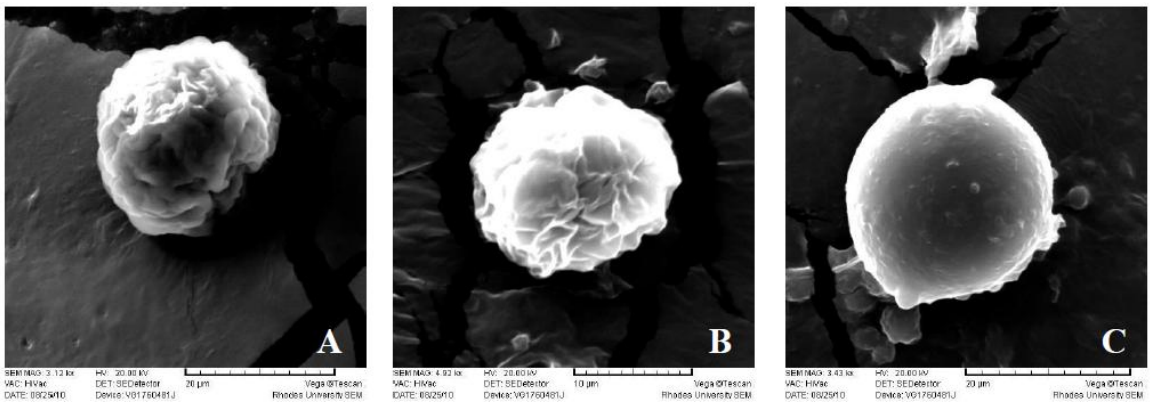

Figure 5.11 SEM images of KTZ-loaded SLM manufactured using 3 (A, SLM 23), 4 (B, SLM 24) and 5 (C, SLM 15) homogenization cycles on the day of manufacture

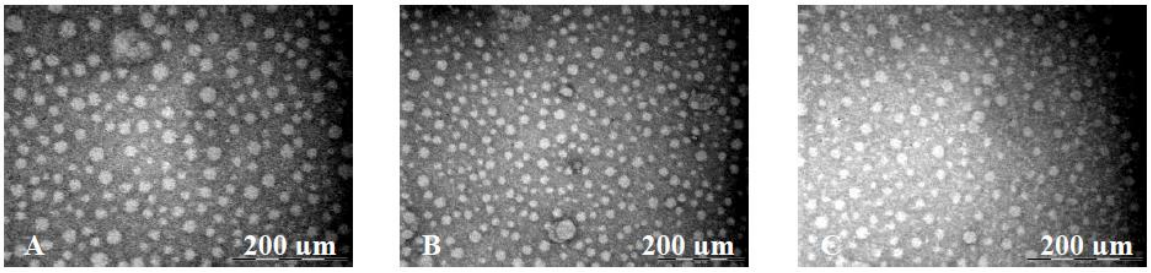

Figure 5.12 TEM images of KTZ-loaded SLM manufactured using 3 (A, SLM 23), 4 (B, SLM 24) and 5 (C, SLM 15) homogenization cycles on the day of manufacture

Table 5.5 PS, ZP, DLC and EE of KTZ-loaded SLM manufactured using 3 (A, SLM 23), 4 (B, SLM 24) and 5 (C, SLM 15) homogenization cycles on the day of manufacture

Number of homogenization cycles	**3 (SLM 23)**	**4 (SLM 24)**	**5 (SLM 15)**
Parameter	**Day 0**	**Day 0**	**Day 0**
PS (µm)	42.7 ± 6.9	17.8 ± 7.1	18.6 ± 3.6
ZP (mV)	-27.5 ± 0.2	-29.7 ± 0.1	-30.1 ± 0.2
DLC (%)	20.7 ± 1.9	19.1 ± 3.9	23.6 ± 1.8
EE (%)	43.8 ± 2.8	42.3 ± 2.5	58.2 ± 2.3

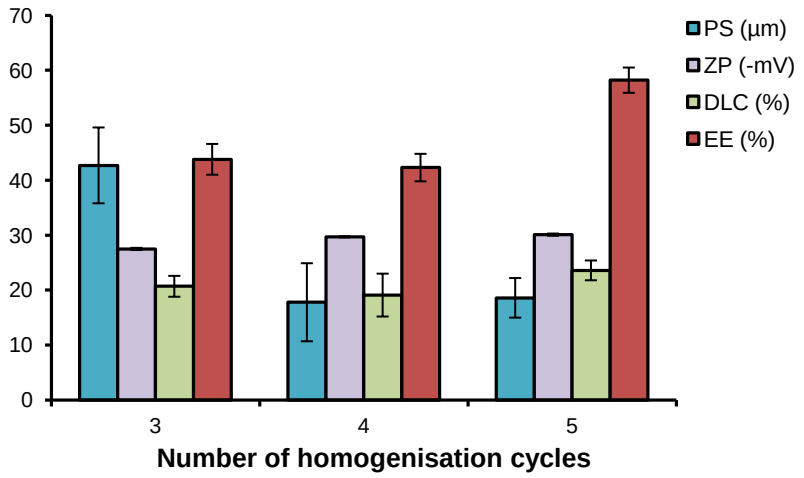

Figure 5.13 PS, ZP, DLC and EE of KTZ-loaded SLM manufactured using 3 (A, SLM 23), 4 (B, SLM 24) and 5 (C, SLM 15) homogenization cycles on the day of manufacture

Process parameters such as the number of homogenization cycles have a direct impact on particle size as the formation of a finer and more homogenous emulsion permits stabilization of smaller particles [451]. Similar observations have also been reported for the preparation of nano-dispersions using a reversible salting-out effect [455]. The mean particle size measured using TEM (Figure 5.12) and the data obtained from these studies reveal that increasing the number of homogenization cycles during production of SLM results in a reduction in the mean PS for the formulations tested on the day of manufacture. The SEM micrographs depicted in Figure 5.11 reveal a change in surface morphology of the particles when using five homogenization cycles and the surface of the particles in KTZ-loaded SLM C appeared smoother and more regular compared to the surface of particles produced using fewer homogenization cycles (A and B). Further studies using a higher number of homogenization cycles were not undertaken so as to maintain the simplicity of the production process and ensure that the duration of production was reasonably short. A slight increase in the ZP of the SLM formulations tested during these studies as the number of homogenization cycles was increased was noted. The higher ZP values obtained using a higher number of homogenization cycles were close to -30 mV indicating improved stability of the SLM formulations possibly due to a reduction in PS. The use of five homogenization cycles also led to the production of particles with higher KTZ entrapment efficiency as shown in Table 5.5 and Figure 5.13. Therefore, the production of KTZ-loaded SLM using a modified micro-emulsion technique was achieved by passing the micro-emulsion through an Ultra-Turrax® homogenizer at 24 000 rpm for 5 minutes prior to homogenization for five cycles using an Erweka GmbH homogenizer.

5.5.5. Stability assessment of optimized SLM formulations

The optimized formulations identified through formulation development studies were found to be comprised of 10% w/v solid lipid Labrafil® M2130 CS, 5% w/v KTZ and a combination of Pluronic® F-68, sodium cholate and Tween® 80. At a concentration of 10% w/v of the solid lipid and 5% w/v KTZ the use of different concentrations of each surfactant produced good quality KTZ-loaded SLM on the day of manufacture in terms of particle shape, surface morphology, PS, ZP, DLC and EE. Therefore, for the purposes of these studies two formulations were selected *viz.*, SLM 15 and SLM 16 were used for further studies and were stabilized with 4% w/v and 5% w/v Pluronic® F-68 respectively, 2% w/v and 1% w/v Tween 80 respectively and 1% w/v sodium cholate in both cases (Table 5.1).

The stability of the optimized products was assessed using stability chambers (Binder GmbH, KBF 240, E5.2, Tuttlingen, Germany) set to 25°C/65% RH and 40°C/75% RH as specified by ICH Q1A guidelines for stability testing of new drug substances and products [456]. The formulations were tested on days 0, 3, 7 and 30 following manufacture as signs of instability were observed after one month of storage. The stability of each SLM formulation was evaluated by assessing the PS, ZP, DLC and EE on days 0, 3, 7 and 30 after manufacture. SEM and TEM were used to evaluate the PS, shape and surface morphology of the formulations and the ZP was established using a Nano-ZS Zetasizer set in the Laser Doppler Anemometry (LDA) mode. The entrapment efficiency was also assessed on days 0, 3, 7 and 30 as it was considered to be an essential indicator of stability of the SLM formulations that may exert an effect on KTZ release [246].

A summary of the PS, ZP, DLC, EE data generated on days 0, 3, 7, 30 at 25°C/60% RH and 40°C/75% RH for SLM 15 and SLM 16 respectively is listed in Tables 5.6 and 5.7.

Table 5.6 PS, ZP, DLC and EE of KTZ-loaded SLM 15 manufactured using 10% w/v solid lipid, 5% w/v KTZ, 4% w/v Pluronic® F-68, 2% w/v Tween 80 and 1% w/v sodium cholate on days 0, 3, 7 and 30 after manufacture and after storage at 25°C/60% RH and 40°C/75% RH

SLM 15		**25°C/60% RH**		
Parameters	**day 0**	**day 3**	**day 7**	**day 30**
PS (µm)	18.6 ± 3.6	22.5 ± 2.9	26.7 ± 2.8	29.7 ± 2.4
ZP (mV)	-30.1 ± 0.2	-30.2 ± 0.1	-29.3 ± 0.2	-31.2 ± 0.3
DLC (%)	23.6 ± 1.8	21.8 ± 2.1	22.4 ± 3.8	22.9 ± 4.6
EE (%)	58.2 ± 2.3	59.2 ± 4.2	56.9 ± 3.6	57.8 ± 7.5
SLM 15		**40°C/75% RH**		
Parameters	**day 0**	**day 3**	**day 7**	**day 30**
PS (µm)	18.6 ± 3.6	30.1 ± 4.2	46.3 ± 7.5	60.6 ± 8.4
ZP (mV)	-30.1 ± 0.2	-28.4 ± 0.3	-27.6 ± 0.3	-28.6 ± 0.2
DLC (%)	23.6 ± 1.8	15.4 ± 4.3	8.4 ± 3.6	4.7 ± 1.9
EE (%)	58.2 ± 2.3	30.2 ± 5.1	17.6 ± 2.4	6.2 ± 2.3

Table 5.7 PS, ZP, DLC and EE of KTZ-loaded SLM 16 manufactured using 10% w/v solid lipid, 5% w/v KTZ, 5% w/v Pluronic® F-68, 1% w/v Tween 80 and 1% w/v sodium cholate on days 0, 3, 7 and 30 after manufacture and after storage at 25°C/60% RH and 40°C/75% RH

SLM 16		**25°C/60% RH**		
Parameters	**day 0**	**day 3**	**day 7**	**day 30**
PS (µm)	15.6 ± 2.1	25.8 ± 3.7	29.8 ± 1.2	30.6 ± 5.8
ZP (mV)	-31.6 ± 0.1	-29.4 ± 0.2	-28.5 ± 0.1	-32.1 ± 0.3
DLC (%)	18.6 ± 0.3	16.5 ± 4.3	17.1 ± 1.8	17.9 ± 3.5
EE (%)	43.2 ± 1.4	41.5 ± 3.2	39.9 ± 2.4	42.6 ± 6.2
SLM 16		**40°C/75% RH**		
Parameters	**day 0**	**day 3**	**day 7**	**day 30**
PS (µm)	25.6 ± 2.2	35.7 ± 4.9	48.9 ± 7.6	70.7 ± 5.1
ZP (mV)	-31.6 ± 0.1	-26.3 ± 0.2	-25.8 ± 0.1	-24.1 ± 0.3
DLC (%)	18.6 ± 0.3	10.4 ± 2.6	6.7 ± 1.9	3.2 ± 0.6
EE (%)	43.2 ± 1.4	31.2 ± 4.3	12.6 ± 3.1	5.6 ± 2.5

5.5.5.1. Particle size analysis

The PS data listed in Table 5.6 reveal that the mean PS of microparticles of batch SLM 15 were less than 35 µm following storage at 25°C/60% RH for 30 days. An increase in PS was observed on storage of SLM 15 at 25°C/60% RH (Table 5.6 and Figure 5.20). Particles of SLM 15 after storage at 25°C/60% RH for up to 30 days are depicted in Figure 5.14. The SEM micrographs shown in Figure 5.14 depict spherical and smooth particles that exhibited signs of flocculation from the day of manufacture and an increase in flocculation was noted after storage at 25°C/60% RH for one month. The particles depicted in Figure 5.14 D for SLM formulation 15 reveals the presence of clusters following storage at 25°C/60% RH for 30 days which could indicate early signs of instability due to coalescence or Ostwald ripening. Coalescence describes the aggregation of flocculated particles into a larger droplet and may be caused by a loss of the interfacial film between approaching particles in the aqueous phase [457]. Furthermore, the

particles depicted in Figure 5.14 D also appear less spherical than those obtained on the day of manufacture as depicted in Figure 5.14 A. However, an aqueous suspension of SLM 15 could easily be redispersed and no signs of caking were observed. In addition there were no changes in state of the dispersion and the lipid microparticles remained in the solid state with no signs of gel formation after exposure to 25°C/60% RH for up to 30 days.

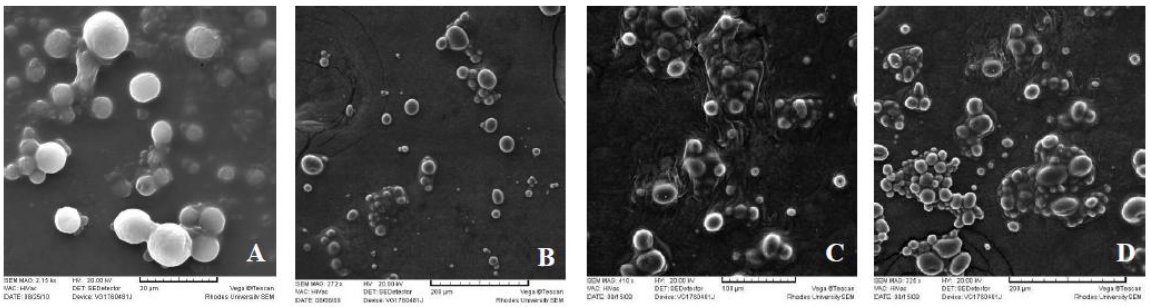

Figure 5.14 SEM micrographs of SLM formulation 15 after storage at 25°C/60% RH on day 0 (A), 3 (B), 7 (C), 30 (D) after manufacture

Particles of SLM 15 after storage at 40°C/75% RH for up to 30 days are depicted in Figure 5.15. The data obtained from the SEM reveal a progressive increase in the mean PS of SLM 15 when stored at 40°C/75% RH (from 18.6 µm to 60.6 µm) (Table 5.6 and Figure 5.20). The SEM micrographs depicted in Figure 5.15 B reveal clusters of particles from day 3 and larger particles possibly resulting from a combination of coalescence and Ostwald ripening from day 7 (Figure 5.15 C). Furthermore, a slight change in state from a solid to semi-solid state was observed from day 7 when stored under these conditions. A change in physical appearance from a uniform aqueous dispersion to a semi-solid gel was observed on day 30 following storage of SLM 15 at 40°C/75% RH and the product was not easily redispersed on shaking. Therefore, storage of an aqueous dispersion of SLM 15 at 40°C/75% RH for 30 days resulted in caking and revealed potential instability. The SEM micrograph of particles of batch SLM 15 generated on day 30 following storage at 40°C/75% RH (Figure 5.15 D) revealed clusters of very large and small particles, a phenomenon that is characteristic of Ostwald ripening which may be the mechanism of instability within this dispersion.

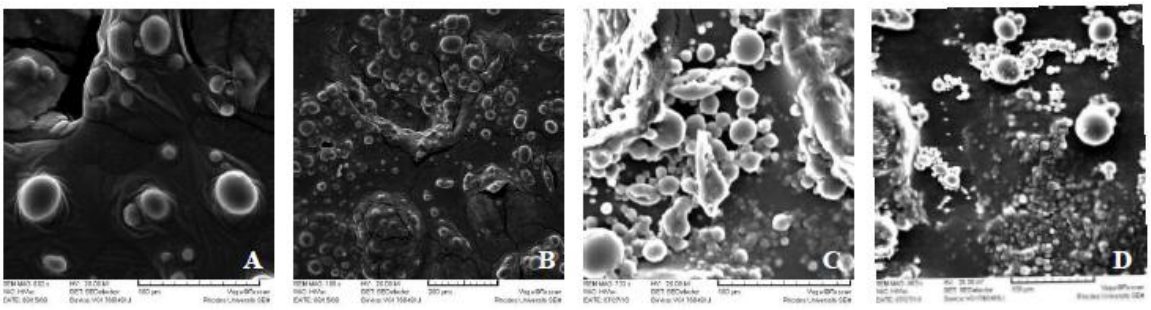

Figure 5.15 SEM micrographs of SLM formulation 15 after storage at 40°C/75% RH on day 0 (A), 3 (B), 7 (C), 30 (D) after manufacture

The TEM micrographs obtained on day 30 for aqueous dispersion SLM 15 revealed an increase in the mean PS of the SLM after storage at 40°C/75% RH (Figure 5.16 B) compared to storage at 25°C/60% RH (Figure 5.16 A). The particles in Figure 5.16 B seem to be rough and non-spherical and indicate the physical instability of the dispersion due to coalescence or Ostwald ripening. Therefore, SLM 15 was not deemed stable under high temperature and humidity conditions thirty days after its manufacture. Storage of SLM 15 at 25°C/60% RH appeared to be suitable as the stability of the aqueous dispersion did not appear to be altered significantly. The slight aggregation of particles noted in the aqueous dispersion of SLM 15 at 25°C/60% RH was easily redispersed on shaking of the product.

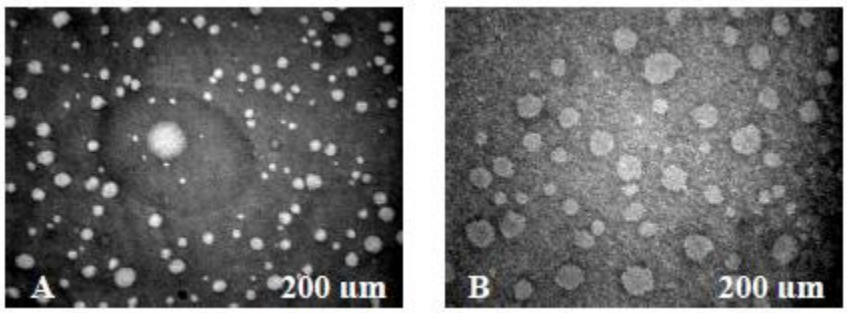

Figure 5.16 TEM micrographs of SLM formulation 15 after storage at 25°C/60% RH (A) and 40°C/75% RH (B) on day 30

SEM micrographs of SLM 16 following storage at 25°C/60% RH are depicted in Figure 5.17 and reveal that the mean PS was between 15.6 ± 2.1 µm and 30.6 ± 5.8 µm on days 0 and 30 respectively (Table 5.7). The particles in aqueous dispersion of SLM 16 were relatively spherical and discrete on the day of manufacture. Slight particle growth was observed on days 3 and 7 and larger particles surrounded by smaller particles were observed on day 7 possibly indicating that aggregation due to Ostwald ripening was occurring. However, the aqueous dispersion of SLM 16 was easily redispersed into a uniform product for up to 7 days without any sign of gel formation

or caking. Some non-spherical particles and presence of a few lipid aggregates are observed in Figure 5.17 D.

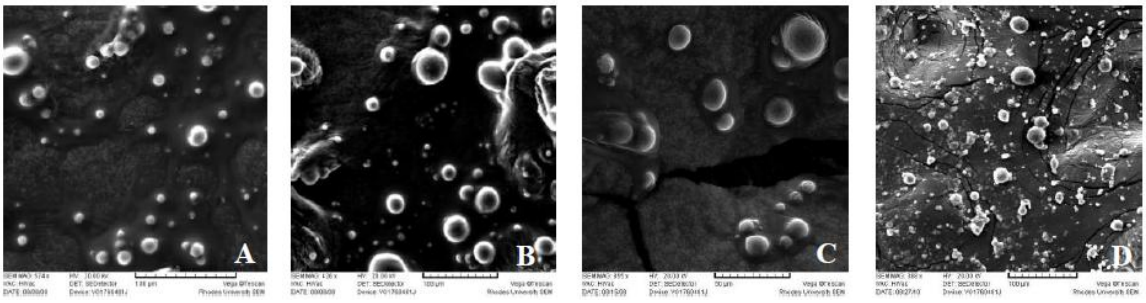

Figure 5.17 SEM micrographs of SLM formulation 16 after storage at 25°C/60% RH on day 0 (A), 3 (B), 7 (C), 30 (D) after manufacture

Following storage of SLM 16 at 40°C/75% RH large particles were observed from the day of manufacture. The mean PS following storage of SLM 16 at 25°C/60% RH was 15.6 ± 2.1 µm whilst storage at 40°C/75% RH for the same time period (2 hours) resulted in particles with a mean diameter of 25.6 ± 2.2 µm (Table 5.7). Furthermore, the particles of SLM 16 were non-spherical following storage at 40°C/75% RH. The aqueous dispersion of SLM 16 exhibited signs of physical instability from day 3 as the dispersion was not easily redispersible on shaking and a compact layer had been formed at the bottom container. SEM micrographs taken on day 3 and 7 are depicted in Figure 5.18 B and C reveal the presence of non-discrete particles connected by a layer of film. The mean PS was 70.7 ± 5.1 µm after 30 days which indicates that an increase in PS had occurred since the day of manufacture. The degree of caking was more pronounced after one month of storage of SLM 16 at 40°C/75% RH further revealing the instability of the dispersion under these conditions at this temperature.

The presence of solidification within the aqueous dispersion at higher storage temperatures could be due to crystal growth that results in the formation of a solid, lipid network. Subsequent recrystallisation into platelets or rods-like structures may occur and promote the formation of a lipid network. The extent of solidification is thought to be related to the amount of stable lipid modification [448]. Higher kinetic energy of particles will lead to collisions between particles which in turn may disrupt the stabilizing surfactant layer around the particles. The formation of resulting unprotected interfaces within the dispersion at high temperatures increases the likelihood of particles approaching each other from unprotected sides leading to aggregation [448].

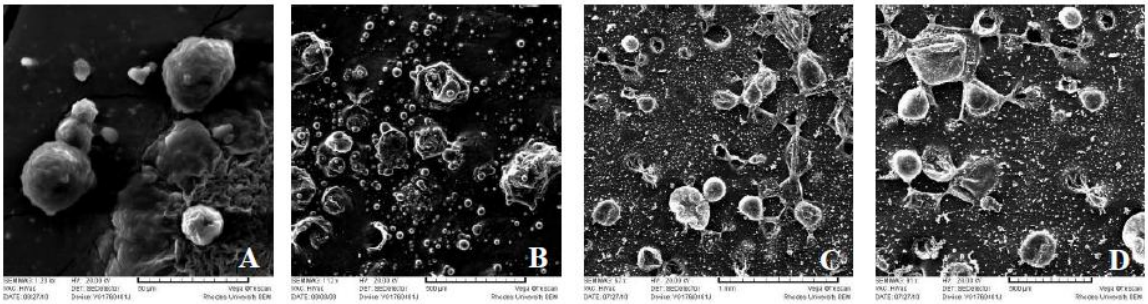

Figure 5.18 SEM micrographs of SLM formulation 16 after storage at 40°C/75% RH on day 0 (A), 3 (B), 7 (C), 30 (D) after manufacture

The instability of the aqueous dispersion of SLM 16 following storage at 40°C/75% RH was also observed in the TEM micrographs (Figure 5.19). On day 30 clusters of large particles were seen within the aqueous dispersion as observed in Figure 5.19 B. The high degree of particle growth and caking observed after one month of storage revealed an unstable aqueous dispersion for SLM 16 when stored at 40°C/75% RH.

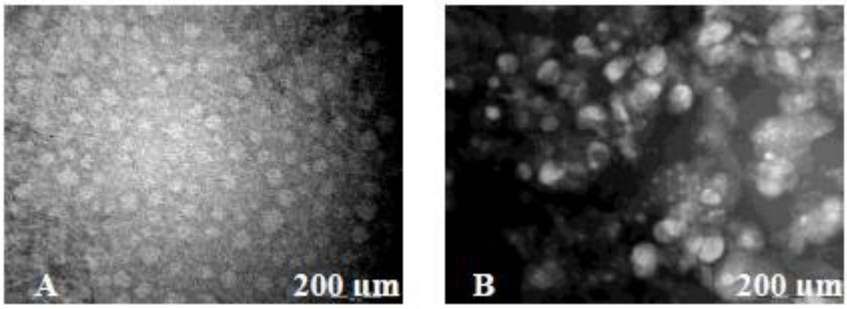

Figure 5.19 TEM micrographs of SLM formulation 16 after storage at 25°C/60°C RH (A) and 40°C/75°C RH (B) on day 30

A comparison of the particle growth in the aqueous dispersions of SLM 15 and SLM 16 after storage at 25°C/60% RH and 40°C/75% RH is depicted in Figure 5.20. An increase in mean PS was observed for both SLM 15 and SLM 16 on storage and exposure to higher temperatures appeared to aggravate the extent of particle growth. The TEM micrograph depicted in Figure 5.19 B reveals the presence of cluster of lipid. Furthermore, a higher degree of particle growth and physical instability were observed for SLM 16 following storage at 40°C/75% RH indicating that the dispersion cannot be stored for more than three days under high temperature and humidity conditions. Therefore, these stability studies indicate that particle growth and subsequent solidification may be induced through an increase in kinetic energy at high temperatures coupled with possible changes in lipid crystallinity, particle film rigidity and steric effects [448].

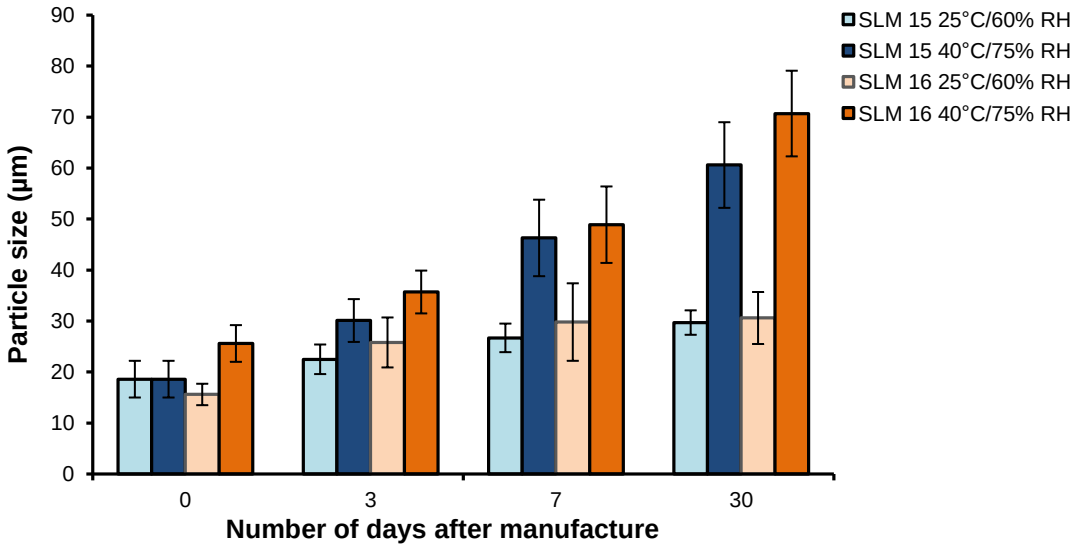

Figure 5.20 Particle size (PS) of SLM formulations 15 and 16 after storage at 25°C/60% RH and 40°C/75% RH on day 0, 3, 7 and 30 after manufacture

5.5.5.2. Zeta potential analysis

The assessment of ZP over the storage period is a good indicator of changes in stability within aqueous disperse systems. The change in ZP observed following storage of SLM 15 and SLM 16 respectively over the one-month period is depicted in Figure 5.21. The changes in ZP were not significantly different between batches SLM 15 and SLM 16 on the day of manufacture and following storage at 25°C/60% RH ($p > 0.05$). However, a drop in ZP was observed as from three days when SLM dispersions were stored at 40°C/75% RH and this observation may explain the increase in aggregation observed following storage at high temperature.

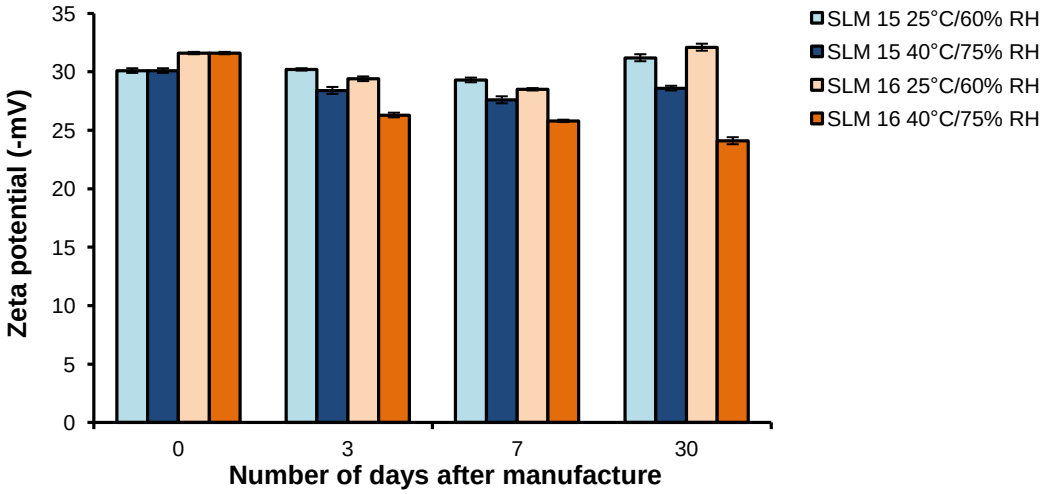

Figure 5.21 Zeta potential (ZP) of SLM formulations 15 and 16 after storage at 25°C/60% RH and 40°C/75% RH on day 0, 3, 7 and 30 after manufacture

A decrease in the magnitude of the ZP from -30.1 ± 0.2 mV to -28.6 ± 0.2 mV was observed for batch SLM 15 when stored for 30 days at 40°C/75% RH. A larger drop in ZP was noted for batch SLM 16 after storage at 40°C/75% RH as the ZP decreased from -31.6 ± 0.1 mV to -24.1 ± 0.3 mV (Table 5.7). The reduction in ZP indicates a decrease in the surface charge of the particles and subsequently a reduction in the repulsion potential of the particles. The resulting increase in flocculation observed for batches SLM 15 and SLM 16 at 40°C/75% RH may be attributed to the decrease in ZP, thereby promoting aggregation. Limited flocculation is known to occur at ZP values between 5 and 15 mV and rapid flocculation occurs at potentials < 5 mV. In these stability studies rapid flocculation was observed at higher ZP values following storage at 40°C/75% RH and this may be attributed to the high kinetic energy and velocity of the particles that exist at higher temperatures leading to an increase in number of collisions and contact time between dispersed particles. High temperatures and the presence of light are known to increase the kinetic energy of systems and such prevailing conditions in combination with a lower ZP is likely to promote aggregation and gelation of the SLM dispersions [448]. Under storage conditions of 40°C/75% RH the cumulative steric and electrostatic effects of Tween 80 and sodium cholate appear to be inadequate to prevent agglomeration that was observed for dispersion of batches SLM 15 and SLM 16.

The reduction in ZP may also be due to a shift in the shear plane subsequently resulting in insufficient potential energy necessary for electrostatic repulsion that is essential for establishing a high quality interface between SLM units. Increasing the energy input into a system may also lead to changes in the crystallinity of lipids and enhance the development of lipid modifications such as an increase in the formation of the β-modification form. Subsequently, an increase in energy input results in crystalline re-orientation that in turn may influence the Nernst potential, the surface charge of the particle and resultant ZP. Storage of SLM at high temperatures may also lead to crystal growth and for one-dimensional crystal growth the charge density on different sides of a crystal may vary, thereby changing the surface ratio of charges that has an impact on the ZP [448]. An increase in the temperature of exposure for these systems results in a reduction in ZP as observed in Figure 5.21.

5.5.5.3. KTZ loading capacity and encapsulation efficiency

The DLC and EE obtained for KTZ-loaded aqueous SLM dispersions during stability studies are important parameters as they reflect the remaining KTZ content that is encapsulated following

storage and provide an indication of the ability of the SLM to retain KTZ. An EE value of at least 50% following storage for 30 days was deemed necessary for KTZ-loaded SLM intended for use in an oral drug delivery system. A reduction of the DLC and EE values on storage implies that expulsion of KTZ from the lipid matrix that can be attributed to changes within the lipid structure would have occurred. Conversion of metastable lipid modifications to their stable forms during storage can result in a change in crystallinity of the lipid from a disordered structure that retains API molecules to an orderly structure that leads to the expulsion of the KTZ [156]. The DLC and EE values observed for batches SLM 15 and SLM 16 following storage at 25°C/60% RH and 40°C/75% RH are depicted in Figures 5.22 and 5.23.

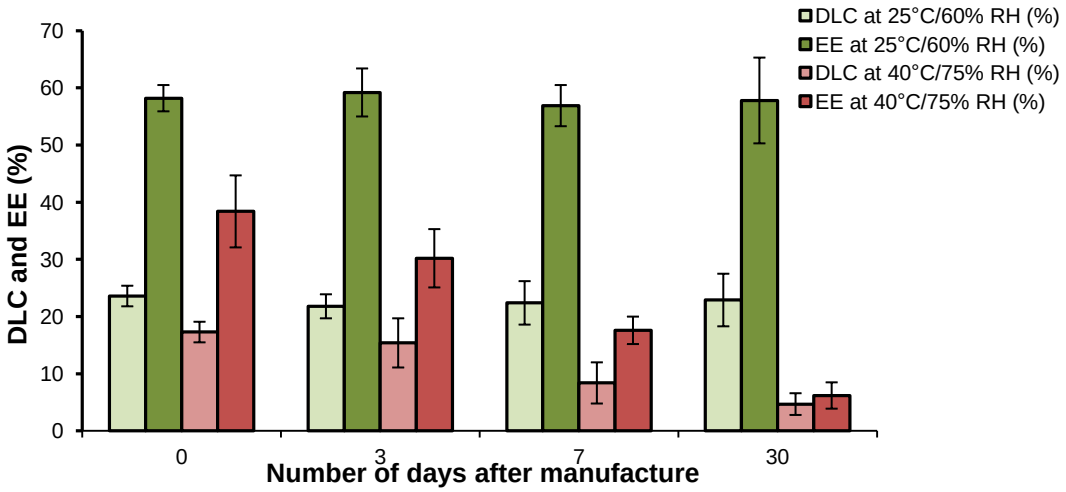

Figure 5.22 Drug loading capacity (DLC) and encapsulation efficiency (EE) of SLM 15 after storage at 25°C/60% RH and 40°C/75% RH on day 0, 3, 7 and 30 after manufacture

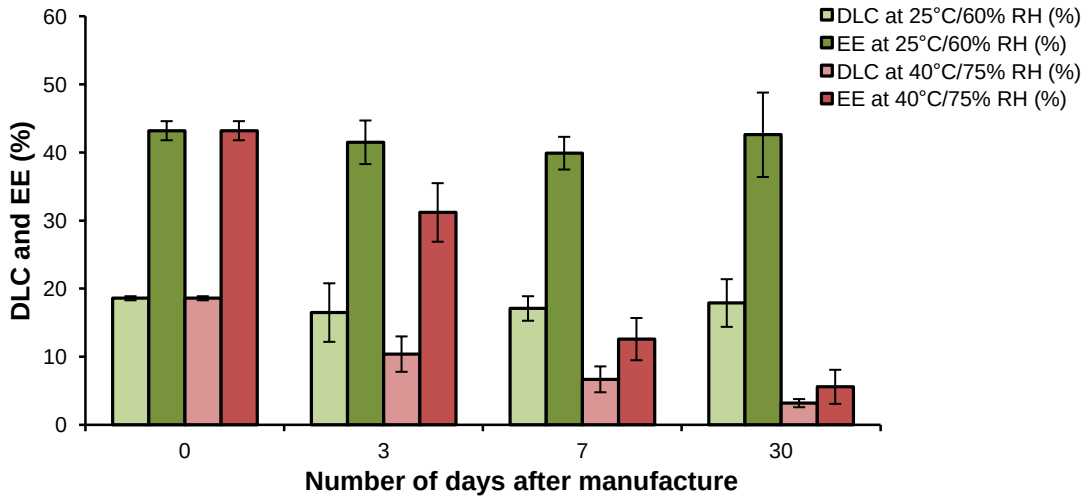

Figure 5.23 Drug loading capacity (DLC) and encapsulation efficiency (EE) of SLM 16 after storage at 25°C/60% RH and 40°C/75% RH on day 0, 3, 7 and 30 after manufacture

The stability data revealed that batches SLM 15 and SLM 16 maintained their DLC and EE after storage at 25°C/60% RH for up to 30 days. However, SEM and TEM micrographs of batch SLM 16 taken following storage at 25°C/60% RH for 30 days revealed the presence of non-spherical particles and lipid aggregates that may be indicative of particle growth through Ostwald ripening which would eventually destabilize the SLM. An increase in particle aggregation as noted from the presence of lipid aggregrates in SLM 16 following storage at 25°C/60% RH would subsequently lead to expulsion of the API. Therefore, batch SLM 15 was deemed to more stable than SLM 16 after storage at 25°C/60% RH for up to 30 days. On the other hand batches SLM 15 and 16 revealed a reduction in DLC and EE following storage at 40°C/75% RH for up to 30 days. The reduction in DLC and EE was more pronounced at storage conditions of 40°C/75% RH for batch SLM 16 when compared to that observed for batch SLM 15 implying that batch SLM 16 was less stable than batch SLM 15. Prolonged storage conditions of KTZ-loaded SLM 16 at 40°C/75% RH may have resulted in a decrease in the crystallinity of KTZ subsequently enhancing its expulsion from the particle. An increase in temperature may result in perturbation of the surfactant layer, resulting in a temporary lack of homogeneity of this layer that may precipitate particle aggregation and KTZ expulsion [458].

The transformation of the lipid to stable polymorphic modifications may also result in instability within SLM dispersions, since physically stable SLM dispersions usually require the coexistence of different modifications [459]. The polymorphic form of a lipid affects the loading capacity of a drug in that lipid in addition to affecting the release rate of drug from the technology [102, 460]. In lipid formulations the lipid tends to re-crystallize partially in the α-form as opposed to preferential re-crystallisation in the β'-form and rapid transformation to the β-form in bulk lipid materials [237]. The formation of the β/β' forms promotes drug expulsion as the crystal lattice tends to become more structured [237, 460]. This polymorphic transformation is slower in long-chain triglycerides [460] and as the thermodynamic stability and lipid packing density increases , drug incorporation rates decrease in the order β-modification > β'-modification > α –modification > supercooled melts [341]. Although the DSC thermogram of the bulk lipid material revealed no significant changes in polymorphic state following exposure to heat (Chapter 4, § 4.4.2.2, *vide infra*), Labrafil® M2130 CS may be subject to polymorphic changes after subsequent exposure to increased temperature. The recrystallization process following production of the micro-emulsion at 60ºC occurs via a cooling step which was reproduced by allowing the lipid to cool to 25ºC during DSC studies. In order to evaluate possible polymorphic changes on reheating an additional heating step to mimic the impact of high temperature storage conditions will be required during

DSC studies to establish whether the structure of Labrafil® M2130 CS changes. Additional thermal analysis of KTZ-loaded SLM dispersion during stability was beyond the scope of this project and therefore not undertaken.

The stability studies undertaken on two optimized SLM formulations *viz.*, SLM 15 and SLM 16 infer that there is some degree of instability of KTZ-loaded dispersions when stored under high temperatures and humidity conditions. The formulation of batch SLM 15 was found to be of better quality and more stable than those of batch SLM 16 when stored at 25°C/60% RH for up to 30 days. Both batches were found to be unstable when stored at 40°C/75% RH. Therefore, batch SLM 15 manufactured using 5% w/v KTZ, 10% w/v Labrafil® M2130 CS, 4% w/v Pluronic® F-68, 2% w/v Tween® 80, 1% w/v sodium cholate was deemed to be an appropriate KTZ-loaded SLM formulation produced in these studies. The product can be stored for up to one month at 25°C/60% RH without a significant loss in stability. It is clear that additional development and optimization of this dosage form would be necessary to ensure that a viable product was produced.

5.6. Conclusions

For the development of KTZ-loaded SLM it was important to establish an appropriate surfactant or combination of surfactants to use in order to stabilize SLM aqueous dispersions during initial formulation studies. The use of Pluronic® F68 in combination with other surfactants such as Soluphor® P, Soluplus®, Lutrol® E400, Tween 80 and the co-surfactant sodium cholate was investigated in order to select an emulsifying system for KTZ-loaded SLM manufacture using Labrafil® M2130 CS. Pluronic® F68 is known to produce stable dispersions particularly when used in combination with other non-ionic surfactants. However, aqueous SLM dispersions manufactured using Lutrol® E400, Soluphor® P, Soluplus® in combination with Pluronic® F68 were found to be unstable and of poor quality in terms of PS, ZP, DLC and EE from the day of manufacture. It was observed that KTZ-loaded SLM dispersions manufactured using Lutrol® E400, Soluphor® P, Soluplus® exhibited signs of gelation, particle agglomeration and a low DLC and EE. Conversely, the use of Pluronic® F68 in combination with Tween 80 and sodium cholate produced particles of better quality and these surfactants were therefore selected for the further development of an optimized KTZ-loaded SLM aqueous dispersion.

A simple micro-emulsion technique in which an Ultra-Turrax® homogenizer operated at 24 000 rpm for 5 minutes followed by homogenization with an Erweka GmbH homogenizer was used to manufacture KTZ-loaded SLM dispersions. The addition of increasing amounts of Labrafil® M2130 CS did not seem to affect the ZP of KTZ-loaded SLM dispersions. High concentrations of solid lipid however resulted in particles with a lower DLC, EE and a large PS. Therefore, an optimum concentration of 10% w/v solid lipid was used to manufacture KTZ-loaded SLM. Increasing the ratio of KTZ to Labrafil® M2130 CS did not affect the ZP of the particles and concentrations in excess of 5% w/v KTZ led to a reduction in DLC and EE and an increase in PS. In order to improve particle characteristics of KTZ-loaded SLM dispersions the effect of process parameters such as the number of homogenization cycles on the quality of particles was established and the results revealed that at least five homogenization cycles using the Erweka GmbH homogenizer were necessary to produce particles of acceptable ZP, PS, surface morphology, DLC and EE.

An assessment of the stability of the KTZ-loaded SLM aqueous dispersions under different temperatures and humidity conditions was essential to establish if changes in the quality of dispersions was likely to occur on storage. Optimised KTZ-loaded SLM formulations were produced using Labrafil® M2130 CS, KTZ and a combination of the non-ionic surfactants. Pluronic® F-68, sodium cholate and Tween 80. The PS, surface morphology, ZP, DLC and EE were evaluated following storage at 25°C/65% RH and 40°C/75% RH for up to 30 days following manufacture as specified in the ICH Q1A guidelines. The formulations were tested on days 0, 3, 7 and 30 and stability studies revealed that batch SLM 15 manufactured using 10% w/v Labrafil® M2130 CS, 5% w/v KTZ and a combination of 4% w/v Pluronic® F-68, 2% w/v Tween 80 and 1% w/v sodium cholate was the most stable when stored at 25°C/65% RH for up to 30 days, yet storage at 40°C/75% RH revealed the formulation was unstable. Storage at 40°C/75% RH resulted in an increase in PS, agglomeration of the particles into a solid lipid network, lower ZP and KTZ expulsion which may be caused by a disruption of the interfacial film surrounding the particles leading to a reduction in electrostatic repulsion of the particles. Changes in the crystallinity of the solid lipid during storage may have resulted in the formation of stable polymorphic forms which do not retain KTZ within the solid lipid matrix. Additional studies using thermal analysis and X-ray scattering would be necessary to investigate changes in the polymorphic nature of the lipid matrices used to manufacture the SLM during and after storage.

The results of these studies reveal the feasibility of incorporating KTZ into SLM and suggest it is a suitable candidate for inclusion into physiologically compatible lipid matrices as it is lipophilic in nature. It has been shown that aqueous dispersions of KTZ-loaded SLM can be manufactured using a simple micro-emulsion technique and that aqueous SLM dispersions of KTZ were stable for up to 30 days when stored at 25°C/60% RH. The method of manufacture of SLM formulations developed in these studies permits small-scale production of KTZ-loaded SLM with a reasonable DLC and EE for the oral administration of KTZ to paediatric patients who may not be able to swallow large solid oral dosage forms. Further optimization studies are required to improve the DLC and EE of KTZ on storage. The research reveals the potential for use of SLM as a means to avoid extemporaneous preparation of KTZ dispersions prepared using crushed tablets which is common practice in South Africa.

CHAPTER SIX

CONCLUSIONS

Ketoconazole (KTZ) is a broad-spectrum imidazole antifungal agent used for the treatment of oral and topical mycoses in immuno-compromised patients suffering from cancer and paediatric patients requiring antifungal therapy. The mechanism of action of KTZ involves inhibition of sterol 14α-demethylase which results in the depletion of ergosterol in fungal cells, thereby impacting on cell growth and proliferation patterns. KTZ is a BCS Class II compound and has physicochemical and pharmacological properties including a high degree of lipophilicity and adequate systemic activity which make it an ideal candidate for incorporation into an oral lipid formulation. The lack of availability of antifungal medicines in an appropriate form for paediatric use, particularly in developing countries, requires that extemporaneous preparations of KTZ in suspension form must be prepared to achieve appropriate antifungal therapy in some public hospitals. Solid oral dosage forms that are intended for adult use are usually manipulated by breaking or crushing and mixing with a suspension vehicle such as methylcellulose by care-givers. This may lead to under or over-dosing if providers are not well-informed and are not trained in product manipulation. This commonly used practice in South Africa can also exacerbate the problem of resistance, thereby further impacting the quality of life of patients. Cold chain storage requirements in developing countries due to high temperature and humidity conditions are often ignored and the dearth of information on the stability of the extemporaneous KTZ formulations prepared in these countries can lead to ineffective antifungal therapy and may further complicate the problem of resistance. Therefore, it is essential that research and development is focused on the development of novel drug delivery systems with well-established chemical and physical stability to circumvent extemporaneous preparation and improve antifungal therapy, particularly amongst paediatric patients.

Solid lipid carriers are promising colloidal drug delivery systems that may be used as potential carriers for the oral administration of KTZ to paediatric patients. Solid lipid nanoparticles (SLN) and microparticles (SLM) combine the advantages of traditional colloidal carriers such as liposomes, nano-emulsions, nano-suspensions and polymeric nanoparticles as they consist of lipid matrices that are manufactured using physiologically well-tolerated lipid excipients including glycerides of fatty acid esters or fatty acids that have GRAS status. In addition SLN and SLM

demonstrate physicochemical stability, enhanced bioavailability, have the possibility of sustaining drug release and drug targeting. The use of solid lipids instead of liquid lipids in the manufacture of solid lipid carriers not only leads to a reduction in the variability of plasma profiles but also enables better characterization of lipid excipients and offers a greater possibility of scale-up of the manufacturing process. Furthermore, better control can be exercised over the release kinetics of encapsulated compounds when solid lipid carriers are used. The drug content has been found to be higher for carriers manufactured with solid lipid carriers and these systems may be used for the encapsulation of hydrophilic and hydrophobic drugs.

Furthermore, as KTZ is known to undergo chemical degradation, the protection of the API by the lipid matrix offers an additional advantage for the administration of KTZ. The objective of this study was to investigate the feasibility of developing SLM as a carrier system for the oral administration of KTZ to patients in an attempt to circumvent the disadvantages of extemporaneously prepared formulations of KTZ and to improve the stability of KTZ. The study involved the development and characterization of a KTZ solid lipid micro-particle (SLM) formulation containing 5% w/v KTZ and an investigation of the stability of the KTZ-loaded aqueous SLM dispersion on storage.

Prior to initiating formulation development studies, it is crucial that a suitable analytical method that can be used for the quantitation of KTZ and the characterization of the dosage form during the development and assessment process is developed and validated. One of the difficulties encountered in the analysis of lipid formulations is interference due to formulation excipients that are usually present in technologies with a complex composition. RP-HPLC is a widely used powerful and reliable analytical tool that may be used for the *in vitro* analysis of formulations manufactured using a complex combination of adjuvants and has been applied to the analysis of gels, ointments, creams and suspensions. Separation and quantitative data may be generated using RP-HPLC and interference challenges can be successfully eliminated. Most of the RP-HPLC methods that have been reported for the analysis of KTZ from pharmaceutical dosage forms involve extensive sample pre-treatment, lack specificity and are costly and tedious to perform. There was a need to develop a simple, rapid, sensitive and selective analytical method to quantitate the DLC and EE of KTZ-loaded SLM. The initial phases of this project entailed the development, optimization and validation of a suitable RP-HPLC method for the quantitative determination of KTZ in aqueous KTZ-loaded SLM dispersions during formulation optimization and stability studies. The chromatographic separation of KTZ and the internal standard,

clotrimazole (CLZ) was achieved using a binary mobile phase consisting of acetonitrile and 50 mM potassium dihydrogen phosphate buffer adjusted to pH 6.0 using 1 M sodium hydroxide in a ratio of 60:40. A flow rate of 1 ml/min was used and the analysis was performed at room temperature (22°C) using a Beckman Coulter® ODS column (5µm, 150 × 4.6 mm I.D.). The method was developed using a modular isocratic reversed-phase HPLC-UV system at a wavelength of 206 nm. The optimized liquid chromatographic conditions were achieved by manipulation of the mobile phase composition, buffer pH, molarity and flow rate. The analytical run time was 12 min and KTZ and CLZ eluted at 3.7 and 8.7 min, respectively. The RP-HPLC analytical method was validated according to USP and ICH guidelines and was found to be linear, precise, accurate, specific, sensitive and suitable for the intended purpose of quantitation of KTZ. KTZ was found to be stable in methanol following storage at 4°C for at least 7 days and thus all calibration standards were prepared using methanol, were stored at 4°C and analyzed within 7 days after which fresh calibration standards were prepared.

Different methods of preparation of solid lipid carriers exist and include high pressure homogenization, micro-emulsion, solvent-evaporation and spray congealing techniques. The inclusion of KTZ into SLM manufactured using the solid lipid, Labrafil® M2130 CS was achieved using a modified form of the micro-emulsion technique that is relatively simple and relies on the use of routinely available homogenizers. This micro-emulsion technique was used as it requires relatively low mechanical energy input and imparts good theoretical stability to the particles that are produced. The incorporation of a drug into solid lipid carriers depends on the solubility of the drug in the lipid, the physicochemical properties of the drug, the chemical and physical structure of the lipids, the surfactants used and the production method used to produce the particles. One of the pre-requisites to obtain adequate drug loading is a sufficiently high solubility of the drug in the lipid melt. Formulation development of KTZ-loaded SLM was preceded by studies that were conducted to determine the lipid with the best solubilising potential for KTZ. The lipids that were screened for use were Precirol® ATO 5, Compritol® 888, Labrafil® M2130 CS, Gelucire® 44/14 and Gelucire® 50/13. KTZ was found to be poorly to moderately soluble in all lipids tested. Labrafil® M2130 CS was found to exhibit the best solubilising potential for KTZ and was therefore selected as the lipid for use in the manufacture of KTZ-loaded SLM as the solubility of the API in the solid lipid is likely to influence the DLC and EE.

The crystalline nature of the lipid can also influence drug loading as lipids that tend to form highly crystalline particles with a perfect orderly lattice structure are prone to drug expulsion and

thus unexpected dynamics of polymeric transitions may be one of the disadvantages of solid lipid carriers. The micro-emulsion method required that KTZ was dissolved in the solid lipid and subjected to heating to 60°C. Methods that involve the heating of the solid lipid during manufacture of SLM may lead to changes in the polymorphic and crystalline states of the SLM in relation to those of the bulk lipid from which the microparticles are manufactured. Differential Scanning Calorimetry (DSC) and wide-angle X-ray diffraction (WAXD) are widely used to investigate the crystallinity and polymorphic modification of the lipid. The polymorphic behavior of the solid lipid and KTZ was therefore investigated using DSC. Infrared and Raman spectroscopy are useful to determine the structural properties of lipids and Fourier-transform Infra-Red (FTIR) was used in conjunction with DSC to identify polymorphic modifications, if any, of the solid lipid and KTZ. It was necessary to elucidate the thermal behavior of KTZ and the Labrafil® M2130 CS prior to and after exposure of 1 hour to a temperature of 60°C prior to initiating formulation studies. Thermal and spectroscopic analyses of a 1:1 mixture of KTZ and Labrafil® M2130 CS were also conducted to investigate if Labrafil® M2130 CS interacts with KTZ prior to and after heating to production temperatures for 1 hour. DSC and FTIR studies revealed that no changes in crystallinity of KTZ or Labrafil® M2130 CS occurred after heating to 60°C for 1 hour. A slight shift in the melting endotherm of Labrafil® M2130 CS was noted. However, no changes in chemical bond shift, broadening of peaks or occurrence of unique bands were observed in the FTIR spectrum of the lipid suggesting that there are no major polymorphic changes within the lipid. Similarly, no potential interaction of KTZ and the lipid was detected after heating to 60°C for 1 hour as the DSC thermogram revealed the presence of peaks that were due to Labrafil® M2130 CS and KTZ and these occurred at their respective melting points. These data show that KTZ is molecularly dispersed in the lipid. The FTIR spectrum of the KTZ-lipid mixture shows a superimposition of the bands of KTZ and Labrafil® M2130 CS, thereby confirming the lack of physicochemical interaction within the drug-lipid mixture as an interaction would result in new bond formation and thus result in the occurrence of additional absorption bands.

The incorporation of KTZ into SLM was investigated by developing and manufacturing an aqueous micro-particulate dispersion consisting of 10% w/v solid lipid Labrafil® M2130 CS using a modified micro-emulsion technique that required the use of an Ultra-Turrax® homogenizer set at 24 000 rpm for 5 minutes followed by the use of the Erweka GmbH homogenizer. Particle growth and an unpredictable gelation tendency may impair the stability of solid lipid particles and successful formulation development requires optimization of the production method, conditions

and composition of the formulation including the surfactant/surfactant mixture, properties of the lipid and the API to ensure that a product of good quality is manufactured.

A number of characterization techniques may be used to investigate the physical and chemical properties of solid lipid nanoparticles and microparticles and for the control of the quality of the product during formulation development and optimization procedures. Parameters that tend to have a direct impact on the stability and release kinetics of solid lipid carriers include particle size (PS), zeta potential (ZP), degree of crystallinity and lipid modification. The co-existence of additional structures and dynamic phenomena within the system must also be evaluated. Photon correlation spectroscopy (PCS) and laser diffractometry (LD) are used for routine measurement of particle size. However, PCS may only be used to measure particles from a few nanometers to about 3 micrometers in size. Electron microscopy may also be used to obtain direct information about particle size and shape and was used in these studies. Scanning Electron Microscopy (SEM) was used for the morphological examination of the particles and Transmission Electron Microscopy (TEM) was used to measure the particle size and gather information regarding the physical characteristics of particles. The ZP of the nano- or microparticles is used to predict the stability of aqueous dispersions of SLN and SLM on storage and was measured using Laser Doppler anemometry (LDA) coupled to a Zetasizer. The evaluation of DLC and EE is of prime importance since it in part influences the release characteristics of incorporated drug. The factors that determine the loading capacity of the drug in the lipid are the solubility of the drug in the molten lipid, the miscibility of the drug in the lipid melt, the physicochemical properties of the solid lipid matrix and the polymorphic state of the lipid material. The amount of API entrapped in the particle is determined after separation of the encapsulated API from the SLM formulation using techniques such as ultracentrifugation, centrifugation filtration and gel permeation chromatography. The extent of KTZ entrapment was assessed indirectly by determining the amount of drug remaining in the supernatant following filtration centrifugation using the RP-HPLC method that was developed and validated for the quantitation of KTZ.

Initial formulation development studies were conducted to select a surfactant or combination of surfactants that would ensure the production of stable KTZ-loaded SLM formulations. The selection of an emulsifying system was based on an ability to produce SLM of acceptable size, shape and surface morphology and to stabilize KTZ-loaded SLM dispersions on the day of manufacture. Pluronic® F68 was used in combination with surfactants such as Soluphor® P, Soluplus®, Lutrol® E400, Tween 80 and sodium cholate to determine an appropriate emulsifying

system for KTZ-loaded SLM manufactured using the solid lipid Labrafil® M2130 CS. Aqueous drug-free SLM dispersions manufactured using Pluronic® F68 (4% w/v) in combination with Lutrol® E400 (3% w/v), Soluphor® P (3% w/v), Soluplus® (3% w/v) (SLM 1, SLM 2 and SLM 3) and KTZ-loaded SLM dispersions using the same combination of surfactants (SLM 10, SLM 11 and SLM 12) were found to be unstable and of poor quality in terms of PS, ZP, DLC and EE from the day of manufacture. The KTZ-loaded SLM dispersions manufactured using 3% w/v Lutrol® E400, Soluphor® P, Soluplus® exhibited signs of instability such as a gelation tendency, particle agglomeration and particularly low DLC and EE on the day of manufacture. The results also revealed that the use of Pluronic® F68 alone and in combination with Tween 80 and/or sodium cholate produced drug-free SLM of better quality (SLM 4, SLM 5, SLM 6, SLM 7, SLM 8 and SLM 9) than drug-free SLM produced using Lutrol® E400, Soluphor® P, Soluplus® (SLM 1, SLM 2 and SLM 3). Therefore, Pluronic® F68 in combination with Tween 80 and/or sodium cholate was further investigated in these initial studies and it was found that a combination of 4% w/v Pluronic® F68, 2% w/v Tween 80 and 1% w/v sodium cholate produced the most stable drug-free SLM dispersion (SLM 6).

The use of increasing amounts of Labrafil® M2130 CS was investigated and it was found that high concentrations of solid lipid produced particles with lower DLC and EE and larger PS. In contrast, the ZP of KTZ-loaded SLM dispersions produced with varying concentrations of Labrafil® M2130 CS was not significantly affected. An optimum concentration of 10% w/v Labrafil® M2130 CS was used to manufacture the KTZ-loaded SLM in further formulation development studies. The effect of KTZ loading on the quality of SLM was investigated and concentrations in excess of 5% w/v KTZ led to a reduction in DLC and EE and an increase in PS. Conversely, an increasing ratio of KTZ to Labrafil® M2130 CS did not appear to influence the ZP of the aqueous SLM dispersions. The effect of process variables such as the number of homogenization cycles on the quality of the particles produced was investigated and the results suggest that at least five homogenization cycles using the Erweka GmbH homogenizer after initial homogenisation with an Ultra-Turrax® homogenizer at 24 000 rpm for 5 minutes were required for the production of particles with acceptable surface morphology and size. The number of homogenisation cycles appeared to influence the surface morphology and particle size (PS) using a higher number of homogenisation cycles produced particles with a smoother surface and lower PS.

In order to establish the potential use of an aqueous KTZ-loaded SLM dispersion in developing countries, it was essential to assess stability under different storage conditions. The high temperature and humidity conditions encountered in many developing countries require that aqueous preparations be stored under cold chain conditions. However, cold chain facilities are sometimes not readily available in these countries and it was deemed appropriate to investigate the stability of the KTZ-loaded aqueous dispersion at 25°C/65% RH and 40°C/75% RH as specified by the ICH Q1A guidelines for up to 30 days following manufacture in order to establish the stability of the KTZ-loaded dispersion in cases where cold chain facilities are not available. Two optimized KTZ-loaded formulations (SLM 15 and SLM 16) were produced and their PS, surface morphology, ZP, DLC and EE were evaluated on days 0, 3, 7 and 30 following manufacture and storage at 25°C/65% RH and 40°C/75% RH. The results of these studies revealed that SLM 15 manufactured using 10% w/v of Labrafil® M2130 CS, 5% w/v KTZ and a combination of 4% w/v Pluronic® F-68, 2% w/v Tween 80 and 1% w/v sodium cholate was the most stable when stored at 25°C/65% RH for up to 30 days. However, storage at 40°C/75% RH resulted in the formulation exhibiting instability. Storage at temperatures and humidity conditions of 40°C/75% RH is likely to cause an increase in PS and agglomeration of the particles into a solid, lipid network with destabilization of the formulation. This phenomenon of aggregation may be a consequence of Ostwald ripening due to a relatively large PS distribution observed in these formulations. In addition the ZP is lowered and the decrease in DLC and EE infers the expulsion of KTZ from the lipid matrix on storage. The chain of events leading to the destabilization of KTZ-loaded SLM formulations could arise from the disruption of the interfacial film around the particles leading to a reduction in electrostatic repulsion forces and changes in the crystallinity of the solid lipid to stable polymorphic forms which do not retain KTZ within the solid lipid matrix.

This research has shown that it is feasible to incorporate KTZ into SLM using a simple micro-emulsion manufacturing technique. The long-term stability of the optimized formulation, SLM 15, must be established and improved to enable storage at 25°C/60% RH for longer than 30 days and increase the stability of the formulation at 40°C/75% RH. The narrowing of the PS and PS distribution may assist in preventing particle growth through Ostwald ripening. Elucidation of the mechanism of instability using DSC in conjunction with WAXD to investigate potential polymorphic modifications and crystallographic changes during storage of the SLM dispersions is necessary. The use of DSC and WAXD may also improve the detection of dynamic phenomena and co-existence of addition structures that may form during prolonged storage of the SLM system. Furthermore, it is important to evaluate the *in vitro* release rate of KTZ from the SLM

dispersion using conventional or novel methods prior to the use of this alternative drug delivery system as a carrier for KTZ. *In vitro* release of KTZ from SLM may be achieved using a dialysis bag diffusion technique or an agitation technique followed by ultracentrifugation or centrifugal ultrafiltration. In addition, further studies may require an investigation into the biocompatibility of the SLM formulation. Although the solid lipid Labrafil® M2130 CS has a GRAS status and is known to be approved for its use in oral drug delivery, it may be worthwhile to determine the biocompatibility of the SLM formulation, for instance by performing cell culture studies using the mouse connective tissue fibroblast L929 cell line in order to investigate its *in vitro* cytotoxicty as specified in the ICH S2 guidelines. Since KTZ is a BCS Class II compound exhibiting poor water solubility the potential of SLM as a bioavailability enhancer may be investigated using an *in vitro* method requiring side by side diffusion cells with an artificial or biological membrane or an *ex vivo* method to determine the permeability of KTZ across the gut. Should the KTZ-loaded SLM formulation exhibit acceptable physicochemical and biopharmaceutical properties the use of this innovative solid lipid carrier system for the oral administration of KTZ can be investigated by conducting an *in vivo* study to confirm that appropriate levels of KTZ are reached *in vivo* during antifungal therapy. The addition of a taste enhancer to improve the palatability of the formulation is important if it is intended for paediatric use. The incorporation of additional excipients in the SLM formulation may affect stability and therefore further stability studies may be necessary.

This research has revealed that the inclusion of KTZ in SLM is possible and there is the potential to improve oral delivery of KTZ for paediatric patients. This approach may facilitate the delivery of KTZ in a liquid dosage form, which would circumvent the need for extemporaneous preparation of KTZ dispersions made from crushed solid dosage forms. This approach may result in enhanced bioavailability of KTZ and improved stability of KTZ, thereby bettering the quality of life of patients requiring antifungal therapy in developing countries.

APPENDIX I

BATCH SUMMARY REPORTS

The batch summary reports for Batches SLM 1 to SLM 24 are included here.

RHODES UNIVERSITY, Faculty of Pharmacy, Grahamstown, South Africa

BATCH SUMMARY REPORT

Formulator: Henusha Jhundoo

Product name: Solid Lipid Microparticle (SLM) aqueous dispersion

Batch ID: SLM 1

Manufacturing date: 19.07.2010 **Batch size:** 50 ml

Homogenizing time: 25-30 min

Formula

Material	% (w/v)	Amount added (g)
Labrafil® M2130 CS	10.00	5.06
Pluronic® F-68	4.00	2.12
Lutrol® E400	3.00	1.54
Aqua	83.0	41.5

Production equipment used:

Water bath: Model NB-34980 Colora Ultra-Thermostat
Homogenizer 1: Model 6-105 AF Virtis Ultra-Turrax®
Homogenizer 2: Model HO/HHO Erweka AR400, Erweka GmbH

Parameters evaluated on day of manufacture:

Particle size, PS (µm)	43.7 ± 3.1
Zeta potential, ZP (mV)	-18.3 ± 0.5

Comments / Observations

- White to off-white aqueous dispersion was produced
- Dispersion was clumpy and non-homogenous on the day of manufacture
- Particles were non-discrete, non-spherical and had irregular surfaces
- Signs of gelation and particle aggregation were visible on the day of manufacture

RHODES UNIVERSITY, Faculty of Pharmacy, Grahamstown, South Africa

BATCH SUMMARY REPORT

Formulator: Henusha Jhundoo

Product name: Solid Lipid Microparticle (SLM) aqueous dispersion

Batch ID: SLM 2

Manufacturing date: 19.07.2010 **Batch size:** 50 ml

Homogenizing time: 25-30 min

Formula

Material	% (w/v)	Amount added (g)
Labrafil® M2130 CS	10.00	5.16
Pluronic® F-68	4.00	2.09
Soluphor® P	3.00	1.57
Aqua	83.0	41.2

Production equipment used:

Water bath: Model NB-34980 Colora Ultra-Thermostat
Homogenizer 1: Model 6-105 AF Virtis Ultra-Turrax®
Homogenizer 2: Model HO/HHO Erweka AR400, Erweka GmbH

Parameters evaluated on day of manufacture:

Particle size, PS (µm)	17.3 ± 4.4
Zeta potential, ZP (mV)	-13.9 ± 0.2

Comments / Observations

- White to off-white aqueous dispersion was produced
- Dispersion was clumpy and non-homogenous on the day of manufacture
- Particles were non-discrete and had irregular surfaces
- Signs of sedimentation and particle aggregation were visible on the day of manufacture

RHODES UNIVERSITY, Faculty of Pharmacy, Grahamstown, South Africa

BATCH SUMMARY REPORT

Formulator: Henusha Jhundoo

Product name: Solid Lipid Microparticle (SLM) aqueous dispersion

Batch ID: SLM 3

Manufacturing date: 19.07.2010 **Batch size:** 50 ml

Homogenizing time: 25-30 min

Formula

Material	% (w/v)	Amount added (g)
Labrafil® M2130 CS	10.00	5.05
Pluronic® F-68	4.00	2.12
Soluplus®	3.00	1.58
Aqua	83.0	41.3

Production equipment used:

Water bath: Model NB-34980 Colora Ultra-Thermostat
Homogenizer 1: Model 6-105 AF Virtis Ultra-Turrax®
Homogenizer 2: Model HO/HHO Erweka AR400, Erweka GmbH

Parameters evaluated on day of manufacture:	
Particle size, PS (µm)	21.7 ± 8.6
Zeta potential, ZP (mV)	-14.8 ± 0.6

Comments / Observations

- White to off-white aqueous dispersion was produced
- Dispersion was non-homogenous on the day of manufacture
- Particles were non-spherical and formed aggregates
- Fast rate of sedimentation was observed on the day of manufacture
- Signs of gelation were observed on the day of manufacture

RHODES UNIVERSITY, Faculty of Pharmacy, Grahamstown, South Africa

BATCH SUMMARY REPORT

Formulator: Henusha Jhundoo

Product name: Solid Lipid Microparticle (SLM) aqueous dispersion

Batch ID: SLM 4

Manufacturing date: 02.08.2010 **Batch size:** 50 ml

Homogenizing time: 25-30 min

Formula

Material	% (w/v)	Amount added (g)
Labrafil® M2130 CS	10.00	5.07
Pluronic® F-68	4.00	2.03
Tween 80	3.00	1.63
Aqua	83.0	41.3

Production equipment used:

Water bath: Model NB-34980 Colora Ultra-Thermostat
Homogenizer 1: Model 6-105 AF Virtis Ultra-Turrax®
Homogenizer 2: Model HO/HHO Erweka AR400, Erweka GmbH

Parameters evaluated on day of manufacture:

Particle size, PS (µm)	37.4 ± 6.5
Zeta potential, ZP (mV)	-18.7 ± 0.9

Comments / Observations

- White to off-white aqueous dispersion was produced
- Dispersion was homogenous on the day of manufacture
- Particles were spherical with improved surface characteristics
- Sedimentation was observed on the day of manufacture
- A wide particle size distribution (PSD) was noted

RHODES UNIVERSITY, Faculty of Pharmacy, Grahamstown, South Africa

BATCH SUMMARY REPORT

Formulator: Henusha Jhundoo

Product name: Solid Lipid Microparticle (SLM) aqueous dispersion

Batch ID: SLM 5

Manufacturing date: 02.08.2010 **Batch size:** 50 ml

Homogenizing time: 25-30 min

Formula

Material	% (w/v)	Amount added (g)
Labrafil® M2130 CS	10.00	5.09
Pluronic® F-68	4.00	2.04
Tween 80	1.00	0.59
Sodium cholate	2.00	1.13
Aqua	83.0	41.2

Production equipment used:

Water bath: Model NB-34980 Colora Ultra-Thermostat
Homogenizer 1: Model 6-105 AF Virtis Ultra-Turrax®
Homogenizer 2: Model HO/HHO Erweka AR400, Erweka GmbH

Parameters evaluated on day of manufacture:

Particle size, PS (µm)	40.6 ± 9.2
Zeta potential, ZP (mV)	-11.6 ± 0.7

Comments / Observations

- White to off-white aqueous dispersion was produced
- Dispersion was homogenous on the day of manufacture
- Particles were large and spherical
- A wide particle size distribution (PSD) was noted
- Signs of aggregation were observed

RHODES UNIVERSITY, Faculty of Pharmacy, Grahamstown, South Africa

BATCH SUMMARY REPORT

Formulator: Henusha Jhundoo

Product name: Solid Lipid Microparticle (SLM) aqueous dispersion

Batch ID: SLM 6

Manufacturing date: 02.08.2010 **Batch size:** 50 ml

Homogenizing time: 25-30 min

Formula

Material	% (w/v)	Amount added (g)
Labrafil® M2130 CS	10.00	5.13
Pluronic® F-68	4.00	2.06
Tween 80	2.00	1.14
Sodium cholate	1.00	0.53
Aqua	83.0	41.1

Production equipment used:

Water bath: Model NB-34980 Colora Ultra-Thermostat
Homogenizer 1: Model 6-105 AF Virtis Ultra-Turrax®
Homogenizer 2: Model HO/HHO Erweka AR400, Erweka GmbH

Parameters evaluated on day of manufacture:

Particle size, PS (µm)	25.5 ± 2.6
Zeta potential, ZP (mV)	-31.1 ± 0.2

Comments / Observations

- White to off-white aqueous dispersion was produced
- Dispersion was homogenous on the day of manufacture
- Particles were smooth, small and spherical
- High ZP and low rate of sedimentation

RHODES UNIVERSITY, Faculty of Pharmacy, Grahamstown, South Africa

BATCH SUMMARY REPORT

Formulator: Henusha Jhundoo

Product name: Solid Lipid Microparticle (SLM) aqueous dispersion

Batch ID: SLM 7

Manufacturing date: 25.08.2010 **Batch size:** 50 ml

Homogenizing time: 25-30 min

Formula

Material	% (w/v)	Amount added (g)
Labrafil® M2130 CS	10.00	5.03
Pluronic® F-68	5.00	2.58
Tween 80	1.00	0.54
Sodium cholate	1.00	0.59
Aqua	83.0	41.3

Production equipment used:

Water bath: Model NB-34980 Colora Ultra-Thermostat
Homogenizer 1: Model 6-105 AF Virtis Ultra-Turrax®
Homogenizer 2: Model HO/HHO Erweka AR400, Erweka GmbH

Parameters evaluated on day of manufacture:

Particle size, PS (µm)	22.6 ± 4.1
Zeta potential, ZP (mV)	-32.7 ± 0.1

Comments / Observations

- White to off-white aqueous dispersion was produced
- Dispersion was homogenous on the day of manufacture
- Particles were small, spherical but tended to aggregate
- High ZP and low rate of sedimentation

RHODES UNIVERSITY, Faculty of Pharmacy, Grahamstown, South Africa

BATCH SUMMARY REPORT

Formulator: Henusha Jhundoo

Product name: Solid Lipid Microparticle (SLM) aqueous dispersion

Batch ID: SLM 8

Manufacturing date: 25.08.2010 **Batch size:** 50 ml

Homogenizing time: 25-30 min

Formula

Material	% (w/v)	Amount added (g)
Labrafil® M2130 CS	10.00	5.15
Pluronic® F-68	6.00	3.18
Sodium cholate	1.00	0.61
Aqua	83.0	41.1

Production equipment used:

Water bath: Model NB-34980 Colora Ultra-Thermostat
Homogenizer 1: Model 6-105 AF Virtis Ultra-Turrax®
Homogenizer 2: Model HO/HHO Erweka AR400, Erweka GmbH

Parameters evaluated on day of manufacture:

Particle size, PS (µm)	22.2 ± 7.9
Zeta potential, ZP (mV)	-19.3 ± 0.3

Comments / Observations

- White to off-white aqueous dispersion was produced
- Dispersion was homogenous on the day of manufacture
- Particles were small, smooth and spherical
- Low rate of sedimentation and signs of aggregation were noted on the day of manufacture
- A wide particle size distribution (PSD) was noted

RHODES UNIVERSITY, Faculty of Pharmacy, Grahamstown, South Africa

BATCH SUMMARY REPORT

Formulator: Henusha Jhundoo

Product name: Solid Lipid Microparticle (SLM) aqueous dispersion

Batch ID: SLM 9

Manufacturing date: 25.08.2010 **Batch size:** 50 ml

Homogenizing time: 25-30 min

Formula

Material	% (w/v)	Amount added (g)
Labrafil® M2130 CS	10.00	5.25
Pluronic® F-68	7.00	3.52
Aqua	83.0	41.2

Production equipment used:

Water bath: Model NB-34980 Colora Ultra-Thermostat
Homogenizer 1: Model 6-105 AF Virtis Ultra-Turrax®
Homogenizer 2: Model HO/HHO Erweka AR400, Erweka GmbH

Parameters evaluated on day of manufacture:

Particle size, PS (µm)	33.4 ± 5.8
Zeta potential, ZP (mV)	-15.5 ± 0.3

Comments / Observations

- White to off-white aqueous dispersion was produced
- Dispersion was homogenous on the day of manufacture
- Particles were larger with irregular surfaces
- Sedimentation was observed
- A wide particle size distribution (PSD) was noted

RHODES UNIVERSITY, Faculty of Pharmacy, Grahamstown, South Africa

BATCH SUMMARY REPORT

Formulator: Henusha Jhundoo

Product name: KTZ-loaded Solid Lipid Microparticle (SLM) aqueous dispersion

Batch ID: SLM 10

Manufacturing date: 06.09.2010 **Batch size:** 50 ml

Homogenizing time: 25-30 min

Formula

Material	% (w/v)	Amount added (g)
KTZ	5.00	2.53
Labrafil® M2130 CS	10.00	5.16
Pluronic® F-68	4.00	2.16
Lutrol® E400	3.00	1.59
Aqua	78.0	38.6

Production equipment used:

Water bath: Model NB-34980 Colora Ultra-Thermostat
Homogenizer 1: Model 6-105 AF Virtis Ultra-Turrax®
Homogenizer 2: Model HO/HHO Erweka AR400, Erweka GmbH

Parameters evaluated on day of manufacture:

Particle size, PS (µm)	39.2 ± 8.1
Zeta potential, ZP (mV)	-18.3 ± 0.5
Drug loading capacity, DLC (%)	0.04 ± 0.007
Encapsulation Efficiency, EE (%)	0.09 ± 0.006

Comments / Observations

- White to off-white homogeneous aqueous dispersion was produced
- Dispersion was physically unstable
- Signs of gelation and particle aggregation were visible
- Very low DLC and EE

RHODES UNIVERSITY, Faculty of Pharmacy, Grahamstown, South Africa

BATCH SUMMARY REPORT

Formulator: Henusha Jhundoo

Product name: KTZ-loaded Solid Lipid Microparticle (SLM) aqueous dispersion

Batch ID: SLM 11

Manufacturing date: 06.09.2010 **Batch size:** 50 ml

Homogenizing time: 25-30 min

Formula

Material	% (w/v)	Amount added (g)
KTZ	5.00	2.59
Labrafil® M2130 CS	10.00	5.14
Pluronic® F-68	4.00	2.08
Soluphor® P	3.00	1.61
Aqua	78.0	38.6

Production equipment used:

Water bath: Model NB-34980 Colora Ultra-Thermostat
Homogenizer 1: Model 6-105 AF Virtis Ultra-Turrax®
Homogenizer 2: Model HO/HHO Erweka AR400, Erweka GmbH

Parameters evaluated on day of manufacture:

Particle size, PS (µm)	33.6 ± 4.4
Zeta potential, ZP (mV)	-13.9 ± 0.2
Drug loading capacity, DLC (%)	0.89 ± 0.02
Encapsulation Efficiency, EE (%)	1.85 ± 0.09

Comments / Observations

- White to off-white homogeneous aqueous dispersion was produced
- Dispersion was physically unstable
- Signs of gelation and particle aggregation were visible
- Very low DLC and EE

RHODES UNIVERSITY, Faculty of Pharmacy, Grahamstown, South Africa

BATCH SUMMARY REPORT

Formulator: Henusha Jhundoo

Product name: KTZ-loaded Solid Lipid Microparticle (SLM) aqueous dispersion

Batch ID: SLM 12

Manufacturing date: 06.09.2010 **Batch size:** 50 ml

Homogenizing time: 25-30 min

Formula

Material	% (w/v)	Amount added (g)
KTZ	5.00	2.55
Labrafil® M2130 CS	10.00	5.04
Pluronic® F-68	4.00	2.18
Soluplus®	3.00	1.51
Aqua	78.0	38.7

Production equipment used:

Water bath: Model NB-34980 Colora Ultra-Thermostat
Homogenizer 1: Model 6-105 AF Virtis Ultra-Turrax®
Homogenizer 2: Model HO/HHO Erweka AR400, Erweka GmbH

Parameters evaluated on day of manufacture:	
Particle size, PS (µm)	15.7 ± 8.6
Zeta potential, ZP (mV)	-14.8 ± 0.6
Drug loading capacity, DLC (%)	0.97 ± 0.07
Encapsulation Efficiency, EE (%)	1.93 ± 0.18

Comments / Observations

- White to off-white homogeneous aqueous dispersion was produced
- Dispersion was physically unstable
- Sedimentation was observed
- Very low DLC and EE

RHODES UNIVERSITY, Faculty of Pharmacy, Grahamstown, South Africa

BATCH SUMMARY REPORT

Formulator: Henusha Jhundoo

Product name: KTZ-loaded Solid Lipid Microparticle (SLM) aqueous dispersion

Batch ID: SLM 13

Manufacturing date: 13.09.2010 **Batch size:** 50 ml

Homogenizing time: 25-30 min

Formula

Material	% (w/v)	Amount added (g)
KTZ	5.00	2.51
Labrafil® M2130 CS	10.00	5.05
Pluronic® F-68	4.00	2.03
Tween 80	3.00	1.56
Aqua	78.0	38.9

Production equipment used:

Water bath: Model NB-34980 Colora Ultra-Thermostat
Homogenizer 1: Model 6-105 AF Virtis Ultra-Turrax®
Homogenizer 2: Model HO/HHO Erweka AR400, Erweka GmbH

Parameters evaluated on day of manufacture:	
Particle size, PS (µm)	24.4 ± 5.2
Zeta potential, ZP (mV)	-18.3 ± 0.4
Drug loading capacity, DLC (%)	6.9 ± 1.2
Encapsulation Efficiency, EE (%)	11.5 ± 1.8

Comments / Observations

- White to off-white homogeneous aqueous dispersion was produced
- Low rate of sedimentation was observed
- Particles were spherical with irregular surfaces
- Low DLC and EE
- A wide particle size distribution (PSD) was noted

RHODES UNIVERSITY, Faculty of Pharmacy, Grahamstown, South Africa

BATCH SUMMARY REPORT

Formulator: Henusha Jhundoo

Product name: KTZ-loaded Solid Lipid Microparticle (SLM) aqueous dispersion

Batch ID: SLM 14

Manufacturing date: 25.10.2010 **Batch size:** 50 ml

Homogenizing time: 25-30 min

Formula

Material	% (w/v)	Amount added (g)
KTZ	5.00	2.53
Labrafil® M2130 CS	10.00	5.02
Pluronic® F-68	4.00	2.03
Sodium cholate	2.00	1.04
Tween 80	1.00	0.54
Aqua	78.0	38.8

Production equipment used:

Water bath: Model NB-34980 Colora Ultra-Thermostat
Homogenizer 1: Model 6-105 AF Virtis Ultra-Turrax®
Homogenizer 2: Model HO/HHO Erweka AR400, Erweka GmbH

Parameters evaluated on day of manufacture:

Particle size, PS (µm)	23.6 ± 7.7
Zeta potential, ZP (mV)	-30.9 ± 0.8
Drug loading capacity, DLC (%)	7.3 ± 0.18
Encapsulation Efficiency, EE (%)	13.3 ± 0.74

Comments / Observations

- White to off-white homogeneous aqueous dispersion was produced
- Low rate of sedimentation was observed and dispersion was stable on the day of manufacture
- Higher ZP indicating higher stability
- Particles were smooth, small, spherical and discrete
- Low DLC and EE
- A wide particle size distribution (PSD) and signs of agglomeration was noted

RHODES UNIVERSITY, Faculty of Pharmacy, Grahamstown, South Africa

BATCH SUMMARY REPORT

Formulator: Henusha Jhundoo

Product name: KTZ-loaded Solid Lipid Microparticle (SLM) aqueous dispersion

Batch ID: SLM 15

Manufacturing date: 25.10.2010 **Batch size:** 50 ml

Homogenizing time: 25-30 min

Formula

Material	% (w/v)	Amount added (g)
KTZ	5.00	2.51
Labrafil® M2130 CS	10.00	5.04
Pluronic® F-68	4.00	2.08
Tween 80	2.00	1.10
Sodium cholate	1.00	0.506
Aqua	78.0	36.5

Production equipment used:

Water bath: Model NB-34980 Colora Ultra-Thermostat
Homogenizer 1: Model 6-105 AF Virtis Ultra-Turrax®
Homogenizer 2: Model HO/HHO Erweka AR400, Erweka GmbH

Parameters evaluated on the day of manufacture, after storage at 25°C/60% RH and 40°C/75% RH for 30 days:

	Day of manufacture	25°C/60% RH	40°C/75% RH
Particle size, PS (µm)	18.6 ± 3.6	29.7 ± 2.4	60.6 ± 8.4
Zeta potential, ZP (mV)	-30.1 ± 0.2	-31.2 ± 0.3	-28.6 ± 0.2
Drug loading capacity, DLC (%)	23.6 ± 1.8	22.9 ± 4.6	4.7 ± 1.9
Encapsulation Efficiency, EE (%)	58.2 ± 2.3	57.8 ± 7.5	6.2 ± 2.3

Comments / Observations

- White to off-white homogeneous aqueous dispersion was produced
- Dispersion was physically stable on the day of manufacture
- Particles were discrete, small, smooth and spherical
- No signs of gelation or particle aggregation were visible on the day of manufacture
- High DLC and EE and no significant reduction in DLC and EE on storage at 25°C/60% RH for up to 30 days
- Storage at 40°C/75% RH for 30 days led to instability of the SLM dispersion and loss of KTZ retention

RHODES UNIVERSITY, Faculty of Pharmacy, Grahamstown, South Africa

BATCH SUMMARY REPORT

Formulator: Henusha Jhundoo

Product name: KTZ-loaded Solid Lipid Microparticle (SLM) aqueous dispersion

Batch ID: SLM 16

Manufacturing date: 25.10.2010 **Batch size:** 50 ml

Homogenizing time: 25-30 min

Formula

Material	% (w/v)	Amount added (g)
KTZ	5.00	2.57
Labrafil® M2130 CS	10.00	5.04
Pluronic® F-68	5.00	2.58
Tween 80	1.00	1.03
Sodium cholate	1.00	0.501
Aqua	78.0	38.3

Production equipment used:

Water bath: Model NB-34980 Colora Ultra-Thermostat
Homogenizer 1: Model 6-105 AF Virtis Ultra-Turrax®
Homogenizer 2: Model HO/HHO Erweka AR400, Erweka GmbH

Parameters evaluated on the day of manufacture, after storage at 25°C/60% RH and 40°C/75% RH for 30 days:

	Day of manufacture	25°C/60% RH	40°C/75% RH
Particle size, PS (µm)	15.6 ± 2.1	30.6 ± 5.8	70.7 ± 5.1
Zeta potential, ZP (mV)	-31.6 ± 0.1	-32.1 ± 0.3	-24.1 ± 0.3
Drug loading capacity, DLC (%)	18.6 ± 0.3	17.9 ± 3.5	3.2 ± 0.6
Encapsulation Efficiency, EE (%)	43.2 ± 1.4	42.6 ± 6.2	5.6 ± 2.5

Comments / Observations

- White to off-white homogeneous aqueous dispersion was produced
- Dispersion was physically stable on the day of manufacture
- Particles were discrete, small, smooth and spherical
- No signs of gelation or particle aggregation were visible on the day of manufacture
- High DLC and EE and no significant reduction in DLC and EE on storage at 25°C/60% RH for up to 30 days
- Storage at 40°C/75% RH for 30 days led to instability of the SLM dispersion and loss of KTZ retention
- Particle growth was observed on storage at 40°C/75% RH for 30 days and the dispersion was unstable and exhibited particle aggregation and gelation

RHODES UNIVERSITY, Faculty of Pharmacy, Grahamstown, South Africa

BATCH SUMMARY REPORT

Formulator: Henusha Jhundoo

Product name: KTZ-loaded Solid Lipid Microparticle (SLM) aqueous dispersion

Batch ID: SLM 17

Manufacturing date: 28.10.2010 **Batch size:** 50 ml

Homogenizing time: 25-30 min

Formula

Material	% (w/v)	Amount added (g)
KTZ	5.00	2.52
Labrafil® M2130 CS	10.00	5.05
Pluronic® F-68	6.00	3.08
Sodium cholate	1.00	0.511
Aqua	78.0	38.8

Production equipment used:

Water bath: Model NB-34980 Colora Ultra-Thermostat
Homogenizer 1: Model 6-105 AF Virtis Ultra-Turrax®
Homogenizer 2: Model HO/HHO Erweka AR400, Erweka GmbH

Parameters evaluated on the day of manufacture:

Particle size, PS (µm)	24.2 ± 6.5
Zeta potential, ZP (mV)	-20.7 ± 0.3
Drug loading capacity, DLC (%)	17.4 ± 0.1
Encapsulation Efficiency, EE (%)	29.7 ± 0.9

Comments / Observations

- White to off-white homogeneous aqueous dispersion was produced
- Dispersion was physically stable on the day of manufacture
- Particles were discrete and spherical
- Average DLC and EE
- A wide particle size distribution (PSD) was noted

RHODES UNIVERSITY, Faculty of Pharmacy, Grahamstown, South Africa

BATCH SUMMARY REPORT

Formulator: Henusha Jhundoo

Product name: KTZ-loaded Solid Lipid Microparticle (SLM) aqueous dispersion

Batch ID: SLM 18

Manufacturing date: 28.10.2010 **Batch size:** 50 ml

Homogenizing time: 25-30 min

Formula

Material	% (w/v)	Amount added (g)
KTZ	5.00	2.52
Labrafil® M2130 CS	10.00	5.04
Pluronic® F-68	7.00	3.59
Aqua	78.0	38.9

Production equipment used:

Water bath: Model NB-34980 Colora Ultra-Thermostat
Homogenizer 1: Model 6-105 AF Virtis Ultra-Turrax®
Homogenizer 2: Model HO/HHO Erweka AR400, Erweka GmbH

Parameters evaluated on the day of manufacture:	
Particle size, PS (µm)	28.4 ± 8.8
Zeta potential, ZP (mV)	-15.6 ± 0.2
Drug loading capacity, DLC (%)	10.1 ± 0.2
Encapsulation Efficiency, EE (%)	17.9 ± 0.4

Comments / Observations

- White to off-white homogeneous aqueous dispersion was produced
- Particles were discrete and spherical but had irregular surfaces
- Sedimentation was observed on the day of manufacture
- Low DLC and EE
- A wide particle size distribution (PSD) was noted

RHODES UNIVERSITY, Faculty of Pharmacy, Grahamstown, South Africa

BATCH SUMMARY REPORT

Formulator: Henusha Jhundoo

Product name: KTZ-loaded Solid Lipid Microparticle (SLM) aqueous dispersion

Batch ID: SLM 19

Manufacturing date: 28.10.2010 **Batch size:** 50 ml

Homogenizing time: 25-30 min

Formula

Material	% (w/v)	Amount added (g)
KTZ	5.00	2.56
Labrafil® M2130 CS	5.00	2.54
Pluronic® F-68	4.00	2.01
Sodium cholate	1.00	0.52
Tween® 80	2.00	1.01
Aqua	83.0	41.4

Production equipment used:

Water bath: Model NB-34980 Colora Ultra-Thermostat
Homogenizer 1: Model 6-105 AF Virtis Ultra-Turrax®
Homogenizer 2: Model HO/HHO Erweka AR400, Erweka GmbH

Parameters evaluated on the day of manufacture:

Particle size, PS (µm)	40.2 ± 3.5
Zeta potential, ZP (mV)	-30.2 ± 0.3
Drug loading capacity, DLC (%)	24.5 ± 2.1
Encapsulation Efficiency, EE (%)	59.3 ± 3.5

Comments / Observations

- White to off-white homogeneous aqueous dispersion was produced
- Particles were discrete, smooth and spherical
- Reasonable DLC and EE
- Aggregation was observed
- A wide particle size distribution (PSD) was noted

RHODES UNIVERSITY, Faculty of Pharmacy, Grahamstown, South Africa

BATCH SUMMARY REPORT

Formulator: Henusha Jhundoo

Product name: KTZ-loaded Solid Lipid Microparticle (SLM) aqueous dispersion

Batch ID: SLM 20

Manufacturing date: 28.10.2010 **Batch size:** 50 ml

Homogenizing time: 25-30 min

Formula

Material	% (w/v)	Amount added (g)
KTZ	5.00	2.58
Labrafil® M2130 CS	15.00	7.53
Pluronic® F-68	4.00	2.03
Sodium cholate	1.00	0.51
Tween® 80	2.00	1.04
Aqua	73.0	36.3

Production equipment used:

Water bath: Model NB-34980 Colora Ultra-Thermostat
Homogenizer 1: Model 6-105 AF Virtis Ultra-Turrax®
Homogenizer 2: Model HO/HHO Erweka AR400, Erweka GmbH

Parameters evaluated on the day of manufacture:

Particle size, PS (µm)	32.2 ± 4.2
Zeta potential, ZP (mV)	-29.5 ± 0.1
Drug loading capacity, DLC (%)	15.1 ± 0.23
Encapsulation Efficiency, EE (%)	32.9 ± 0.34

Comments / Observations

- White to off-white homogeneous aqueous dispersion was produced
- Particles were discrete, smooth and spherical
- Lower DLC and EE with higher concentration of Labrafil® M2130 CS
- Aggregation was observed
- A wide particle size distribution (PSD) was noted

RHODES UNIVERSITY, Faculty of Pharmacy, Grahamstown, South Africa

BATCH SUMMARY REPORT

Formulator: Henusha Jhundoo

Product name: KTZ-loaded Solid Lipid Microparticle (SLM) aqueous dispersion

Batch ID: SLM 21

Manufacturing date: 28.10.2010 **Batch size:** 50 ml

Homogenizing time: 25-30 min

Formula

Material	% (w/v)	Amount added (g)
KTZ	10.00	5.08
Labrafil® M2130 CS	10.00	5.02
Pluronic® F-68	4.00	2.01
Sodium cholate	1.00	0.54
Tween® 80	2.00	1.01
Aqua	73.0	36.3

Production equipment used:

Water bath: Model NB-34980 Colora Ultra-Thermostat
Homogenizer 1: Model 6-105 AF Virtis Ultra-Turrax®
Homogenizer 2: Model HO/HHO Erweka AR400, Erweka GmbH

Parameters evaluated on the day of manufacture:

Particle size, PS (µm)	28.3 ± 3.8
Zeta potential, ZP (mV)	-28.1 ± 0.1
Drug loading capacity, DLC (%)	19.4 ± 0.37
Encapsulation Efficiency, EE (%)	49.5 ± 0.79

Comments / Observations

- White to off-white homogeneous aqueous dispersion was produced
- Particles were discrete, smooth and spherical
- Slightly lower DLC and EE
- DLC and EE decreased slightly

RHODES UNIVERSITY, Faculty of Pharmacy, Grahamstown, South Africa

BATCH SUMMARY REPORT

Formulator: Henusha Jhundoo

Product name: KTZ-loaded Solid Lipid Microparticle (SLM) aqueous dispersion

Batch ID: SLM 22

Manufacturing date: 28.10.2010 **Batch size:** 50 ml

Homogenizing time: 25-30 min

Formula

Material	% (w/v)	Amount added (g)
KTZ	3.30	1.65
Labrafil® M2130 CS	10.00	5.01
Pluronic® F-68	4.00	2.03
Sodium cholate	1.00	0.52
Tween® 80	2.00	1.01
Aqua	79.7	39.8

Production equipment used:

Water bath: Model NB-34980 Colora Ultra-Thermostat
Homogenizer 1: Model 6-105 AF Virtis Ultra-Turrax®
Homogenizer 2: Model HO/HHO Erweka AR400, Erweka GmbH

Parameters evaluated on the day of manufacture:

Particle size, PS (µm)	27.5 ± 4.9
Zeta potential, ZP (mV)	-30.8 ± 0.6
Drug loading capacity, DLC (%)	22.5 ± 1.2
Encapsulation Efficiency, EE (%)	48.5 ± 2.9

Comments / Observations

- White to off-white homogeneous aqueous dispersion was produced
- Particles were discrete, smooth and spherical
- DLC and EE decreased slightly with lower concentration of KTZ

RHODES UNIVERSITY, Faculty of Pharmacy, Grahamstown, South Africa

BATCH SUMMARY REPORT

Formulator: Henusha Jhundoo

Product name: KTZ-loaded Solid Lipid Microparticle (SLM) aqueous dispersion

Batch ID: SLM 23

Manufacturing date: 28.10.2010 **Batch size:** 50 ml

Homogenizing time: 25-30 min

Formula

Material	% (w/v)	Amount added (g)
KTZ	5.00	2.51
Labrafil® M2130 CS	10.00	5.02
Pluronic® F-68	4.00	2.01
Sodium cholate	1.00	0.53
Tween® 80	2.00	1.02
Aqua	78.0	38.9

Production equipment used:

Water bath: Model NB-34980 Colora Ultra-Thermostat
Homogenizer 1: Model 6-105 AF Virtis Ultra-Turrax®
Homogenizer 2: Model HO/HHO Erweka AR400, Erweka GmbH (3 cycles)

Parameters evaluated on the day of manufacture:

Particle size, PS (µm)	42.7 ± 6.9
Zeta potential, ZP (mV)	-27.5 ± 0.2
Drug loading capacity, DLC (%)	20.7 ± 1.9
Encapsulation Efficiency, EE (%)	43.8 ± 2.8

Comments / Observations

- White to off-white homogeneous aqueous dispersion was produced
- Particles were discrete, spherical and had irregular surfaces
- Larger PS with lower number of homogenization cycles
- Low DLC and EE with three (3) homogenization cycles

RHODES UNIVERSITY, Faculty of Pharmacy, Grahamstown, South Africa

BATCH SUMMARY REPORT

Formulator: Henusha Jhundoo

Product name: KTZ-loaded Solid Lipid Microparticle (SLM) aqueous dispersion

Batch ID: SLM 24

Manufacturing date: 28.10.2010 **Batch size:** 50 ml

Homogenizing time: 25-30 min

Formula

Material	% (w/v)	Amount added (g)
KTZ	5.00	2.50
Labrafil® M2130 CS	10.00	5.01
Pluronic® F-68	4.00	2.03
Sodium cholate	1.00	0.54
Tween® 80	2.00	1.03
Aqua	78.0	38.9

Production equipment used:

Water bath: Model NB-34980 Colora Ultra-Thermostat
Homogenizer 1: Model 6-105 AF Virtis Ultra-Turrax®
Homogenizer 2: Model HO/HHO Erweka AR400, Erweka GmbH (4 cycles)

Parameters evaluated on the day of manufacture:

Particle size, PS (µm)	17.8 ± 7.1
Zeta potential, ZP (mV)	-29.7± 0.1
Drug loading capacity, DLC (%)	19.1 ± 3.9
Encapsulation Efficiency, EE (%)	42.3 ± 2.5

Comments / Observations

- White to off-white homogeneous aqueous dispersion was produced
- Particles were discrete, spherical and had irregular surfaces
- PS is reduced with higher number of homogenization cycles
- Low DLC and EE with four (4) homogenization cycles

APPENDIX II

BATCH PRODUCTION RECORDS

Note that only the production record for Batch SLM 15 is included here. The batch production records for all other formulations manufactured and tested during formulation development and optimization studies are available on request.

RHODES UNIVERSITY, Faculty of Pharmacy, Grahamstown, South Africa

BATCH PRODUCTION RECORD

Product name: KTZ-loaded SLM **Page 1 of 5**
Batch ID: SLM 15 **Batch size:** 50 ml

MANUFACTURING APPROVALS

Batch record issued by_____ **Date**_____

Master record issued by_____ **Date**_____

RHODES UNIVERSITY, Faculty of Pharmacy, Grahamstown, South Africa

BATCH PRODUCTION RECORD

Product name: KTZ-loaded SLM **Page 2 of 5**
Batch ID: SLM 15 **Batch size:** 50 ml

Item	Material	Quantity (% w/v)	Amount/ Batch (g)	Amount dispensed	Dispensed by	Checked by
1	KTZ	5.00	2.50	2.51		
2	Labrafil® M2130 CS	10.00	5.00	5.04		
3	Pluronic® F-68	4.00	2.00	2.08		
4	Tween® 80	2.00	1.00	1.10		
5	Sodium cholate	1.00	0.500	0.506		
6	Aqua	73.0	36.5	36.5		

RHODES UNIVERSITY, Faculty of Pharmacy, Grahamstown, South Africa

BATCH PRODUCTION RECORD

Product name: KTZ-loaded SLM **Page 3 of 5**
Batch ID: SLM 15 **Batch size:** 50 ml

EQUIPMENT VERIFICATION			
Description	**Type**	**Verified by**	**Confirmed by**
Water bath	Model NB-34980 Colora Ultra-Thermostat		
Homogenizer	Model 6-105 AF Virtis Ultra-Turrax®		
Homogenizer	Model HO/HHO Erweka AR400, Erweka GmbH		

RHODES UNIVERSITY, Faculty of Pharmacy, Grahamstown, South Africa

BATCH PRODUCTION RECORD

Product name: KTZ-loaded SLM **Page 4 of 5**
Batch ID: SLM 15 **Batch size:** 50 ml

MANUFACTURING PROCEDURE				
Step	**Procedure**	**Time**	**Done by**	**Checked by**
1	Weigh all materials.			
2	Heat water bath to 60°C for at least 30 min.			
3	Pipette 5 ml of distilled water in a test tube and store at 4°C for at least 20 min.			
4	Measure 36.5 ml of distilled water using a measuring cylinder and transfer to a 250 ml beaker. Store in a freezer for at least 15 min or until temperature is between 2-3°C.			
5	Heat lipid Labrafil® M2130 CS until melted to 60°C in water bath.			
6	Dissolve Pluronic® F-68 in 5 ml of water stored at 4°C for at least 30 min (from step 3) and mix using a Vortex mixer until complete dissolution.			
7	Add co-surfactant sodium cholate, followed by Tween 80 to solution of Pluronic® F-68 (from step 5) and mix using a Vortex mixer until complete dissolution to obtain aqueous surfactant solution.			
8	Heat aqueous surfactant solution in water bath to 60°C for at least 15 min.			
9	Add heated surfactant solution to molten lipid at 60°C and mix briefly using a Vortex mixer to form microemulsion. Store microemulsion in water bath at 60°C.			
9	Disperse hot microemulsion in beaker containing cold water maintained at 2-3°C from step 4.			
10	Homogenize aqueous dispersion using an Ultra-Turrax® homogenizer at 24 000 rpm for 5 minutes.			
11	Homogenize resulting aqueous dispersion with an Erweka GmbH homogenizer for five cycles.			
12	Store samples at room temperature (22°C) prior to characterization.			

RHODES UNIVERSITY, Faculty of Pharmacy, Grahamstown, South Africa

BATCH PRODUCTION RECORD

Product name: KTZ-loaded SLM
Batch ID: SLM 15

Batch size: 50 ml

SIGNATURE AND INITIAL REFERENCE			
Full name (Print)	**Signature**	**Initials**	**Date**

REFERENCES

1. J. Lederberg. *Encyclopedia of Microbiology*. Academic Press, London, 2000.

2. D. Thienpont, J. Van Cutsem, F. Van Gerven, J. Heeres, P.A.J. Janssen. Ketoconazole, a broad-spectrum orally active antimycotic. *Experientia*, 1979, **35** (5), 606-607.

3. D. Borelli, J.L. Bran, J. Fuertes, R. Legendre, E. Leiderman, H.B. Levine, M.A. Restrepo, D.A. Stevens. Ketoconazole, an oral antifungal: Laboratory and clinical assessment of imidazole drugs. *Postgraduate Medical Journal*, 1979, **55** (647), 657-661.

4. J.R. Graybill, D.J. Drutz. Ketoconazole: A major innovation for treatment of fungal disease. *Annals of Internal Medicine*, 1980, **93** (6), 921-923.

5. R.C. Heel, R.N. Brogden, A. Carmine, P.A. Morley, T.M. Speight, G.S. Avery. Ketoconazole: A review of its therapeutic efficacy in superficial and systemic fungal infections. *Drugs*, 1982, **23** (1-2), 1-36.

6. M. Borgers, H. Van den Bossche, M. De Brabander. The mechanism of action of the new antimycotic ketoconazole. *American Journal of Medicine*, 1983, **74** (1B), 2-8.

7. H.B. Levine. *Ketoconazole in the management of fungal disease*. ADIS Press, New York, 1982.

8. F.C. Odds. Antifungal agents: their diversity and increasing sophistication. *Mycologist*, 2003, **17** (2), 51-55.

9. News: Jan Heeres is Awarded the 2008 IUPAC-Richter Prize. http://old.iupac.org/news/archives/2008/Heeres_Richter-prize.html, last accessed 21-03-2014.

10. H.B. Levine, J.M. Cobb. Oral therapy for experimental coccidioidomycosis with R 41400 (ketoconazole), a new imidazole. *American Review of Respiratory Diseases*, 1981, **118**, 715-721.

11. J. Heeres, H. Van den Bossche. Antifungal chemotherapy. In: Hess (editor): *Annual Reports in Medicinal Chemistry*. New York: Academic Press, 1980, pp. 139-148.

12. J. Symoens, M. Moens, J. Dom, H. Scheijgrond, J. Dony, V. Schuermans, R. Legendre, N. Finestine. An Evaluation of Two Years of Clinical Experience with Ketoconazole. *Reviews of Infectious Diseases*, 1980, **2** (4), 674-691.

13. D. Thienpont, J. Van Cutsem, M. Borgers. Ketoconazole in experimental candidosis. *Review of Infectious Diseases*, 1980, **2**, 570-577.

14. G.E. Schutze, S.L. Hickerson, E.M. Fortin, D.E. Schellhase, T.Darville, P.O.Gubbins, R.F. Jacobs. Blastomycosis in Children. *Clinical Infectious Diseases*, 1996, **22** (3), 496-502.

15. K. Parfitt. *Martindale: The Complete Drug Reference*. Pharmaceutical Press, 2005.

16. R.F. Hector. An overview of antifungal drugs and their use for treatment of deep and superficial mycoses in animals. *Clinical Techniques in Small Animal Practice*, 2005, **20** (4), 240-249.

17. W.H. Beggs, F.A. Andrews, G.A. Sarosi. Action of imidazole-containing antifungal drugs. *Life Sciences,* 1981, **28** (2), 111-118.

18. FDA Approval History of Ketoconazole. http://www.drugs.com/pro/ketoconazole-tablets.html, last accessed on 21-03-2014.

19. The 2008 IUPAC-Richter Prize in Medicinal Chemistry has been awarded to Jan Heeres, formerly of the Centrum for Molecular Design and Janssen Pharmaceutica, Beerse, BE. http://www.highbeam.com/doc/1G1-184746111.html, last accessed on 21-03-2014.

20. M.G. Lee. *British Pharmacopoeia*. 2009, The Stationery Office, London.

21. S. Pandey, V. Devmurari, M. Goyani, D. Pandey. Formulation, Optimization and In-Vitro Evaluation of Ketoconazole Cream. *Der Pharmacia Lettre* 2009, **1**(2), 18-24.

22. Using a Portfolio of Particle Growth Technologies to Enable Delivery of Drugs With Poor Water Solubility. Drug Delivery Technology 4. http://www.drugdeliverytech.com/ME2/dirmod.asp?sid=&nm=&type=Publishing&mod=Publications%3A%3AArticle&mid=8F3A7027421841978F18BE895F87F791&tier=4&id=51EA11B6268048338C15D4DD2D00C55C, last accessed on 21-03-2014.

23. G. Van den Mooter, M. Wuyts, N. Blaton, R. Busson, P. Grobet, P. Augustijns, R. Kinget. Physical stabilisation of amorphous ketoconazole in solid dispersions with polyvinylpyrrolidone K25. *European Journal of Pharmaceutical Sciences*, 2011, **12** (3), 261-269.

24. H. van de Waterbeemd, B. Testa. Drug bioavailability: estimation of solubility, permeability, absorption and bioavailability. Methods and Principles in Medicinal Chemistry, 2nd Ed. 2010, Wiley-Vch, Weinheim, pp. 22.

25. U. Holzgrabe, I. Wawer, B. Diehl. NMR Spectroscopy in Pharmaceutical Analysis. 2010, Elsevier, Amsterdam, p. 208.

26. J.A. Carlson, H.J. Mann, D.M. Canafax. Effect of pH on disintegration and dissolution of ketoconazole tablets. *American Journal of Hospital Pharmacy*, 1983, **40** (8), 1334-1336.

27. W.A. Ritschel. Compilation of pharmacokinetic parameters of beta-adrenergic blocking agents. *Drug Intelligence and Clinical Pharmacokinetics*, 1980, **14**, 746-756.

28. D. Cordoba-Diaz, M. Cordoba-Diaz, S. Awad, M. Cordoba-Borrego. Effect of pharmacotechnical design on the *in vitro* interaction of ketoconazole tablets with non-systemic antacids. *International Journal of Pharmaceutics*, 2001, **226** (1-2), 61-68.

29. W.H. Beggs. Protonation of ketoconazole in relation to fungistatic activity. *Mycopathologia*, 2010, **116** (1), 3-4.

30. P.T. Mannisto, S. Nykanen, U. Lamminsivu, P. Ottoila. Impairing effect of food on ketoconazole absorption. *Antimicrobial Agents and Chemotherapy*, 1982, **21** (5), 730-733.

31. Partition coefficient Log D. Cerep, http://www.cerep.fr/cerep/users/pages/Downloads/Documents/Marketing/Pharmacology%20&%20ADME/Application%20notes/partitioncoefficient, last accessed on 3-12-2010.

32. M. Aleksic, S. Eric, D. Agbaba, J. Odovic, D. Milojkovic-Opsenica, Z. Tesic. Estimation of the hydrophobicity of antimycotic compounds by planar chromatography. *Journal of Planar Chromatography*, 2002, **15**, 414-417.

33. A. Pyka, M. Babuśka, M. Zachariasz. A comparison of theoretical methods of calculation of partition coefficients for selected drugs. *Acta Poloniae Pharmaceutica ñ Drug Research*, 2006, **63** (3), 159-167.

34. Ketoconazole (USP 34), Arasto Pharmaceutical Chemicals Inc. http://en.arasto.com/products.10, last accessed on 21-03-2014.

35. D.L. Pavia, G.M. Lampman, G.S. Kriz. *Introduction to Spectroscopy*. 2001, Thomson Learning, Inc., Washington.

36. D.H. Whiffen. *Spectroscopy*. 1966, Longman, London.

37. M. Hesse, H. Meier, B. Zeeh. *Spectroscopic Methods in Organic Chemistry*. 1997, Stuggart, New York.

38. N.M. Gray, R.L. Woosley. Methods and compositions of (-) ketoconazole for treating fungal yeast and dermatophyte infections. Sepracor Inc. Marlborough MA/USA. U.S. Patent 166, 09/314 229, 2000.

39. J. Heeres, L.J.J. Backx, J.H. Mostmans, J. Van Cutsem. Antimycotic imidazoles. Part 4. Synthesis and antifungal activity of ketoconazole, a new potent orally active broad-spectrum antifungal agent. *Journal of Medicinal Chemistry*, 1979, **22** (8), 1003-1005.

40. M. Zehender, S. Hohnloser, H. Just. QT-Interval prolonging drugs: Mechanisms and clinical relevance of their arrhythmogenic hazards. *Cardiovascular Drugs Therapy*, 1991, **5**, 515-530.

41. C. Viseras, I. Ismail Salem, I.C. Rodriguez Galan, A. Cerezo Galan, A. Lopez Galindo. The effect of recrystallization on the crystal growth, melting point and solubility of ketoconazole. *Thermochimica Acta*, 1995, **268**, 143-151.

42. H. Van den Bossche, J.M. Ruysschaert, F. Defrise-Quertain, G. Willemsens, F. Cornelissen, P. Marichal, W. Cools, J. Van Cutsem. The interaction of miconazole and ketoconazole with lipids. *Biochemical Pharmacology*, 1982, **31**, 2609-2617.

43. H. Minagawa, K. Kitora, N. Nakamizo. Effects of pH on the activity of ketoconazole against Candida albicans. *Antimicrobial Agents and Chemotherapy*, 1983, **23** (1), 105-107.

44. M. Skiba, M. Skiba-Lahiani, H. Marchais, R. Duclos, P. Arnaud. Stability assessment of ketoconazole in aqueous formulations. *International Journal of Pharmaceutics*, 2000, **198**, 1-6.

45. S. Patil. Synthesis of ketoconazole impurity by novel method. *Journal of Chemical and Pharmaceutical Research*, 2010, **2** (3), 117-119.

46. K. Mielech-Lukasiewicz, H. Puzanowska-Tarasiewicz, A. Niedzielko. Electrooxidation of some antifungal agents and their square-wave voltammetric determination in cosmetics and pharmaceutics. *Analytical Letters*, 2011, **44** (6), 955-967.

47. M. Shamsipur, K. Farhadi. Electrochemical behavior and determination of ketoconazole from pharmaceutical preparations. *Electroanalysis*, 2000, **12** (6), 429-433.

48. M. Shamsipur, F. Jalali. Preparation of a ketoconazole ion-selective electrode and its application to pharmaceutical analysis. *Analytical Sciences*, 2000, **16**, 549-552.

49. K.P. Kumer, A.D. Okonomah, W.G. Bradshaw, K.F.A. Soliman. Stability of ketoconazole in ethanolic solutions. *Drug Development and Industrial Pharmacy*, 1991, **17** (4), 577-580.

50. N.H. Georgopapadakou. Antifungals: mechanism of action and resistance, established and novel drugs. *Current Opinion in Microbiology*, 1998, **1**, 547-557.

51. J.G. Hardman, L.E. Limbird. *Goodman and Gilman's, The Pharmacological Basis of Therapeutics*. 2001, McGraw Hill Medical Publishing Division, New York.

52. J.H. Van Tyle. Ketoconazole. Mechanism of action, spectrum of activity, pharmacokinetics, drug interactions, adverse reactions and therapeutic use. *Pharmacotherapy*, 1984, **4** (6), 343-373.

53. J.J. Sheets, J.I. Mason. Ketoconazole: a potent inhibitor of cytochrome P-450 dependent drug metabolism in rat liver. *Drug Metabolism and Disposition*, 1984, **12**, 603-606.

54. M. Borgers. Mechanism of Action of Antifungal Drugs, with Special Reference to the Imidazole Derivatives. *Reviews of Infectious Diseases*, 1980, **2** (4), 520-534.

55. M. Borgers, H. Van den Bossche. The Mode of Action of Antifungal drugs. In: H.B. Levine (editor): *Ketoconazole in the management of fungal disease*. 1982, Adis Press, New York, pp. 25-47.

56. P. Loli, M.E. Berselli, M. Tagliaferri. Use of Ketoconazole in the Treatment of Cushing's Syndrome. *Journal of Clinical Endicronology and Metabolism*, 2010, **63** (6), 1365-1371.

57. M.H. Beers. *The Merck Manual of Diagnosis and Therapy*. 2006, West Point: Merck & Co., Pennsylvania.

58. T.H. Schurmeyer, E. Nieschlag. Effect of ketoconazole and other imidazole fungicides on testosterone biosynthesis. *Acta Endocrinologica*, 1984, **105** (2), 275-280.

59. J. Uno, M.L. Shi, M.L. Shigematsu, T.Arai. Primary site of action of ketoconazole on Candida albicans. *Antimicrobial Agents and Chemotherapy*, 1982, **21** (6), 912-918.

60. T.A. Miettinen. Cholesterol metabolism during ketoconazole treatment in man. *Journal of Lipid Research*, 1988, **29**:43-51.

61. C.J. Gibbon. *South African Medicines Formulary*. 2008, Health and Medical Publishing Group, Cape Town.

62. M.K. Polano. *Topical Skin Therapeutics*. 1984, Churchill Livingstone, New York.

63. A.L. Hume, T.M. Kerkering. Ketoconazole. *Drug Intelligence Clinical Pharmacy* 1983, **17** (3), 169-174.

64. C.W. Stratton. Antifungal agents. *Infectious Diseases Newsletter*, 1990, **9** (6).

65. J.R. Graybill. Antifungal agents of the 1980's. *The Antimicrobic newsletter*, 1988, **5** (7), 45-52.

66. C.Dollery. *Therapeutic drugs*. 1991, Churchill Livingstone, New York.

67. A.W. Maksymiuk, H.B. Levine, G.P. Bodey. Pharmacokinetics of ketoconazole in patients with neoplastic diseases. *Antimicrobial Agents and Chemotherapy,* 1982, **22** (1), 43-46.

68. D. Sanglard, K. Kuchler, F. Ischer, J.L. Pagani, M. Monod, J. Bille. Mechanisms of resistance to azole antifungals in Candida albicans isolates from AIDS patients involve specific multidrug transporters. *Antimicrobial Agents and Chemotherapy,* 1995, **39** (11), 2378-2386.

69. H. Van den Bossche, F. Dromer, I. Improvisi, M. Lozano-Chiu, J.H. Rex, D. Sanglard. Antifungal drug resistance in pathogenic fungi. *Medical Mycology,* 1998, **36** (Suppl 1), 119-128.

70. M. Sanguinetti, B. Posteraro, B. Fiori, S. Ranno, R. Torelli, G. Fadda. Mechanisms of azole resistance in clinical isolates of Candida glabrata collected during a hospital survey of antifungal resistance. *Antimicrobial Agents and Chemotherapy,* 2005, **49** (2), 668-679.

71. O. Rollman, L. Loof. Hepatic toxicity of ketoconazole. *British Journal of Dermatology* 1983, **108** (3), 376-378.

72. T.K. Daneshmend, D.W. Warnock. Clinical Pharmacokinetics of ketoconazole. *Clinical Pharmacokinetics,* 1988, **14**, 13-34.

73. A.J. Magnasco, L.D. Magnasco. Interaction of ketoconazole and ethanol. *Clinical Pharmacy,* 1986, **5** (6), 522-523.

74. K. Boughton. Ketoconazole and hepatic reactions. *South African Medical Journal,* 1983, **63** (25), 955.

75. E. Giavini, E. Menegola. Are azole fungicides a teratogenic risk for human conceptus? *Toxicology Letters,* 2010, **198**, 106-111.

76. Z. Kazy, E. Puho, A.E. Czeizel. Population-based case-control study of oral ketoconazole treament for birth outcomes. *Congenital Anomalies,* 2005, **45** (1), 5-8.

77. C. Brass, J.N. Galgiani, T.F. Blaschke, R. Defelice, R.A. O'Reilly, D.A. Stevens. Disposition of ketoconazole, an oral antifungal in humans. *Antimicrobial Agents and Chemotherapy,* 1982, **21** (1), 151-158.

78. C. Brass. Antimycotic therapy: A critical appraisal. *The Antimicrobic newsletter,* 1984, **1** (5), 35-42.

79. E.W. Gascoigne, G.J. Barton, M. Michaels, W. Meuldermans, J. Heykants. The kinetics of ketoconazole in animals and man. *Clinical Research Reviews,* 1981, **1**, 177-187.

80. J.W.M. Van Der Meer, J.J. Keuning, H.W. Scheijgrond, J. Heykants, J. Van Cutsem, J. Brugmans. The influence of gastric acidity on the bioavailability of ketoconazole. *Journal of Antimicrobial Chemotherapy,* 1980, **6** (4), 552-554.

81. J.D. Hoeschele, A.K. Roy, V.L. Pecoraro, P.L. Carver. *In vitro* analysis of the interaction between sucralfate and ketoconazole. *Antimicrobial Agents and Chemotherapy,* 1994, **38** (2), 319-325.

82. G. Lake-Bakkar, W. Tom, D. Lake-Bakkar, N. Gupta, S. Beidas, M. Elsakr, E. Straus. Gastropathy and ketoconazole malabsorption in the acquired immunodeficiency syndrome (AIDS). *Annals of Internal Medicine,* 1988, **109** (6), 471-473.

83. L.S. Welage, P.L. Carver, S. Revankar, C. Pierson, C.A. Kauffman. Alterations in gastric acidity in patients with Human Immunodeficiency Virus. *Clinical Infectious Diseases* 1995, **21** (6), 1431-1438.

84. M.J. Knapp, R.R. Berardi, J.B. Dressman, J.M. Rider, P.L. Carver. Modification of gastric pH with oral glutamic acid hydrochloride. *Clinical Pharmacy*, 1991, **10**, 866-869.

85. W.E. Fibbe, J.W.M. Van Der Meer, J. Thompson, R.P. Mouton. CSF concentrations of ketoconazole. *Journal of Antimicrobial Chemotherapy*, 1980, **6** (5), 681.

86. Y.C. Huang, J.C. Colaizzi, R.H. Bierman, R. Woestenborghs, J. Heykants. Pharmacokinetics and dose proportionality of ketoconazole in normal volunteers. *Antimicrobial Agents and Chemotherapy*, 1986, **30** (2), 206-210.

87. T.K. Daneshmend, D.W. Warnock, A. Turner, C.J.C. Roberts. Pharmacokinetics of ketoconazole in normal subjects. *Journal of Antimicrobial Chemotherapy*, 1981, **8** (4), 299-304.

88. T.K. Daneshmend, D.W. Warnock, M.D. Ene, E.M. Johnson, M.R. Potten. Influence of food on the pharmacokinetics of ketoconazole. *Antimicrobial Agents and Chemotherapy*, 1984, **25** (1), 1-3.

89. I.M. Hann, H.G. Prentice, M. Keaney, R. Corringham, H.A. Blacklock, J. Fox, E.W. Gascoigne, J. Van Cutsem. The pharmacokinetics of ketoconazole in severely immunocompromised patients. *Journal of Antimicrobial Chemotherapy*, 1982, **10** (6), 489-496.

90. J.E. Diederichs, R.H. Müller. *Future Strategies for Drug Delivery Particulate Systems*. 1998, Medpharm GmbH Scientific Publishers, Stuttgart.

91. S.S. Davis, L. Illum, J.G. McVie, E. Tomlinson. *Microspheres and drug therapy: Pharmaceutical, Immunological and Medical Aspects*. 1984, Elsevier Science Publishers, Amsterdam.

92. E. Touitou, H.E. Junginger, N.D. Weiner, T. Nagai, M. Mezei. Liposomes as carriers for topical and transdermal delivery. *Journal of Pharmaceutical Sciences*, 1994, **83** (9), 1189-1203.

93. Y. Barenholz, D.J. Crommelin. Liposomes as pharmaceutical dosage forms. In: J. Swarbrick, J.C. Boylan (editors): *Encyclopedia of Pharmaceutical Technology*. 1994, Marcel Dekker Inc., New York, pp. 1-39.

94. A. Sharma, U.S. Sharma. Liposomes in drug delivery: Progress and limitations. *International Journal of Pharmaceutics*, 1997, **154** (2), 123-140.

95. S. Heuschkel, A. Goebel, R.H. Neubert. Microemulsions: modern colloidal carrier for dermal and transdermal drug delivery. *Journal of Pharmaceutical Sciences*, 2008, **97** (2), 603-631.

96. J. Kreuter. Nanoparticle-based drug delivery systems. *Journal of Controlled Release*, 1991, **16**, 169-176.

97. J. Kreuter. Nanoparticles. In: J. Kreuter (editor): *Colloidal Drug Delivery Systems*. 1994, Marcel Dekker Inc., New York, pp. 219-342.

98. V. Bhardwaj, M.N.V.R. Kumar. Polymeric nanoparticles for oral drug delivery. In: R. Gupta, U.B. Kompella (editors): *Nanoparticle Technology for Drug Delivery*. 2006, Taylor and Francis, New York, pp. 231-272.

99. S. Jaspart, G. Piel, L. Delattre, B. Evrard. Solid lipid microparticles: formulation, preparation, characterisation, drug release and applications. *Expert Opinion in Drug Delivery*, 2005, **2** (1), 75-87.

100. A. zur Mühlen, C. Schwarz, W. Mehnert. Solid lipid nanoparticles (SLN) for controlled drug delivery - Drug release and and release mechanism. *European Journal of Pharmaceutics and Biopharmaceutics*, 1998, **45**, 149-155.

101. R.H. Müller, K. Mäder, S. Gohla. Solid lipid nanoparticles (SLN) for controlled drug delivery - a review of the state of the art. *European Journal of Pharmaceutics and Biopharmaceutics*, 2000, **50**, 161-177.

102. W. Mehnert, K. Mäder. Solid lipid nanoparticles: production, characterization and applications. *Advanced Drug Delivery Reviews*, 2001, **47**, 165-196.

103. S. Chakraborty, D. Shukla, B. Mishra, S. Singh. Lipid - An emerging platform for oral delivery of drugs with poor bioavailability. *European Journal of Pharmaceutics and Biopharmaceutics*, 2009, **73**, 1-15.

104. P. Barthelemy. *Recent advances in the formulation and development of poorly-soluble drugs*. 1999, 33rd Journeé Galéniques, Bulletin Technique Gattefossé, 92, pp. 21-28.

105. S. Stegemann, F. Leveiller, D. Franchi, H. de Jong, H. Linden. When poor solubility becomes an issue: From early stage to proof of concept. *European Journal of Pharmaceutical Sciences*, 2007, **31**, 249-261.

106. C. Schwarz, W. Mehnert. Solid lipid nanoparticles (SLN) for controlled drug dleivery; drug incorporation and physicochemical characterization. *Journal of Microencapsulation*, 1999, **16** (2), 205-213.

107. M. Radtke, E.B. Souto, R.H. Müller. Nanostructured lipid carriers: A novel generation of solid lipid drug carriers. *Pharmaceutical Technology Europe*, 2005, **17** (4), 45-50.

108. R.H. Müller, M. Radtke, S.A. Wissing. Nanostructured lipid matrices for improved microencapsulation of drugs. *International Journal of Pharmaceutics*, 2002, **242** (1-2), 121-128.

109. R.H. Müller, C.M. Keck. Drug delivery to the brain-realization by novel drug carriers. *Journal of Nanoscience and Nanotechnology*, 2004, **4** (5), 471-483.

110. I. Pal Kaur, R. Bhandari, S. Bhandari, V. Kakkar. Potential of solid lipid nanoparticles in brain targeting. *Journal of Controlled Release*, 2007, **127**, 97-109.

111. T.M. Göppert, R.H. Müller. Polysorbate-stabilized solid lipid nanoparticles as colloidal carriers for intravenous targeting of drugs to the brain: comparison of plasma protein adsorption patterns. *Journal of Drug Targeting*, 2005, **13** (3), 179-187.

112. L.E. van Vlerken, M.M. Amiji. Multi-functional polymeric nanoparticles for tumour-targeted drug delivery. *Expert Opinion on Drug Delivery*, 2006, **3** (2), 205-216.

113. A.A. Date, M.D. Joshi, V.B. Patravale. Parasitic diseases: Liposomes and polymeric nanoparticles versus lipid nanoparticles. *Advanced Drug Delivery Reviews,* 2007, **59**, 505-521.

114. A.D. Bangham. Liposomes: realizing their promise. *Hospital Practice (Office Ed),* 1992, **27** (12), 51-56.

115. D.D. Verma, S. Verma, G. Blume, A. Fahr. Liposomes increase skin penetration of entrapped and non-entrapped hydrophilic substances into human skin: a skin penetration and confoccal laser scanning microscopy study. *European Journal of Pharmaceutics and Biopharmaceutics,* 2003, **55** (3), 271-277.

116. D.J. Crommelin, H. Schreier. Liposomes. In: J. Kreuter (editor): *Colloidal Drug Delivery Systems*. 1994, Marcel Dekker Inc., New York, pp. 73-190.

117. F.J. Martin. Pharmaceutical manufacturing of liposomes. In: P. Tyle (editor): *Specialized Drug Delivery Systems: Manufacturing and Production technology*. 1990, Marcel Dekker Inc., New York, pp. 267-316.

118. G. Gregoriadis, A.T. Florence, H.M. Patel. Liposomes in drug delivery. In: A.T.Florence, G.Gregoriadis (editors): *Drug Targeting and Delivery*. 1993, Harwood Academic Publishers GmBH, Langhorne, USA.

119. M.J. Choi, H.I. Maibach. Liposomes and niosomes as topical drug delivery systems. *Skin Pharmacology and Physiology,* 2005, **18** (5), 209-219.

120. R. Cortesi, C. Nastruzzi. Liposomes, micelles and microemulsions as new delivery systems for cytotoxic alkaloids. *Pharmaceutical Science and Technology Today*, 1999, **2** (7), 288-298.

121. S. Benita, D. Friedman, M. Weinstock. Phytostigmine emulsion: a new injectible controlled release delivery system. *International Journal of Pharmaceutics,* 1986, **30** (1), 47-55.

122. S. Benita, M.Y. Levy. Submicron emulsions as colloidal drug carriers for intraveous administration: comprehensive physicochemical characterization. *Journal of Pharmaceutical Sciences,* 1993, **82** (11), 1069-1079.

123. P. Kocbek, S. Baumgartner, J. Kristl. Preparation and evaluation of nanosuspensions for enhancing the dissolution of poorly soluble drugs. *International Journal of Pharmaceutics,* 2006, **312**, 179-186.

124. R. Bodmeier, H. Chen. Indomethacin polymeric nanosuspensions prepared by microfluidization. *Journal of Controlled Release,* 1990, **12** (3), 223-233.

125. R.H. Müller, S. Benita, B. Bohm. *Emulsions and Nanosuspensions for the Formulation of Poorly Soluble Drugs.* 1998, Medpharm Scientific Publishers, Stuttgart.

126. A. Lamprecht, Y. Bouligand, J.P. Benoit. New lipid nanocapsules exhibit sustained release properties for amiodarone. *Journal of Controlled Release,* 2002, **84** (1-2), 59-68.

127. C. Mayer. Nanocapsules as drug delivery systems. *International Journal of Artificial Organs,* 2005, **28** (11), 1163-1171.

128. M. Aboubakar, F. Puisieux, P. Couvreur, C. Vauthier. Physicochemical characterization of insulin-loaded poly(isobutylcyanoacrylate) nanocapsules obtained by interfacial polymerization. *International Journal of Pharmaceutics,* 1999, **183** (1), 63-66.

129. R. Alverez-Roman, G. Barre, R.H. Guy, H. Fessi. Biodegradable polymer nanocapsules containing a sunscreen agent: preparation and photoprotection. *European Journal of Pharmaceutics and Biopharmaceutics,* 2001, **52** (2), 191-195.

130. T. Pitaksuteepong, N.M. Davies, I.G. Tucker, T. Rades. Factors influencing the entrapment of hydrophilic compounds in nanocapsules prepared by interfacial polymerization of water-in-oil microemulsions. *European Journal of Pharmaceutics and Biopharmaceutics,* 2002, **53** (3), 335-342.

131. V. Andrieu, H. Fessi, M. Dubrasquet, J.P. Devissaguet, F. Puisieux, S. Benita. Pharmacokinetic evaluation of indomethacin nanocapsules. *Drug Design and Delivery,* 1989, **4** (4), 295-302.

132. A. Smith, I.M. Hunneyball. Evaluation of poly(lactic acid) as a biodegradable drug delivery system for parenteral administration. *International Journal of Pharmaceutics,* 1986, **30** (2-3), 215-220.

133. F. Kaneko, K. Tashiro, M. Kobayashi. Polymorphic transitions during crystallization processes of fatty acids studied with FT-IR spectroscopy. *Journal of Crystal Growth,* 1999, **198-199** (2), 1352-1359.

134. G. Puglisi, G. Giammona, M. Fresta, B. Carlisi, N. Micali, A.Villari. Evaluation of polyalkylcyanoacrylate nanoparticles as a potential drug carrier: preparation, morphological characterization and loading capacity. *Journal of Microencapsulation,* 1993, **10** (3), 353-366.

135. H. Fessi, F. Puisieux, N. Ammoury, S. Benita. Nanocapsule formation by interfacial polymer deposition following solvent displacement. *International Journal of Pharmaceutics,* 1989, **55**, R1-R4.

136. K.S. Soppimath, T.M. Aminabhavi, A.R. Kulkarni, W.E. Rudzinski. Biodegradable polymeric nanoparticles as drug delivery devices. *Journal of Controlled Release,* 2001, **70** (1-2), 1-20.

137. L. Illum, M.A. Khan, E. Mak, S.S. Davis. Evaluation of carrier capacity and release characteristics for poly(butyl 2-cyanoacrylate) nanoparticles. *International Journal of Pharmaceutics,* 1986, **30** (1), 17-28.

138. M.C. Vernier-Julienne, J.P. Benoit. Preparation, purification and morphology of polymeric nanoparticles as drug carriers. *Pharmaceutica Acta Helvetiae,* 1996, **71** (2), 121-128.

139. M. Savolainen, J. Herder, C. Khoo, K. Lovqvist, C. Dahlqvist, H. Glad, A.M. Juppo. Evaluation of polar lipid-hydrophilic polymer microparticles. *International Journal of Pharmaceutics,* 2003, **262** (1-2), 47-62.

140. M. Vert. Polyvalent polymeric drug carriers. *Critical Reviews in Therapeutic Drug Carrier Systems,* 1986, **2** (3), 291-327.

141. P. Couvreur, C. Vauthier. Polyalkylcyanoacrylate nanoparticles as drug carriers: present state and perspectives. *Journal of Controlled Release,* 1991, **17**, 187-198.

142. T. Eldem, P. Speiser, H. Altorfer. Polymorphic behaviour of sprayed lipid micropellets and its evaluation by differential scanning calorimetry and scanning electron microscopy. *Pharmaceutical Research,* 1991, **8** (2), 178-184.

143. Y. Akiyama, M. Yoshioka, H. Horibe, S. Hirai, N. Kitamori, H. Toguchi. Novel oral controlled-release microspheres using polyglycerol esters of fatty acids. *Journal of Controlled Release,* 1993, **26** (1), 1-10.

144. A. Estella-Hermoso de Mendoza, M. Rayo, F. Mollinedo, M.J. Blanco-Prieto. Lipid nanoparticles for alkyl lysophospholipid edelfosine encapsulation: Development and in vitro characterization. *European Journal of Pharmaceutics and Biopharmaceutics,* 2008, **68**, 207-213.

145. A.J. Almeida, E. Souto. Solid lipid nanoparticles as a drug delivery system for peptides and proteins. *Advanced Drug Delivery Reviews,* 2007, **59**, 478-490.

146. D. Hou, C. Xie, K. Huang, C. Zhu. The production and characteristics of solid lipid nanoparticles (SLNs). *Biomaterials,* 2003, **24** (10), 1781-1785.

147. F.Q. Hu, H. Yuan, H.H. Zhang, M. Fang. Preparation of solid lipid nanoparticles with clobetasol propionate by a novel solvent diffusion method in aqueous system and physicochemical characterization. *International Journal of Pharmaceutics,* 2002, **239**, 121-128.

148. H. Bunjes, T. Unruh. Characterization of lipid nanoparticles by differential scanning calorimetry, X-ray and neutron scattering. *Advanced Drug Delivery Reviews,* 2007, **59**, 379-402.

149. J. Pardeike, A. Hommoss, R.H. Müller. Lipid nanoparticles (SLN, NLC) in cosmetic and pharmaceutical dermal products. *International Journal of Pharmaceutics,* 2009, **366**, 170-184.

150. K. Westesen, B. Siekmann, M.H.J. Koch. Investigations on the physical state of lipid nanoparticles by synchrotron radiation X-ray diffraction. *International Journal of Pharmaceutics*, 1993, **93** (1-3), 189-199.

151. K. Westesen, H. Bunjes, M.H.J. Koch. Physicochemical characterization of lipid nanoparticles and evaluation of their drug loading capacity and sustained release. *Journal of Controlled Release,* 1997, **48**, 223-236.

152. M.D. Joshi, R.H. Müller. Lipid nanoparticles for parenteral delivery of actives. *European Journal of Pharmaceutics and Biopharmaceutics,* 2009, **71**, 161-172.

153. M. Goutayer, S. Dufort, V. Josserand, A. Royere, E. Heinrich, F. Vinet, J. Bibette, J. Coll, I. Texier. Tumor targeting of functionalized lipid nanoparticles: Assessment by in vivo fluorescence imaging. *European Journal of Pharmaceutics and Biopharmaceutics,* 2010, **75**, 137-147.

154. R.K. Subedi, K. Kanga, H. Choi. Preparation and characterization of solid lipid nanoparticles loaded with doxorubicin. *European Journal of Pharmaceutics and Biopharmaceutics,* 2009, **37**, 508-513.

155. V. Jenning, M. Schafer-Korting, S. Gohla. Vitamin A-loaded solid lipid nanoparticles for topical use: drug release properties. *Journal of Controlled Release*, 2000, **66**, 115-126.

156. V. Venkateswarlu, K. Manjunath. Preparation, characterization and in vitro release kinetics of clozapine solid lipid nanoparticles. *Journal of Controlled Release,* 2004, **95**, 627-638.

157. W. Weyenberg, P. Filev, D. Van den Plas, J. Vandervoort, K. De Smet, P. Sollie, A. Ludwig. Cytotoxicity of submicron emulsions and solid lipid nanoparticles for dermal application. *International Journal of Pharmaceutics,* 2007, **337** (1-2), 291-298.

158. R.M. Mainardes, L.P. Silva. Drug delivery systems: past, present and future. *Current Drug Targets,* 2004, **5** (5), 449-455.

159. E. Allemann, R. Gurny, E. Doelker. Drug-loaded nanoparticles: preparation methods and drug targeting issues. *European Journal of Pharmaceutics and Biopharmaceutics,* 1993, **39** (5), 173-191.

160. H. Reithmeier, J. Hermann, A. Gopferich. Development and characterization of lipid microparticles as a drug carrier for somatostatin. *International Journal of Pharmaceutics,* 2001, **218**, 133-143.

161. L. Brannon-Peppas. Recent advances on the use of biodegradable microparticles and nanoparticles in controlled drug delivery devices. *International Journal of Pharmaceutics,* 1995, **116** (1), 1-9.

162. X.M. Zeng, G.P. Martin, C. Marriott. The controlled delivery of drugs to the lung. *International Journal of Pharmaceutics,* 1995, **124** (2), 149-164.

163. S. Jaspart, P. Bertholet, G. Piel, J. Dogne, L. Delattre, B. Evrard. Solid lipid microparticles as a sustained release system for pulmonary drug delivery. *European Journal of Pharmaceutics and Biopharmaceutics,* 2007, **65**, 47-56.

164. R.H. Müller, J.S. Lucks. Arzneistoffträger aus festen Lipidteilchen, Feste Lipidnanospharen (SLN). 1996, European Patent no. 0605497, Germany, In: R. H Müller, M. Radtke, S. A. Wissing. Nanostructured lipid matrices for improved microencapsulation of drugs. *International Journal of Pharmaceutics,* 2002, **242**, 121-128.

165. K. Jores, A. Haberland, S. Wartewig, K. Mäder, W.Mehnert. Solid Lipid Nanoparticles (SLN) and oil-loaded SLN studied by spectrofluorometry and Raman spectroscopy. *Pharmaceutical Research,* 2005, **22**, 1887-1897.

166. R.H. Müller, A. Lippacher, S. Gohla. Solid Lipid Nanoparticles (SLN) as a carrier system for the controlled release of drugs. In: D.L.Wise (editor): *Handbook of Pharmaceutical Controlled Release Technology*, 2000, pp. 377-389.

167. A. Samad, Y. Sultana, M. Aqil. Liposomal drug delivery systems: an update review. *Current Drug Delivery*, 2007, **4** (4), 297-305.

168. A. Manosroi, L. Kongkaneramit, J. Manosroi. Stability and transdermal absorption of topical amphotericin B liposome formulations. *International Journal of Pharmaceutics,* 2004, **270** (1-2), 279-286.

169. M.M. Elsayed, O.Y. Abdallah, V.F. Naggar, N.M. Khalafallah. Lipid vesicles for skin delivery of drugs. *International Journal of Pharmaceutics,* 2007, **332** (1-2), 1-16.

170. R. Janknegt, S. de Marie, I.A. Bakker-Woudenberg, D.J. Crommelin. Liposomal and lipid formulations of amphotericin B. clinical pharmacokinetics. *Clinical Pharmacokinetics,* 1992, **23** (4), 279-291.

171. L.C. Collins-Gold, R.T. Lyons, L.C. Bartholow. Parenteral emulsions for drug delivery. *Advanced Drug Delivery Reviews*, 1990, **5**, 189-208.

172. R.J. Prankerd, V.J. Stella. The use of oil-in-water emulsions as a vehicle for parenteral drug administration. *Journal of Parenteral Science and Technology*, 1990, **44** (3), 139-149.

173. R.H. Müller, M. Radtke, S.A. Wissing. Solid lipid nanoparticles (SLN) and nanostructured lipid carriers (NLC) in cosmetic and dermatological preparations. *Advanced Drug Delivery Reviews*, 2002, **54** (1), S131-S155.

174. A. Dingler, R.P. Blum, H. Niehus, R.H. Müller, S. Gohla. Solid lipid nanoparticles (SLN/Lipopearls): a pharmaceutical and cosmetic carrier for the application of vitamin E in dermal products. *Journal of Microencapsulation*, 1999, **16** (6), 751-767.

175. B. Magenheim, M.Y. Levy, S. Benita. A new in vitro technique for the evaluation of drug release profile from colloidal carriers - ultrafiltration technique at low pressure. *International Journal of Pharmaceutics*, 1993, **94** (1-3), 115-123.

176. S. Benita, D. Friedman, M. Weinstock. Pharmacological evaluation of an injectible prolonged release emulsion of phytostigmine in rabbits. *Journal of Pharmacy and Pharmacology*, 1986, **38** (9), 653-658.

177. L. Mu, S.S. Feng. PLGA/TPGS nanoparticles for controlled release of paclitaxel: effects of the emulsifier and drug loading ratio. *Pharmaceutical Research*, 2003, **20** (11), 1864-1872.

178. C. Lherm, R.H. Müller, F. Puisieux, P. Couvreur. Alkylcyanoacrylate Drug Carriers II: cytotoxicity of cyanoacrylate nanoparticles with different alkyl chain length. *International Journal of Pharmaceutics*, 1992, **84** (1), 13-22.

179. A. Saez, M. Guzman, J. Molpeceres, M.R. Aberturas. Freeze-drying of polycaprolactone and poly(D,L-lactic-glycolic) nanoparticles induce minor particle size changes affecting the oral pharmacokinetics of loaded drugs. *European Journal of Pharmaceutics and Biopharmaceutics*, 2000, **50** (3), 379-387.

180. U. Edlund, A.C. Albertsson, S.K. Singh, I. Fogelberg, B.O. Lundgren. Sterilization, storage stability and in vivo biocompatibility of poly(trimethylenecarbonate)/poly(adipic anhydride) blends. *Biomaterials*, 2000, **21** (9), 945-955.

181. C. Schwarz, W. Mehnert, J.S. Lucks, R.H. Müller. Solid lipid nanoparticles (SLN) for controlled drug delivery. I. Production, characterization and sterilization. *Journal of Controlled Release*, 1993, **30**, 83-96.

182. R.H. Müller, W. Mehnert, J.S. Lucks, C. Schwarz, A. zur Mühlen, H. Wyhers, C. Freitas, D. Rühl. Solid lipid nanoparticles (SLN): an alternative colloidal carrier system for controlled drug delivery. *European Journal of Pharmaceutics and Biopharmaceutics*, 1995, **41** (1), 62-69.

183. M.R. Gasco. Solid lipid nanospheres from warm micro-emulsions. *Pharmaceutical Technology Europe*, 1997, **9**, 52-58.

184. M.R. Gasco. Method for producing solid lipid microspheres having a narrow size distribution. United States of America Patent, no 5250236, 1993.

185. B. Siekmann, K. Westesen. Sub-micron sized parenteral carrier systems based on solid lipids. *Pharmaceutical and Pharmacological Letters*, 1992, **1**, 123-126.

186. R. Cavalli, E. Marengo, L. Rodriguez, M.R. Gasco. Effects of some experimental factors on the production process of solid lipid nanoparticles. *European Journal of Pharmaceutics and Biopharmaceutics,* 1996, **43** (2), 110-115.

187. B. Siekmann, K. Westesen. Melt-homogenized solid lipid nanoparticles stabilized by the nonionic surfactant tyloxapol. *Pharmaceutical and Pharmacological Letters,* 1994, **3**, 194-197.

188. L. Zhang, Y. Qian, C. Long, Y. Chen. Systematic procedures for formulation design of drug-loaded solid lipid microparticles: selection of carrier material and stabilizer. *Industrial and Engineering Chemical Research,* 2008, **47**, 6091-6100.

189. C. Erni, C. Suard, S. Freitas, D. Dreher, H.P. Merkle, E. Walter. Evaluation of cationic solid lipid microparticles as synthetic carriers for the targeted delivery of macromolecules to phagocytic antigen-presenting cells. *Biomaterials,* 2002, **23**, 4667-4676.

190. D.B. Masters, A.J. Domb. Liposphere local anesthetic timed-release for perineural site application. *Pharmaceutical Research,* 1998, **15** (7), 1038-1045.

191. G. Yener, T. Incegul, N. Yener. Importance of using solid lipid microspheres as carriers for UV filters on the example octyl methoxy cinnamate. *International Journal of Pharmaceutics*, 2003, **258**, 203-207.

192. H.K. Frederiksen, H.G. Kristensen, M. Pedersen. Solid lipid microparticle formulations of the pyrethroid gamma-cyhalothrin - incompatibility of the lipid and the pyrethroid and biological properties of the formulations. *Journal of Controlled Release,* 2003, **86**, 243-252.

193. H. Reithmeier, J. Hermann, A. Gopferich. Lipid microparticles as parenteral controlled release device for peptides. *Journal of Controlled Release,* 2001, **73**, 339-350.

194. L.I. Giannola, V. Di Stefano, V. De Caro. White beeswax microspheres: a comparative *in vitro* evaluation of cumulative release of the anticancer agents fluorouracil and ftorafur. *Pharmazie,* 1993, **48** (2), 123-126.

195. L. Rodriguez, N. Passerini, C. Cavallari, M. Cini, P. Sancin, A. Fini. Description and preliminary evaluation of a new ultrasonic atomizer for spray-congealing processes. *International Journal of Pharmaceutics,* 1999, **183** (2), 133-143.

196. M.D. Del Curto, D. Chicco, M. D'Antonio, V. Ciolli, H. Dannan, S. D'Urso, B. Neuteboom, S. Pompili, S. Schiesaro, P. Esposito. Lipid microparticles as sustained release system for a GnRH antagonist (Antide). *Journal of Controlled Release,* 2003, **89**, 297-310.

197. M. Demirel, Y. Yazan, R.H. Müller, F. Kilic, B. Bozan. Formulation and *in vitro-in vivo* evaluation of piribedil solid lipid micro- and nanoparticles. *Journal of Microencapsulation,* 2001, **18** (3), 359-371.

198. N. Passerini, B. Perissutti, M. Moneghini, V. Voinovich, B. Albertini, C. Cavallari, L. Rodriguez. Characterization of carbamazepine-Gelucire 50/13 microparticles prepared by a spray-congealing process using ultrasounds. *Journal of Pharmaceutical Sciences,* 2002, **91** (3), 699-707.

199. N. Passerini, B. Perissutti, B. Albertini, D. Voinovich, M. Moneghini, L. Rodriguez. Controlled release of verapamil hydrochloride from waxy microparticles prepared by spray congealing. *Journal of Controlled Release*, 2003, **88** (2), 263-275.

200. R. Bodmeier, J. Wang, H. Bhagwatkar. Process and formulation variables in the preparation of wax microparticles by a melt dispersion technique. I. Oil-in-water technique for water-insoluble drugs. *Journal of Microencapsulation,* 1992, **9** (1), 89-98.

201. R. Bodmeier, J. Wang, H. Bhagwatkar. Process and formulation variables in the preparation of wax microparticles by a melt dispersion technique. II.W/O/W multiple emulsion technique for water-soluble drugs. *Journal of Microencapsulation,* 1992, **9** (1), 99-107.

202. S. Benita, O. Zouai, J.P. Benoit. 5-Fluorouracil: carnauba wax microspheres for chemoembloization: an *in vitro* evaluation. *Journal of Pharmaceutical Sciences,* 1986, **75** (9), 847-851.

203. T. Eldem, P. Speiser, A. Hincal. Optimization of spray-dried and congealed lipid micropellets and characterization of their surface morphology by scanning electron microscopy. *Pharmaceutical Research,* 1991, **8** (1), 47-54.

204. V. Sanna, N. Kirschvink, P. Gustin, E. Gavini, I. Roland, L. Delattre, B. Evrard. Preparation and *in vivo* toxicity study of solid lipid microparticles as carrier for pulmonary administration. *AAPS PharSciTech,* 2004, **5** (2), Article 27.

205. E.B. Souto. PhD Thesis, SLN and NLC for Topical Delivery of Antifungals. 2005, Chemie, Pharmazie der Freien Universität Berlin, Berlin.

206. S.A. Wissing, R.H. Müller. The development of an improved carrier system for sunscreen formulations based on crystalline lipid nanoparticles. *International Journal of Pharmaceutics,* 2002, **242**, 373-375.

207. S.A. Wissing, O. Kayser, R.H. Müller. Solid lipid nanoparticles for parenteral drug delivery. *Advanced Drug Delivery Reviews,* 2004, **56**, 1257-1272.

208. S.C. Yang, L.F. Lu, Y. Cai, J.B. Zhu, B.W. Liang, C.Z. Yang. Body distribution in mice of intravenously injected camptothecin solid lipid nanoparticles and targeting effect on the brain. *Journal of Controlled Release,* 1999, **59**, 299-307.

209. S.C. Yang, J.B. Zhu, Y. Lu, B.W. Liang, C.Z. Yang. Body distribution of camptothecin solid lipid nanoparticles after oral administration. *Pharmaceutical Research,* 1999, **16** (5), 751-757.

210. K. Wa Kasongo, R.H. Müller, R.B. Walker. Investigation of solid lipid nanocarriers as potential vehicles for the oral delivery of didanosine to paediatric patients. International Symposium on Controlled Release of Bioactive Materials, 2010, Portland/Oregon.

211. R. Cavalli, M.R. Gasco, P. Chetoni, S. Burgalassi, M.F. Saettone. Solid lipid nanoparticles (SLN) as ocular delivery system for tobramycin. *International Journal of Pharmaceutics,* 2002, **238**, 241-245.

212. A. Salgueiro, M.A. Egea, M. Espina, O. Valls, M.L. Garcia. Stability and occular tolerance of cyclophosphamide-loaded nanospheres. *Journal of Microencapsulation,* 2004, **21** (2), 213-223.

213. M.A. Videira, A.J. Almeida, M.F. Botelho, A.C. Santos, C. Gomes, J.J.P. de Lima. Lymphatic uptake of radiolabelled solid lipid nanoparticles administered by the pulmonary route. *European Journal of Nuclear Medicine,* 1999, **26** (9), 1168.

214. S. Jaspart, P. Bertholet, L. Delattre, B. Evrard. Study of solid lipid microparticles as sustained release delivery system for pulmonary administration. 15th International Symposium on Microencapsulation, 2005, Parma, Italy.

215. M. Sznitowska, M. Gajewska, S. Janicki, A. Radwanska, G. Lukowski. Bioavailability of diazepam from aqueous-organic solution, submicron emulsion and solid lipid nanoparticles after rectal administration to rabbits. *European Journal of Pharmaceutics and Biopharmaceutics,* 2001, **52**, 159-163.

216. J. Kristil, B. Volk, M. Gasperlin, M. Sentjurc, P. Jurkovic. Effects of colloidal carriers on ascorbyl palmitate stability. *European Journal of Pharmaceutical Sciences,* 2003, **19** (4), 181-189.

217. M. Savolainen, C. Khoo, H. Glad, C. Dahlqvist, A.M. Juppo. Evaluation of controlled-release of polar lipid microparticles. *International Journal of Pharmaceutics,* 2002, **244**, 151-161.

218. K. Westesen, H. Bunjes. Do nanoparticles prepared from lipids solid at room temperature always possess a solid lipid matrix. *International Journal of Pharmaceutics,* 1995, **115**, 62-69.

219. C. Schwarz. PhD thesis, Feste Lipidnanopartikel: Herstellung, Charakterisierung, Arzneistoffinkorporation undfreisetzung, Sterilisation und Lyophilisation. 1995, Free University of Berlin, Berlin, Germany.

220. F. Han, S. Li, R. Yin, H. Liu, L. Xu. Effect of surfactants on the formation and characterisation of a new type of colloidal drug delivery system. *Colloids and Surfaces A: Physicochemical and Engineering Aspects,* 2008, **315** (1-3), 210-216.

221. Q. Xia, X. Hao, Y. Lu, W. Xu, H. Wei, Q. Ma, N. Gu. Production of drug-loaded lipid nanoparticles based on phase behaviours of special hot microemulsions. *Colloids and Surfaces A: Physicochemical Engineering Aspects,* 2008, **313-314**, 27-30.

222. K. Westesen, B. Siekmann. Investigation of the gel formation of phospholipid stabilized solid lipid nanoparticles. *International Journal of Pharmaceutics,* 1997, **151** (1), 35-45.

223. A. zur Mühlen, W. Mehnert. Drug release and release mechanism of prednisolone loaded solid lipid nanoparticles. *Pharmazie,* 1998, **53**, 552.

224. M. Muchow, P. Maincent, R.H. Müller. Lipid nanoparticles with a solid matrix (SLN®, NLC®, LDC®) for oral drug delivery. *Drug Development and Industrial Pharmacy,* 2008, **34** (12), 1394-1405.

225. E.B. Souto, R.H. Müller. Lipid nanoparticles (SLN and NLC) for drug delivery. In: A.J. Domb, Y. Tobata, M.N.V.R. Kumar, S. Farber (editors): *Nanoparticles for Pharmaceutical Applications*. 2007, Stevenson Ranch, California: American Scientific Publishers, pp. 103-122.

226. M. Igartua, P. Saulnier, B. Heurtault, B. Pech, J.E. Proust, J.L. Pedraz, J.P. Benoit. Development and characterization of solid lipid nanoparticles loaded with magnetite. *International Journal of Pharmaceutics,* 2002, **223** (1-2), 149-157.

227. B. Sjöström, B. Bergenstå. Preparation of submicron drug particles in lecithin stabilized o/w emulsions: I. Model studies of the precipitation of cholesteryl acetate. *International Journal of Pharmaceutics,* 1992, **88** (1), 53-62.

228. R. Cortesi, E. Esposito, G. Luca, C. Nastruzzi. Production of lipospheres as carriers for bioactive compounds. *Biomaterials,* 2002, **23** (11), 2283-2294.

229. S. Sugiura, M. Nakajima, J. Tong, H. Nabetani, M. Seki. Preparation of monodispersed solid lipid microspheres using a microchannel emulsification technique. *Journal of Colloid and Interface Science,* 2000, **227**, 95-103.

230. T. Kawakatsu, G. Tragardh, C. Tragardh. Production of W/O/W emulsions and S/O/W pectin microcapsules by microchannel emulsification. *Colloid Surface A,* 2001, **189**, 257-264.

231. M.J. Killeen. Spray drying and spray congelaing of pharmaceuticals. In: J. Swarbrick, J.C. Boylan (editors): *Encyclopedia of Pharmaceutical Technology*, 2000, Marcel Dekker Inc., New York, pp. 207-221.

232. K. Wa Kasongo, R.H. Müller, R.B. Walker. The use of hot and cold HPH to enhance the LC and EE of nanostructured lipid carriers for the hydrophilic antiretroviral drug, didanosine for potential administration to paediatric patients. *Pharmaceutical Development and Technology,* 2012, **17** (3), 353-362.

233. A. De Labouret, O. Thioune, H. Fessi, J.P. Devissaguet, F. Puisieux. Application of an original process for obtaining colloidal dispersions of some coating polymers: Preparation, characterisation and industrial scaling up. *Drug Development and Industrial Pharmacy,* 1995, **21**, 229-241.

234. B. Siekmann, K. Westesen. Investigations on solid lipid nanoparticles prepared by precipitation in o/w emulsions. *European Journal of Pharmaceutics and Biopharmaceutics,* 1996, **43**, 104-109.

235. A. Dubes, H. Parrot-Lopez, W. Abdelwahed, G. Degobert, H. Fessi, P. Shahgaldian, A.W. Coleman. Scanning electron microscopy and atomic force microscopy imaging of solid lipid nanoparticles derived from amphiphilic cyclodextrins. *European Journal of Pharmaceutics and Biopharmaceutics,* 2003, **55**, 279-282.

236. D. Danino, Y. Talmon, R. Zana. Vesicle-to-micelle transformation in systems containing dimeric surfactants. *Journal of Colloid and Interface Science,* 1997, **185**, 84-93.

237. B. Heurtault, P. Saulnier, B. Pech, J. Benoit. Physico-chemical stability of colloidal lipid particles. *Biomaterials,* 2003, **24**, 4283-4300.

238. A. Radomska-Soukharev. Stability of lipid excipients in solid lipid nanoparticles. *Advanced Drug Delivery Reviews,* 2007, **59**, 411-418.

239. Y.C. Kuo, T.W. Lin. Electrophoretic mobility, zeta potential and fixed charge density of bovine knee chondrocytes, methyl methacrylate-sulphonyl methacryalte, polybutylcyanocrylate and solid lipid nanoparticles. *Journal of Physical Chemistry B,* 2006, **110** (5), 2202-2208.

240. C. Freitas, R.H. Müller. Correlation between long-term stability of solid lipid nanoparticles (SLN^{TM}) and crystallinity of the lipid phase. *European Journal of Pharmaceutics and Biopharmaceutics,* 1999, **47**, 125-132.

241. E.B. Souto, W. Mehnert, R.H. Müller. Polymorphic behaviour of compritol 888 ATO as bulk lipid and as SLN and NLC. *Journal of Microencapsulation,* 2006, **23** (4), 417-433.

242. H. Bunjes, K. Westesen, M.H.J. Koch. Crystallization tendency and polymorphic transitions in triglyceride nanoparticles. *International Journal of Pharmaceutics,* 1996, **129** (1-2), 159-173.

243. E.B. Souto, S.A. Wissing, C.M. Barbosa, R.H. Müller. Development of a controlled release formulation based on SLN and NLC for topical clotrimazole delivery. *International Journal of Pharmaceutics,* **278**, 71-77.

244. G. Lukowski, J. Kasbohm, P. Pflegel, A. Illing, H. Wuff. Crystallographic investigation of cetylpalmitate solid lipid nanoparticles. *International Journal of Pharmaceutics,* 2000, **196** (2), 201-205.

245. V. Teeranachaideekul, E.B. Souto, V.B. Junyaprasert, R.H. Müller. Cetyl palmitate-based NLC for topical delivery of Coenzyme Q10 - Development, physicochemical characterization and *in vitro* release studies. *European Journal of Pharmaceutics and Biopharmaceutics,* 2007, **67** (1), 141-148.

246. M. Joshi, V. Patravale. Nanostructured lipid carrier (NLC) based gel of celecoxib. *International Journal of Pharmaceutics,* 2007, **346**, 124-132.

247. J. You, F. Wan, F. de Cui, Y. Sun, Y.Z. Du, F.Q. Hu. Preparation and characterization of vinorelbine bitartrate-loaded solid lipid nanoparticles. *International Journal of Pharmaceutics,* 2007, **343** (1-2), 270-276.

248. F.Q. Hu, S.P. Jiang, Y.Z. Du, H. Yuan, Y.Q. Ye, S. Zeng. Preparation and characteristics of monostearin nanostructured lipid carriers. *International Journal of Pharmaceutics,* 2006, **314**, 83-89.

249. C.M. Riley. Determination of ketoconazole in the plasma, liver, lung and adrenal of the rat by high-performance liquid chromatography. *Journal of Chromatography,* 1986, **377**, 287-294.

250. F.A. Andrews, L.R. Peterson, W.H. Beggs, D. Crankshaw, G.A. Sarosi. Liquid chromatographic assay of ketoconazole. *Antimicrobial Agents and Chemotherapy,* 1981, **19** (1), 110-113.

251. K.H. Yuen, K.K. Peh. Simple high-performance liquid chromatographic method for determination of ketoconazole in human plasma. *Journal of Chromatography B,* 1998, **715**, 436-440.

252. L. Ramos, N. Brignol, R. Bakhtiar, T. Ray, L.M. Mc Mahon, F.L. Tse. High-throughput approaches to the quantitative analysis of ketoconazole, a potent inhibitor of cytochrome P450 3A4, in human plasma. *Rapid communications in mass spectrometry,* 2000, **14** (23), 2282-2293.

253. M.V. Vertzoni, C. Reppas, H.A. Archontaki. Optimization and validation of a high-performance liquid chromatographic method with UV detection for the determination of ketoconazole in canine plasma. *Journal of Chromatography B,* 2006, **839**, 62-67.

254. P. de Bruijn, D.F.S. Kehrer, J. Verweij, A. Sparreboom. Liquid chromatographic determination of ketoconazole, a potent inhibitor of CYP3A4-mediated metabolism. *Journal of Chromatography B,* 2001, **753**, 395-400.

255. S. Bajad, R.K. Johri, K. Singh, J. Singh, K.L. Bedi. Simple high-performance liquid chromatography method for the simultaneous determination of ketoconazole and piperine in rat plasma and hepatocyte culture. *Journal of Chromatography A,* 2002, **949**, 43-47.

256. S.F. Swezey, K.M. Glacomini, A. Abang, C. Brass, D.A. Stevens, T.F. Blaschke. Measurement of ketoconazole, a new antifungal agent, by high-performance liquid chromatography. *Journal of Chromatography,* 1982, **227**, 510-515.

257. Y. Chen, L. Felder, X. Jiang, S. Vladimirov. Determination of ketoconazole in human plasma by high-performance liquid chromatography-tandem mass spectrometry. *Journal of Chromatography B,* 2002, **774**, 67-78.

258. K.B. Alton. Determination of the antifungal agent, ketoconazole, in human plasma by high-performance liquid chromatography. *Journal of Chromatography,* 1980, **221**, 337-344.

259. J.H. Jorgensen, G.A. Alexander, J.R. Graybill, D.J. Drutz. Sensitive bioassay for ketoconazole in serum and cerebrospinal fluid. *Antimicrobial Agents and Chemotherapy,* 1981, **20** (1), 59-62.

260. A.M. Di Pietra, V. Cavrini, V. Andrisano, R. Gatti. HPLC analysis of imidazole antimycotic drugs in pharmaceutical formulations. *Journal of Pharmaceutical and Biomedical Analysis,* 1992, **10** (10-12), 873-879.

261. B.A. Mousa, N.M. El-Kousy, R.I. El-Bagary, N.G. Mohamed. Stability-indicating methods for the determination of some anti-fungal agents using densitometric and RP-HPLC methods. *Chemical and pharmaceutical bulletin,* 2008, **56** (2), 143-149.

262. E.M. Abdel-Moety, F.I. Khattab, K.M. Kelani, A.M. AbouAl-Alamein. Chromatographic determination of clotrimazole, ketoconazole and fluconazole in pharmaceutical formulations. *Il Farmaco,* 2002, **57**, 931-938.

263. E.R.M. Kedor-Hackmann, M.M.F. Nery, M.I.R.M. Santoro. Determination of ketoconazole in pharmaceutical preparations by ultraviolet spectrophotometry and high-performance liquid chromatography. *Analytical Letters,* 1994, **27** (2), 363-376.

264. E.R.M. Kedor-Hackmann, M.I.R.M. Santoro, A.K. Singh, A.C. Peraro. First-derivative ultraviolet spectrophotometric and high performance liquid chromatographic determination of ketoconazole in pharmaceutical emulsions. *Brazilian Journal of Pharmaceutical Sciences,* 2006, **42** (1), 91-98.

265. L.V. Allen, M.A. Erickson. Stability of ketoconazole, metolazone, metronidazole, procainamide hydrochloride and spironolactone in extemporaneously compounded oral liquids. *American Journal of Health-System Pharmacy,* 1996, **53** (17), 2073-2078.

266. M. Skiba, M. Skiba-Lahiani, H. Marchais, R. Duclos, P. Arnaud. Stability assessment of ketoconazole in aqueous formulations. *International Journal of Pharmaceutics,* 2000, **198**, 1-6.

267. P.Y. Khashaba, S.R. El-Shabouri, K.M. Emara, A.M. Mohamed. Analysis of some antifungal drugs by spectrophotometric and spectrofluorimetric methods in different pharmaceutical dosage forms. *Journal of Pharmaceutical and Biomedical Analysis,* 2000, **22**, 363-376.

268. Y.V. Heyden, A.N.M. Nguyet, M.R. Detaevernier, D.L. Massart, J. Plaizier-Vercammen. Simultaneous determination of ketoconazole and formaldehyde in a shampoo: liquid

chromatography method development and validation. *Journal of Chromatography A*, 2002, **958**, 191-201.

269. I. Staub, E.E.S. Schapoval, A.M. Bergold. Microbiological assay of ketoconazole in shampoo. *International Journal of Pharmaceutics*, 2005, **292**, 195-199.

270. C. Zhang, F. von Heeren, W. Thormann. Separation of hydrophobic, positively-chargeable substances by capillary electrophoresis. *Analytical Chemistry*, 1995, **67**, 2070-2077.

271. I. Velikinac, O. Cudina, I. Jankovic, D. Agbaba, S. Vladimirov. Comparison of capillary zone electrophoresis and high performance liquid chromatography methods for quantitative determination of ketoconazole in drug formulations. *Il Farmaco*, 2004, **59**, 419-424.

272. C.A. Turner, A. Turner, D.W. Warnock. High performance liquid chromatographic determination of ketoconazole in human serum. *Journal of Antimicrobial Chemotherapy*, 1986, **18** (6), 757-763.

273. P.L. Carver, R.R. Berardi, M.J. Knapp, J.M. Rider, C.A. Kauffman, S.F. Bradley, M. Atassi. *In vivo* interaction of ketoconazole and sucralfate in healthy volunteers. *Antimicrobial Agents and Chemotherapy*, 1994, **38** (2), 326-329.

274. C.F. Simpson. *Techniques in liquid chromatography*. 1982, Wiley Heyden Ltd., Great Britain.

275. C. Horvath. High Performance Liquid Chromatography: Advances and Perspectives. 1980, Academic Press, New York, pp. 113-229.

276. G.D. Christian. *Analytical Chemistry*. 1977, John Wiley & Sons, New York.

277. H.A. Laitinen, W.E. Harris. Applications of chromatography. 1975, McGraw Hill, New York, pp. 499-530.

278. I.W. Wainer. *Liquid Chromatography in Pharmaceutical Development: An Introduction*. 1985, Aster Publishing Corporation, Springfield.

279. J. Swarbrick, J.C. Boylan. *Encyclopedia of Pharmaceutical Technology*. 1990, Marcel Dekker Inc., New York and Basel.

280. K.A. Connors. *A textbook of Pharmaceutical analysis*. 1967, John Wiley & Sons, Inc., New York.

281. P.A. Bristow. *Liquid chromatography in practice*. 1976, Laboratory Data Control, UK.

282. J.J. Kirkland. *Modern Practice of Liquid Chromatography*. 1971, Wiley-Interscience, a Division of John Wiley & Sons, Inc., New York.

283. L.R. Snyder, J.J. Kirkland. *Introduction to modern liquid chromatography*. 1979, John Wiley & Sons, Inc., New York.

284. L.R. Snyder, J.J. Kirkland, J.L. Glajch. *Practical HPLC Method Development*. 1997, John Wiley & Sons, Inc., New York.

285. S. Ahuja. Selectivity and detectability optimizations in HPLC. In: J.D. Winefordner, I.M. Kolthoff (editors): *Chemical Analysis: A Series of Monographs on Analytical Chemistry and its Applications*. 1989, John Wiley and Sons, New York, p. 2.

286. L. Ohannesian, A.J. Streeter. *Handbook of Pharmaceutical Analysis*. 2002, Marcel Dekker Inc., New York.

287. P.C. Sadek. *The HPLC Solvent Guide*. 1996, John Wiley & Sons, Inc., New York.

288. J.A. Jonsson. *Chromatographic Theory and Basic Principles*. 1987, Marcel Dekker Inc., New York.

289. J. Nawrocki. The silanol group and its role in liquid chromatography. *Journal of Chromatography A*, 1997, **779**, 29-71.

290. N. Tanaka, K. Sakagami, M. Araki. Effect of alkyl chain length of the stationary phase on retention and selectivity in reversed-phase liquid chromatography. *Journal of Chromatography*, 1980, **199**, 327-337.

291. N. Tanaka, K. Kimata, K. Hosoya, H. Miyanishi, T. Araki. Stationary phase effects in reversed-phase liquid chromatography. *Journal of Chromatography A*, 1993, **656**, 265-287.

292. F. Bailey. Applications of high-performance liquid chromatography in the pharmaceutical industry. *Journal of Chromatography A*, 1976, **122**, 73-84.

293. F.E. Regnier, K.M. Gooding. High-performance liquid chromatography of proteins. *Analytical Biochemistry*, 1980, **103**, 1-25.

294. D. Kasiske, K.D. Klinmuller, M. Sonneborn. Application of high-performance liquid chromatography to water pollution analysis. *Journal of Chromatography*, 1978, **149**, 703-710.

295. P.C. Sadek. *Troubleshooting HPLC systems: A Bench Manual*. 2000, John Wiley & Sons, Inc., New York.

296. S. Kromidas. *Practical Problem Solving in HPLC*. 2002, Wiley-Vch, Weinheim.

297. S. Kromidas. *More Practical Problem Solving in HPLC*. 2005, Wiley-Vch, Weinheim.

298. C.M. Ginsburg, G.H. McCracken Jr, K. Olsen. Pharmacology of ketoconazole suspension in infants and children. *Antimicrobial Agents and Chemotherapy*, 1983, **23**, 787-789.

299. L.K. Pershing, J. Corlett, C. Jorgensen. *In vivo* pharmacokinetics and pharmacodynamics of topical ketoconazole and miconazole in human stratum corneum. *Antimicrobial Agents and Chemotherapy*, 1994, **38** (1), 90-95.

300. T.W.F. Chin, M. Loeb, I.W. Fong. Effects of an acidic beverage (Coca-Cola) on absorption of ketoconazole. *Antimicrobial Agents and Chemotherapy*, 1995, **39** (8), 1671-1675.

301. D. Cordoba-Diaz, M. Cordoba-Diaz, S. Awad, M. Cordoba-Borrego. Effect of pharmacotechnical design on the in vitro interaction of ketoconazole tablets with non-systemic antacids. *International Journal of Pharmaceutics*, 2001, **226**, 61-68.

302. K. Karch, S. Sebestian, I. Halasz. Preparation and properties of reversed phases. *Journal of Chromatography*, 1976, **122**, 3-16.

303. J.J. Kirkland. *Modern Practice of Liquid Chromatography*. 1971, Wiley-Interscience, a Division of John Wiley & Sons, Inc., New York.

304. L.R. Snyder, J.J. Kirkland. Introduction to modern liquid chromatography. 1979, John Wiley & Sons, Inc., New York, pp. 125-165.

305. I.W. Wainer. *Liquid Chromatography in Pharmaceutical Development: An Introduction*. 1985, Aster Publishing Corporation, Springfield.

306. P.A. Bristow. *Liquid chromatography in practice*. 1976, hetp, Macclesfield, pp. 134-136.

307. C.F. Simpson. *Techniques in liquid chromatography*. 1982, Wiley Heyden Ltd., New York.

308. R.P.W. Scott. *Liquid chromatography detectors*. 1977, Elsevier Scientific Publishing Company, Amsterdam.

309. T.M. Vickrey. *Liquid chromatography detectors*. 1983, Marcel Dekker, Inc., New York.

310. L.R. Snyder, J.J. Kirkland, J.L. Glajch. *Practical HPLC Method Development*. 1997, John Wiley & Sons, Inc., New York.

311. D.C. Harries. *Quantitative chemical analysis*. 1999, W.H. Freeman and Company, New York.

312. K. Hammarstrand. Internal standard in gas chromatography. *Varian Instrument Applications*, 1976, **10** (1), 10-11.

313. L.C. Tan, P.W. Carr. Study of retention in reversed-phase liquid chromatography using linear solvation energy relationships II: the mobile phase. *Journal of Chromatography A*, 1998, **799** (1-2), 1-19.

314. The United States Pharmacopeia incorporating 'The National Formulary'. 2006, The United States Pharmacopoeial Convention Inc., Rockville.

315. C.M. Riley, T.W. Rosanske. *Development and Validation of Analytical Methods*. 1996, Elsevier Science Ltd, Amsterdam.

316. U.S. Department of Health and Human Services FDA. *Guidance for industry: Bioanalytical methods validation*. 2001, Center for Drug Evaluation and Research and Center for Veterinary Medicine, Rockville.

317. H. Rosing, W.Y. Man, E. Doyle, A. Bult, J.H. Beijnen. Bioanalytical liquid chromatographic method validation: a review of current practices and procedures. *Journal of Liquid Chromatography and Related Technologies*, 2000, **23** (3), 329-354.

318. L. Huber. Validation of analytical methods and processes. In: R.A. Nash, A.H. Wachter (editors): *Pharmaceutical Process Validation*. 1993, Marcel Dekker Inc., New York, pp. 507-524.

319. S.R.G. Braggio, R.J. Barnaby, P. Grossi, M. Cugola. A strategy for validation of bioanalytical methods. *Journal of Pharmaceutical and Biomedical Analysis*, 1996, **14** (4), 375-388.

320. G.A. Shabir. Validation of high-performance liquid chromatography methods for pharmaceutical analysis: Understanding the differences and similarities between validation requirements of the US Food and Drug Administration, the US Pharmacopeia and the International Conference on Harmonization. *Journal of Chromatography A*, 2003, **987** (1-2), 57-66.

321. U.S. Department of Health and Human Services FDA. *Reviewer Guidance: Validation of chromatographic methods*. 1994, Center for Drug Evaluation and Research and Center for Veterinary Medicine, Rockville.

322. J. Ermer. Validation of Pharmaceutical Analysis. Part I: An integrated approach. *Journal of Pharmaceutical and Biomedical Analysis*, 2001, **24**, 755-767.

323. ICH Topic Q2A. *ICH Harmonised Tripartite Guidelines: validation of analytical methods: definitions and terminology*. 1995, International Conference on Harmonization, London.

324. ICH Topic Q2B. *ICH Harmonised Tripartite Guidelines: validation of analytical procedures: Methodology*. 1996, International Conference on Harmonization, London.

325. Food and Drug Administration. *Guidance for industry. Validation of analytical procedures for Type C medicated feeds*. 2005, Food and Drug Administration and Centre for Veterinary Medicine, Rockville.

326. G.C. Hokanson. A life cycle approach to the validation of analytical methods during pharmaceutical product development, Part I: The Initial Method Validation Process. *Pharmaceutical Technology* 1994 (September) 118-130.

327. M.E. Swartz, I.S. Krull. Validation of Chromatographic methods. *Pharmaceutical Technology*, 1998, **22**, 104-118.

328. B. Dejaegher, Y.V. Heyden. Ruggedness and robustness testing. *Journal of Chromatography A*, 2007, **1158**, 138-157.

329. J.M. Green. A practical guide to analytical method validation. *Analytical Chemistry*, 1996, **68** (News and features) 305A-309A.

330. A. Segall, M. Vitale, V. Perez, F. Hormaechea, M. Palacios, M.T. Pizzorno. A stability-indicating HPLC method to determine cyproterone acetate in tablet formulations. *Drug Development and Industrial Pharmacy*, 2000, **26** (8), 867-872.

331. R. Wood. How to validate analytical methods. *Trends in Analytical Chemistry*, 1999, **18** (9 & 10), 624-632.

332. I.S. Krull, M.E. Swartz. Regulatory Review of Method Validation. *LCGC*, 2000, **18** (6), 620-625.

333. T.C. Paino, A.D. Moore. Determination of the LOD and LOQ of an HPLC method using four different techniques. *Pharmaceutical Technology*, 1999, **23** (10), 82-90.

334. I.S. Krull, M.E. Swartz. *Analytical Method Development and Validation*. 1997, Marcel Dekker Inc., New York.

335. I. Taverniers, M. De Loose, E. van Bockstaele. Trends in quality in the analytical laboratory. II. Analytical method validation and quality assurance. *Trends in Analytical Chemistry*, 2004, **23** (8), 535-552.

336. R.D. McDowell. The role of laboratory information systems (LIS) in analytical method development. *Analytica Chemica Acta*, 1999, **391**, 149-158.

337. D. Dadgar, P.E. Burnett. Issues in evaluation of bioanalytical method selectivity and drug stability. *Journal of Pharmaceutical and Biomedical Analysis*, 1995, **14** (1-2), 23-31.

338. A.R. Buick, M.V. Doig, S.C. Jeal, G.S. Land, R.D. McDowell. Method validation in the bioanalytical laboratory. *Journal of Pharmaceutical and Biomedical Analysis*, 1990, **8** (8-12), 629-637.

339. A strategy for validation of bioanalytical methods. *Journal of Pharmaceutical and Biomedical Analysis*, 1996, **14** (4), 375-388.

340. U. Timm, M. Wall, D. Dell. A new approach for dealing with the stability of drugs in biological fluids. *Journal of Pharmaceutical Sciences*, 1985, **74** (9), 972-977.

341. R.H. Müller, K. Mäder, S. Gohla. Solid lipid nanoparticles (SLN) for controlled drug delivery - a review of the state of the art. *European Journal of Pharmaceutics and Biopharmaceutics*, 2000, **50**, 161-177.

342. E.B. Souto, C. Anselmi, M. Centini, R.H. Müller. Preparation and characterization of n-dodecyl-ferulate-loaded solid lipid nanoparticles (SLN®). *International Journal of Pharmaceutics*, 2005, **295** (1-2), 261-268.

343. E.B. Souto, R.H. Müller. SLN and NLC for topical delivery of ketoconazole. *Journal of Microencapsulation*, 2005, **22** (5), 501-510.

344. R.H. Müller, S.S. Runge, V. Ravelli, A.F. Thünemann, W. Mehnert, E.B. Souto. Cyclosporine-loaded topical SLN formulations - Preparation, storage stability, mechanism on skin. *European Journal of Pharmaceutics and Biopharmaceutics*, 2008, **68** (3), 535-544.

345. J.W. Dodd, K.H. Tonge. Differential thermal analysis/Differential scanning calorimetry - nature and instrumentation. In: B.R. Currell (editor): *Thermal methods*. 1987, Crown Copyright, London, pp. 110-143.

346. M.I. Pope, M.D. Judd. *Differential thermal analysis, A guide to the technique and its applications*. 1980, Heyden & Son Ltd., London.

347. E.M. Barrall II, J.F. Johnson. Differential scanning calorimetry theory and applications. In: P.E. Slade Jr, L.T. Jenkins (editors): *Thermal characterization techniques*. 1970, Marcel Dekker Inc., New York, pp. 1-39.

348. M.E. Brown. *Introduction to thermal analysis: techniques and applications*. 1988, Chapman and Hall, London.

349. T. Hatakeyama, Z. Liu. *Handbook of thermal analysis*. 1998, John Wiley & Sons, Sussex.

350. N. Chieng, T. Rades, J. Aaltonen. An overview of recent studies on the analysis of pharmaceutical polymorphs. *Journal of Pharmaceutical and Biomedical Analysis*, 2011, **55**, 618-644.

351. A. Rossi, A. Savioli, M. Bini, D. Capsoni, V. Massarotti, R. Bettini, A. Gazzaniga, M.E. Sangalli, F. Giordano. Solid-state characterization of paracetamol metastable polymorphs formed in binary mixtures with hydroxypropylmethylcellulose. *Thermochimica Acta*, 2003, **406**, 55-67.

352. C. McGregor, E. Bines. The use of high-speed differential scanning calorimetry (Hyper-DSC) in the study of pharmaceutical polymorphs. *International Journal of Pharmaceutics*, 2008, **350**, 48-52.

353. M. Tomassetti, A. Catalani, V. Rossi, S. Vecchio. Thermal analysis study of the interactions between acetaminophen and excipients in solid dosage forms and in some binary mixtures. *Journal of Pharmaceutical and Biomedical Analysis,* 2005, **37**, 949-955.

354. L. Bond, S. Allen, M.C. Davies, C.J. Roberts, A.P. Shivji, S.J.B. Tendler, P.M. Williams, J. Zhang. Differential scanning calorimetry and scanning thermal microscopy analysis of pharmaceutical materials. *International Journal of Pharmaceutics,* 2002, **243**, 71-82.

355. S. Lin, C. Liao, G. Hsiue, R. Liang. Study of a theophylline-Eudragit L mixture using a combined system of microscopic Fourier-transform infrared spectroscopy and differential scanning calorimetry. *Thermochimica Acta,* 1995, **245**, 153-166.

356. P.G. Royall, D.Q.M. Craig, D.M. Price, M. Reading, T.J. Lever. An investigation into the use of microthermal analysis for the solid state characterisation of an HPMC tablet formulation. *International Journal of Pharmaceutics,* 1999, **192**, 97-103.

357. S. Clas, C.R. Dalton, B.C. Hancock. Differential scanning calorimetry: applications in drug development. *PSTT,* 1999, **2** (8), 311-320.

358. J.L. Ford, T.E. Mann. Fast-Scan DSC and its role in pharmaceutical physical form characterisation and selection. *Advanced Drug Delivery Reviews,* 2012, **64**, 422-430.

359. R.F. Speyer. Differential thermal analysis. In: R.F. Speyer (editor): *Thermal analysis of materials*. 1994, Marcel Dekker Inc., New York, pp. 35-90.

360. A.A. Attama, B.C. Schicke, C.C. Müller-Goymann. Further characterization of theobroma oil-beeswax admixtures as lipid matrices for improved drug delivery systems. *European Journal of Pharmaceutics and Biopharmaceutics,* 2006, **64**, 294-306.

361. B. Kowalski. Determination of oxidative stability of edible vegetable oils by pressure differential scanning calorimetry. *Thermochimica Acta,* 1989, **156**, 347-358.

362. C.G. Biliaderis. Differential scanning calorimetry in food research - A review. *Food Chemistry,* 1983, **10**, 239-265.

363. J.B. Brubach, V. Jannin, B. Mahler, C. Bourgaux, P. Lessieur, P. Roya, M. Ollivon. Structural and thermal characterization of glyceryl behenate by X-ray diffraction coupled to differential calorimetry and infrared spectroscopy. *International Journal of Pharmaceutics,* 2007, **336**, 248-256.

364. L. Yu, G. Christie. Measurement of starch thermal transitions using differential scanning calorimetry. *Carbohydrate Polymers,* 2001, **46**, 179-184.

365. A.C. Eliasson. Starch-lipid interactions studied by differential scanning calorimetry. *Thermochimica Acta,* 1985, **95**, 369-374.

366. Z. Zhong, X.S. Sun. Thermal characterization and phase behaviour of cornstarch studied by differential scanning calorimetry. *Journal of Food Engineering,* 2005, **69**, 453-459.

367. R. Hilfiker. *Polymorphism in the pharmaceutical industry*. 2006, Wiley, Weinheim.

368. H. Weber-Anneler, R.W. Arndt. Thermal methods of analysis/Differential scanning calorimetry in theory and application. *Thermochimica Acta,* 1985, **85**, 267-270.

369. J. Haleblian, W. McCrone. Pharmaceutical applications of polymorphism. *Journal of Pharmaceutical Sciences,* 1969, **58**, 911-929.

370. P. Corvi Mora, M. Cirri, P. Mura. Differential scanning calorimetry as a screening technique in compatibility studies of DHEA extended release formulations. *Journal of Pharmaceutical and Biomedical Analysis,* 2006, **42**, 3-10.

371. P. Mura, M.T. Faucci, A. Manderioli, G. Bramanti, L. Ceccarelli. Compatibility study between ibuproxam and pharmaceutical excipients using differential scanning calorimetry, hot-stage microscopy and scanning electron microscopy. *Journal of Pharmaceutical and Biomedical Analysis,* 1998, **18**, 151-163.

372. K. Daniel, T. Plivelic, Y. Cerenius. Characterizing lipid nanostructures: A SAXS/WAXS and DSC study. http://www.aidic.it/isic18/webpapers/276Kalnin.pdf, last accessed on 22-03-2014

373. C. Allais, G. Keller, P. Lesieur, M. Ollivon, F. Artzner. X-Ray diffraction/calorimetry coupling, a tool for polymorphism control. *Journal of Thermal Analysis and Calorimetry,* 2003, **74**, 723-728.

374. A. Salari, R.E. Young. Application of attenuated total reflectance FTIR spectroscopy to the analysis of mixtures of pharmaceutical polymorphs. *International Journal of Pharmaceutics,* 1998, **163**, 157-166.

375. J.E. Stewart. *Infrared Spectroscopy*. 1970, Marcel Dekker, New York.

376. M. Sorrenti, L. Catenacci, G. Bruni, B. Luppi, F. Bigucci, G. Bettinetti. Solid-state characterization of tacrine hydrochloride. *Journal of Pharmaceutical and Biomedical Analysis,* 2012, **63**, 53-61.

377. S. Agatonovic-Kustrin, I.G. Tucker, D. Schmierer. Solid state assay of ranitidine-HCl as a bulk drug and as active ingredient in tablets using DRIFT spectroscopy with artificial neural networks. *Pharmaceutical Research,* 1999, **16**, 1477-1482.

378. F.E.B. Silva, M.F. Ferrão, G. Parisotto, E.I. Müller, E.M.M. Flores. Simultaneous determination of sulphamethoxazole and trimethoprim in powder mixtures by attenuated total reflection-Fourier transform infrared and multivariate calibration. *Journal of Pharmaceutical and Biomedical Analysis*, 2009, **49**, 800-805.

379. D. Bach, I.R. Miller. Attenuated total reflection (ATR) Fourier transform infrared spectroscopy of dimyristoyl phosphatidylserine–cholesterol mixtures. *Biochimica et Biophysica Acta*, 2001, **1514**, 318-326.

380. A. Rohman, Y.B. Che Man. Fourier transform infrared (FTIR) spectroscopy for analysis of extra virgin olive oil adulterated with palm oil. *Food Research International* 2010, **43**, 886-892.

381. M. Jackson, P.I. Haris, D. Chapman. Fourier transform infrared spectroscopic studies of lipids, polypeptides and proteins. *Journal of Molecular Structure*, 1989, **214**, 329-355.

382. D.A. Mannock, P.E. Harper, S.M. Gruner, R.N. McElhaney. The physical properties of glycosyl diacylglycerols. Calorimetric, X-ray diffraction and Fourier transform spectroscopic studies of a homologous series of 1,2-di-O-acyl-3-O-(ß-d-galactopyranosyl)-sn-glycerols. *Chemistry and Physics of Lipids,* 2001, **111**, 139-161.

383. K. Brandenburg, U.Seydel. Infrared spectroscopy of glycolipids. *Chemistry and Physics of Lipids*, 1998, **96**, 23-40.

384. M.D. Guillén, N. Cabo. Infrared spectroscopy in the study of edible oils and fats. *Journal of the Science of Food and Agriculture*, 1997, **75** (1), 1-11.

385. P. Samyn, D. Van Nieuwkerke, G. Schoukens, L. Vonck, D. Stanssens, H. Van Den Aabbeele. Quality and statistical classification of Brazilian vegetable oils using mid-infrared and Raman spectroscopy. *Applied Spectroscopy*, 2012, **66** (5), 552-565.

386. J. Salimon, N. Farhan. Physiochemical properties of Saudi extra virgin olive oil. *International Journal of Chemical and Environmental Engineering*, 2012, **3** (3), 205-208.

387. G. Reich. Near-infrared spectroscopy and imaging: Basic principles and pharmaceutical applications. *Advanced Drug Delivery Reviews*, 2005, **57**, 1109-1143.

388. M.E. Auer, U.J. Griesser, J. Sawatzki. Qualitative and quantitative study of polymorphic forms in drug formulations by near infrared FT-Raman spectroscopy. *Journal of Molecular Structure*, 2003, **661-662**, 307-317.

389. H.G. Brittain, K.R. Morris, D.E. Bugay, A.B. Thakur, A.T.M. Serajuddin. Solid-state NMR and IR for the analysis of pharmaceutical solids: Polymorphs of fosinopril sodium. *Journal of Pharmaceutical and Biomedical Analysis*, 1993, **11** (11-12), 1063-1069.

390. A.M. Tudor, M.C. Davies, C.D. Melia, D.C. Lee, R.C. Mitchell, P.J. Hendra, S.J. Church. The applications of near-infrared Fourier transform Raman spectroscopy to the analysis of polymorphic forms of cimetidine. *Spectrochimica Acta*, 1991, **47A** (9/10), 1389-1393.

391. B. Zimmermann, G. Baranovic. Thermal analysis of paracetamol polymorphs by FT-IR spectroscopies. *Journal of Pharmaceutical and Biomedical Analysis*, 2011, **54**, 295-302.

392. W.P. Findlay, D.E. Bugay. Utilization of Fourier transform-Raman spectroscopy for the study of pharmaceutical crystal forms. *Journal of Pharmaceutical and Biomedical Analysis*, 1998, **16**, 921-930.

393. P. Ekambaram, H.S.A. Abdul. Formulation and Evaluation of Solid Lipid Nanoparticles of Ramipril. *Journal of Young Pharmacists*, 2011, **3** (3), 216-220.

394. P.R. Griffiths, J.A. deHaseth. *Fourier transform infrared spectroscopy*. 1986, Wiley, New York.

395. D.B. Chase, J.F. Rabolt. *Fourier transform Raman spectroscopy*. 1994, Academic Press, New York.

396. B. Schrader. *Infrared and Raman Spectroscopy*. 1995, VCH, Weinheim.

397. D. Steele. Infrared spectroscopy: theory. In: J.M. Chalmers, P.R. Griffiths (editors): *Handbook of vibrational spectroscopy*. 2002, John Wiley & Sons Ltd., Chichester, pp. 44-70.

398. B. Van Eerdenbrugh, L.S. Taylor. Application of mid-IR spectroscopy for the characterization of pharmaceutical systems. *International Journal of Pharmaceutics*, 2011, **417**, 3-16.

399. Perkin Elmer Technical Note. FT-IR Spectroscopy, Attenuated total reflectance. http://www.utsc.utoronto.ca/~traceslab/ATR_FTIR.pdf, last accessed on 22-03-2014

400. K. Wa Kasongo, J. Pardeike, R.H. Müller, R.B. Walker. Selection and characterization of suitable lipid excipients for use in the manufacture of didanosine-loaded solid lipid nanoparticles and nanostructured lipid carriers. *Journal of Pharmaceutical Sciences*, 2011, **100** (12), 5185-5196.

401. N. Schöler, C. Olbrich, K. Tabatt, R.H. Müller, H. Hahn, O. Liesenfeld. Surfactant, but not the size of solid lipid nanoparticles (SLN) influences viability and cytokine production of macrophages. *International Journal of Pharmaceutics*, 2001, **221**, 57-67.

402. H. Weyhers, S. Ehlers, H. Hahn, E.B. Souto, R.H. Müller. Solid lipid nanoparticles (SLN)-effect of lipid composition on in vitro degradation and in vivo toxicity. *Pharmazie*, 2005, **61**, 539-544.

403. N.A. Armstrong. Glyceryl palmitostearate. In: R.C.Rowe, P.J.Sheskey, M.E.Quinn (editors): *Handbook of pharmaceutical excipients*. 2003, The Pharmaceutical Press, London, pp. 293-294.

404. M. Ash, I. Ash. *Handbook of pharmaceutical additives*. 1995, Hartnolls Ltd, Cornwall.

405. J. Hamdani, A.J. Moës, K. Amighi. Physical and thermal characterisation of Precirol® and Compritol as lipophilic glycerides used for the preparation of controlled-release matrix pellets. *International Journal of Pharmaceutics*, 2003, **260**, 47-57.

406. Gattefossé. Precirol® ATO 5. Gattefossé Pharmaceuticals. http://www.gattefosse.com/en/applications/precirol-ato5.html, last accessed on 22-03-2014.

407. R.C. Rowe, P.J. Sheskey, P.J. Weller. *Handbook of pharmaceutical excipients: Glyceryl behenate*. 2003, American Pharmaceutical Association, Washington, D.C.

408. *British Pharmacopoeia*. 2013, Stationery Office Books, London.

409. Gattefossé. Compritol® 888 ATO. Gattefossé Pharmaceuticals. http://www.gattefosse.com/en/applications/compritol-888-ato.html, last accessed on 22-03-2014.

410. Gattefossé. Labrafil® M2130CS. Gattefossé Pharmaceuticals. http://www.gattefosse.com/node.php?articleid=9? , last accessed on 22-03-2014.

411. M. Ambühl, B. Haeberlin, B. Lückel, A. Meinzer, O. Lambert, L. Marchal. Pharmaceutical compositions, United States Patent Application. Free patents online, http://www.freepatentsonline.com/y2010/0215734.html, last accessed on 22-03-2014.

412. Gattefossé. Gelucire® 44/14. Gattefossé Pharmaceuticals. http://www.gattefosse.com/en/applications/gelucire-4414.html, last accessed on 22-03-2014.

413. R. Jadhav. Gelucires: Pharmaceutical applications. Pharmainfo.net. http://www.pharmainfo.net/reviews/gelucires-pharmaceutical-applications, last accessed on 22-03-2014.

414. A. Svensson, C. Neves, B. Cabane. Hydration of an amphiphilic excipient, Gelucire 44/14. Archives ouvertes. http://hal.archives-ouvertes.fr/docs/00/05/22/09/PDF/articlegelucire.pdf, last accessed on 22-03-2014.

415. Gattefosse. Gelucire® 50/13. Gattefosse Pharmaceuticals. http://www.gattefosse.com/en/applications/gelucire-5013.html, last accessed on 22-03-2014.

416. C. Viseras, I. Ismail Salem, I.C. Rodriguez Galan, A. Cerezo Galan, A. Lopez Galindo. The effect of recrystallization on the crystal growth, melting point and solubility of ketoconazole. *Thermochimica Acta*, 1995, **268**, 143-151.

417. J.L. Ford, P. Timmins. *Pharmaceutical Thermal Analysis*. 1989, Ellis Horwood Ltd, London.

418. M.D. Guillén, N. Cabo. Some of the most significant changes in the Fourier transform infrared spectra of edible oils under oxidative conditions. *Journal of the Science of Food and Agriculture*, 2000, **80**, 2028-2036.

419. M. Safar, D. Bertrand, P. Roder, M.F. Devaux, C. Genot. Characterization of edible oils, butter and margarines by Fourier transform infrared spectroscopy with attenuated total reflectance. *Journal of the American Oil Chemists' Society*, 1994, **71**, 371-377.

420. M.C. Nahata, L.V. Allen. Extemporaneous drug formulations. *Clinical Therapeutics* 2008, **30** (11), 2112-2119.

421. L.V. Allen. Dosage form design and development. *Clinical Therapeutics* 2008; **30** (11), 2102-2111.

422. Soluphor® P. BASF SE, http://www.basf.com/group/corporate/wind-energy/en/overview-page:/Brand+Soluphor, last accessed on 22-03-2014.

423. Soluphor® P. BASF Pharma Ingredients. BASF Corporation. http://www.pharma-ingredients.basf.com/Statements/Technical%20Informations/EN/Pharma%20Solutions/EMP%20030747e_Soluphor%20P.pdf, last accessed on 22-03-2014.

424. Soluphor® P. Signet. The Complete Excipients Company. http://www.signetchem.com/Signet-The-Complete-Excipients-Company-Product-Soluphor-P, last accessed on 22-03-2014.

425. S.Ali. Soluplus BASF. BASF Pharma Ingredients. http://www.pharma-ingredients.basf.com/Products.aspx?PRD=30446233, last accessed on 22-03-2014.

426. S.Ali. Soluplus®. BASF Pharma Ingredients. BASF The Chemical Company. http://www.pharma-ingredients.basf.com/Documents/ENP/Brochure/EN/RZ_BASF_Broschure_Soluplus.pdf, last accessed on 22-03-2014.

427. Soluplus. Chemanager Europe. http://www.chemanager-online.com/en/products/pharma-biotech-processing/soluplus-polymeric-solubilizer-effective-drug-delivery, last accessed on 22-03-2014.

428. S.Ali. Lutrol® E 400 Polyethylene Glycol. BASF Pharma Ingredients . BASF The Chemical Company. http://www.pharma-ingredients.basf.com/Products.aspx?PRD=30035160, last accessed on 22-03-2014.

429. S.Ali. Lutrol® E liquid grades. BASF Pharma Ingredients. BASF The Chemical Company. http://www.pharma-ingredients.basf.com/Statements/Technical%20Informations/EN/Pharma%20Solutions/03_030734e_Lutrol%20E%20-%20Liquid%20Grades.pdf, last accessed on 22-03-2014.

430. Lutrol® E 400. SpecialChem. http://www.specialchem4cosmetics.com/tds/lutrol-e-400/basf/1267/index.aspx, last accessed on 22-03-2014.

431. Kollisolv PEG (Lutrol E). Signet. http://www.signetchem.com/Signet-The-Complete-Excipients-Company-Product-Kollisolv-PEG-Lutrol-E, last accessed on 22-03-2014.

432. J.H. Collett. Poloxamer. In: R.C. Rowe, P.J. Sheskey, M.E. Quinn (editors): *Handbook of Pharmaceutical Excipients*. 2009, The Pharmaceutical Press, London, pp. 506-509.

433. R.C. Scott, G.S. Kwon. The effects of Pluronic block copolymers on the aggregation state of nystatin. *Journal of Controlled Release,* 2004; **95**:161-171.

434. Sodium cholate hydrate. Sigma Aldrich. http://www.sigmaaldrich.com/catalog/product/sigma/c1254?lang=de&region=DE, last accessed on 22-03-2014.

435. C9282 Sigma Sodium cholate hydrate. Sigma Aldrich. http://www.sigmaaldrich.com/catalog/product/sigma/c9282?lang=en&region=ZA, last accessed on 22-03-2014.

436. Product Specification: Sodium cholate hydrate. Sigma-Aldrich. http://www.sigmaaldrich.com/Graphics/COfAInfo/SigmaSAPQM/SPEC/C9/C9282/C9282-BULK SIGMA .pdf, last accessed on 22-03-2014.

437. Safety data sheet: Sodium cholate hydrate. Sigma Aldrich. http://www.sigmaaldrich.com/MSDS/MSDS/DisplayMSDSPage.do?country=DE&language=de&productNumber=C9282&brand=SIGMA&PageToGoToURL=http%3A%2F%2Fwww.sigmaaldrich.com%2Fcatalog%2Fproduct%2Fsigma%2Fc9282%3Flang%3Dde, last accessed on 22-03-2014.

438. D. Zhang. Polyoxyetylene sorbitan fatty acid esters. In: R.C. Rowe, P.J. Sheskey, M.E. Quinn (editors): *Handbook of Pharmaceutical Excipients*. 2009, The Pharmaceutical Press, London, pp. 549-553.

439. C.S. Chauhan, H.S. Udawat, P.S. Naruka, N.S. Chouhan, M.S. Meena. Micellar solubilization of poorly water soluble drug using non ionic surfactant. *International Journal of Advanced Research in Pharmaceutical & Bio Sciences,* 2012, **1** (1), 1-8.

440. Product information: Tween 80. Sigma Aldrich. http://www.sigmaaldrich.com/etc/medialib/docs/Sigma-Aldrich/Product_Information_Sheet/p8074pis.Par.0001.File.tmp/p8074pis.pdf, last accessed on 22-03-2014.

441. A. Kovacevic, S. Savic, G. Vuleta, R.H. Müller, C.M. Keck. Polyhydroxy surfactants for the formulation of lipid nanoparticles (SLN and NLC): Effects on size, physical stability and particle matrix structure. *International Journal of Pharmaceutics*, 2011, **406** (1-2), 163-172.

442. C. Olbrich, O. Kayser, R.H. Müller. Enzymatic degradation of Dynasan 114 SLN – effect of surfactants and particle size. *Journal of Nanoparticle Research*, 2002, **4**, 121-129.

443. M. Uner, S.A. Wissing, G. Yener, R.H. Müller. Influence of surfactants on the physical stability of solid lipid nanoparticle (SLN) formulations. *Pharmazie*, 2004, **59** (4), 331-332.

444. A.A. Attama, B.C. Schicke, T. Paepenmüller, C.C. Müller-Goymann. Solid lipid nanodispersions containing mixed lipid core and a polar heterolipid: characterization. *European Journal of Pharmaceutics and Biopharmaceutics*, 2007, **67** (1), 48-57.

445. S-J. Lim, C-K. Kim. Formulation parameters determining the physicochemical characteristics of solid lipid nanoparticles loaded with all-trans retinoic acid. *International Journal of Pharmaceutics*, 2002, **243** (1-2), 135-146.

446. Y. Liang, N. Hilal, P. Langston, V. Starov. Interaction forces between colloidal particles in liquid: theory and experiment. *Advances in Colloid and Interface Science*, 2007, **134** (135), 151-166.

447. R.T. Gupta. MSc Thesis, Surface-active solid lipid nanoparticles for emulsion stabilization , Ryerson University, 2011. http://digitalcommons.ryerson.ca/islandora/object/RULA%3A1305/datastream/OBJ/download/Surface-active_solid_lipid_nanoparticles_for_emulsion_stabilization.pdf, last accessed on 22-03-2014.

448. C. Freitas, R.H. Müller. Effect of light and temperature on zeta potential and physical stability in solid lipid nanoparticle (SLN) dispersions. *International Journal of Pharmaceutics*, 1998, **168**, 221-229.

449. E. Aboutaleb, M. Noori, N. Gandomi, F. Atyabi, M.R. Fazeli, H. Jamalifar, R. Dinarvand. Improved antimycobacterial activity of rifampin using solid lipid nanoparticles. *International Nano Letters*, 2012, **2** (33), 1-8.

450. Y. Luo, D. Chen, L. Ren, X. Zhao, J. Qin. Solid lipid nanoparticles for enhancing vinpocetine's oral bioavailability. *Journal of Controlled Release*, 2006, **114**, 53-59.

451. D. Quintanar-Guerreroa, D. Tamayo-Esquivel, A. Ganem-Quintanar, E. Allémann, E. Doelker. Adaptation and optimization of the emulsification-diffusion technique to prepare lipidic nanospheres. *European Journal of Pharmaceutical Sciences*, 2005, **26** (2), 211-218.

452. J-C. Leroux, E. Allémann, E. Doelker, R. Gurny. New approach for the preparation of nanoparticles by an emulsification-diffusion method. *European Journal of Pharmaceutics and Biopharmaceutics*, 1995, **41** (1), 14-18.

453. M.A. Schubert, C.C. Müller-Goymann. Solvent injection as a new approach for manufacturing lipid nanoparticles – evaluation of the method and precess parameters. *European Journal of Pharmaceutics and Biopharmaceutics*, 2003, **55** (1), 125-131.

454. S.J. Lim, C.K. Kim. Formulation parameters determining the physicochemical characteristics of solid lipid nanoparticles loaded with all-trans retinoic acid. *International Journal of Pharmaceutics*, 2002, **243** (1-2), 135-146.

455. E. Allémann, R. Gurny, E. Doelker. Preparation of aqueous polymeric nanodispersions by a reversible salting-out process: influence of process parameters on particle size. *International Journal of Pharmaceutics*, 1992, **87**, 247-253.

456. European Agency for the Evaluation of Medicinal Products. *Stability testing of new drug substances and products: ICH Harmonised Tripartite Guidelines (ICH Q1A)*. 1993, ICH - Technical Coordination, London.

457. T. Tadros. Application of rheology for assessment and prediction of the long-term physical stability of emulsions. *Advances in Colloid and Interface Science*, 2004, **108-109**, 227-258.

458. H. Heiati, R. Tawashi, N.C. Phillips. Drug retention and stability of solid lipid nanoparticles containing azidothymidine palmitate after autoclaving, storage and lyophilization. *Journal of Microencapsulation*, 1998, **15** (2), 173-184.

459. P. Ekambaram, A. Abdul Hasan Sathali, K. Priyanka. Solid lipid nanoparticles: A review. *Scientific Reviews & Chemical Communications*, 2012, **2** (1), 80-102.

460. R.H. Müller, M. Radtke, S.A. Wissing. Nanostructured lipid matrices for improved microencapsulation of drugs. *International Journal of Pharmaceutics*, 2002, **242** (1-2), 121-128.